OPERATION AND CONTROL OF A MICROGRID WITH DISTRIBUTED GENERATION SYSTEMS

Thesis

submitted in partial fulfillment of the requirements for the degree of

DOCTOR OF PHILOSOPHY

by

CHETHAN RAJ D

DEPARTMENT OF ELECTRICAL AND ELECTRONICS ENGINEERING

NATIONAL INSTITUTE OF TECHNOLOGY KARNATAKA

SURATHKAL, MANGALORE - 575 025

FEBRUARY, 2020

D E C L A R A T I O N

by the Ph.D. Research Scholar

I hereby *declare* that the Research Thesis entitled **OPERATION AND CONTROL OF A MICROGRID WITH DISTRIBUTED GENERATION SYSTEMS** which is being submitted to the **National Institute of Technology Karnataka, Surathkal** in partial fulfilment of the requirements for the award of the Degree of **Doctor of Philosophy** in department of Electrical and Electronics Engineering is a *bonafide report of the research work carried out by me*. The material contained in this Research Thesis has not been submitted to any University or Institution for the award of any degree.

CHETHAN RAJ D

(121176EE12F01)

(Register Number, Name & Signature of the Research Scholar)

Department of Electrical and Electronics Engineering

Place: NITK-Surathkal

Date:

C E R T I F I C A T E

This is to certify that the Research Thesis entitled **OPERATION AND CONTROL OF A MICROGRID WITH DISTRIBUTED GENERATION SYSTEMS** submitted by **CHETHAN RAJ D** (Register Number: 121176EE12F01) as the record of the research work carried out by him, is *accepted as the Research Thesis submission* in partial fulfilment of the requirements for the award of degree of **Doctor of Philosophy.**

(Dr D N Gaonkar)
Research Guide
(Name and Signature with Date and Seal)

Chairman-DRPC
(Signature with Date and Seal)

ACKNOWLEDGEMENTS

It gives me immense pleasure and great sense of satisfaction to express my heartfelt gratitude to those who made this dissertation possible.

I take this opportunity to sincerely thank my research supervisor Dr D N Gaonkar for all his invaluable guidance, patience, encouragement, timely advice and support. He has been a constant source of inspiration throughout this journey. I feel proud to have worked under his guidance.

I thank National Institute of Technology Karnataka for giving me an opportunity for doing research and Ministry of Human Resource Department(MHRD)-Government of India for awarding research scholarship.

I wish to thank my research progress assessment committee (RPAC) members Dr. A. Karthikeyan and Dr. Ramesh M R, for their constructive feedback and guidance from research problem definition stage to thesis submission stage. Without their help the thesis would not have taken this shape.

I would like to thank Prof. K.P.Vittal, former HOD for providing the necessary resources in the department to carry out my research. Also, I would like to thank HOD, Dr Venkatesa Perumal for encouragement and providing valuable suggestions.

I take this opportunity to thank all teaching and non-teaching staff of EEE Department, NITK Surathkal.

I express my gratitude and thanks to the Prof Josep M Guerrero,Dr. Yajuan Guan, Dr Xu Haizhen, Dr Liaoyuan Li,Dr. Yong Shi,Qian Ping Mai.

My stay at NITK Surathkal was a sweet and memorable in the company of my fellow researchers who never let me knew that I am away from home. Big thanks to all the research scholars.

Finally, I would like to thank my Guru, Family members for their patience, care and love which drew me with inspiration to carry out my research.

CHETHAN RAJ D

ABSTRACT

The energy has always played a crucial role in the development and progress of human society. People have long been aware of the drawbacks of traditional fossil energy, such as the limited resources, resulting in environmental pollution and other defects. However, due to the needs of social development and the constraints of backward technology, people have to use fossil energy as the main energy source. In recent years, with the rapid development of science and technology, how to effectively use renewable energy to generate electricity has become the focus of attention in many countries. Because of its unique advantages in the use of new energy, microgrids have received more and more research and development.

The distributed power generation system based on microgrid technology is an important way to develop renewable energy, increase the reliability of power supply, and expand the capacity of the power supply system. The power supply of the distributed power system can be formed by a variety of energy sources through power conversion. The power supply units of the distributed power system are distributed and are all connected to the AC grid bus. The power supply unit of distributed generation micro-power system is generally a parallel inverter, and there are many parallel modes of inverter and the parallel mode of inverter power without interconnection line is especially suitable for distributed power generation system with grid-connected inverter. The ideal distributed generation microgrid system includes parallel DG inverter power modules, output line impedance, AC bus and loads connected to the AC bus. The DG inverter is the core of the distributed power generation system, which is responsible for transforming the distributed energy into electric energy and realizing the parallel network operation of the system.This thesis studies the droop controlled distributed generation inverters power decoupling and the restoration of frequency and voltage under resistive and inductive impedance microgrid environment.

Summarized the research background, definition and characteristics of microgrid. Summarizes the existing control structure of the microgrid. The classification, comparison and analysis of control methods for power electronic converters,

especially distributed generation inverters in microgrids are focused on. The topology of the distributed generation inverter main circuit and the filter circuit was chosen and filter parameters were designed. Then the mathematical model of distributed generation inverter in different coordinate were established. Since the output voltage strategy and output impedance of an distributed generation inverter always have an important influence on the DG inverter parallel system and power distribution. The instantaneous voltage closed-loop control in three-phase stationary coordinate and the inverter output voltage decoupling control strategy in dq rotating coordinate were analysized, in order to reduce variable numbers, while ensuring the DG inverter output voltage tracking with no difference to the reference voltage, the DG inverter output voltage control strategy based PI controller in dq coordinate is implemented and the influence of the controller parameters on closed-loop transfer function of output voltage and inverter equivalent output impedance were analysized.

The droop control is widely employed when multiple distributed generation inverters operate in parallel. However, due to inconsistent line impedance and the local load, there exists power sharing errors when the droop control is adopted, thereby reducing the efficiency of the system. In addition, there is a coupling between the active power and reactive power with the direct droop control, which affects the stability of the system. Though the traditional power decoupling control is able to realize power decoupling, the actual real power and reactive power cannot be shared equally. To deal with the power sharing and power coupling problem, this chapter explicitly analyzes the causes of the power sharing error and power coupling with the direct droop control respectively, quantizes the power sharing error and the extent of power coupling and also gives the basic solution to reducing the power sharing error and solving the problem of power coupling. To solve the inaccurate power sharing problem of the direct droop control, virtual inductance is adopted. By adding the virtual inductance, can decouple the active and reactive power, but also achieve accurate power sharing. The simulation results verify the accuracy and effectiveness of the adopted control scheme.

Using direct droop control, the active power and reactive power can be decoupled when the line impedance is mainly inductive. However, it is not applicable to the microgrid with low voltage when the line impedance is resistive. As a result, the

active power and reactive power will be coupled and errors in preset ratio of power sharing will arise. Aiming at solving the problem about the inapplicability of direct droop control in low voltage micrigrid, this chapter implements reverse droop control. The influence of transmission impedance of distributed generation inverter to public load on power distribution, introduces virtual resistor and then uses reverse droop control strategy to distribute load in low voltage distributed power generation system. Analyzes the conditions that need to be met to accurately share the load according to the ratio of rated capacity for inverter power supply. In the actual distributed generation system, due to the distributed location of the distributed inverter power supply, the impedance of the line is uncertain and the traditional reverse droop control has certain limitations. The simulation model of DG inverter parallel operation is built under the matlab/simulink environment, the reverse droop control and the improved power allocation strategy using virtual resistance are simulated and compared, the correctness and validity of the adopted improved strategy are validated.

The traditional centralized control method cannot solve the problem of the various modes of microgrid operation, for example, the probem of controlling the microgrid systems induced by hard to collect information signals and low controllable. But the distributed secondary control method based on direct and reverse droop control has obvious advantage to solve the problem of parallel connected DG inverters operation. Aiming at the problem of voltage and frequency differences caused by the direct and reverse droop control and considering the actual situation of inductive and resistive line impedance mismatch, this thesis proposes a distributed secondary control. The simulation verifies that the proposed distributed secondary control method can guarantee the voltage amplitude and frequency recovery.

Keywords: Distributed Generation, Direct droop control, Reverse droop control, Microgrid, Virtual resistors, Virtual inductors, Parallel DG inverter, Distributed secondary control.

CONTENTS

LIST OF FIGURES

LIST OF TABLES

ABBREVIATIONS

UPS	:	Uninterruptible Power Supply
DG	:	Distributed Generation
MG	:	Microgrid
PCC	:	Point of Common Coupling
3C	:	Circular Chain Control
PLC	:	Power Line Communication
FCP	:	Frequency controlled power
VCP	:	Voltage controlled power
APFC	:	Active power factor correction
PLL	:	Phase Lock Loop
PI	:	Propotional Integral
EMC	:	Energy Management Centre
IM	:	Impedance Matching
PWM	:	Pulse Width Modulation
SPWM	:	Sine Pulse width modulation
Hz	:	Hertz
MGCC	:	Microgrid Central Controller
IEEE	:	International Electrical and Electronics Engineering
KW	:	Kilo Watt
KVAR	:	Kilo Volt Ampere Reactive

Chapter 1

1 INTRODUCTION

1.1 BACKGROUND AND SIGNIFICANCE

In the industrial revolution, countries around the world have gradually established a system of industrialized development relying on energy [Dugan and Mcdermott (2002)]. With the rapid development of the world economy, fossil fuels such as coal, oil and natural gas have been consumed at an alarming rate and have caused severe environmental problems such as acid rain, fog and global warming [Khattam and Salama (2004)]. With the depletion of fossil energy, the overall energy supply and demand relationship has been strained. "2014 World Energy Outlook" pointed out that: It is estimated that global energy demand will increase by 37% between 2012 and 2040 and global coal demand will grow by 15% [Maria (2014)]. At the same time, economic development in developing countries is accompanied by a great deal of energy waste. Therefore, renewable energy has received great attention from people. Accelerating the change of energy structure and developing renewable energy are particularly important for the sustainable development of the economy and the improvement of the environment [Ackermann et al.(2001)].

As a clean, efficient secondary energy source, electric energy plays an irreplaceable role in the country's economic development, social operation and people's lives. At the same time as social progress and economic prosperity, the electric power industry has also experienced rapid development. However, electrical energy is also a major consumer of fossil energy. Traditional energy consumption methods and power supply models have brought huge driving forces and economic benefits to social development, but have also caused serious environmental pollution problems [Ackermann and Knyazkin (2002)]. In order to prevent drastic climate change from causing harm to humans, how to use wind energy, solar energy and other renewable energy to generate electricity and reduce fossil energy consumption is the key to transforming the energy structure and achieving sustainable economic development and is the future direction of development of the power industry [Ahmed and Istvn (2005), Nunna and Dolla (2012)].

Based on the above factors, the development of distributed generation has become a necessary way to solve the above problems. Distributed generation can effectively use new energy sources such as wind power generation and photovoltaic power generation to ease the energy crisis and be environmentally friendly during operation[Guerrero et al.,(2010)]. Distributed power generation and large power grids can complement each other, improving the reliability of power supply; Distributed generation can supply power to local loads nearby, which can greatly reduce investment in transmission and distribution equipment [Guerrero et al., (2013)].

1.1.1 Distributed Generation Technology

Distributed generation technologies mainly include new energy sources such as fuel cells, wind power and photovoltaic power generation, energy storage devices such as storage batteries, small internal combustion engine generators, and conventional fossil fuel generators[Zhang et al., (2017), Debanth and Chatterjee (2016)]. Usually, the distributed generator set has a capacity of several kilowatts to several tens of megawatts and is directly connected to the low voltage or medium voltage distribution network where the load is located through a modular and decentralized method. Distributed generation technology has the following advantages over conventional large-scale power generation technologies [Pesaran et al.,(2017), Jordehi et al., (2016)]:

(1) The distributed generation technology uses green clean and renewable energy to generate electricity. It is not affected by the shortage of traditional energy sources. It realizes the diversification of energy utilization, which saves energy and increases energy efficiency.

(2) Flexible position, decentralized, well adapted to the distribution of decentralized resources and power demand, improve the use of renewable energy sources.

(3) The construction period is short, the area is small, the investment is reduced, and the electrical and physical distance between the electricity load and the power generation equipment is shortened, thereby reducing the huge cost required for the network loss and the upgrading of the transmission and distribution network.

(4) Distributed generation is an effective support and powerful supplement for large power grids. The mutual backup for large power grids also improves the reliability of power supply[Kayalvizhi and Kumar (2017)].

Therefore, the DG system can not only comprehensively use energy, save costs, solve the problem of long-distance transmission while using electricity in remote areas and improve the flexibility and reliability of power supply.

Although the advantages of grid-connected distributed generation technologies mentioned above are prominent, an increasing number of distributed power sources also highlight their own shortcomings. First of all, the distributed power supply has high cost of single machine access and complex control [Bansal et al., (2016)]. It is difficult to coordinate with existing power systems and other issues. Secondly, if a large number of distributed power sources are directly integrated into the power grid, it will have many impacts on the structure, mode, and stability issues of power system operation, such as the impact of power quality, the impact of network loss, etc[Blaabjerg et al., (2004)]. Therefore, the distributed power supply is treated as an uncontrollable source. In addition, the distributed power supply uses renewable energy with unstable output power and its independent power supply capacity is weak. The installed capacity is relatively small compared to traditional power generation energy, and has an unpredictable impact on the stability of the large power grid. Therefore, the large power grid often requires distributed power, limit and isolate to reduce its impact on large systems[Gao et al., (2008)].

In order to avoid the impact of distributed power on the large power grid, the United States has formulated IEEE I547 regulations that require the distributed power supply to immediately exit operation when a major power grid fails [IEEE std. 1547 (2003)]. However, the energy efficiency of the distributed power supply after exiting is greatly reduced. In order to more efficiently integrate multiple new energy sources in distributed power sources and improve the performance of distributed power sources, in the early 21st century, the American Electric Reliability Technology Solution Association (CERTS) proposed a the organizational form of potential power generation technology—Microgrid [Lassetter et al., (2002)].

1.1.2 Basic Concepts and Significance of Microgrid

Micro-Grid is one of the most important forms of distributed generation [Hatziargyriou et al., (2007)] and it is also the most effective form of integration into large power grids. Micro-grid refers to a small-scale power generation and distribution system composed of distributed power supplies, loads, protection devices, monitoring systems and energy management systems. It can realize relatively independent autonomous systems for self-control, protection, management and can be integrated with large-scale power grids and can also be run in isolation [Lasseter et al., (2011)].The micro-grid will become an important part of the smart grid[Nunna and Dolla (2012), Nunna and Srinivasan (2017). According to the definition of the above microgrid, its main advantages are as follows [Katiraei et al., (2006), Shuai et al., (2016)]:

(1) Improve power supply system reliability:

Microgrids can increase the reliability of local power supply, reduce power consumption and ensure power quality. Furthermore, it is concluded that the flexible parallel operation mode of microgrid can play a demand side management (DSM) role in the large power grid, which greatly improves the safety and stability of the large power grid[Meng et al., (2016), Nunna and Dolla (2012)].

(2) Flexible mode of operation

Microgrids have two modes of operation: grid connection and islanding. When the micro-grid is connected to the grid, the microgrid needs to generate electricity according to the instructions of the large power grid, power dispatching of the micro-grid and the load of the micro-grid can accept the power supply of micro-grid or large power grid. If the large power grid is disturbed, various faults or intermittent fluctuations of renewable energy of distributed generation, the micro-power grid can realize fast and large power grid solution, smooth transition to the island operating mode and to ensure that the distributed power, large power grid, load are not affected [Micallef et al., (2015)].When microgrid is operated islanding mode, it can meet the reliability of local load power supply. When the grid collapses, the microgrid can act as a black-start device, improving post-disaster emergency support capabilities and helping the system return to normal operation [Pecaslopes et al., (2005), Barik et al., (2015)].

(3) Improve energy efficiency

By analyzing the electricity demand of the load, the microgrid can rationally optimize the allocation of resources, increase resource utilization, reduce resource waste and reduce environmental pollution. At the same time, distributed generation based on renewable energy is closer to the load, reducing transmission distance and reducing line losses and maintenance costs[Dahraie et al., (2018)].

(4) Promote the development of the electric power industry

The microgrid integrates distributed power sources of various forms and locations into the same physical network, changing the traditional one way power transmission mode. The microgrid, as an independent entity in the power market, participates in the marketization operation, which is conducive to uniform energy scheduling[LEE et al., (2011)]. Energy management, improve the service efficiency and service level of the power industry and then promote the sound development of the electricity market. At the same time, the widespread use of microgrids can reduce electricity prices and maximize economic benefits[Mohan et al., (2017)]. Enterprises can save energy and reduce consumption, rural electrification, and greatly improve the quality of power supply. Microgrid, as an integral part of the smart grid, is of great significance. As the effective use of distributed power supply and the effective supplement of large power grid, micro-power network not only gives full play to the benefits of distributed power supply for users and power grids, but also solves the disadvantage of distributed power supply and improves the potential value of distributed power supply. Microgrid has received more attention and its development potential is enormous[Vluski et al., (2017)].

1.2 MICROGRID DEVELOPMENT STATUS

In recent years, with the continuous increase of energy demand and environmental problems, the United States, Europe and Japan have represented the developed countries. The region has increased investment in distributed generation and adopted active and effective measures and policies. It has vigorously carried out research on microgrids, combined with actual conditions in various countries, based on the sustainable development of the economy and practical problems of its own power system, to initially establish distributed energy sources. The microgrid model and simulation analysis tools have independently developed control and protection

strategies and communication protocols for domestic microgrid construction and established laboratory tests and on-site demonstration projects to verify that microgrid operation and protection have been resolved. The effective integration, flexible and intelligent control of distributed power supply by microgrids has led to widespread attention and recognition in solving distributed energy grid-connected problems [Shuai et al., (2016)].

1.United States

The United States first proposed the concept of a microgrid. The US Department of Energy attaches great importance to the construction of microgrids. In the "Grid2030" development strategy, the United States has developed a microgrid as an important component of its research and development plan for the US power system in the coming decades [Lasseter et al., (2011)]. The research focus of the US microgrid focuses on meeting various power quality requirements, improving reliability of power supply, reducing costs, and achieving intelligence. CERTS published the "Micro-grid Concept White Paper" in 2003, laying the foundation for its influence in the field of global micro-grid research. Development of microgrid has entered the on-site demonstration stage of operation from simulation analysis and experimental research since 2005. The MadRiver Microgrid, built by the northern United States power system, is the first micro-grid demonstration project in the United States [LYNCH [2006)]. The U.S. Department of Energy and GE also jointly funded the second "GE Global Research" program. The GE Micro Grid focuses on the development of external monitoring circuits, energy utilization and optimization of operating costs. The research content of the distributed performance integration test platform funded by the California Energy Commission in 2004 mainly includes research on the effects of high penetration rate of distributed power sources on distribution networks, voltage and frequency adjustment of microgrids, measurement, analysis of power quality and relay protection[Stevens et al., (2004)].

In addition, from 2009 to 2012, the US Department of Energy funded Oracle Group’s $7.2 million to participate in the development of G&E microgrid projects responsible for the development and application of power off/distribution management systems (DMS). The federal government has signed a contract with NEXTEK Power Systems to establish a direct-coupled microgrid for assessing the

feasibility of direct use of microgrids for larger-scale use and the DC photovoltaic power supply built in 2011.The annual energy saving effect is 3,000 US dollars. Enhancing the power supply reliability of important loads, satisfying a variety of power quality requirements customized by users, reducing costs and achieving intelligence are the focus of the development of the US microgrid [Driesen et al., (2008), Stevens et al., (2007)].

2.Europe

European countries not only have basically realized the interconnection of power systems, but also have a high utilization rate of new energy and renewable energy. Therefore, they attach great importance to the research and development of microgrids. In 2005, Europe put forward the concept of "SmartPowerNetworks" and in 2006 it introduced a technology plan for the implementation of a smart grid project as a development goal for Europe in 2007 and subsequent years[European comission]. The plan points out that in the future, European grids should be flexible, accessible, reliable and economical. In the EU 5th Framework Program (FP5), a special fund of 4.5 million euros is allocated to research on microgrid modeling and simulation, local black-start strategy, agent-based control strategy, distribution network parallel operation, related protection and grounding programs[Hatziargyriou (2007)]. The EU 6th framework program (FP6) has funded 8.5 million euros, emphasizing the interaction between multiple microgrids and distribution networks, including coordinated control strategies, hierarchical energy management, protection, scheduling and microgrid penetration. The EU's 7th Framework Program (FP7) was launched in 2007 to realize the current transition from a trial network to a more flexible and interactive grid, remove barriers to large-scale integration of renewable energy and develop demonstrations of key technologies including energy storage technologies. All microgrid research programs in Europe are considered in terms of reliability, accessibility, and flexibility [Braun et al., (2006)]. The micro-grid demonstration projects established in Europe mainly include the Greek Gesnos microgrid, the demonstration project of the Wallstadt residential district in Mannheim, Germany, LA Leisure in Spain, the Portuguese EDP project and the Danish ELTRA project [Michael and Natalie (2011)].

3. Japan

Japan’s economic development is constrained by the current situation of domestic resource shortage. Its development goals for microgrid research are mainly targeted at diversifying energy supply, reducing pollution, and satisfying users’ individualized electricity requirements [Morozumi (2006)]. Japan has established a new energy and industrial technology development Organization (NEDO) to improve the research and development of new energy and its applications with domestic universities, enterprises and national key laboratories. NEDO has achieved a lot in the research of microgrid. NEDO established three microgrid pilot projects in Aomori, Aichi and Kyoto in the "Regional Power Grid with Renewable Energy esources Project" in 2003. The research focuses on renewable energy and local distribution networks. In 2005 Shimizu Corp of Shimizu Construction Co., Ltd. launched the "Shimizu microgrid" project to establish a small microgrid, focusing on load-tracking technology research. In 2006 Tokyo gas company microgrid project, to achieve local voltage control, high-quality power supply[Morozumi and Nara (2007)]. At present, Japan is a world leader in the construction of microgrid demonstration projects and its Fuel cell and batteries have a high penetration rate in microgrid systems. This is because these two types of units have the characteristics of flexible control and quick start-up[Shinji et al., (2009)].

Japanese scholars have proposed flexible reliability and intelligent electrical systems.Energy delivery system (FRIENDS), which uses FACTS components for fast and flexible control performance to optimize the distribution network energy structure[Morozumi (2007)].

4.India

In the past few years, India's renewable energy generation has increased significantly.The growth of this renewable energy installation is a joint role of the regional energy development agency, the ministry of new and renewable energy (MNRE) and the private sector.Government support policies are also promoting the installation of renewable energy.The Indian Planning Commission has issued the Integrated Energy Policy Report (IEPR), which highlights the need to maximize domestic supply programmes and diversify energy sources to achieve sustainable energy supplies[Khaparde (2007)].

According to the IEPR, renewable energy could account for 11-13% of India's energy mix by 2032. Various problems and feasible solutions related to the large-scale deployment of renewable energy technologies in India are presented in the reference[Khaparde (2007)].The grid interactive energy developed in India is solar, wind, small hydro and bioenergy.It is estimated that with India's abundant biofuels available in various forms, biofuels could play a key role in the coming decades.In the field of distributed energy, with the financial support of MNRE, the country has installed a total of 33 grid-interactive solar photovoltaic power plants and coordinated with a small amount of bioenergy.The total installed capacity of these plants is a peak of 2.125 MW and is estimated to generate about 2.5 million units of electricity per year[Balijepalii et al.,(2010); Khaparde (2007)].

1.Sagar island microgrid-sundarban area [Balijepalii et al.,(2010);MNRE(2015)]:

There are many isolated areas for coordinated action development in the country. One of the most popular is The MicroGrid on Sagar Island.The project is co-financed by MNRE, the Government of India, the Environment Fund of India and Canada (ICEF) and the West Bengal Renewable Energy Development Agency (WBREDA).

At present, Sagar Island's electricity demand is met by a total capacity of 250 kilowatts of solar energy and 400 kilowatts of diesel generators.However, a large number of potential consumers are waiting for electricity. To meet these requirements, WBREDA has decided to build a 500-kW wind-diesel hybrid power plant.Overall, WBREDA has conducted activities in Sundarban region on renewable energy programs.A three-tier electricity price structure has been developed based on the actual electricity consumption of household, commercial and industrial consumers.The electricity price is Rs 5/kWh domestic users, Rs 5.5/ kWh for commercial users and Rs 6 / kWh for industrial users.

5.China

China's research on the microgrid project started late, but the government has given great importance to it. The Ministry of Science and Technology has included the microgrid technology in the project of the year 2007. The 973 project "Related basic research on distributed generation systems for power generation" mainly focuses on the interaction mechanism between microgrids and large grids [Hatziargyriou et al.,(2007),Xie et al.,(2017)].

At present, China's microgrid pilot projects include Henan Zhengzhou Finance Specialized Photoelectric Storage Microgrid Pilot Project, Zhejiang Dongfushan Island Scenery Storage, Firewood and Seawater Desalination Integrated System Project, Tianjin Zhongxin Eco City Smart Business Office Microgrid Pilot Project, Zhejiang Wenzhou Nanlu Island Scenery diesel storage distributed generation integrated system, Turpan new energy demonstration area, etc. [Dong et al.,(2016)]. The first phase of the Turpan New Energy Demonstration Zone was built in 2012 to realize the integration of photovoltaic buildings and smart microgrid functions and zero-carbon emissions from all public transportation are used[Zhao et al., (2016)].

At present, colleges and universities have also started research on microgrids, but they are still at the stage of basic theoretical research. Although they have made certain progress, they are also composed of research institutes, manufacturers, and electric power companies in Europe, the United States and Japan. Compared with the huge research team, there is still a big gap in research efforts and achievements, mainly in the following areas [Wang et al.,(2016),Dong et al., (2016), Hatziargyriou et al.,(2007)]:

1) Lack of unified and standardized microgrid system technical standards and specifications:At present, there are no unified and standardized microgrid system technical standards and specifications, which greatly affect the research of microgrid technology and the construction of demonstration projects. The main reference standard in the world was in 2003, IEE published the “Distributed Power Grid Interconnection Standard” (IEE1547), in which the “Establishment Guide for Design, Operation and Integration of Distributed Island Power Systems” IEEE 1547.4 introduced the microgrid. The concept of planning islands, which is also commonly referred to as the "DR island system," covers the main considerations for planning and operating microgrids: Voltage effects, frequency, power quality, protection plans and modifications, monitoring, information exchange and control, and customer load requirements. In addition, we must understand the characteristics of the DR, determine the interaction between the steady state and transient conditions, generators, energy storage equipment, demand response, load shedding and additional functions of the inverter.

2) The application level of power electronics in microgrid is not high: The development of micro-grid technology is closely related to advanced power electronics technology, computer drawing technology and communication technology. According to the special needs of the microgrid, it is necessary to develop the applicable power electronics technology and develop new types of power electronic equipment such as grid-connected inverters, static switches and power control devices. At present, the bottleneck of various renewable energy sources connected to the power grid has not yet been solved and the electrical and electronic technologies applicable to microgrid systems are still being researched and developed.

3) The protection and control technology of microgrid is not yet mature: Microgrid protection and control techniques include power supply, load control technologies, energy management technologies, microgrid power quality comprehensive monitoring technologies, communications protocols and microgrid safety and protection technologies. At present, related technologies are aimed at the traditional distribution network structure. How to carry out transformation, optimization, upgrade on this basis and the micro-grid protection and control technology still needs further research and development.

4) The analysis and decision-making technology for operation and analysis of microgrid needs in-depth research: Micro-grid operation analysis and decision-making technology includes energy exchange, coordinated control technology of micro-grid and large-scale power grid, optimized operation technology of micro-grid, new distribution network economic dispatching technology including micro-grid and economic evaluation and quantification of micro-grid. At present, these technologies are all in the research stage. To achieve industrialization, we must also gradually deepen the construction of laboratory verification and demonstration projects. Therefore, according to the current situation of the domestic microgrid technology is still in the stage of basic theoretical research and demonstration projects, it is necessary to focus on the research including microgrid control and protection, distributed generation,energy storage devices, inverter devices and isolation devices. The future research and development goal is to develop advanced control strategies, integrate the interactions between multiple microgrids and distribution management

systems and carry out standardized design to achieve on-site experiments to further verify the effectiveness of control strategies in actual microgrids.

1.3 MICROGRID AND ITS MODE OF OPERATION

1.3.1 Basic structure of the microgrid

Figure 1.1 shows a schematic diagram of a typical microgrid system that includes a number of distributed power sources, power electronics converters (such as inverters) and energy storage components (such as batteries, super capacitors). These systems and components are coupled to the load. Distributed power sources include renewable energy power generation systems such as photovoltaic power generation, wind power generation and fuel cell power generation. The load in the microgrid includes both conventional power loads, cooling and heat loads in residential or commercial buildings. The microgrid system can work in both the on-grid and off-grid modes and is connected to the external grid through a point of common coupling (PCC). When the PCC disconnects from the main grid, the system can operate in the network mode, power is continuously supplied to important loads in the microgrid [Guerrero et al., (2013), Katiraei et al., (2006)].

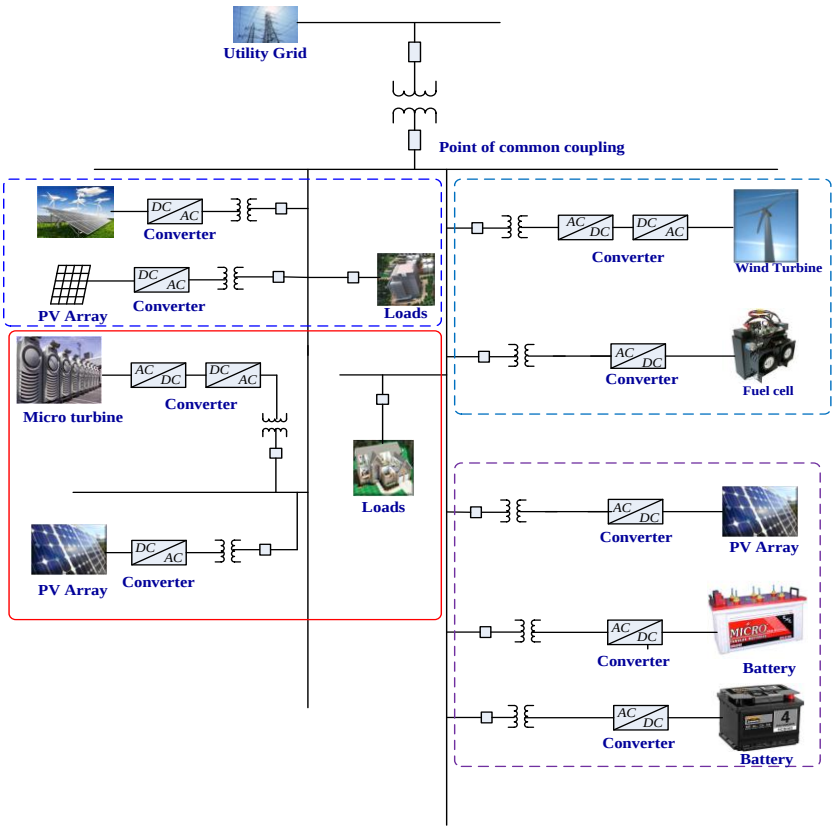

Figure 1.1: Typical microgrid system architecture

The microgrid can be regarded as a small power system, because of its own energy management function [Shuai et al., (2016)], it can effectively maintain the optimal distribution and balance of energy in the microgrid and ensure the economical efficiency of the microgrid.

In addition, the microgrid can be viewed as a "virtual" power source or load in the distribution system. Through the coordinated control of distributed power output in the network, can play the role of load shifting to the grid and it is also possible to achieve constant or fixed range control of the power exchange between the microgrid and the external distribution network. Reduces the impact of distributed renewable energy generation power fluctuations on external distribution networks and effectively reduce the difficulty of system operation personnel scheduling[Meng et al., (2016)].

A microgrid generally refers to a networked microgrid. This microgrid has two different operating modes: grid-tied and off-grid (island). In the grid-connected operating state, the micro-grid is connected to the low-voltage distribution network in parallel to achieve grid-connected operation. The two are supported by each other to achieve two-way flow of energy. When an external power distribution network fails or enters a planned island, the microgrid can be switched to an off-grid operation mode, continue to supply power for important loads in the network and improve the reliability of power supply for important loads. Through the use of advanced control methods and control strategies, it is possible to achieve smooth switching between the two operating states of the microgrid while ensuring that the microgrid is powered by high power quality power supply [Vluski et al., (2017), Lopes et al.,(2006), Pecaslopes et al., (2005), Chengshan et al., (2008)].

1.3.2 Microgrid Classification

The microgrid is classified according to the network structure and functional characteristics and can be divided into AC microgrids[Eid et al., (2016)], DC microgrids[Augustine et al., (2016)] and AC-DC hybrid microgrids[Gupta et al., (2018), Sen and Kumar (2018)].

(1) AC micro-grid

The AC microgrid is currently the main form of microgrid [Rajesh et al., (2017), Xiaofei et al., (2011), Rocabert et al., (2012)]. In the AC microgrid, distributed power

supplies, energy storage devices, etc., must be connected to the AC bus through power electronic inverters, as shown in Figure 1.2. By controlling the on-grid/off-network switch at the common contact point PCC, it is possible to switch between the grid-connected operation of the microgrid and the islanding operation mode. The conventional AC bus microgrid, a new high frequency AC (HFAC) microgrid is proposed in [Xiaofei et al., (2011)]. In this microgrid, all distributed power DGs and energy storage devices are connected to high frequency bus, and then supply power to the user's load. HFAC microgrids have certain advantages in terms of miniaturization of equipment, reduction of harmonic influence, improvement of power quality and easy access to AC energy storage equipment due to their high frequency of operation.

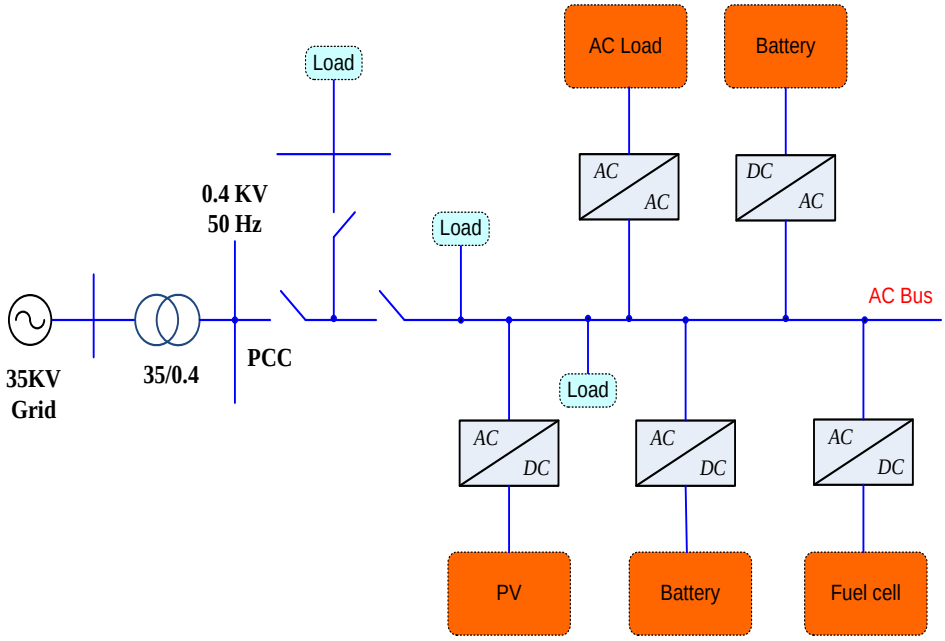

Figure 1.2: AC microgrid structure

(2) DC microgrid

The characteristic of the DC microgrid [Dragicevic et al., (2016)] is that the distributed power source, energy storage device and load in the system are all connected to the DC bus. The DC network is connected to the external AC grid through the power electronic inverter device, as shown in Figure 1.3. DC micropower grids can provide power to AC and DC loads with different voltage levels through power electronic converters and load fluctuations can be regulated by the energy storage device in the DC side[Augustine et al., (2015), Kakigano et al., (2009),Ricchiuto et al., (2013)]. Considering the characteristics of distributed power

supply and the demand of users for different levels of power quality, two or more DC micro-grids can form dual or multiple circuit power supply mode [Ricchiuto et al., (2013)]. A DC feeder connected to a distributed power source with relatively obvious intermittent characteristics for supplying power to common types of loads.

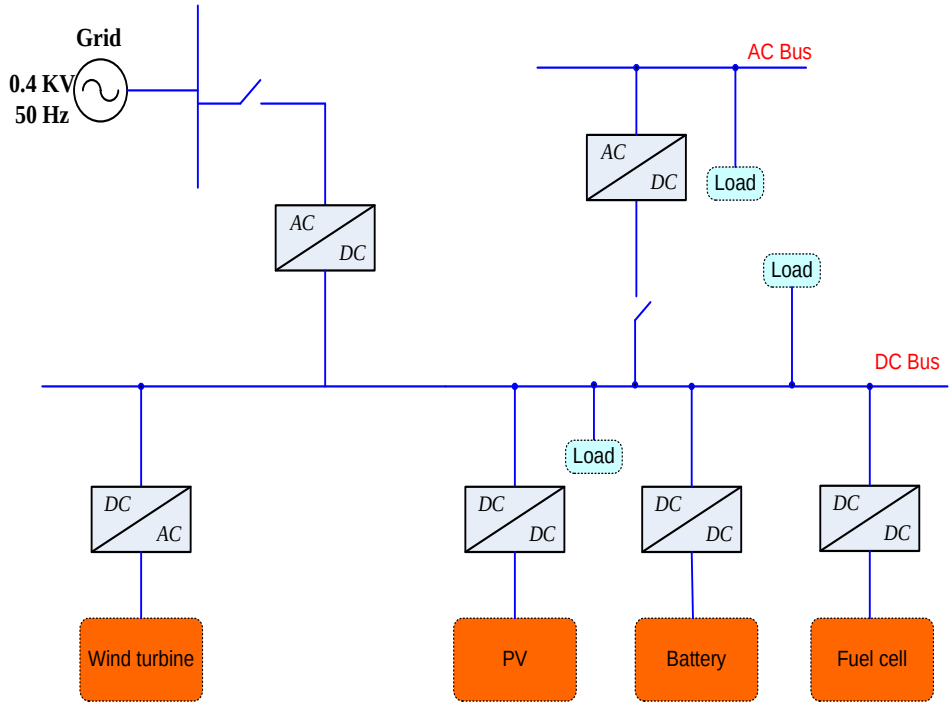

Figure 1.3: DC microgrid structure

A DC feed line connects distributed power sources and energy storage devices with relatively smooth running characteristics to provide power to higher-demand types of loads. Compared with the AC microgrid, the DC microgrid has only one level of voltage conversion equipment between each distributed power source and the DC bus, which reduces the construction cost of the entire system and makes it easier to implement the control. At the same time, since there is no need to consider the synchronization problem between distributed power sources, it is more advantageous to suppress the circulation between different distributed power sources.

(3) AC-DC Hybrid Microgrid

The AC-DC hybrid microgrid structure is shown in Figure 1.4.

In this microgrid, it contains both AC bus and DC bus. It can supply DC to AC loads and can directly supply DC loads and for the hybrid AC/DC microgrid [Vnamuno et al., (2015), Mortezapour et al., (2017)], but from the overall structural

analysis, it can still be regarded as an AC microgrid and the DC microgrid can be regarded as a unique power source that is connected to the AC bus through the power electronic inverter [Poh et al., (2011), Majumder et al., (2014)].

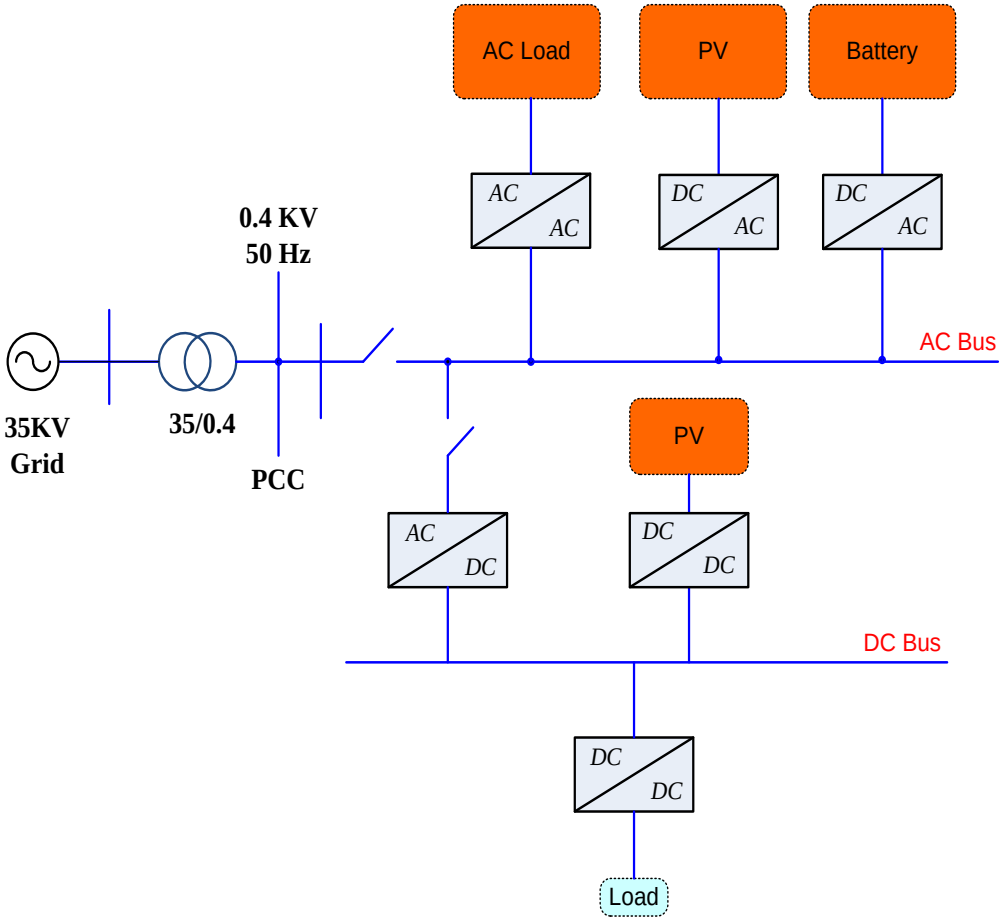

Figure 1.4: AC and DC microgrid structure

1.4 LITERATURE REVIEW OF DISTRIBUTED GENERATION INVERTER PARALLEL CONTROL TECHNOLOGY

The research of the early multi DG inverter parallel technology realizes that each parallel unit is divided into: signal interconnect line method and without signal interconnect line method and multi agent method[Nunna and Srinivasan (2017)]. Signal interconnect line method includes centralized control, master-slave control, decentralized logic control [Guerrero et al., (2008), Kaur et al., (2016)]. The parallel DG units with these methods cannot realize the independent parallel operation, the DG inverter module needs to rely on the interactive key information to support the parallel operation, once the information interaction is interrupted, the parallel system will not be able to continue to operate reliably. The DG inverter based on droop

control can realize the autonomous parallel operation in the case that the DG inverter has no information interaction.

1.4.1 Distributed generation inverter parallel technology relying on information interaction

The parallel technology of DG inverter with information interaction needs to add the signal interconnect line between the parallel DG units or use the technology of wireless communication, power line communication and common mode current communication to realize the information interaction. This limits the flexibility of the DG inverter's spatial distribution and reduces the redundancy of the parallel system, while the high reliance on the interaction signals reduces the reliability of the system[Guerrero et al., (2008), Chandorkar et al., (1993)]. However, such methods are capable of achieving higher current sharing and output voltage quality. At present, parallel DG technology with information interaction is generally an DG inverter parallel system with a common AC bus[Kaur et al., (2016)].

1.Centralized control :

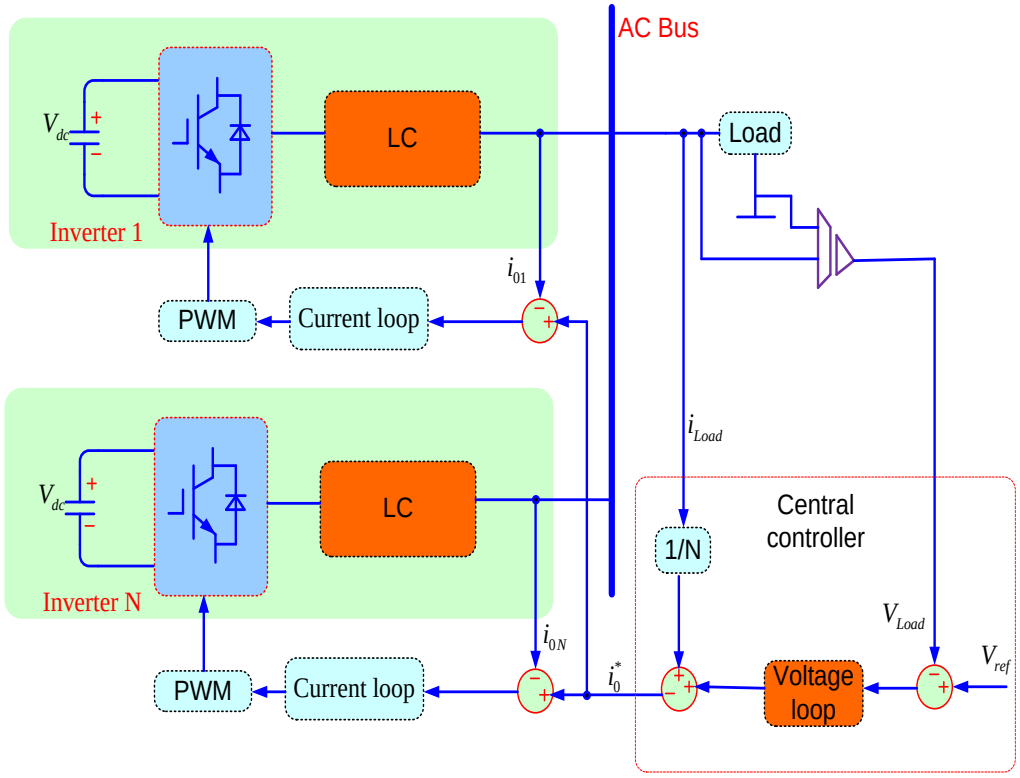

Figure 1.5: Centralized control DG inverter parallel control block diagram

The centralized control mode appears in the initial stage of the DG inverter parallel control and it has a central controller module which is independent of the DG inverter,

which is responsible for generating the unified control signal and sending the parallel units to realize the equalization of output voltage and output current of the inverter[Chen et al., (2003)].

Figure 1.5 shows a typical centralized control parallel scheme, the central controller is integrated with an output voltage control loop, which is used to adjust the load voltage, the output is added to the average load current value, as the current reference value of each DG inverter and the local controller of each DG inverter has only the current loop. For centralized control, the central controller is the core to ensure the normal operation of the parallel system. If it fails, the parallel system will collapse[Martin et al., (1995), Iwade et al., (2003)].

2. Master-slave control

The master-slave control mode is developed from the centralized control mode. Master-Slave control cancels the central controller, making one of the inverters assume the function of the central controller, and as the main inverter, typical master-slave control scheme, as shown in Figure 1.6. The main inverter voltage loop to control the output voltage and its output as all inverter current loop reference, to achieve the control of each parallel unit. At this time, the main inverter is the voltage source control mode and the inverter is controlled by the current source type[Brock et al., (1998), Siri et al., (1992)]. The reliability of master-slave control method is higher than the centralized control strategy and the fault of the inverter does not affect the operation of the parallel system. In the main inverter failure, you can set the rules in advance to switch from the inverter to the main inverter, to ensure the continuous operation of the parallel system [Brock et al., (1998)]. However, the process of switching from inverter to main inverter is accompanied by the change of control strategy, which increases the complexity of control. If the switch fails, the parallel system crashes [Brock et al., (1998), Pei et al.,(2004)].

The literature [Pei et al.,(2004)] proposed an automatic master-slave parallel technology. The control block diagram is shown in Figure 1.7. It has an active power bus P_{BUS} and a reactive power bus Q_{BUS}. Taking the competition mechanism, the inverter with the largest active power output is the active main module and drives the P_{BUS} and the rest is the active slave module.

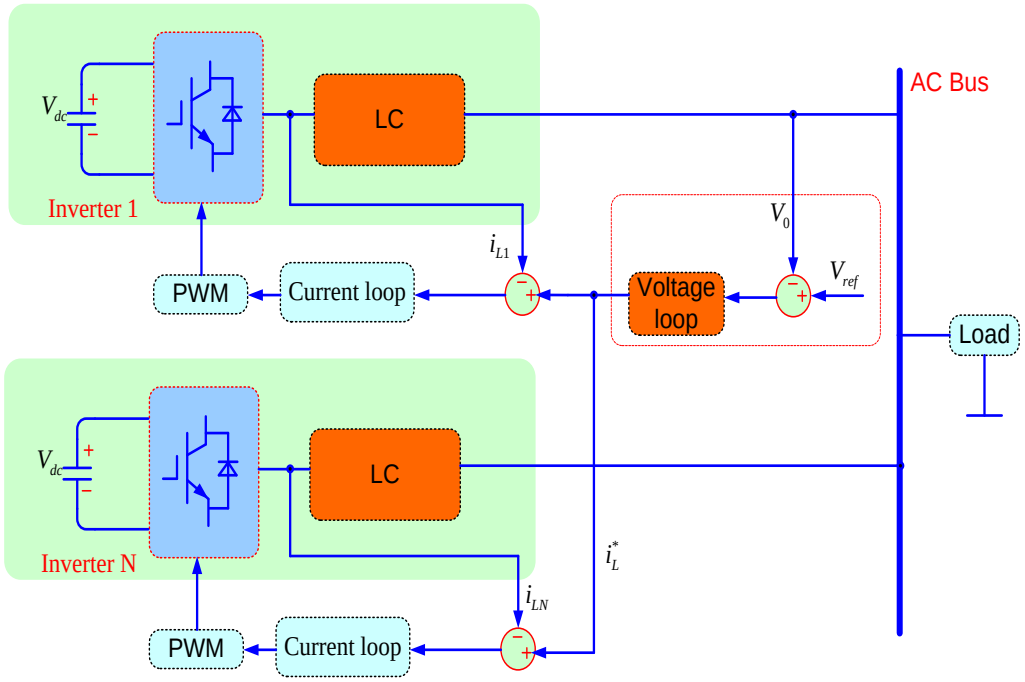

Figure 1.6: Block diagram of inverter parallel control with shared voltage outer loop.

The inverter with the largest output reactive power is the reactive main module and drives Q_{BUS} and the rest is the reactive slave module. Each parallel unit calculates the difference between its output active and reactive power and the P_{BUS} and Q_{BUS}, adjusts the phase and amplitude of the output voltage and realizes the equalization of active and reactive power. The automatic master-slave parallel technology solves the problem of the main module switching, but the introduction of the power bus reduces the system reliability and increases the system cost[Lee et al., (2004)].

In the paper [Mazumder et al., (2005)], a master-slave control scheme based on radio frequency communication technology is proposed, which cancels the interconnection signal line between modules and proposes two ways of wireless transmission of PWM signal and current sharing signal. The experimental results show that the parallel current-sharing accuracy needs to be improved. In addition, the wireless transmission delay has a greater impact on the system. In [Cheng et al., (2006)] a parallel scheme of inverter based on common mode current communication is proposed, which uses common-mode current for information interaction and no signal interconnection between modules.

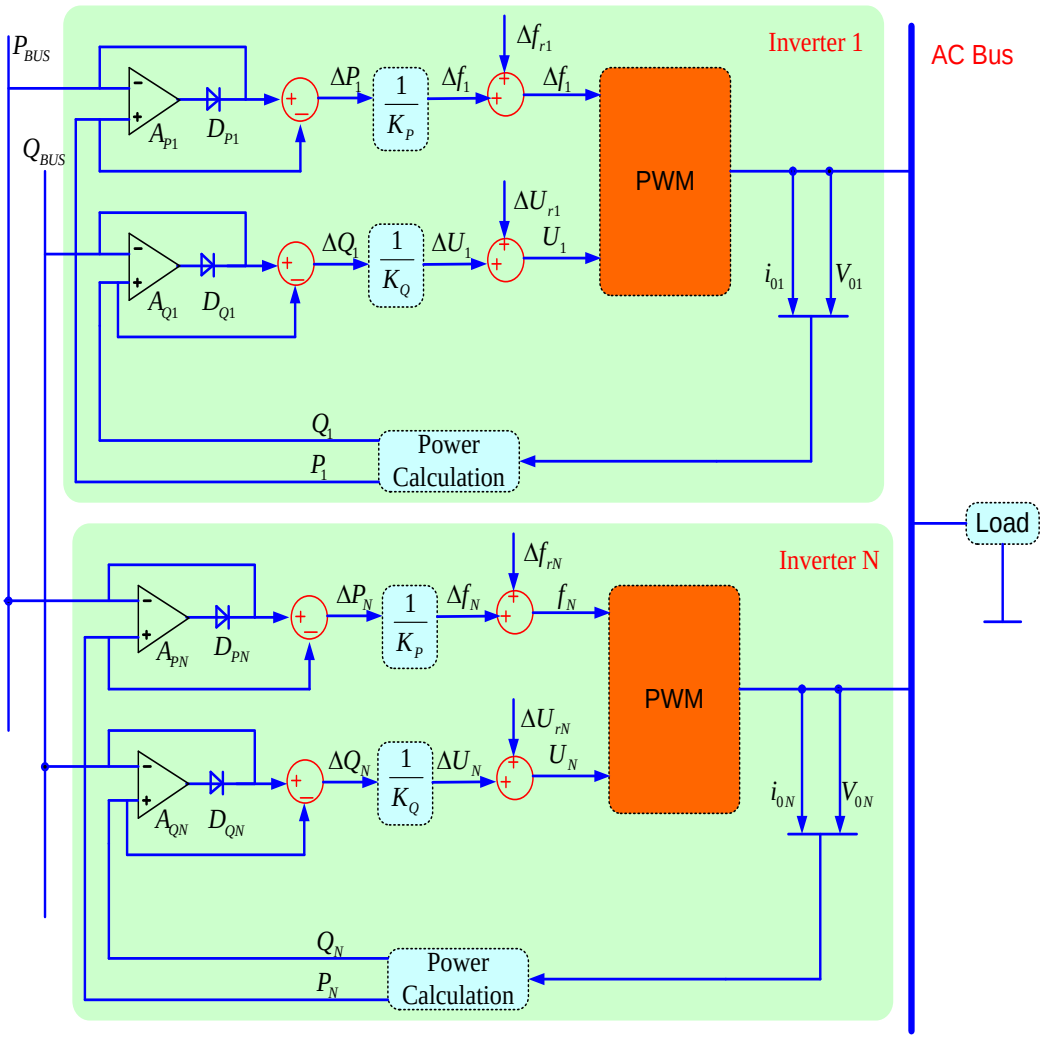

Figure 1.7: The Parallel control block diagram of automatic master-slave inverter.

3. Decentralized logic control

In order to further improve the reliability of the parallel system, the main module is eliminated, the parallel controller is dispersed in each module and the parallel units are equal in the system, which is the idea of decentralized logic control. Using decentralized logic control, each inverter equally interacts with the same information, such as voltage, current, power, frequency and phase, while maintaining the independence of its own detection and control[Qinglin et al., (2006), Xing et al.,(2002)]. The typical decentralized logic control methods are mainly the following.

a.Average load sharing control method

The average load sharing control includes an average current control scheme [Sun et al.,(2003), Shah and Sensarma et al.,(2010), Hsieh et al., (2005)] and an average

power control scheme[Sun et al., (2006), Shanxu et al., (2004)]. The two ideas are basically the same, both need a synchronous bus, the main difference is the difference of the load sharing bus. As shown in Figure 1.8, the average current scheme uses the average current bus. The average power scheme uses the average power bus, as shown in Figure 1.9. Each module tracks the reference value of the load sharing bus through a certain control strategy to achieve parallel current sharing. In [Tianzhi et al., (2008)], the load current feedforward is introduced on the basis of the average current control scheme to improve the output voltage external characteristics while ensuring the current sharing accuracy. In [Wei et al., (2016)], the virtual loop current impedance is introduced into the average current control scheme to achieve loop suppression while maintaining the external characteristics of the parallel system consistent with a single inverter. For the average current method, the average current transmitted on the communication bus is the AC signal and the average power transmission on the average power bus is direct flow, so has lower bandwidth requirements for signal transmission and better anti-interference ability[Tan et al.,(2003), Shanxu et al., (2004)].

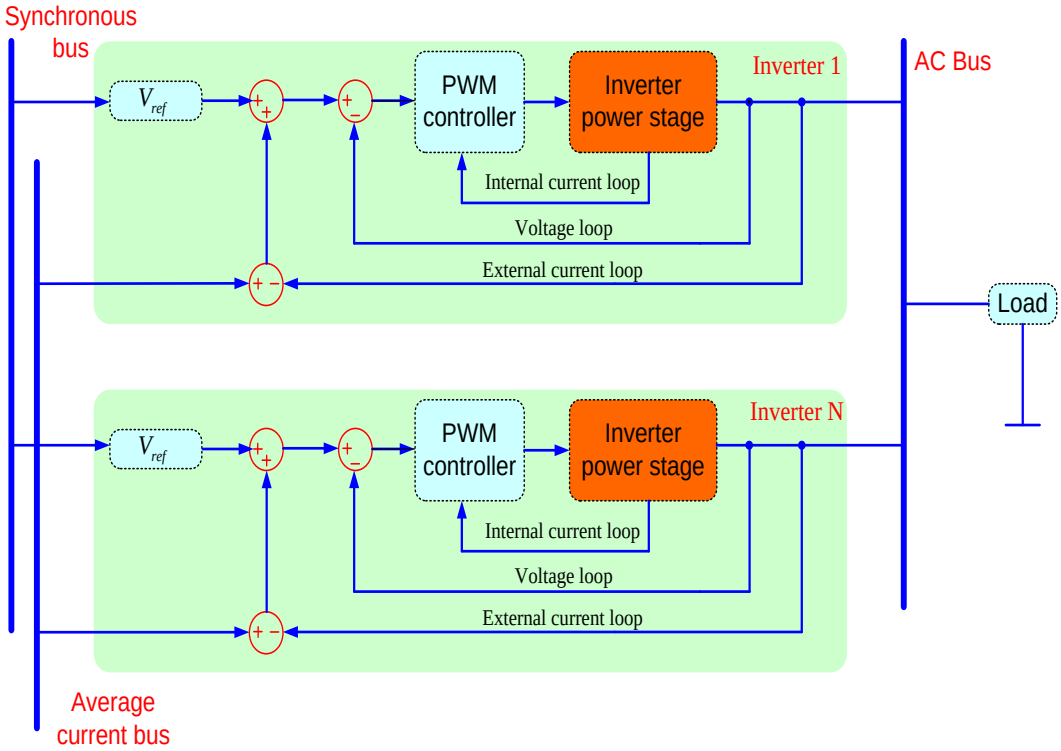

Figure 1.8: Parallel control block diagram of inverter based on average current method.

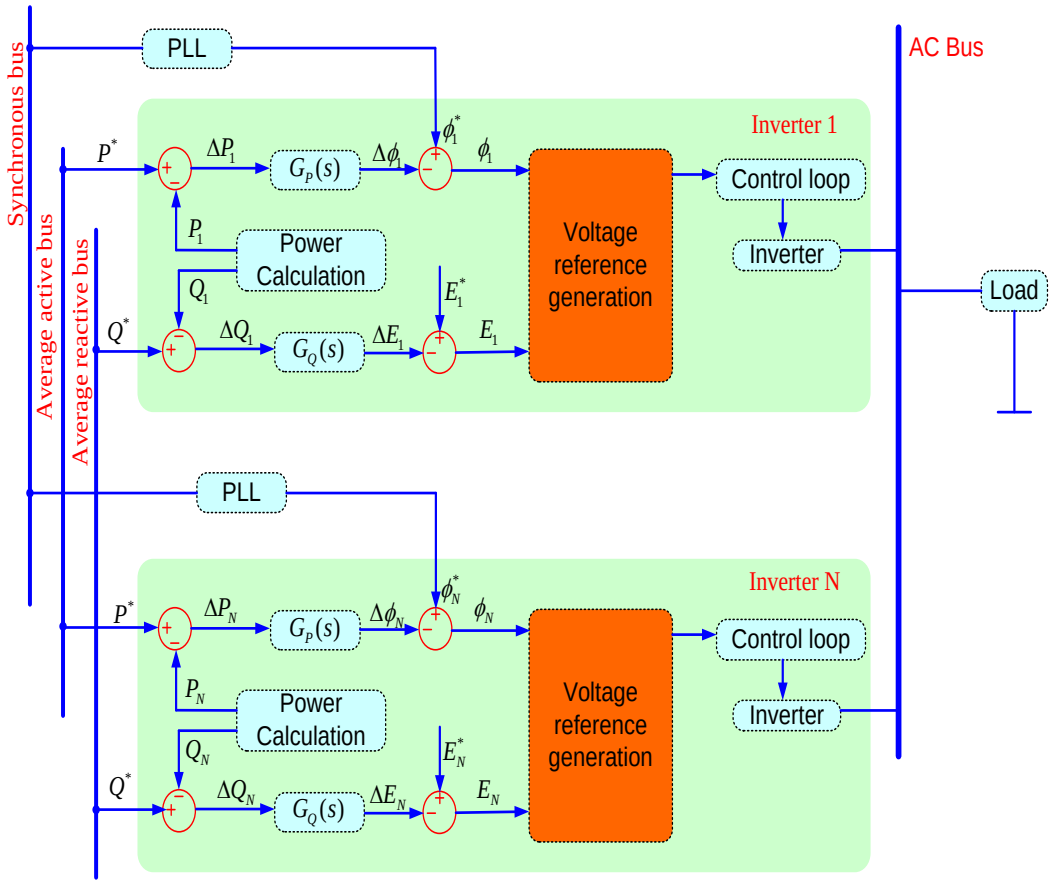

Figure 1.9: Block diagram of inverter parallel control based on average power method.

b) 3C control method:

3C (Circular Chain Control) control is also called current loop chain control, and each parallel unit is connected in a ring shape with the same status[Wu et al., (2000)]. As shown in Figure 1.10, the current signal of the previous inverter in the loop is used as the current reference of the next inverter. All parallel units in the parallel system have strong coupling, which avoids the calculation of average current or average power [Chiang et al., (2004)]. However, when the fault module exists in the parallel system, it is necessary to take some logic control to make the remaining normal module form the ring chain structure, otherwise the system will not operate normally, which increases the complexity of the control and the reliability needs to be improved[Piboonwattanakit et al., (2007)].

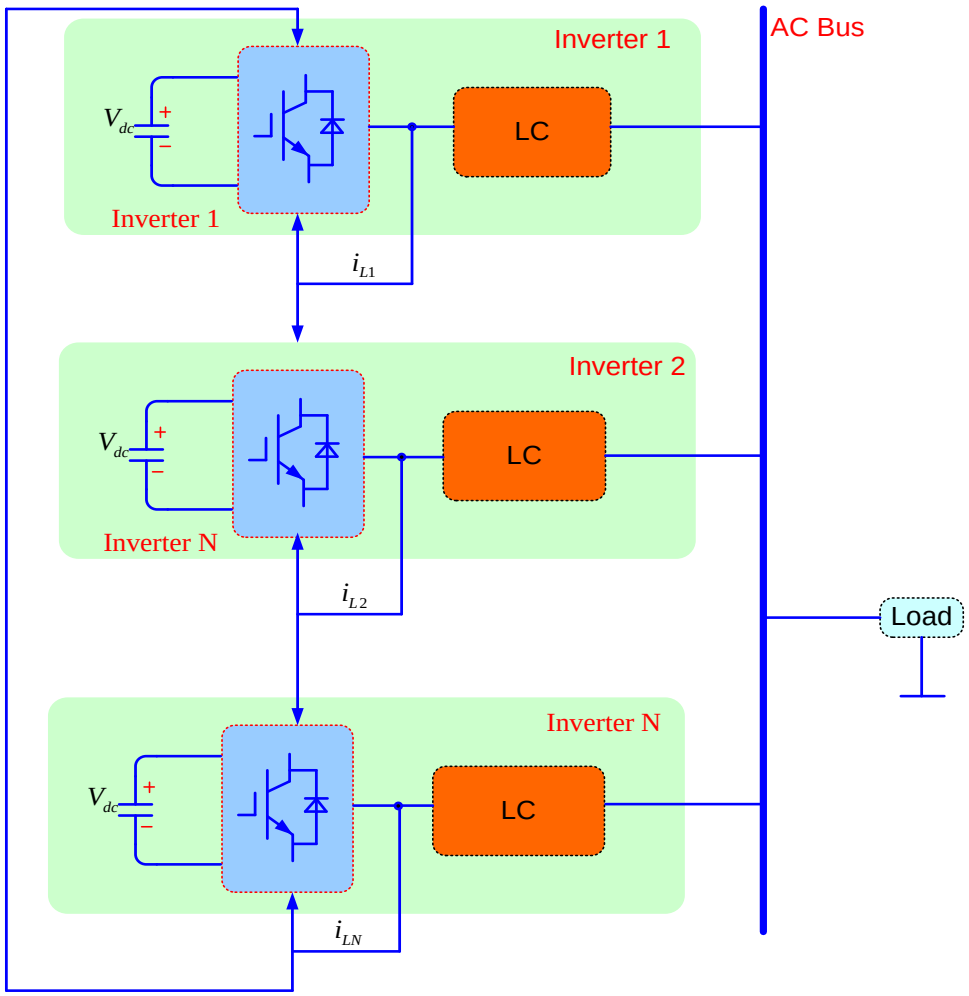

Figure 1.10: Block Diagram of Inverter Control Based on 3C Control.

c) Inverter parallel technology combined with power line carrier communication.

Power line Communication(PLC) technology uses the transmission medium of electric circuit as carrier signal, adopts serial transmission data to realize information exchange and has more application in the field of power system. In the inverter parallel system, the common interactive information has frequency, phase and power signal, so as to realize operation of the parallel unit[Zhongyi et al., (2010)]. Topologically, there is no need to add additional signal lines between the inverter modules using this method, but it is necessary to superimpose high-frequency harmonics on the power lines, which will reduce the quality of the inverter output voltage. In addition, if the parallel inverter output has an isolation transformer, it will block the power carrier signal and additional cost will be added across the transformer communication [He et al., (2008), Shanxu et al., (2003)].

1.4.2 Parallel technology of DG inverter based on droop control

In order to meet the demand of the distributed inverter, it is necessary to realize the control method of the autonomous parallel system without information interaction between the parallel modules. The characteristics of the droop control technology are in line with this demand and have been widely used in distributed inverter parallel systems[Guerrero et al., (2006)]. Droop control, also known as voltage frequency droop control or PQ droop control, the theory is based on the theory of power flow, and realizes the independent parallel of DG inverter module by imitating the characteristics of synchronous generator's self synchronization and voltage droop, adjusting output voltage amplitude and frequency (or phase) according to the output power of the DG inverter [Brabandere et al., (2007)].

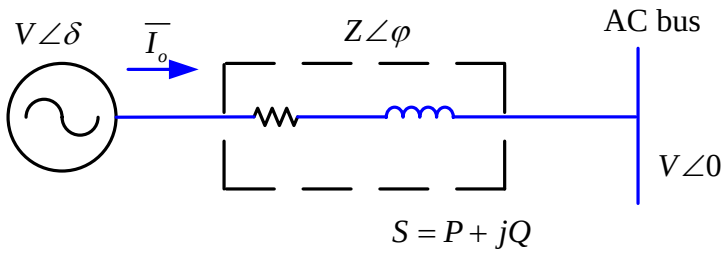

Figure 1.11: The Thevenin equivalent model of a parallel inverter unit

According to the thevenin theorem, the DG inverter can be equivalent to a controlled voltage source series equivalent impedance form, as shown in Figure 1.11. The sum of the line impedance and the equivalent output impedance of the DG inverter is considered as the total impedance is Z, the impedance angle is φ, the voltage source DG inverter and the AC bus are considered as two nodes, the power flow calculation is carried out and the relationship between the output active power and reactive power of the DG inverter and the amplitude and phase angle of the voltage source is determined by the characteristic of the total impedance. Principle of the droop control technology adjusts the power, namely adjusts the output voltage amplitude and the frequency (or the phase) of the DG inverter to adjust the output active and reactive power(Vasquez et al., (2009)].

According to the characteristics of the total impedance, there are five types of DG inverter and droop equation [Chen et al., (2016)], which are summarized in table 1.1, wherein V^* and ω^* are rated output voltage load and angular frequency, V_i and ω_i are set values, k_{PV}, k_{qV}, $k_{P\omega}$ and $k_{q\omega}$ are droop coefficients.

Table 1.1 Five types of inverter and droop control

Types	Impedance angle	Droop equation
L type	$\varphi = 90^0$	$V_i = V^* - k_{qv}Q$ $\omega_i = \omega^* - k_{p\omega}P$
R type	$\varphi = 0^0$	$V_i = V^* - k_{pv}P$ $\omega_i = \omega^* + k_{q\omega}Q$
C type	$\varphi = -90^0$	$V_i = V^* + k_{qv}Q$ $\omega_i = \omega^* + k_{p\omega}P$
RL type	$0^0 \le \varphi \le 90^0$	$V_i = V^* - k_{pv}P - k_{qv}Q$ $\omega_i = \omega^* - k_{p\omega}P + k_{q\omega}Q$
RC type	$-90^0 \le \varphi \le 0^0$	$V_i = V^* - k_{pv}P + k_{qv}Q$ $\omega_i = \omega^* + k_{p\omega}P + k_{q\omega}Q$

The application of droop control technology to multi DG inverter parallel systems has the following advantages [Ye et al., (2015), Hua et al., (2016)]:

1. Inverter module eliminates the need for signal interconnection, can reduce the cost of system control.

2. Droop control is a voltage-type control, based on the Droop control of the inverter parallel system, such as microgrid, can be operated in the grid and Off-grid mode switching without changing the control structure, you can achieve two modes of smooth switching.

3. Adjusting droop curve and combining with virtual impedance method, the distribution of active and reactive power of parallel DG inverter can be realized.

However, the traditional droop control has its inherent defects, the specific performance is [Hua et al.,(2016), Guerrero et al., (2007), Ye et al., (2015)] :

1. Existence of low pass filter in the calculation of average power, it is generally believed that the dynamic performance of the current and power distribution of multiple DG inverter parallel systems based on droop control is not accurate.

2. The frequency and voltage set points deviate from the rated value and the degree of deviation is related to the droop coefficient and the load. To a certain extent, the

larger droop coefficient can obtain higher load distribution accuracy, but correspondingly cause a greater frequency and voltage offset.

3. Compared with the traditional synchronous generator, the DG inverter has a small inertia. Under the large load disturbance, the voltage amplitude and frequency will be abrupt, which puts higher requirements on the stability control of the system.

4. The total impedance of each parallel DG unit needs to meet certain matching conditions, otherwise the power regulated by voltage will not be allocated accurately according to the predetermined target. Parallel systems with mesh-like structures, the addition and exit of parallel inverters and loads can cause impedance and network structure changes between nodes and the situation is more complicated.

5. Relies on its self synchronization characteristic to realize independent parallel connection needs certain impedance support.

In order to solve the above problems of droop control, that is, minimizing the circulating circulation of the inverter, distributing the active and reactive power and harmonic power accurately, improving the output voltage quality and system stability, scholars all over the world put forward various improved droop control.

The DG inverter equivalent model in Figure 1.11 is used as the basis of analyzing power flow in parallel system. The existing improved droop control can be roughly classified into two categories: Based on the improved Droop equation, the amplitude and phase of the equivalent voltage source are adjusted, including the shift of the droop curve and the change of slope and the deformation of the droop equation. The virtual impedance based method corresponds to adjusting the equivalent output impedance of the inverter.

1.Control scheme based on improved droop equation

a) Introduce power differential and integral terms.

Because of the low bandwidth of low-pass filter in the power calculation and the limited ability of the power loop pole to be configured by droop coefficient, the dynamic performance of the system is restricted, so that the average power flow of the parallel system is slow. By introducing a derivative term or an integral term in the drooping equation, the degree of freedom of the power loop pole configuration is increased[Xin et al., (2017), Guerrero et al., (2007)].

$$\begin{aligned}\phi &= -m\int_{-\infty}^{t} P d\tau - m_p P - m_d \frac{dP}{dt} \\ E &= E^* - nQ - n_d \frac{dQ}{dt}\end{aligned} \tag{1.4.2.1}$$

As shown in the equation (1.4.2.1), the literature [Guerrero et al., (2004)] uses the phase droop to replace the frequency droop and adds the differential and integral of the power, the additional parameter m_P, m_d and n_d are helpful to adjust the position of the system characteristic root in s left half plane, and to some extent can improve the dynamic performance of the DG inverter system. The method of introducing power differential and integral term is mainly used in the current sharing control of the parallel system of the inverter with small feeder impedance, that is, each inverter is equally responsible for the load power[Mohamed et al., (2008)].

b) Droop coefficient adjustment method.

The common droop coefficient adjustment method is to set the droop coefficient as active and reactive functions, have a linear function [Meiqin et al., (2015), Jun et al., (2015), Wei et al., (2009)] and two times function [Rokrok et al., (2010)] and other adjustment methods, dynamically adjust the slope of the droop curve, reduce the steady state error. In [Yongwei et al., (2013)], the island frequency non-stationary difference, the island voltage amplitude offset reduction and the grid-connected constant power output are realized by adaptively adjusting the droop coefficient.

If the power reference can be obtained by communication system, the droop coefficient can be adaptively adjusted by simple integration or PI operation of the power difference [Mahmood et al., (2015), Xiaofeng et al., (2014)]. Equation (1.4.2.2), because of the function of integral link, the reactive power Q will be equal to its reference value Q^* and the exact distribution is realized.

$$\begin{aligned}V_i &= V_o - (n_i + \tilde{n_i})Q_i \\ \tilde{n_i} &= \frac{1}{s}(Q_i - Q_i^*)\end{aligned} \tag{1.4.2.2}$$

c) Common variable method.

The power of frequency droop control can be precisely distributed in steady state, because the frequency is a global quantity in steady state. The voltage is a local amount in the parallel system, so that the power distribution of the voltage control is

affected by the impedance. Therefore, the literature [Sao and lehn (2005), Qingchang (2013)] proposes a droop control method based on a common variable, which uses a common load voltage to give the voltage controlled power a "global quantity" for eliminating its distribution error. The basic principle of the equation (1.4.2.3), the steady state of the reference voltage V_{ref} will be the same (are equal to the public load voltage V_{com}), and the rated voltage V^* as a public quantity, so the output of reactive power of each inverter will be in accordance with its droop coefficient of the inverse distribution.

$$\begin{aligned} V_{ref} &= V^* - D_Q Q_i \\ E_i &= K_q \int (V_{ref} - V_{com}) dt \end{aligned} \tag{1.4.2.3}$$

The paper [Qian et al., (2015), Guo et al., (2016)] is based on the common variable method and realizes the function of AC bus voltage recovery on the basis of eliminating the error of reactive power distribution.

As shown in the formula (1.4.2.4), through the central controller, sampling AC bus voltage, the error PI calculation, its output as the reference of each inverter $n_{qi}Q_i$, the difference is added to the V-Q droop equation. At steady state, the AC bus voltage will return to the reference value V_{com}^* and each inverter $n_{qi}Q_i$ will be equal.

$$\begin{aligned} V_i &= V_o - n_{qi}Q_i + K_E \int (V_{cmp} - n_{qi}Q_i) dt \\ V_{cmp} &= K_{pv}(V_{com}^* - V_{com}) + K_{iv} \int (V_{com}^* - V_{com}) dt \end{aligned} \tag{1.4.2.4}$$

The droop control based on the common variable method can realize the accurate distribution of power and is not affected by the difference of system parameters and has strong robustness. However, in a parallel system such as a multi bus line microgrid system, the common point for determining the common voltage amount is no longer unique and the application is limited to a single AC bus system.

d) Synchronous compensation method

In order to improve the equalization accuracy of reactive power, the paper [He and Li et al., (2012)] records the active power P_{ave} of steady state as active reference value, by injecting a small reactive power perturbation to the frequency droop equation, which causes the change of active power, then adds the active error through

an integrator to the voltage droop equation and puts forward the Droop equation is (1.4.2.5).

This process is triggered by the synchronization signal to ensure that each parallel unit starts the compensation process at the same time. Steady-State integrator input zero, each machine output active power equal to P_{ave}, at the same time frequency droop equation to ensure that each inverter $(D_P .P+D_Q .Q)$, so the theory of both active and reactive power can be accurately distributed. However, if the load changes during the compensation process, the integrator may appear saturation output, not only the error of reactive power equalization cannot be eliminated, but also the error of the sharing of the active power.

$$\begin{aligned} &\omega = \omega_o - (D_p P + D_Q Q) \\ &V = V_o - D_Q Q + \frac{K_C}{s}(P - P_{AVE}) \end{aligned} \tag{1.4.2.5}$$

In the paper [Han et al., (2015)], a new synchronous compensation mechanism is proposed, which includes reactive power compensation and voltage recovery operation, which is triggered by a low bandwidth synchronous pulse signal and the control equation is (1.4.2.6). In each synchronization interval, the voltage droop equation is again subtracted from the computed K_eQ_i in the synchronization interval and the different reactive outputs lead to the shift of the voltage droop curve to varying degrees, which can reduce the reactive power deviation. However, this operation will cause the output voltage to continue to drop, when lowering to the lower threshold, the G from 0 to 1, starting the voltage recovery mechanism. This method is simple to implement, but reactive power compensation and voltage recovery operations will always deviate. If the synchronous pulse is lost, there will be disturbances in the regulation of reactive power.

$$\begin{aligned} &\omega_i = \omega^* - m_p P_i \\ &V_i^k = V^* - n_q Q_i^{k-1} - \sum_{n=1}^{k-1} K_e Q_i^n + \sum_{n=1}^{k-1} G_n \Delta V_o \end{aligned} \tag{1.4.2.6}$$

E) V-I Droop method

In the dq coordinate system, the active power and reactive power can be calculated as follows [Das and chattopadhyay (2015)]:

$$\begin{aligned} P &= V_d I_d \\ Q &= -V_d I_q \end{aligned} \tag{1.4.2.7}$$

Since the output voltage of the inverter is less than V_d, the active current I_d and reactive current I_q play a major role in the power regulation. Therefore, using active and reactive currents instead of active and reactive power to control the amplitude and frequency of output voltage, the output control is realized. The equation (1.4.2.8) is the V-I droop equation [Zhang (2015)] .

$$\begin{aligned} \omega_i &= \omega^* - m(I_{di} - I_{di}^*) \\ E_i &= E^* + n(I_{qi} - I_{qi}^*) \end{aligned} \tag{1.4.2.8}$$

The paper [Golsorkhi and Lu (2015), Yajuan et al., (2016)] uses dq axial current to droop the voltage and considers the influence of feeder impedance. By introducing the GPS (Global positioning System) signal to the parallel inverter, the inverter is controlled by constant frequency, so the frequency droop link is omitted.

Compared with the PQ droop method, the bandwidth of low-pass filter which is used to calculate the dq axis is higher than that of the V-I droop, which is advantageous to the improvement of dynamic performance. But it still can't solve the problem of power allocation error caused by impedance mismatch.

f) Virtual coordinate transformation method.

When the impedance of the system is complex impedance characteristic, the power and reactive power of the inverter are correlated with the amplitude and phase of the output voltage of the inverter, which not only increases the complexity of the control, but also prolongs the transient process and reduces the stability of the system when the L-type or R-type sag is used. In order to decouple the active and reactive power, reference [Brabandere et al., (2009), Vasquez et al., (2009)] transforms the active and reactive power according to the impedance angle φ as the virtual coordinate transformation, as shown in the equation (1.4.2.9). The virtual power deflection $P^{'}$ and $Q^{'}$ are correlated with the frequency and voltage amplitude respectively and can be controlled according to the L-type droop equation.

$$\begin{bmatrix} P^{'} \\ Q^{'} \end{bmatrix} = T \begin{bmatrix} P \\ Q \end{bmatrix} = \begin{bmatrix} \sin\varphi & -\cos\varphi \\ \cos\varphi & \sin\varphi \end{bmatrix} \begin{bmatrix} P \\ Q \end{bmatrix} \tag{1.4.2.9}$$

Similarly, virtual coordinate transformation can be performed on active current and reactive current [Brabandere et al., (2009)], as in equation (1.4.2.10).

$$\begin{bmatrix} I_a^{'} \\ I_r^{'} \end{bmatrix} = T \begin{bmatrix} I_a \\ I_r \end{bmatrix} = \begin{bmatrix} \sin\varphi & -\cos\varphi \\ \cos\varphi & \sin\varphi \end{bmatrix} \begin{bmatrix} I_a \\ I_r \end{bmatrix} \tag{1.4.2.10}$$

Similarly, in reference [Li et al., (2009), Wu et al., (2016)], a virtual frequency voltage conversion control, such as the formula (1.4.2.11), is proposed to transform the voltage amplitude and frequency into virtual coordinates. Then, the virtual frequency ω' and the virtual amplitude V' are droop controlled by the active power and the reactive power, respectively.

$$\begin{bmatrix} \omega^{'} \\ V^{'} \end{bmatrix} = T_{\omega E} \begin{bmatrix} \omega \\ V \end{bmatrix} = \begin{bmatrix} \sin\varphi & \cos\varphi \\ -\cos\varphi & \sin\varphi \end{bmatrix} \begin{bmatrix} \omega \\ V \end{bmatrix} \tag{1.4.2.11}$$

It should be pointed out that the virtual power and the virtual current transformation method can be deduced by the addition and subtraction of the power calculation expression, when the impedance is close to pure inductive or pure resistance, it is easy to see the droop equation degenerate to the L-type droop or the R-type droop equation. The method of virtual frequency voltage conversion can be derived by adding and subtracting the RL type droop equation. Therefore, the essence of both methods is the RL type drooping. The introduction of virtual coordinate transformation method only realizes the decoupling control of active and reactive power in the form of control equation, and still cannot eliminate the cross coupling between active and reactive power under complex impedance. When the impedance is not matched, the power distribution error cannot be eliminated. In addition, the virtual coordinate transformation method needs the impedance angle of the known system, which reduces the practicability of the method.

g) Q-$\dot{V}$ drooping method

Traditional Q-V droop has a reactive power distribution error when the system impedance is mismatched. This paper[Lee et al., (2013)] puts forward the $Q-\dot{V}$ as droop method and uses reactive power Q to droop the voltage change rate $\dot{V}$, which can mitigate the effect of system impedance mismatch and improve the distribution accuracy of reactive power. The $Q-\dot{V}$ droop control equation is:

$$\begin{aligned} \dot{V}_i &= \dot{V}_o - n_i(Q_{oi} - Q_i) \\ V_i^* &= V_o + \int_t \dot{V}_i d\tau \end{aligned} \tag{1.4.2.12}$$

Where n_i is the droop coefficient, Q_{oi} is the set value of the rated reactive power, $\dot{V}_i$ is the rate of change of the voltage amplitude versus time, $\dot{V}_o$ is the rated value of $\dot{V}_i$, set to zero and V_o is the rated voltage amplitude. The inverter output voltage reference value $\dot{V}_i$ is adjusted by integrating the time with respect to V_i^*.

The $Q-\dot{V}$ droop control adjusts the reference voltage slowly due to its integral to $\dot{V}$, so a large droop slope can keep the system stable when the reactive load changes. The traditional *Q-V* droop voltage reference quickly responds to reactive load changes, which can easily cause system instability under large droop coefficients. Therefore, the $Q-\dot{V}$ droop can reduce the reactive power distribution error by using a large voltage droop slope, but in the case of system impedance mismatch, the reactive power distribution error cannot be eliminated. In addition, $Q-\dot{V}$ droop adjustment will cause $\dot{V}$ to deviate from the nominal zero value and $\dot{V}$ must be reset to zero value in steady state.

The reset mechanism proposed in [Lee et al., (2013)] is:

$$\frac{d}{dt}Q_{oi} = K_{res}Q_{Ri}(\dot{V}_o - \dot{V}_i) \tag{1.4.2.13}$$

The reset mechanism in the paper [Guo (2016)] indicates that the additional reactive power allocation error is introduced in the equation (1.4.2.13). An improved $\dot{V}$ reset mechanism based on the change rate of voltage-weighted average value of the inverter is designed, such as the equation (1.4.2.14), so that each inverter still has the same $Q-\dot{V}$ droop curve after the reset.

$$\frac{d}{dt}(n_{qi}Q_{oi}) = -k_R(\dot{\overline{V}} - \dot{V}_o) \tag{1.4.2.14}$$

h) Arctan drooping method.

The paper [Rowe et al., (2013)] presents a frequency droop form of arctan calculation, as shown in the formula (1.4.2.15), $P^{'}$ and $P_o^{'}$ respectively as active power and its reference value. Since the output value of the arctan is within the range $\pm\frac{\pi}{2}$, the droop is naturally limited by frequency boundary ($f_o-\frac{a_p}{2}<f<f_o+\frac{a_p}{2}$). The droop slope can be conveniently adjusted by the parameter ρ. The arctan drooping method has a drooping depth near the power reference that is greater than the proportional drooping depth of the conventional droop control, so the power sharing can be improved to some extent.

$$f=f_o-\frac{\alpha_p}{\pi}(\arctan(\rho(P^{'}-P_o^{'}))) \tag{1.4.2.15}$$

In summary, it can be seen that most of the current literature based on droop control focuses on the steady-state performance of power distribution, but less on dynamic performance and also does not consider output and line impedance.

Therefore, based on the droop control, under the condition of accurate distribution of power of the parallel DG system, further research is needed to realize the problem of power distribution.

1.5 MOTIVATION

Nowadays, the scale of power grids continues to increase as the demand for electricity continues to increase. Countries around the world are gradually becoming aware of the depletion of fossil fuels, renewable energy and distributed electricity generation will be the mainstream direction of future energies and the development of the global power grid will be the focus of the long-term power grid development strategy. At present, the issue of the large-scale access of new energy distributed generation to the power grid, micro-grid as the mainstream method to solve its problems, will become an extremely important part of the development of smart grid in the future. Therefore, the research on the operation control method of microgrid containing multiple distributed power sources has been put on the agenda, which has extremely important theoretical and practical significance. The research of microgrid technology can promote the coordinated development of the power industry, society,

environment, flexibility and efficiency also have important significance for the development of the power grid itself.

This thesis studies the theory and strategy of operation control of microgrid with distributed power supply, meets the needs of the power system and the user's operation and control of microgrid and has important theoretical significance and engineering application value.

1.6 AUTHORS CONTRIBUTIONS IN THE THESIS

The direct droop control and reverse droop control is studied and the line impedance influences the control strategy of distributed generation inverter in a large extent. The direct droop control has a good performance when the line impedance is mainly inductive, while reverse droop control is more suitable when the line impedance is mainly resistive. Finally, on the basis of the theoretical analysis, the control performance of direct and reverse droop control were compared and simulated.

A simulation comparison of direct droop control and improved power allocation strategy verifies the correctness and effectiveness of the adopted improvement control strategy.Impact of the transmission impedance of a distributed generation inverter power supply to a common load on power distribution is studied. The characteristics of line impedance uncertainty and the use of direct droop control have certain limitations. Analyze the conditions that need to be met to accurately share the load according to the ratio of rated capacity of DG inverter.The virtual inductance is introduced and the impedance is designed to be inductive, then the direct droop control strategy is used to distribute the load in the microgrid system. Improved droop control based on virtual inductance eliminates the effect of line impedance on power distribution and achieves accurate distribution of load power in proportion to rated capacity.

A simulation comparison of reverse droop control and improved power allocation strategy verifies the correctness and effectiveness of the adopted improvement control strategy.In low-voltage microgrid systems with multiple distributed generation inverters of rated capacity, the performance of load power distribution according to the proportion of DG capacity is very important for the stable and efficient operation of the microgrid system. The reverse droop control strategy has the problem of power distribution error due to the impedance imbalance of the microgrid line. The

application of virtual resistance can suppress this error. The virtual resistance is introduced and the impedance is designed to be resistive, then the reverse droop control strategy is used to distribute the load in the microgrid system. Therefore, reverse droop control method that introduces virtual resistance is adopted to ensure stable control of voltage and frequency while realizing power proportional distribution.

Simulation results are presented to show the feasibility of the distributed secondary control under different conditions.Distributed secondary control in droop controlled microgrid is presented considering the problems of line and output impedance differences and the distributed generation inverters power allocation. Compared with the conventional approach based on restoring the frequency and amplitude deviations produced by the local direct droop controllers by using an MG central controller, an improved approach is used in order to implement a distributed secondary control. The output voltage amplitude, frequency and the reactive power of each DG inverter are restored by PI controller. The proposed approach is not only able to restore frequency and voltage of the microgrid but also ensures reactive power sharing.

Simulation results are presented to show the feasibility of the distributed secondary control under different conditions.In order to solve the problem of voltage amplitude, frequency accuracy and the active power cannot be reasonably distributed in microgrid by using reverse droop control, proposes an improved scheme for the reverse droop control of the microgrid, which can realize secondary regulation. Compared with the reverse droop control method, the improved reverse droop control method adopts the distributed secondary control. Each DG inverter adjusts the inverter output voltage amplitude, frequency and active power by the PI regulator. This method not only can realize the DG inverter output voltage amplitude and frequency recovery, but also to ensure the rational allocation of active power.

1.7 ORGANISATION OF THE THESIS

Chapter 1: Introduces the development of new energy and the current problems of distributed generation, then introduces the concept and structure of microgrid. Discusses the significance of microgrid for distributed generation to large power grid

and then brings out the main problems and common control strategies in the current research of microgrid. Then, the advantages of droop control in the current control method of microgrid are analyzed.

Chapter 2: The system structure of the three-phase distributed generation inverter in the microgrid and the selection of DG inverter output filter and the parameter calculation are introduced. The mathematical model of the three-phase DG inverter was established in different coordinate systems. Then based on the established mathematical model, the design method of the double closed-loop control of the output voltage of the DG inverter is given, which lays a foundation for the droop control.

Chapter 3: The parallel distributed generation inverters power transmission characteristics and the droop control theory are analyzed. The reason why the actual active power and reactive power cannot achieve equalization when the traditional droop control is used analyzed. Aiming at this problem, this chapter achieves the goal of power sharing and power decoupling by adding virtual inductance control loop. The traditional droop control and the improved power allocation strategy are simulated and compared, the correctness and validity of the adopted improved strategy are validated.

Chapter 4: The basic principle of reverse droop control and power transmission characteristics of the low voltage microgrid are analyzed, the relationship between DG inverter output impedance, line impedance and DG inverter control method is demonstrated. The reverse droop control is improved by virtual resistance method, so that the reverse droop control can be used in low-voltage microgrid and this realizes the decoupling control of active power and reactive power. The influence of the virtual resistance control loop on the output characteristics of the system is analyzed by frequency domain method and the validity of the reverse droop control method based on virtual resistance is verified by simulation analysis of microgrid operation.

Chapter 5: This chapter presents a new type of distributed secondary control method for microgrid. In order to solve the problem of unreasonable power distribution and deviation of output voltage and frequency in the inverter parallel system based on direct and reverse droop control, a parallel DG inverter control strategy based on virtual impedance for voltage, frequency, active and reactive power

adjustment in isolated micro-grid is proposed. The voltage, frequency is adjusted two times so that the voltage and frequency can be maintained at the rated value when the load changes frequently. Simulation results verify the effectiveness of the proposed control strategy.

Chapter 6: The overall conclusions of the thesis and scope for future work are given.

Chapter 2

2 MODELING ANALYSIS OF THREE-PHASE FULL-BRIDGE DISTRIBUTED GENERATION INVERTER

2.1 THREE-PHASE VOLTAGE SOURCE DISTRIBUTED GENERATION INVERTER MATHEMATICAL MODEL

The three-phase voltage source inverter uses a three-phase full-bridge topology [Zhongyi (2008)]. The detailed structure is shown in Figure 2.1. The middle of the three bridge arms of the inverter is connected to the LC filter. The three-phase output voltage is the terminal voltage on the filter capacitor [Wu et al., (2007)].

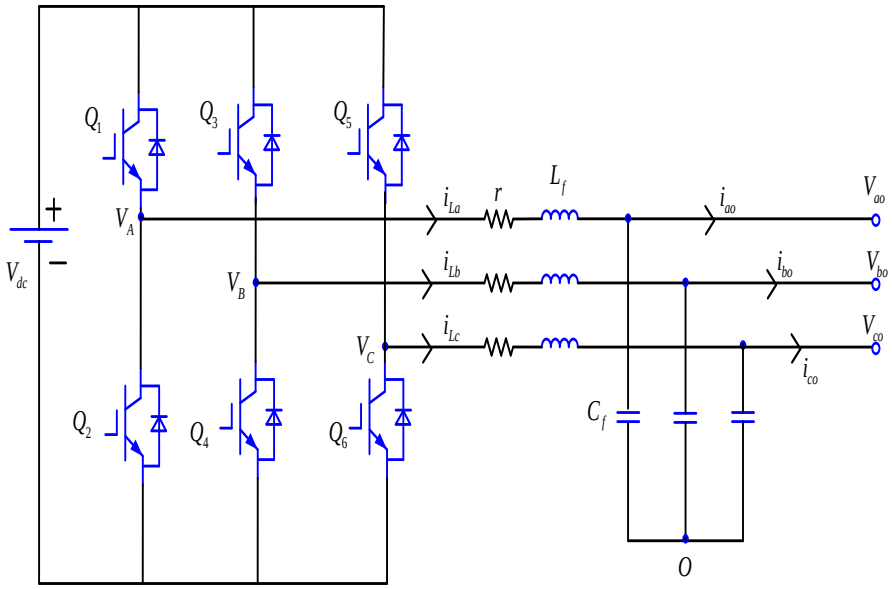

Figure 2.1: Three phase voltage source DG inverter topology

In the figure, V_{dc} is the DC input voltage, L_f is the filter inductor, r is the filter inductor equivalent resistance and C_f is the filter capacitor. A, B, and C three-phase inverter bridge arms from left to right. The midpoint voltage of the inverter arm *is* V_A, V_B, V_C.The three-phase filter capacitor at the output is star-connected and O is the midpoint of the filter capacitor. The output voltage of the inverter is the capacitor voltage V_{ao}, V_{bo} , V_{co}. The three-phase inductor currents are i_{La}, i_{Lb}, i_{Lc} .The three-phase output current of the load side of the inverter is i_{ao}, i_{bo}, i_{co}. The establishment of a mathematical model of a three-phase full-bridge voltage source inverter is the basis for its theoretical analysis and is a prerequisite for the design of reasonable control parameters.

2.2 MATHEMATICAL MODEL IN THREE-PHASE STATIONARY COORDINATE SYSTEM

Select the three-phase filter inductor current and the three-phase filter capacitor voltage as the state variables and write the state equations for the filter inductor and the filter capacitor, respectively, according to the Kirchhoff voltage and current law [Yajuan (2012)]:

$$\begin{aligned} &V_A - v_{ao} = L_f \frac{di_{La}}{dt} + ri_{La}, V_B - v_{bo} = L_f \frac{di_{Lb}}{dt} + ri_{Lb} \\ &V_C - v_{co} = L_f \frac{di_{Lc}}{dt} + ri_{Lc} \\ &i_{La} - i_{ao} = C_f \frac{dv_{ao}}{dt}, i_{La} - i_{bo} = C_f \frac{dv_{bo}}{dt} \\ &i_{Lc} - i_{co} = C_f \frac{dv_{co}}{dt} \end{aligned} \tag{2.2.1}$$

The state equation of the three-phase voltage source inverter in the three-phase stationary coordinate system of abc is as follows:

$$\frac{d}{dt}\begin{bmatrix} i_{La} \\ i_{Lb} \\ i_{Lc} \\ v_{ao} \\ v_{bo} \\ v_{co} \end{bmatrix} = \begin{bmatrix} -\frac{r}{L_f} & 0 & 0 & -\frac{1}{L_f} & 0 & 0 \\ 0 & -\frac{r}{L_f} & 0 & 0 & -\frac{1}{L_f} & 0 \\ 0 & 0 & -\frac{r}{L_f} & 0 & 0 & -\frac{1}{L_f} \\ \frac{1}{C_f} & 0 & 0 & 0 & 0 & 0 \\ 0 & \frac{1}{C_f} & 0 & 0 & 0 & 0 \\ 0 & 0 & \frac{1}{C_f} & 0 & 0 & 0 \end{bmatrix} \begin{bmatrix} i_{La} \\ i_{Lb} \\ i_{Lc} \\ v_{ao} \\ v_{bo} \\ v_{co} \end{bmatrix} + \begin{bmatrix} 0 & 0 & 0 & \frac{1}{L_f} & 0 & 0 \\ 0 & 0 & 0 & 0 & \frac{1}{L_f} & 0 \\ 0 & 0 & 0 & 0 & 0 & \frac{1}{L_f} \\ -\frac{1}{C_f} & 0 & 0 & 0 & 0 & 0 \\ 0 & -\frac{1}{C_f} & 0 & 0 & 0 & 0 \\ 0 & 0 & -\frac{1}{C_f} & 0 & 0 & 0 \end{bmatrix} \begin{bmatrix} i_{ao} \\ i_{bo} \\ i_{co} \\ V_A \\ V_B \\ V_C \end{bmatrix} \tag{2.2.2}$$

Equation (2.2.2) is the mathematical model of three-phase voltage source inverter in abc three-phase static coordinate system.

2.2.1 Mathematical model in two-phase stationary frame

In the three-phase stationary coordinate system of abc, three variables need to be analyzed respectively. In a three-phase symmetric system, only two of the three variables are totally independent. In order to reduce the number of variables and simplify the analysis, the Clark transformation originally applied to motor control is often introduced into the analysis of three-phase inverters. The Clark transform transforms the three variables in the three-phase stationary coordinate system of abc to the two variables in the $\alpha\beta$ two-phase stationary coordinate system as shown in Figure 2.2. [Shang (2013)].

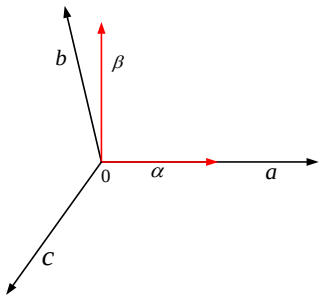

Figure 2.2: abc two phase stationary co-ordinate system $\alpha\beta$ two phase stationary co-ordinate system

In the Figure 2.2, the α axis of the $\alpha\beta$ two-phase stationary coordinate system coincides with the α phase coordinate of the abc three-phase stationary coordinate system, according to the principle of equal amplitude transformation, the transformation matrix is:

$$T_{abc-\alpha\beta} = \frac{2}{3}\begin{bmatrix} 1 & -\frac{1}{2} & -\frac{1}{2} \\ 0 & \frac{\sqrt{3}}{2} & -\frac{\sqrt{3}}{2} \end{bmatrix} \tag{2.2.3}$$

The transformation from the $\alpha\beta$ two-phase stationary coordinate system to the abc three-phase stationary coordinate system is called the Clark inverse transform. The transformation matrix is:

$$T_{\alpha\beta-abc}=\begin{bmatrix} 1 & 0 \\ -\frac{1}{2} & \frac{\sqrt{3}}{2} \\ -\frac{1}{2} & -\frac{\sqrt{3}}{2} \end{bmatrix} \tag{2.2.4}$$

After multiplying the left and right sides of the equation (2.2.2) by the Clark transformation matrix, the state equation of the three-phase voltage source inverter in the αβ two-phase stationary coordinate system can be obtained by sorting:

$$\frac{d}{dt}\begin{bmatrix} i_{L\alpha} \\ i_{L\beta} \\ v_{o\alpha} \\ v_{o\beta} \end{bmatrix}=\begin{bmatrix} -\frac{r}{L_f} & 0 & -\frac{1}{L_f} & 0 \\ 0 & -\frac{r}{L_f} & 0 & -\frac{1}{L_f} \\ \frac{1}{C_f} & 0 & 0 & 0 \\ 0 & \frac{1}{C_f} & 0 & 0 \end{bmatrix}\begin{bmatrix} i_{L\alpha} \\ i_{L\beta} \\ v_{o\alpha} \\ v_{o\beta} \end{bmatrix}+\begin{bmatrix} 0 & 0 & \frac{1}{L_f} & 0 \\ 0 & 0 & 0 & \frac{1}{L_f} \\ -\frac{1}{C_f} & 0 & 0 & 0 \\ 0 & -\frac{1}{C_f} & 0 & 0 \end{bmatrix}\begin{bmatrix} i_{o\alpha} \\ i_{o\beta} \\ v_{\alpha} \\ v_{\beta} \end{bmatrix} \tag{2.2.5}$$

Equation (2.2.5) is the mathematical model of three-phase voltage source inverter in $\alpha\beta$ two-phase stationary coordinate system[Yajuan (2012), Chen (2014)].

2.3 MATHEMATICAL MODEL OF dq TWO-PHASE ROTATING COORDINATES

Equation (2.2.5), we can see that after the Clark transformation, the three variables in the three-phase stationary coordinate system become the two variables in the two-phase stationary coordinate system, the number of variables is reduced, but the transformed control variable is still the AC quantity.

According to the principle of automatic control, when using the traditional PI control, the control of AC volume is always static, in order to achieve the control effect of static error, the AC amount in the $\alpha\beta$ two-phase stationary coordinate system must be transformed into the direct flow under the dq two-phase rotating coordinate system through the park transformation, as shown in Figure 2.3.

The dq two-phase rotating coordinate system rotates counterclockwise at an angular velocity ω with respect to the $\alpha\beta$ two-phase stationary coordinate system,

where ω is the angular frequency of the AC in the stationary coordinate system and θ is the angular difference between the d-axis and the α -axis[Zhang (2013].

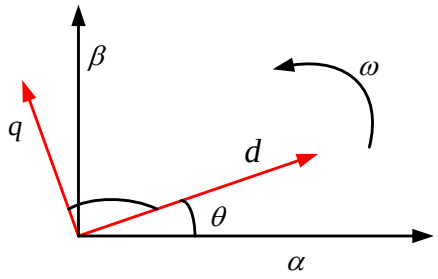

Figure 2.3: αβ two phase stationary co-ordinate system and the dq two-phase rotating co-ordinate system diagram

According to the principle of constant-amplitude transformation, the Park transformation matrix from $\alpha\beta$ two-phase stationary coordinate system to dq two-phase rotating coordinate system is:

$$T_{\alpha\beta-dq}=\begin{bmatrix}\cos(\omega t) & \sin(\omega t)\\ -\sin(\omega t) & \cos(\omega t)\end{bmatrix} \tag{2.3.1}$$

Similarly, the transformation from dq two-phase rotating coordinate system to $\alpha\beta$ two-phase stationary coordinate system is called Park inverse transformation. The transformation matrix is:

$$T_{dq-\alpha\beta}=\begin{bmatrix}\cos(\omega t) & -\sin(\omega t)\\ \sin(\omega t) & \cos(\omega t)\end{bmatrix} \tag{2.3.2}$$

After multiplying the left and right sides of the equation (2.2.5) by the Park transformation matrix, the state equation of the three-phase full-bridge voltage source inverter in the dq two-phase rotating coordinate system can be obtained by sorting:

$$\frac{d}{dt}\begin{bmatrix}v_{od}\\ v_{oq}\\ i_{Ld}\\ i_{Lq}\end{bmatrix}=\begin{bmatrix}0 & \omega & \frac{1}{C_f} & 0\\ -\omega & 0 & 0 & \frac{1}{C_f}\\ -\frac{1}{L_f} & 0 & -\frac{r}{L_f} & \omega\\ 0 & -\frac{1}{L_f} & -\omega & -\frac{r}{L_f}\end{bmatrix}\begin{bmatrix}v_{od}\\ v_{oq}\\ i_{Ld}\\ i_{Lq}\end{bmatrix}+\begin{bmatrix}-\frac{1}{C_f}i_{od}\\ -\frac{1}{C_f}i_{oq}\\ \frac{v_d}{L_f}\\ \frac{v_q}{L_f}\end{bmatrix} \tag{2.3.3}$$

Equation (2.3.3) is the mathematical model of the three-phase voltage source inverter in the dq two-phase rotating coordinate system[Zhang (2013), Wang (2014), Kroutikova et al., (2007)]. Set the three-phase AC flow to:

$$\begin{aligned} v_a &= V_m \cos(\omega t), v_b = V_m \cos(\omega t - \frac{2\pi}{3}) \\ v_c &= V_m \cos(\omega \mathrm{t} + \frac{2\pi}{3}) \end{aligned} \tag{2.3.4}$$

Where Vm is the three-phase AC voltage amplitude, after the above Clark and Park transformations are obtained:

$$\begin{aligned} v_d &= V_m \\ v_q &= 0 \end{aligned} \tag{2.3.6}$$

2.4 VOLTAGE AND CURRENT DECOUPLING CONTROL BASED ON dq ROTATION COORDINATES

Equation (2.3.3), the state equation of the inductor current in the dq two-phase rotating coordinate system of the three-phase voltage source inverter can be rewritten as a differential equation [Xiaodeng (2016), Zhang (2013)]:

$$\begin{aligned} L_f \frac{di_{Ld}}{dt} &= v_d - v_{od} + \omega L_f i_{Lq} - r i_{Ld} \\ L_f \frac{di_{Lq}}{dt} &= v_q - v_{oq} - \omega L_f i_{Ld} - r i_{Lq} \end{aligned} \tag{2.4.1}$$

Where:

$$\begin{aligned} v_d &= K_{PWM} m_d \\ v_q &= K_{PWM} m_q \end{aligned}$$

K_{PWM} is the gain of the three phase full bridge circuit.m_d and m_q are the pwm modulation signal.It can be seen from the above equation that this is a coupled system where the d-axis component and the q-axis component of the current are coupled to each other. Therefore, the q-axis current of the d-axis needs to be decoupled.

In order to achieve decoupling control, the following:

$$\begin{aligned} m_d &= \frac{1}{K_{pwm}} (v_{id} + v_{od} - \omega L_f i_{Lq}) \\ m_q &= \frac{1}{K_{PWM}} (v_{iq} + v_{oq} + \omega L_f i_{Ld}) \end{aligned} \tag{2.4.2}$$

where v_{id} and v_{iq} current loop PI regulator output, namely:

$$v_{id} = \left(K_{pi} + \frac{K_{ii}}{s} \right)(i_{Ldref} - i_{Ld})$$
$$v_{iq} = (K_{pi} + \frac{K_{ii}}{s})(\mathrm{i}_{Lqref} - i_{Lq}) \tag{2.4.3}$$

In the equation above, K_{pi} and K_{ii} are the proportional and integral coefficients of the current loop PI regulator, respectively.

i_{Ldref} and i_{Lqref} are reference currents for the d and q axis.According to the decoupling control scheme of equation (2.4.2), a functional block diagram of current loop decoupling control as shown in Figure 2.4 can be obtained:

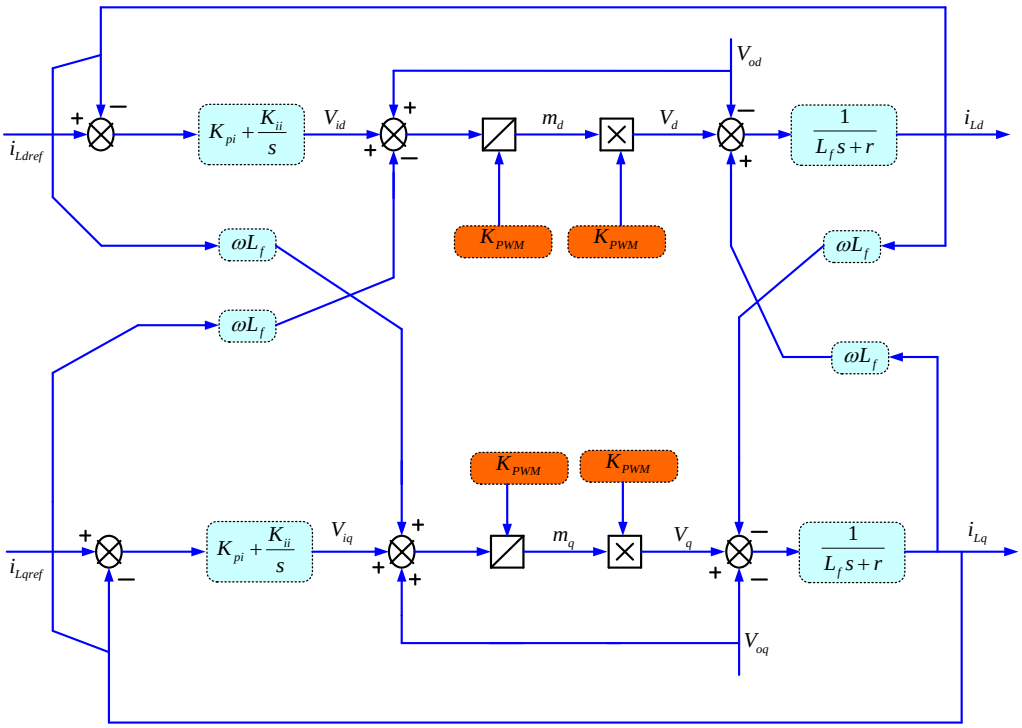

Figure 2.4: Block diagram of the current loop decoupling

After the decoupling control, the differential equation of the inductor current can be obtained as follows:

$$L_f \frac{di_{Ld}}{dt} = v_{id} - ri_{Ld}$$
$$L_f \frac{di_{Lq}}{dt} = v_{iq} - ri_{Lq} \tag{2.4.4}$$

In this way, the above control block diagram can be simplified and the simplified current loop control block diagram is shown in Figure 2.5[Deng et al., (2005), Yangdong (2014), Zhang (2013):

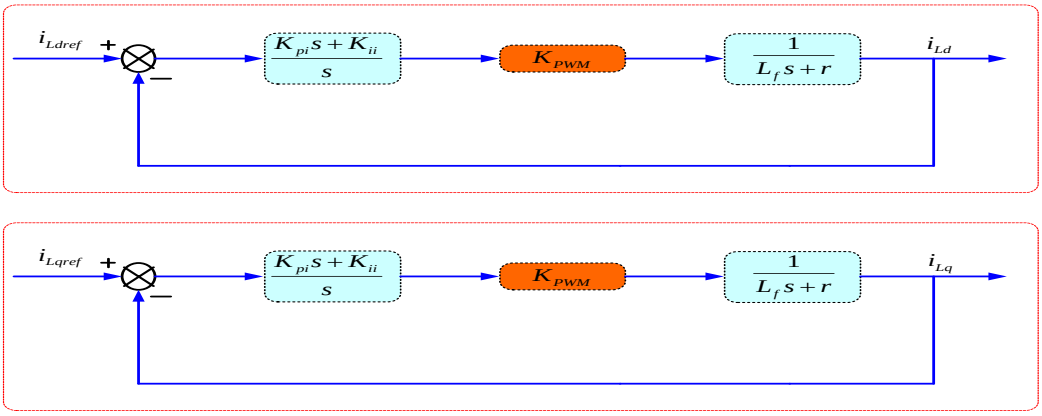

Figure 2.5: Current loop control diagram in dq coordinate system

From this we can get the open loop gain function *l(s)* of the current loop:

$$l(s)=\frac{K_{PWM}G_{pi}(s)}{(L_f s+r)} \tag{2.4.5}$$

As can be seen from the following section, through the rational design of PI parameters, the closed-loop transfer function of the current loop can be equivalent to a first-order inertial link:

$$G_i(s)=\frac{1}{\tau_i s+1} \tag{2.4.6}$$

Where τ_i is the time constant that needs to be designed and this value can affect the dynamic response speed of the system.

According to the idea of current loop decoupling control, similarly, the voltage loop can be analyzed. It can be known from equation (2.3.3) that the state equation of the capacitor voltage of the three-phase voltage source inverter in the dq two-phase rotating coordinate system can be rewritten as differential equation:

$$\begin{aligned} C_f\frac{dv_{od}}{dt}&=i_{Ld}-i_{od}+\omega C_f v_{oq}\\ C_f\frac{dv_{od}}{dt}&=i_{Lq}-i_{oq}-\omega C_f v_{od}\end{aligned} \tag{2.4.7}$$

It is easy to find that the voltage d-axis component and the q-axis component are coupled to each other. Therefore, it is necessary to decouple the d-axis and q-axis voltage. So that, the current loop reference is:

$$\begin{aligned} i_{Ldref}&=v_{vd}-C_f(\omega v_{oq})+i_{od}\\ i_{Lqref}&=v_{vd}+C_f(\omega v_{oq})+i_{oq}\end{aligned} \tag{2.4.8}$$

where v_{vd}, v_{vq} voltage loop PI regulator output, namely:

$$v_{vd} = (K_{pv} + \frac{K_{vi}}{s})(v_{odref} - v_{od})$$
$$v_{vq} = (K_{pv} + \frac{K_{vi}}{s})(v_{oqref} - v_{oq}) \quad (2.4.9)$$

In the equation above, K_{pv} and K_{vi} are the proportional and integral coefficients of the voltage loop PI regulator, respectively. V_{odref}, V_{oqref} is the reference voltage for d axis and q axis.According to the decoupling control scheme of equation (2.4.8), a functional block diagram of decoupling control of the voltage loop as shown in Figure 2.6 can be obtained:

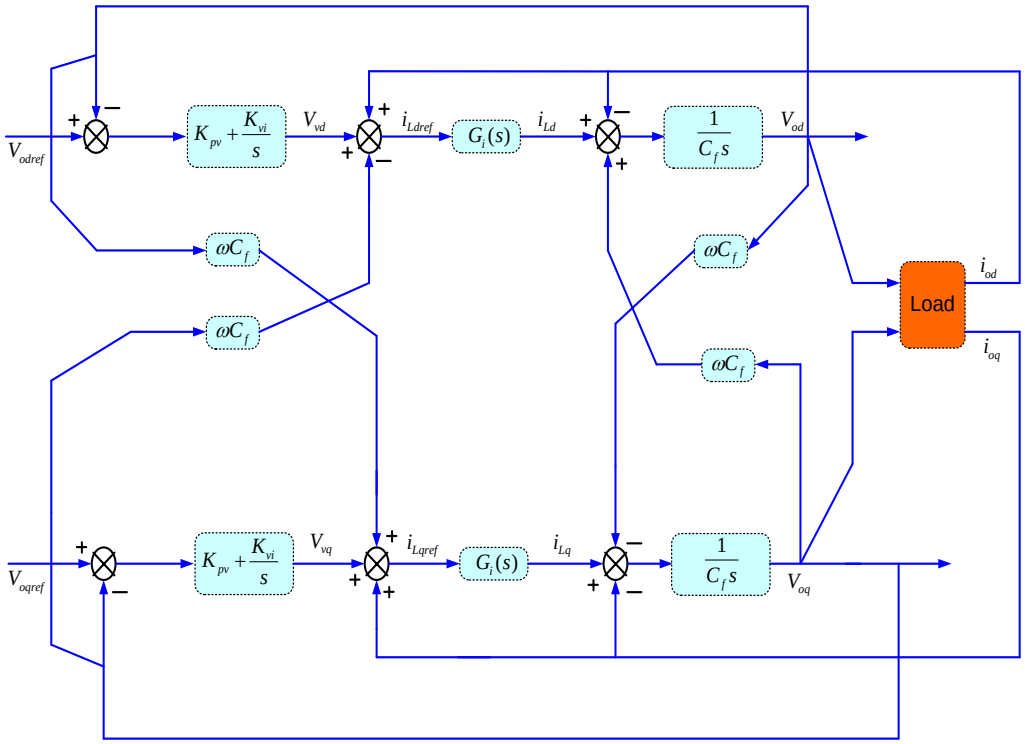

Figure 2.6: Voltage loop decoupling control block diagram

In the figure above, $G_i(s)$ is the closed-loop transfer function of the current loop:

$$i_{Ld}(s) = G_i(s) i_{Ldref}(s)$$
$$i_{Lq}(s) = G_i(s) i_{Lqref}(s) \quad (2.4.10)$$

Substituting the transformed formula (2.4.8) into (2.4.10) yields:

$$i_{Ld}(s) = G_i(s)[v_{vd}(s) - C_f L\{\omega v_{oq}\} + i_{od}(s)]$$
$$i_{Lq}(s) = G_i(s)[v_{vq}(s) + C_f L\{\omega v_{od}\} + i_{oq}(s)] \quad (2.4.11)$$

$$C_f s v_{od}(s) = G_i(s) v_{vd}(s) + C_f[1 - G_i(s)]\mathrm{L}\{\omega \mathrm{v}_{oq}\} - [1 - G_i(s)] i_{od}(s)$$
$$C_f s v_{oq}(s) = \mathrm{G}_i(s) v_{vq}(s) - C_f[1 - G_i(s)] L\{\omega v_{od}\} - [1 - \mathrm{G}_i(s)] \mathrm{i}_{oq}(s) \quad (2.4.12)$$

Equation (2..4.6) can be derived:

$$1 - G_i(s) = \frac{\tau_i s}{\tau_i s + 1} \quad (2.4.13)$$

Since the time constant τ_i of the current loop is small, $1 - G_i(s)$ can be approximately zero over a wide range of frequencies, so the equation (2.4.12) can be simplified as:

$$v_{od} = G_i(s) \frac{1}{C_f s} v_{vd}(s)$$
$$v_{od} = G_i(s) \frac{1}{C_f s} v_{vq}(s) \quad (2.4.14)$$

From the equation (2.4.14), we can see that the d-axis and q-axis components of the output voltage of the inverter are fully decoupled. According to this formula, the simplified control block diagram of the voltage loop can be obtained as shown in the Figure 2.7[Yajuan and Weiyang (2010), Zhang (2013), Kroutikova et al., (2007)]:

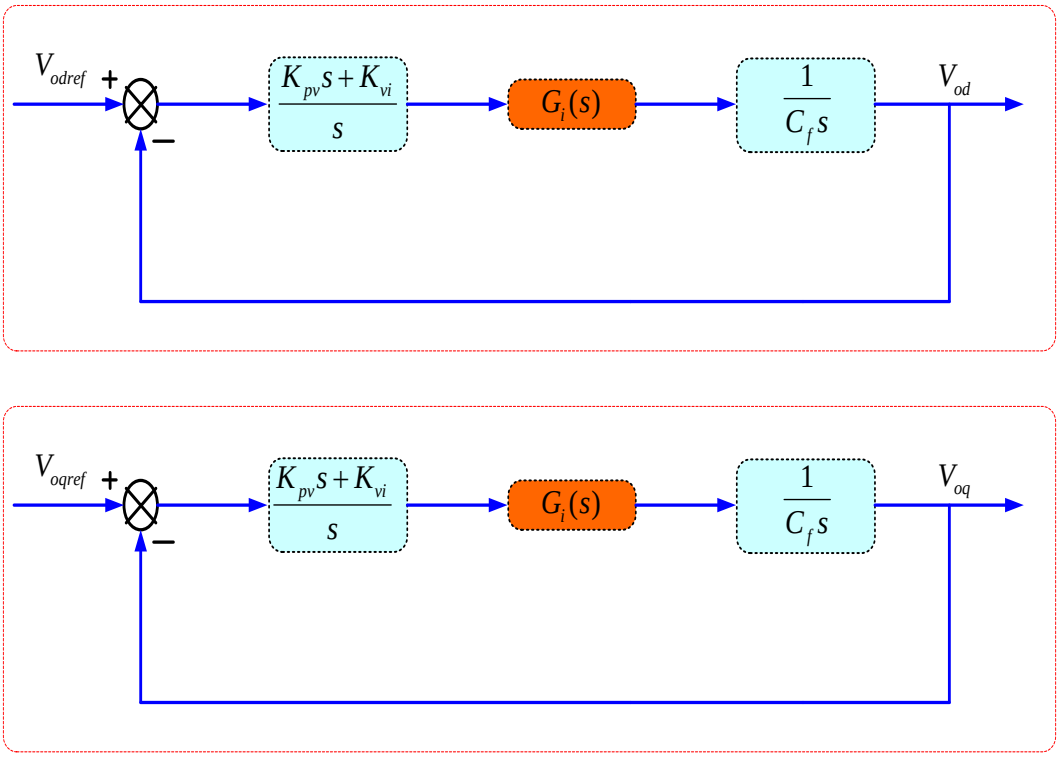

Figure 2.7: Voltage control loop block diagram dq co-ordinates

From the above analysis, it can be seen that the process of decoupling control is actually injecting the components containing the information of other axes into the output of each axis PI regulator. The amount of coupling between the injected component and the controlled object is equal and opposite in direction, thereby canceling out the influence of the coupling amount.

2.5 LC FILTER DESIGN

The filter circuit is an important part of the main circuit, the choice of topological structure and the value of component parameter determine the characteristic of the control distributed generation inverter, which has an important influence on the dynamic and static performance of the inverter output voltage and current control. The intermediate link between the DG inverter bridge and the load, the filter circuit not only satisfies the requirements of the switching frequency harmonics and the side-band harmonics of the DG inverter, but also ensures the output voltage of the DG inverter to track the command voltage and current quickly. The harmonic suppression effect and the dynamic performance of the voltage and current control are mutually restricted. When designing the parameters of the filter circuit, consideration should be given to the trade-off between the two factors[Kim and Sul (2009)].

There are roughly three types of inverter output filter circuits: single-inductor L, LC, and LCL filters, as shown in Figure 2.8[Xiaodong (2016)].

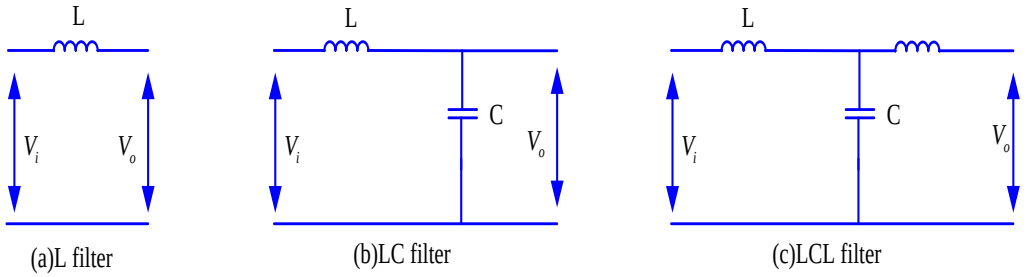

Figure 2.8: Inverter filter circuits

A single-inductance L filter, its design ideas are clear and the structure is simple, but its high frequency filtering effect is not good. Increasing the inductor value or increasing the switching frequency of the power device can improve the filtering effect, but the inductance value of the large filter circuit increases the system cost and adversely affects the dynamic performance of the system. The switching frequency of

the power device is influenced by the device's own parameters, switching losses, system cost and conversion efficiency and cannot be blindly increased[Shang (2013)]. In addition, inverters with single-inductance L filtering cannot directly control the output voltage of the inverter and the DG inverter should have the function of maintaining the frequency stability and need to control the output voltage of the inverter. Inductor L filter circuit is not suitable for distributed generation inverter. The LCL filter circuit, which is itself a three-order system, there is a resonance problem that will affect the stability of the system[Yandong (2014)].

In the design of the controller, it is necessary to consider the resonance suppression, the output voltage of the inverter and the dynamic and static performance of the current control, which increases the complexity of controller design and related parameter selection. According to the demand of the output filter circuit of the DG inverter, this paper chooses the LC filter as the output filter circuit of the inverter[Kim and sul (2009), Changyong et al., (2000)].

The parameters of the main circuit and the control circuit are designed below.L the selection of three-phase inductance according to the design rules, not only to meet the requirements of the system speed and to suppress harmonics, that is, need to meet the following[Shang (2013), Yajuan (2012), Changyong et al., (2000)]:

$$\frac{(2V_{dc}-3V_m)V_m T_s}{2V_{dc}\Delta i_{\max}} \le L_f \le \frac{2V_{dc}}{3I_m\omega} \tag{2.5.1}$$

Substituting the above parameters into equation (2.5.1) yields the range of inductance values as follows:

$$2.5mH \le L_f \le 127mH \tag{2.5.2}$$

According to the above formula, select the filter inductor L_f = 3mH.

The resonant frequency of the LC filter is:

$$f_c = \frac{1}{2\pi\sqrt{L_f C_f}} \tag{2.5.3}$$

The resonant frequency is generally required to be less than 1/5-1/10 of the switching frequency and greater than 10 times the fundamental frequency, ie:

$$10 f_o \le f_c \le \left(\frac{1}{5} \sim \frac{1}{10}\right) f_s \tag{2.5.4}$$

The switching frequency is f_s = 10000Hz and the fundamental frequency is f_o = 50Hz. It can be obtained from equation (2.5.4):

$$500Hz \le f_c \le 1000Hz \tag{2.5.5}$$

Take the filter capacitor 15μF, according to equation (2.5.6) can be obtained:

$$f_c = \frac{1}{2\pi\sqrt{L_f C_f}} \tag{2.5.6}$$

It can be seen that the resonant frequency f_c of the filter is in the range, which meets the design requirements and the filter inductance and capacitance selection parameters are reasonable.

2.6 DG INVERTER VOLTAGE AND CURRENT DOUBLE CLOSED-LOOP CONTROL SYSTEM DESIGN

Through the analysis in the previous section, we obtained the mathematical model of three-phase voltage source DG inverter after decoupling control in dq two-phase rotating coordinate system. In this section, we will develop a double-loop control system for DG inverter voltage and current based on this mathematical model.

Voltage and current dual-loop control [Wang et al., (2015)] is the main inverter control strategy as shown in figure 2.9, in which the current inner loop improves system stability, system dynamic response and damping properties. The inner current loop feedback is of two types, capacitor current mode [Yajuan et al., (2016), Wei et al., (2011)] and inductor current mode [Zhang et al., (2010)]. As compared to the inductor current mode feedback, the feedback capacitor current mode provides better noise immunity, but is unable to carry out inverter current limit protection. In the paper [Mingrui et al., (2014), Wang et al., (2014)] have shown that, for larger values of current controller proportional parameter K_{pi}, better dynamic response of the current loop is achieved. But, if K_{pi} is too large, there is a deterioration in the system stability. On the other hand, the smaller values of voltage controller parameter K_{pv}, the DG inverter output impedance is resistive. If K_{pv} takes larger values, the DG inverter output impedance is inductive. Similarly, the selection of the integral parameter K_{vi} has a significant effect on the characteristics of the inverter output impedance. In other words, the steady-state as well as the dynamic characteristics of DG inverter output depends on the parameter design of the controller. When the control parameter is a fixed value, it is difficult to meet the microgrid island operation in adjusting the voltage amplitude and frequency, during the changes in power supply fluctuations. Therefore, it is necessary to control the use of reasonable structure and parameter tuning method to achieve stable control of microgrid in islanding mode. In Figure 2.9, V_{ref} is the voltage loop reference, V_0 is the DG inverter output voltage,

K_{PWM} is the gain of the three phase full bridge circuit, $G_v(s)$ and $G_i(s)$ respectively are the voltage loop and current loop controllers, i_0 is the output current of the inverter and i_c is the capacitive feedback signal.

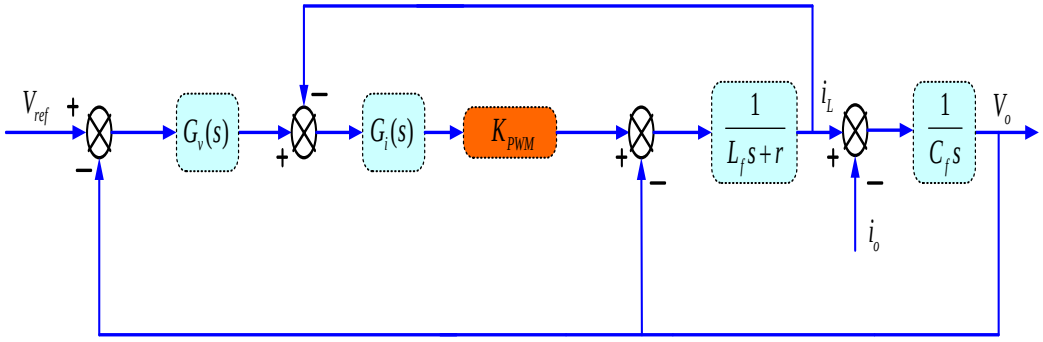

Figure 2.9: Voltage and current dual loop control block diagram

The proportional controller for the current loop is mainly for the quick consideration of the system and the capacitance current feedback is used instead of the inductance current feedback and the capacitance current feedback dynamic response is faster. The voltage loop considers the immunity of the system and uses the proportional integral control method to realize steady output voltage without static error[Chengshan et al., (2009), Zhang (2013)].

(1) Design of current loop control block diagram as shown in Figure 2.10:

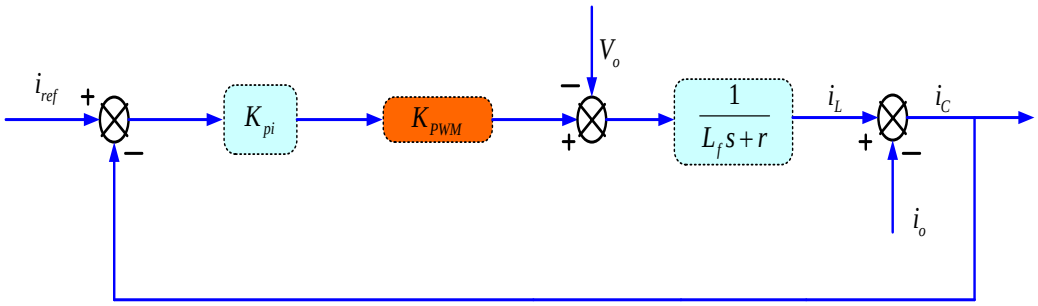

Figure 2.10: Current loop block diagram

To make sure the inner current loop has a better tracking performance under different load conditions, the inner current loop cut off frequency is chosen as $f_{ib} = \frac{1}{5} f_S$ [Zmood et al., (2001), Yajuan et al., (2011)]. The impact of the load

current i_o is neglected. Current loop closed loop block diagram is as shown in Figure 2.10 and the transfer function is given by:

$$G_i(s) = \frac{i_c(s)}{i_{ref}(s)} = \frac{G_i(s)K_{PWM}}{Ls + r + G_i(s)K_{PWM}} \tag{2.6.1}$$

From equation (2.6.1) the amplitude frequency characteristic of the transfer function is:

$$|G_i(j\omega)| = \frac{K_{pi}K_{PWM}}{\sqrt{\omega^2 L^2 + (K_{pi}K_{PWM} + r)^2}} \tag{2.6.2}$$

Current loop control parameter $K_{pi} = 0.2857$ is obtained from the bode diagram as shown in Figure 2.11.

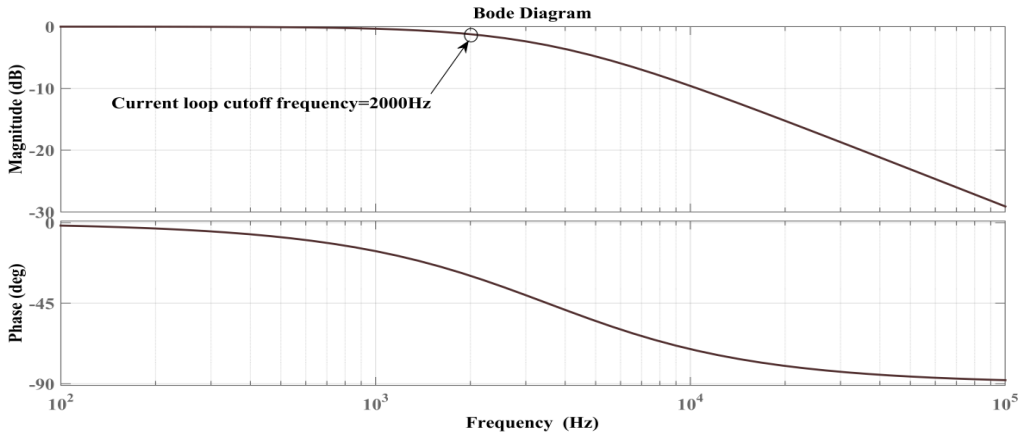

Figure 2.11: Bode diagram of the current loop

The voltage loop control block diagram is shown in Figure 2.12:

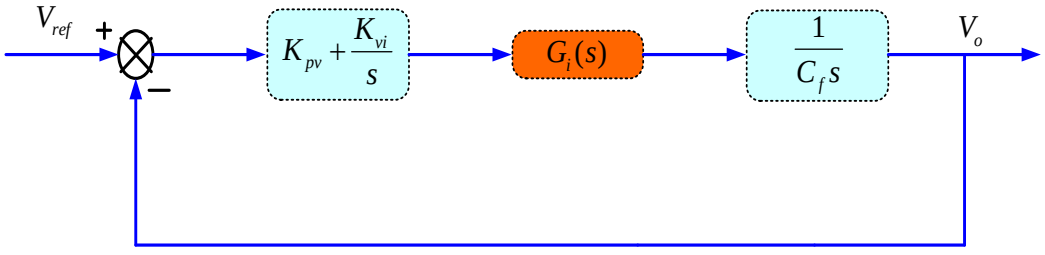

Figure 2.12: Voltage loop block diagram

The closed loop transfer function of the voltage loop can be deduced from Figure 2.9:

In order to avoid mutual coupling on the voltage loop and current loop, the cut off frequency of the voltage loop should be less than half of the current loop bandwidth. Hence, voltage loop cutoff frequency is chosen as 800 Hz [Zmood et al., (2001), Zhang (2013), Shang (2013)]. The transfer function is obtained as:

$$G_v(s) = \frac{(K_{pv} + \frac{K_{vi}}{s})G_i(s)}{C_f s + (K_{pv} + \frac{K_{vi}}{s})G_i(s)} \tag{2.6.3}$$

In equation (2.6.3), at first, integral coefficient K_{vi} is set to 0; the outer voltage cut-off frequency is set to 800 Hz; K_{pv} is obtained as 0.0225. In order to ensure that the system bandwidth is within the required range, the selected system bandwidth is f_{vb} = 900 Hz, then K_{vi} =38 is obtained. Voltage loop bode diagram as shown in the Figure 2.13.

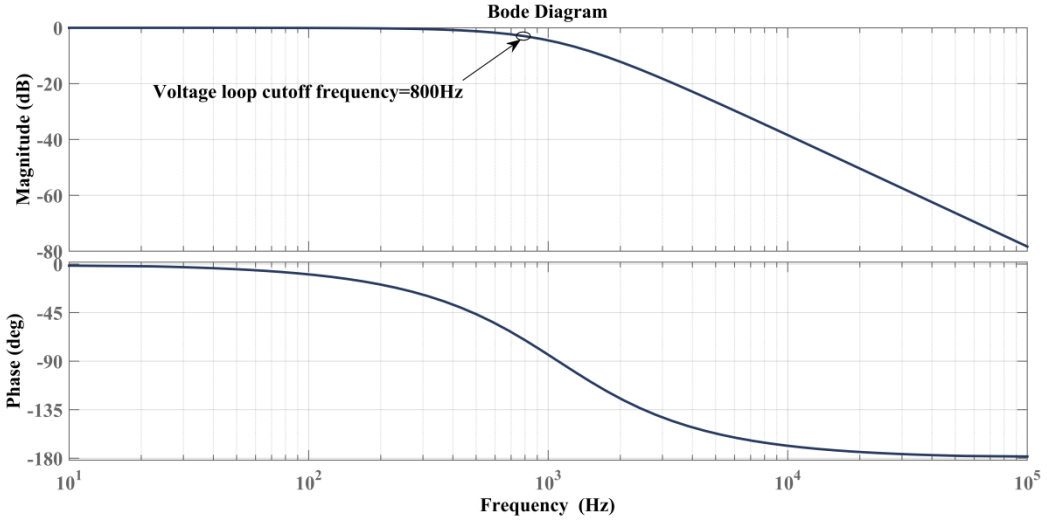

Figure 2.13: Bode diagram of the voltage loop

By control block diagram of inverter shown in Figure 2.9, we can derive the inverter output voltage is:

$$V_0 = \psi(s) * V_{ref} - Z_o(s) * i_0 \tag{2.6.4}$$

where $\psi(s)$ is the transfer function of the voltage, the expression is:

$$\psi(s) = \frac{G_i(s)G_v(s)K_{PWM}}{As^2 + Bs + 1 + G_i(s)G_v(s)K_{PWM}} \tag{2.6.5}$$

$$A = C_f L_f, B = rC_f + G_i(s)K_{PWM}C_f$$

The inverter output impedance transfer function is given by[Yandong (2014), Guerrero et al.,(2005), Shang (2013)]:

$$Z_o(s) = \frac{A_1 s^2 + A_2 s}{A_3 s^3 + A_4 s^2 + A_5 s + A_6} \tag{2.6.6}$$

$$A_1 = L_f, A_2 = r + K_{pi}K_{pwm}, A_3 = L_f C_f, A_4 = K_{pi}K_{pwm}C_f + rC_f,$$
$$A_5 = K_{pi}K_{pwm}K_{pv} + 1, A_6 = K_{pi}K_{pwm}K_{vi}.$$

Due to the presence of the output filter inductor and inductive components of the device parameters, the equivalent output impedance of the inverter is generally considered inductive. But, equivalent output impedance of the closed loop of inverter has a relationship with control strategy adopted [Chengshan et al., (2009), Tao et al.,(2015), Shang et al.,(2013)] by adjusting the inverter control parameters. The equivalent output impedance of the DG inverters can be changed to resistive or inductive.

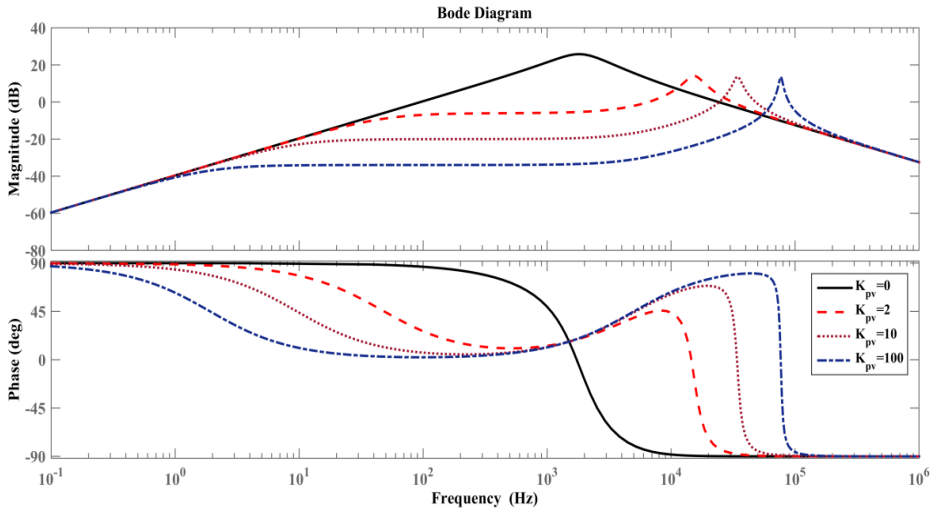

Figure 2.14: Bode diagram of inverter output impedance with different K_{pv}

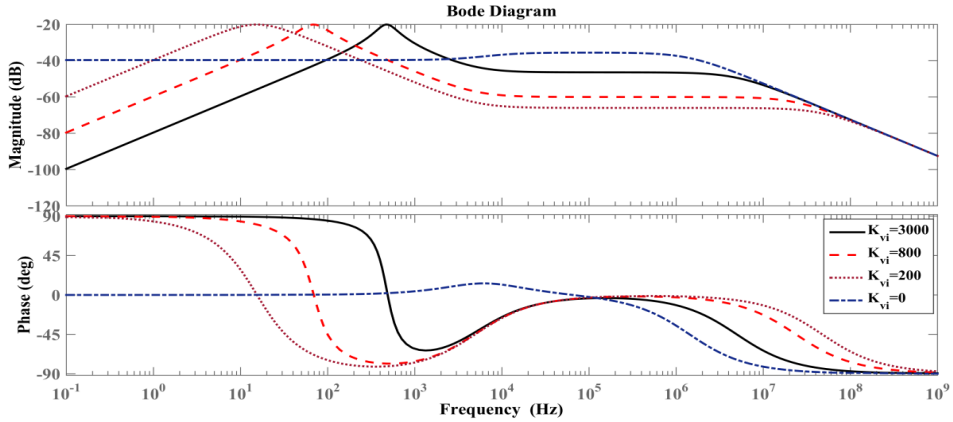

Figure 2.15: Bode diagram of inverter output impedance with different K_{vi}

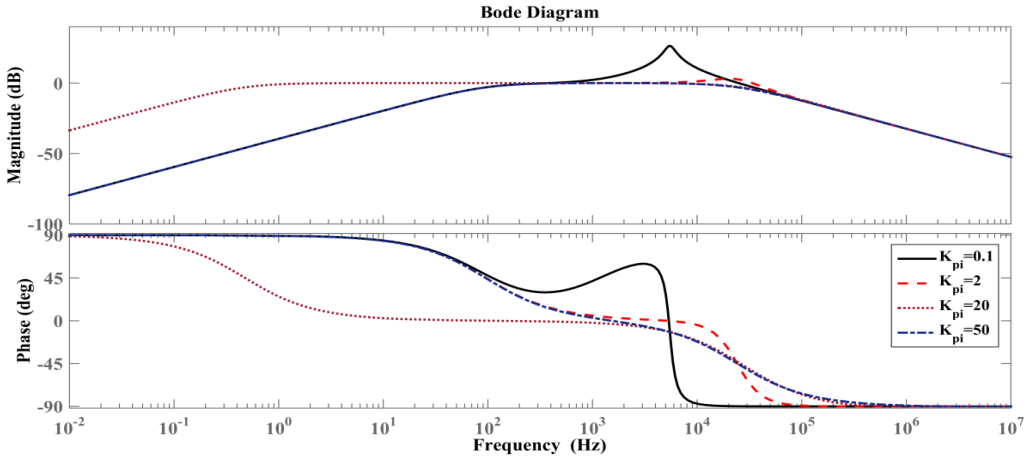

Figure 2.16 Bode diagram of inverter output impedance with different K_{pi}

Figure 2.14 shows that the voltage loop proportional factor has some influence on the DG inverter output impedance. When $K_{pv}=0$, the inverter output impedance at 50 Hz is more inductive. With the increasing K_{pv} value the DG inverter output impedance at 50 Hz is more resistive.

Figure 2.15 shows that the voltage loop integral factor has some influence on the inverter output impedance. When K_{vi}=0, the inverter output impedance at 50 Hz is approximately more resistive, with increasing K_{vi} the output impedance of the DG inverter at 50 Hz is more capacitive.

Taking K_{pi}=0.1, 2, 20, 50 the DG inverter output impedance at 50 Hz is as shown in Figure 2.16. The current loop proportional coefficient has little effect on the output impedance nature of DG inverters.

The output impedance of the DG inverters are calculated using equation (2.6.6). The output impedance angle at 50 Hz is 70° as shown in the Figure 2.17. In ensuring the stability of the microgrid system, the DG inverters output impedance is approximated as inductive for direct droop control and resistive for the reverse droop control. If the DG inverter closed loop output impedance design is reasonable, it can reduce the impact of line impedance imbalance. Different values of the system parameters of the DG inverters output impedance magnitude and angle has a direct impact on power sharing. To further reduce the effect of DG inverter output impedance and line impedance effect on the parallel DG inverters, virtual resistors and inductors are added to the control loop, so that DG inverter output impedance nature is changed to inductive for the direct droop control and resistive for the reverse droop control are discussed in chapter 3, chapter 4.

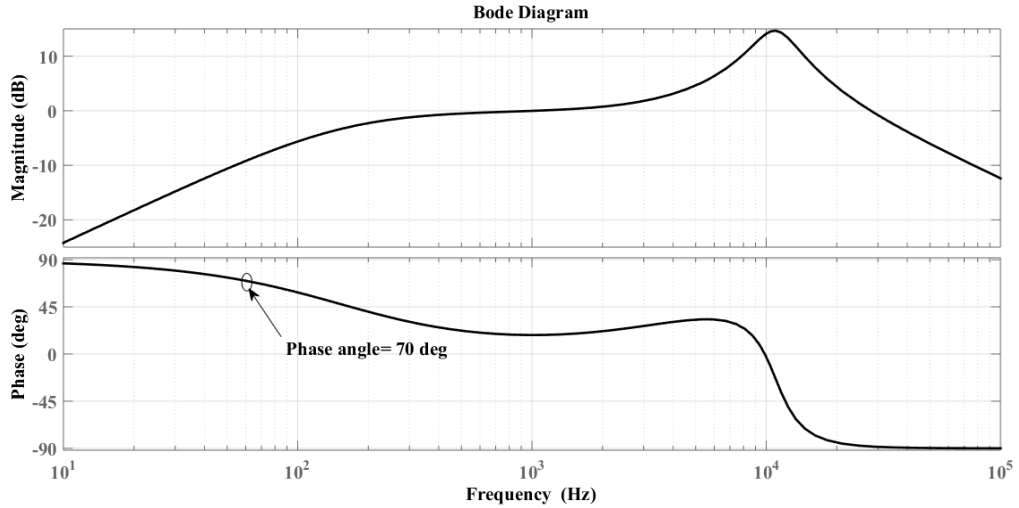

Figure 2.17: Bode diagram of DG inverter output impedance

2.7 CONCLUSION

This chapter introduces the modeling of the three phase DG inverter in the microgrid in the dq coordinate system and the parameter design of the voltage and current double closed loop system controller. The main circuit of the three-phase DG inverter is given and the output LC filter parameters are designed. Then the mathematical model of the three-phase DG inverter in the static three-phase coordinate system is established and then the model of the three-phase inverter in the

synchronous rotating coordinate system is obtained by coordinate transformation. Then the controller parameters of the voltage-current inner loop are designed.

Chapter 3

3 DIRECT DROOP CONTROL (P-F/Q-V) OF PARALLEL DISTRIBUTED GENERATION INVERTERS IN MICROGRID

3.1 INTRODUCTION

As demand for renewable energy grows, more renewable are integrated into the micro-grid. However, due to the intermittent and fluctuating load curves of renewable energy, the high penetration of renewable energy, different types of load show many challenging problems, such as power quality, stability and reliability of power system. In order to deal with these problems, the concept of microgrid network is proposed to realize flexible coordinated control between distributed generation units[Wei et al., (2009)]. The micro-grid is made up of various forms of Distributed Generation(DG), energy storage equipment, load and control unit, such as the collection of the central and low-voltage distribution system, can be connected to the large power grid operation, can also be in an isolated island mode to bear the local load [Peng et al., (2009)].

When the micro-grid is transferred from the grid to the isolated island operation mode, the micro-grid load power is distributed precisely according to the distribution capacity. In order to meet the demand of power distribution, the droop control method simulating the behavior of synchronous generators is widely used in the isolated island mode of microgrid[Peng et al., (2010)]. This method does not need the communication link. However, although the frequency droop control can guarantee the distribution accuracy of the active power, the voltage droop control is difficult to achieve the precise reactive distribution because of the line impedance mismatch[Khaledian et al., (2017), Han et al., (2015)].

In order to solve this problem, many scholars have started the relevant research. In paper [Tuladhar et al., (2000), He et al., (2012), Zhu et al., (2015)] presents a signal injection method to change the active power distribution according to the non frequency signal injected into the system. However, due to the complexity of the signal occurrence and processing, it is difficult to implement this method when there are two distributed generators.

In the paper [Li et al., (2009), Yongwei et al., (2013)] regulates droop control coefficient to improve the accuracy of reactive power distribution, but in order to adjust droop control coefficient in island mode, the coefficient of load curve obtained in grid-connected mode is utilized. The improved voltage droop control method is proposed in the paper [Lee et al., (2013)], but it cannot guarantee the exact distribution of reactive power in the presence of local load. In [Junzhao et al., (2016)] The virtual impedance is introduced to improve the stability of power control and the precision of load power distribution. But this method only considers the output impedance of the inverter and cannot consider the mismatch of line impedances.

The control accuracy of the inverter output voltage amplitude and phase depends on the inverter output voltage control strategy used. In the paper [Guerrero et al., (2005), Guerrero et al., (2007)] the control method of a given feedforward voltage closed-loop PID controller is used to ensure the error-free tracking of the reference voltage at the fundamental frequency of the inverter output voltage. In the paper [Zinxin et al., (2009)], the single voltage loop control method is used to guarantee the accurate control of the output voltage of the inverter, but the controller parameter design is complex and the influence of the controller parameters on the equivalent output impedance of the inverter is not analyzed. In the paper [Hasanzadeh et al., (2010), Shaohua et al., (2015)], the voltage and current double loop control strategy based on proportional resonant controller is adopted, but the design method of the controller parameters is not given. In [Liaoyuan et al., (2016)], the total output impedance of the inverter is designed to be resistive by virtual complex impedance containing both resistive and negative inductive components, wherein the negative inductive component is used to eliminate the inductive output impedance of the inverter.

To sum up, at present, most of the literature cannot completely overcome the microgrid line impedance and other factors on the distribution of load power, it is difficult to apply to a complex microgrid containing multiple DG. The microgrid system with multiple DG sources, an improved direct droop control strategy based on the introduction of virtual inductance is adopted, which can achieve a reasonable sharing of power according to DGs capacities.

3.2 POWER FLOW CHARACTERISTICS BETWEEN DISTRIBUTED GENERATION INVERTERS

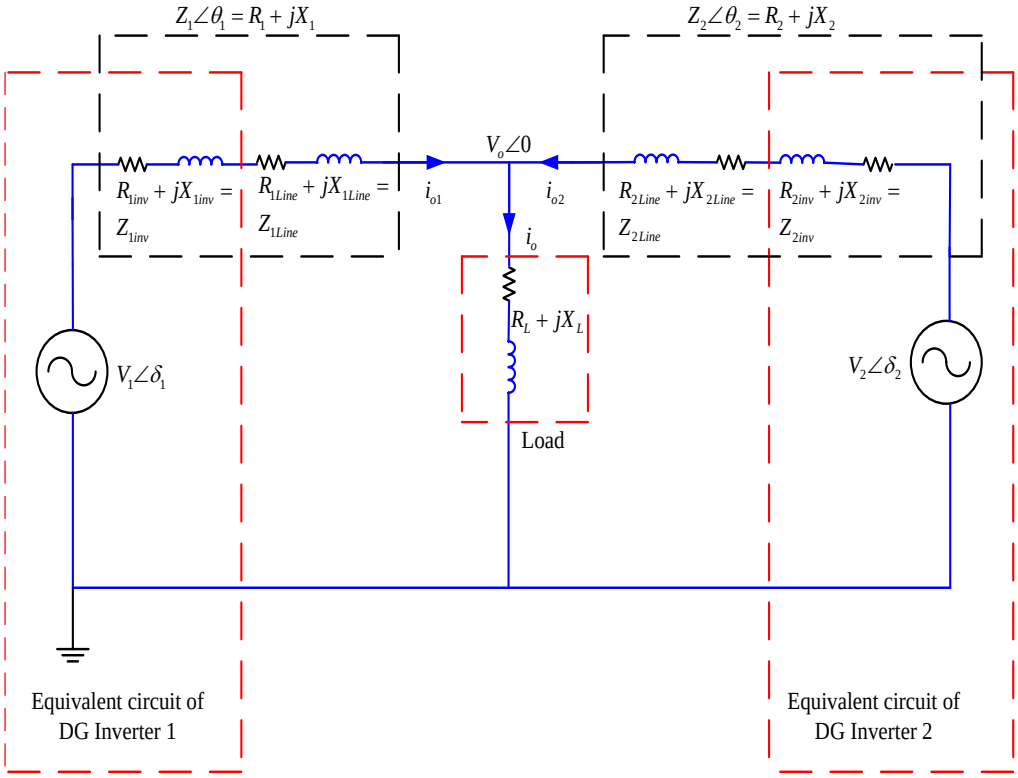

Figure 3.1: Equivalent circuit diagram of DG inverter parallel operation

The voltage source distributed generation inverter is an important way to connect the distributed power supply and the power grid in the microgrid. The regulation characteristics of the DG inverter are crucial for the power distribution between the distributed generation sources. The DG inverter with droop control can adjust its own frequency and power according to measured active and reactive power.

The following is an overview of the basics of droop control using Figure 3.1 to analyses the output power of two DG inverters operating in parallel. The sum of the line and output impedance of the DG inverter1 and DG inverter 2 is given by[Yajuan (2012), Yandong (2014)]:

$$Z_1\angle\theta_1 = R_{1inv} + jX_{1inv} + R_{1Line} + jX_{1Line}$$

$$Z_2\angle\theta_2 = R_{2inv} + jX_{2inv} + R_{2Line} + jX_{2Line}$$

The load equivalent impedance is given by:

$$Z_L = R_L + jX_L$$

Where R_{1inv}, R_{2inv} are the DG inverters equivalent output resistances; X_{1inv}, X_{2inv} are the DG inverters equivalent output reactances; $R_{1Line}, \mathrm{R}_{2Line}$ are the line resistances; X_{1Line}, X_{2Line} are the line reactances; $V_o \angle 0$ is the ac bus voltage amplitude. V_1, V_2 are the DG inverter output voltages; δ_1, δ_2 are the DG inverter output voltage phase angles; θ_1, θ_2 ar the total impedance angles of DG inverters; i_{o1}, i_{o2} are the output currents of DG inverters; i_o is the load current.

The equivalent circuit impedance $Z_n (n = 1, 2)$ is:

$$Z_n = R_n + jX_n \tag{3.2.1}$$

The DG inverters output current (n=1,2) is:

$$i_n = \frac{V_n \angle \delta_n - V_o \angle 0}{Z_n \angle \theta_n} \tag{3.2.2}$$

The output power of DG inverters (n=1,2) is:

$$S_n = P_n + jQ_n = V_n \angle \delta_n . i_n^* \tag{3.2.3}$$

P_n is the output active power of DG inverter n; Q_n is the output reactive power of DG inverter n; i_n^* is the output current conjugate.

$$P_n = \frac{1}{Z_n}[(V_n V_o \cos\delta_n - V_o^2)\cos\theta_n + V_n V_o \sin\delta_n \sin\theta_n)] \tag{3.2.4}$$

$$Q_n = \frac{1}{Z_n}[(V_n V_o \cos\delta_n - V_o^2)\sin\theta_n - V_n V_o \sin\delta_n \cos\theta_n)] \tag{3.2.5}$$

When the impedance of the DG inverter system is inductive $\theta = 90^o$, the active and reactive power of the DG inverter output respectively is:

$$P_n = \frac{V_n V_o}{X_n} \sin\delta_n \tag{3.2.6}$$

$$Q_n = \frac{V_n V_o \cos\delta_n - V_o^2}{X_n} \tag{3.2.7}$$

It is generally considered that the DG inverter outout voltage phase angle δ_n is small, $\cos\delta_n = 1, \sin\delta_n = \delta_n$, so equations (3.2.6) and (3.2.7) further reduced to:

$$P_n = \frac{V_n V_o}{X_n} \delta_n \tag{3.2.8}$$

$$Q_n = \frac{V_o}{X_n}(V_n - V_o) \tag{3.2.9}$$

When the impedance of the DG inverter system is resistive $\theta = 0^o$, the active and reactive power of the DG inverter output respectively is:

$$P_n = \frac{V_o(V_n - V_o)}{R_n} \tag{3.2.10}$$

$$Q_n = -\frac{V_n V_o}{R_n}\delta_n \tag{3.2.11}$$

Droop control is actually controlled by the principle of linear relationship between the power of the inverter output and the amplitude of the system frequency and output voltage. The Droop control method is generally used in the control of distributed generation units in the Peer-to-peer control strategy [Lasseter et al., (2011), Meng et al., (2016)].

(a) Direct droop Control

In order to reduce the line loss, the traditional generation system of generator is usually high voltage long-distance transmission. Equations (3.2.6), (3.2.7) are system power transfer equations that are introduced under inductive line conditions. It can be seen from these two equations: The active power output by the distributed unit is only related to the phase angle difference; Reactive power is only related to the amplitude difference of voltage, so the power angle and voltage amplitude of the interface inverter can be changed by adjusting the active and reactive power output of the system. In practical applications, the phase angle difference is obtained by integrating the frequency and the adjustment frequency is easier to achieve than directly adjusting the phase angle difference. Therefore, the active power output from the DG inverter is adjusted to control the frequency and the reactive power output from the DG inverter is adjusted to control the voltage amplitude. Direct droop control is given by[Guerrero et al., (2011), Lopes et al., (2006), Pecaslopes et al., (2005)]:

$$f_n - f_{ref} = -m_{Pf}(P_n - P_{ref}) \tag{3.2.12}$$

$$V_n - V_{ref} = -n_{QV}(\mathrm{Q}_n - Q_{ref}) \tag{3.2.13}$$

In the equation, f_{ref} is the rated frequency of the system, f is the actual frequency of the system, V_{ref} is the rated voltage of the system, V is the actual output voltage of the

system, P_{ref} is the rated active power of the system and P is the actual output active power. m_{Pf} is the P-f droop coefficient and n_{QV} is the Q-V droop coefficient.

Direct droop control compares the output active power, reactive power with the rated power value and the difference is used to adjust the frequency and voltage amplitude of the inverter output. This control strategy is applicable to grid-connected mode and islanding mode. Figure 3.2 shows the drooping characteristics of direct (*P-f* and *Q-V)*droop control[Zhang et al., (2013)].

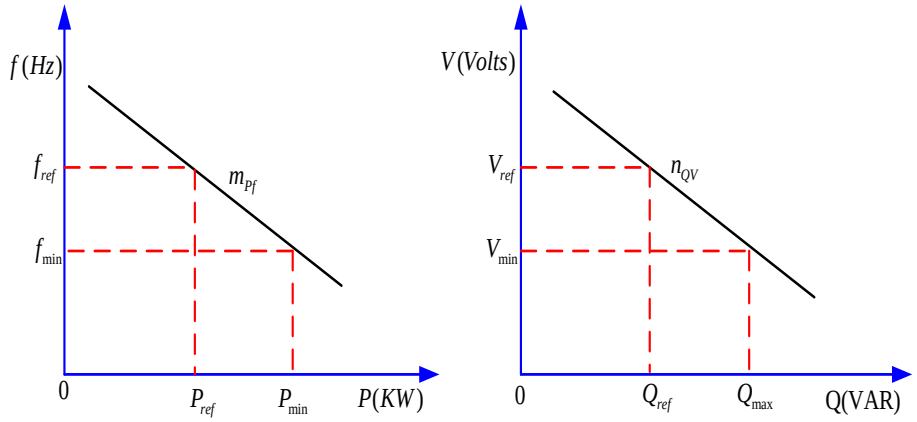

Figure 3.2: Direct droop control curves

f_{min} is the allowable minimum operating frequency of the system, V_{min} is the allowable minimum output voltage amplitude of the system, P_{max} is the maximum active power output of the DG inverter and Q_{max} is the maximum reactive power output of the DG inverter.The droop coefficient has an impact on the dynamic performance and steady-state performance of the system. If the droop coefficient is chosen to be small, although the steady-state characteristics of the system are good, the dynamic response speed of the system is sacrificed.

(b) Reverse droop control

The microgrid is usually connected to the grid through a distribution network, while the distribution network is a low-voltage system and the transmission line is mainly resistive. Obviously, the traditional direct droop control strategy obtained by ignoring the resistance component in the line is no longer applicable. So, reverse droop control is introduced(Wang (2014), Chun et al., (2010)].

In the case of low-voltage resistive transmission lines, the system power transmission equations (3.2.10) and (3.2.11) that are introduced in the absence of line

inductance indicate that: At this time, the active power output by the distributed system is only related to the voltage amplitude difference; Reactive power is only related to the phase angle difference. In this way, the basic principle of reverse(P-V,Q-f) droop control is obtained.The active power output from the inverter is adjusted to control the voltage amplitude and the reactive power output from the inverter is adjusted to control the frequency. In this way, reverse droop control strategy can be derived[Guerrero et al., (2005), Guerrero et al., (2007)]:

$$V_n - V_{ref} = -m_{PV}(P_n - P_{ref}) \tag{3.2.14}$$

$$f_n - f_{ref} = n_{Qf}(Q_n - Q_{ref}) \tag{3.2.15}$$

Where f_{ref} is the nominal frequency of the system and f is the actual frequency of the system; V_{ref} is the rated voltage of the system and V is the actual output voltage of the system. Q_{ref} is the system rated reactive power and Q is the actual output reactive power; m_{PV} is the reverse droop(P-V) coefficient and n_{Qf} is the reverse(Q-f) droop coefficient. Figure 3.3 shows the droop characteristics of reverse droop control[Chen (2014), Wang (2014)].

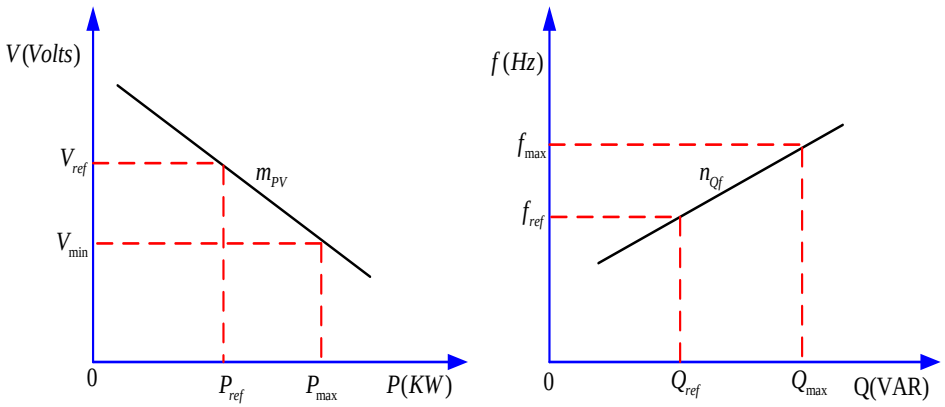

Figure 3.3: Reverse droop control curves

f_{max} is the maximum allowable operating frequency of the system, V_{min} is the allowable minimum output voltage amplitude of the system, P_{max} is the maximum active power output of the inverter, and Q_{max} is the maximum reactive power of the inverter output.

3.3 BLOCK DIAGRAM OF DIRECT DROOP CONTROL (P-F/Q-V)

Microgrid as a whole is composed of a voltage source inverters using direct droop control as shown in the Figure 3.4. then assuming that the inverter dc bus voltage V_{dc} essentially unchanged.L_{f1},L_{f2} are the three phase filter inductor, r_1,r_2 are the filter inductor equivalent resistance, C_{f1},C_{f2} is a three phase filter capacitor.

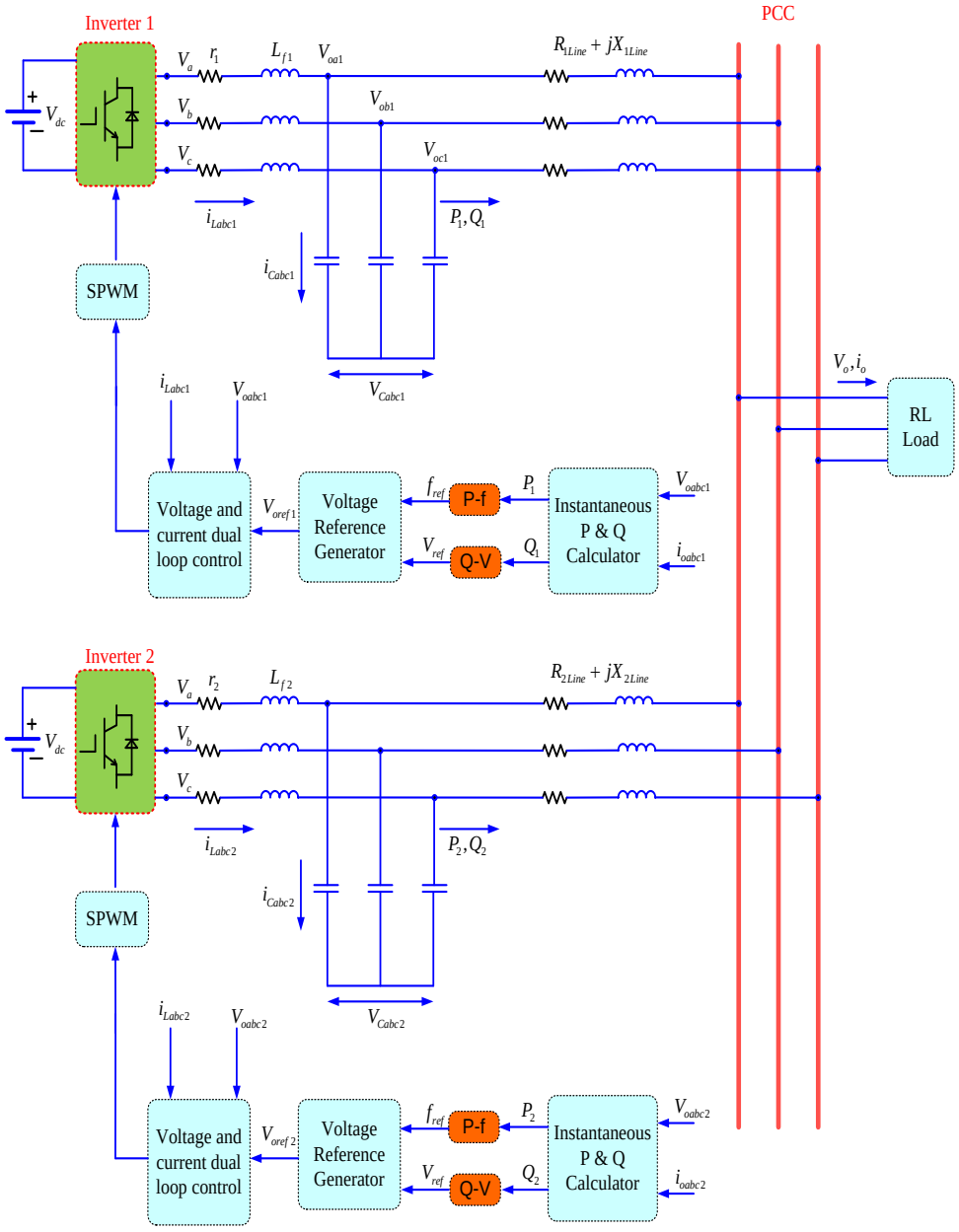

Figure 3.4: Block Diagram of three phase parallel DG inverter in microgrid using direct droop control

Comprehensive equivalent line impedance of the transmission line of two DG inverters is expressed as $Z_1=R_1+jX_1$ $Z_2=R_2+jX_2$.PCC represents a common connection point for DG inverters. In an islanded micro-grid where multiple distributed power supplies are connected in parallel, the distributed power supply not only needs to provide voltage and frequency support, but also in order to improve the reliability and redundancy of the micro-grid, each distributed power supply needs to be autonomous without interconnection lines and adjust the output voltage and frequency to achieve automatic power distribution. The droop control simulates the primary frequency modulation and the primary voltage regulation characteristics of the synchronous generator, which can adjust the voltage amplitude and frequency according to the droop curve and realize the distribution of the voltage controlled distributed power supply and the load power[Yong (2015), Jinxiao (2013)].

The droop control scheme is related to the characteristics of the line impedance. When the line impedance is inductive, direct droop control are generally used. When the line impedance is resistive, reverse droop control are generally used.

3.4 CONTROL DIAGRAM OF DIRECT DROOP CONTROL (P-F/Q-V)

In a microgrid, a direct droop control is actually used to simulate the droop characteristics of the synchronous generator to adjust the voltage and frequency of the DG inverters output, so that the micro-grid can operate under different load requirements. As can be seen from Figure 3.5, where L_f is the filter inductor, C_f is the filter capacitor, r is the filter inductor equivalent resistance and Z_{Load} is the load impedance, the droop control model of microgrid can be divided into two parts: voltage and current loop control model and power droop control model. First, the output voltage and current of the microgrid power supply are obtained by sampling the DG inverter module. The output power of the microgrid power supply is obtained by the power calculation unit and the low-pass filter and then calculated according to the active power droop controller and the reactive power droop controller respectively. The reference voltage values V_{dref} and V_{qref} is finally adjusted by the voltage PI control and i_{dref} and i_{qref} are adjusted by the current P control to obtain controllable sinusoidal modulation signal m to the DG inverter[Meiqin (2013), Xiaodong (2016)].

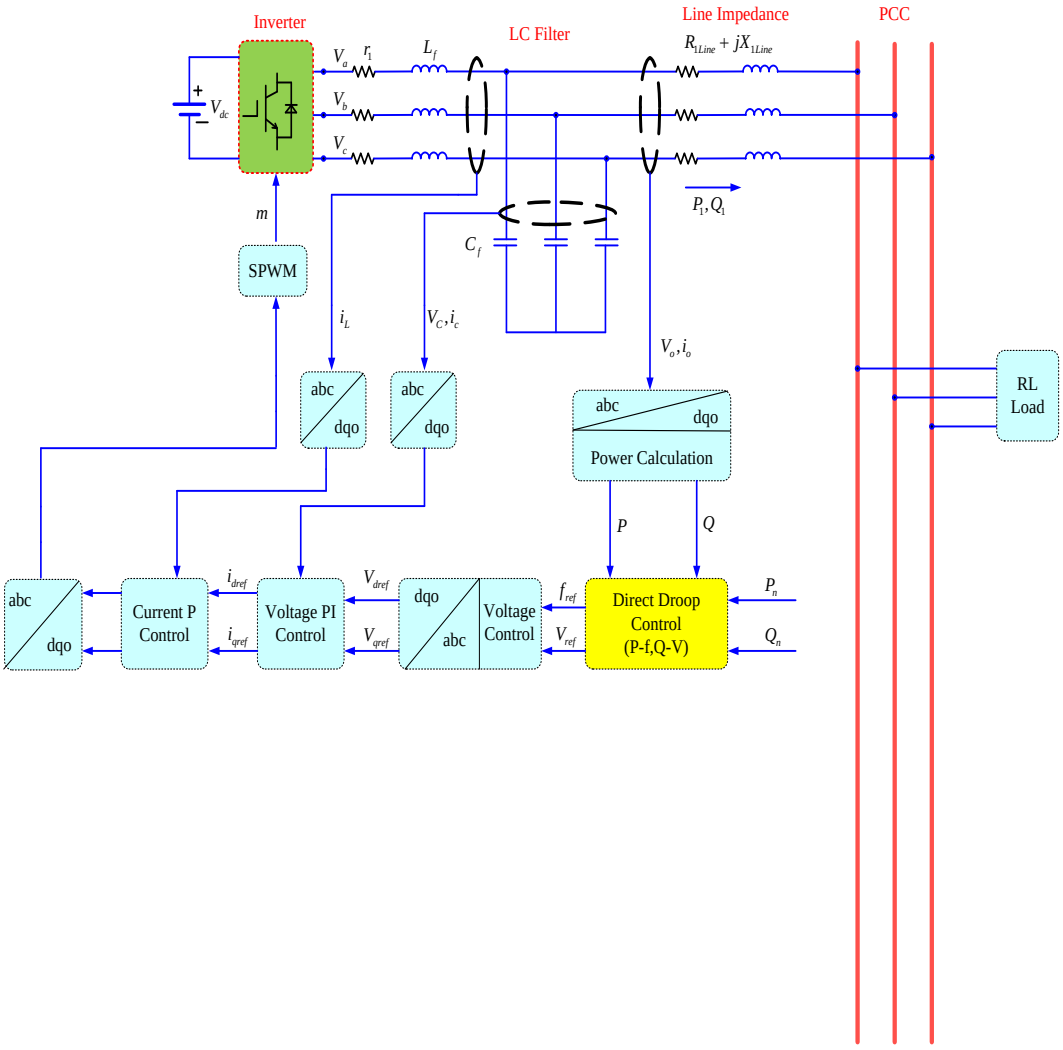

Figure 3.5: Control diagram of direct droop control

3.5 PROPORTIONAL LOAD SHARING OF PARALLEL DISTRIBUTED GENERATION INVERTERS USING DIRECT DROOP CONTROL

If the load is distributed according to the capacity, the droop co efficient needs to be inversely proportional to the capacity, namely:

$$m_{Pf1}P_1 = m_{Pf2}P_2 = ... = m_{Pfn}P_n \quad (3.5.1)$$

$$n_{QV1}Q_1 = n_{QV2}Q_2 = ... = n_{QVn}Q_n \quad (3.5.2)$$

When the distributed inverter power supply with same capacity is running in parallel, it is necessary to realize the exact load sharing according to the rated capacity

and the condition that the droop coefficient of each inverter is inversely proportional to the rated capacity, namely the equation (3.5.1) and (3.5.2).

However, only by setting the droop coefficient and the capacity is inversely proportional to the power cannot be accurately allocated. The following is a detailed analysis of the conditions for the accurate distribution of active and reactive power[Tuladhar et al., (2000), Wei et al., (2011)].

(a) Active power

When the micro-grid island operation reaches steady state operation, each working frequency is the same $f_1=f_2$, therefore, according to equation (3.2.12), it is only necessary to make all DG inverters have the same reference frequency at rated power in the droop control and the droop coefficient is inversely proportional to its rated power, that is, satisfying equations (3.5.3) and (3.5.4).It can achieve the purpose of equalizing the active power of the DG inverter output according to its rated power, as shown in equation (3.5.4)[Xumiao (2015), Meiqin (2013),Junhu et al., (2012)].

$$f_{n1} = f_{n2} \tag{3.5.3}$$

$$m_1 P_{n1} = m_2 P_{n2} \tag{3.5.4}$$

If the active power can be equally divided between the inverters, then equation is given by:

$$m_{Pf1} \frac{V_1 V_o}{X_1} \delta_1 = m_{Pf2} \frac{V_2 V_o}{X_2} \delta_2 \tag{3.5.5}$$

If $\delta_1 = \delta_2, V_1 = V_2$, then

$$\frac{m_{Pf1}}{X_1} = \frac{m_{Pf2}}{X_2} \tag{3.5.6}$$

(b) Reactive power

It can be known from equation (3.2.13), it is necessary to ensure equalization of reactive power, so that the condition for equation is (3.5.8) is $V_1=V_2$[Xumiao (2015), Meiqin (2013)].

$$V_{n1} = V_{n2} \tag{3.5.7}$$

$$n_{QV1} Q_1 = n_{QV2} Q_2 \tag{3.5.8}$$

Since the slope of the reactive/voltage(Q-V) droop curve is small, a slight deviation between the voltages causes a large reactive deviation, which easily causes overcurrent of the inverter.

It can be seen from equation (3.2.13), the voltage difference between the two DG inverters is:

$$\Delta V = V_2 - V_1 \tag{3.5.9}$$

V_1=V_2 can be guaranteed only when equation (3.5.10) is established and reactive power can be achieved between DG inverters according to rated capacity and perform equalization.

$$\frac{X_1}{n_{QV1}} = \frac{X_2}{n_{QV2}} \tag{3.5.10}$$

To sum up, the conditions for the equalization of active and reactive power by traditional droop control are:

$$\begin{aligned} &m_{Pf1}P_1 = m_{Pf2}P_2 \\ &n_{QV1}Q_1 = n_{QV2}Q_2 \\ &f_1 = f_2 \\ &V_1 = V_2 \end{aligned} \tag{3.5.11}$$

$$\begin{aligned} &V_1 = V_2 \\ &\frac{X_1}{n_{QV1}} = \frac{X_2}{n_{QV2}} \end{aligned} \tag{3.5.12}$$

$$\begin{aligned} &\delta_1 = \delta_2 \\ &\frac{X_1}{m_{Pf1}} = \frac{X_2}{m_{Pf2}} \end{aligned} \tag{3.5.13}$$

The equation (3.5.12), (3.5.13) indicate that the following conditions are met[Xumiao (2015), Meiqin (2013), Tuladhar et al., (2000), Wei et al., (2011)]:

1. The reference frequency and the reference voltage setting are the same under the rated power;

2. The droop coefficient is inversely proportional to its capacity;

3. The impedance of the line is inversely proportional to the capacity of the DG inverter;

4. The output voltage amplitude and phase of the DG inverter are the same, so that the active power and reactive power between the different capacities inverters can be achieved.

Therefore, according to the direct droop control method, it is very difficult to realize that the DG inverter can share the load accurately according to the rated proportion and the application in the distributed generation system has certain limitation.So, direct droop control method has to be improved.

3.6 VIRTUAL INDUCTANCE

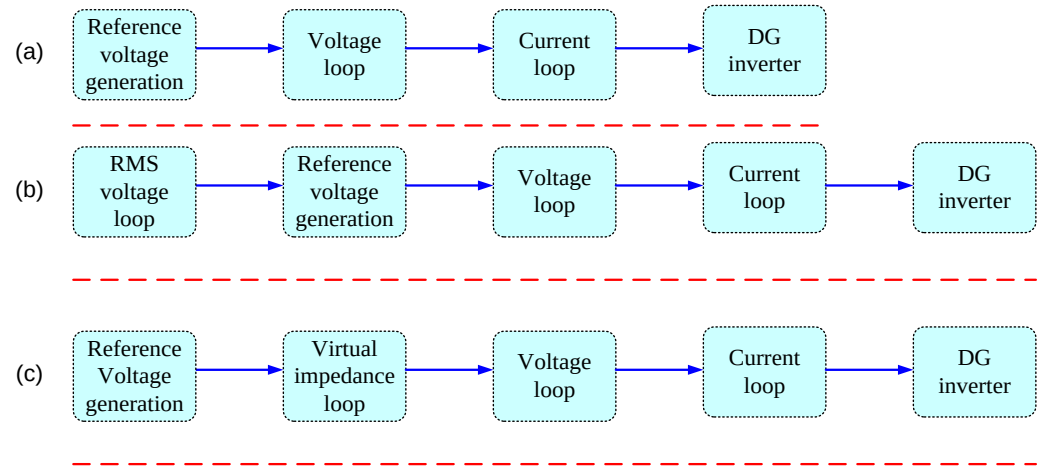

Figure 3.6: Typical control structure of a DG inverter

The classical voltage-current double-closed loop control shown in Figure 3.6(a) is widely used in parallel control of DG inverters due to its simple parameter design, fast dynamic response and small voltage waveform distortion [Jiarong et al., (2009), Zheng et al., (2016), Shitole et al., (2015), Lazzarin e al., (2009)].

In order to improve the voltage regulation accuracy of the DG inverter output voltage, in practical applications, the RMS value is often introduced in the double closed-loop control to adjust the amplitude of the reference voltage [He et al., (2008)], as shown in Figure 3.6(b).Adjusting the DG inverter's equivalent output impedance is also one of the DG inverter control techniques [Qinghai et al., (2014), Zhen et al., (2014)]. The inverter's equivalent output impedance can be used to evaluate the transient drop and overshoot of the output voltage as the load changes. Adjusting the equivalent impedance of the inverter with virtual impedance technology can improve the load regulation rate and optimize the output waveform quality of the inverter. The inverter control structure with virtual impedance added is shown in Figure 3.6(c).

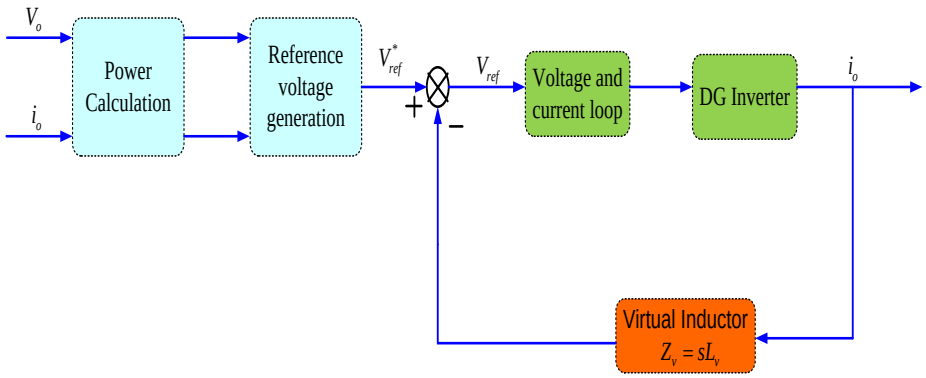

Figure 3.7: Virtual inductance block diagram

The droop control is a voltage type control. If the droop control is neglected for the small adjustment of the output voltage amplitude and phase, the DG inverter parallel system based on the droop control can be understood from the perspective of the voltage source parallel connection: In steady state, its output power is distributed strictly according to the system impedance. In the transient state, in order to ensure the stability and reliability of the parallel system, each parallel unit is required to have a certain impedance support. Therefore, the impedance plays an extremely important role in the power sharing of the DG inverter parallel system. The virtual impedance method can realize the adjustment of the output impedance of the DG inverter, which is of great significance in the field of DG inverter parallel control based on droop control.

The nature of the virtual impedance depends on the phase relationship between the virtual impedance drop and the inverter output current. The most common implementation is shown in Figure 3.7.

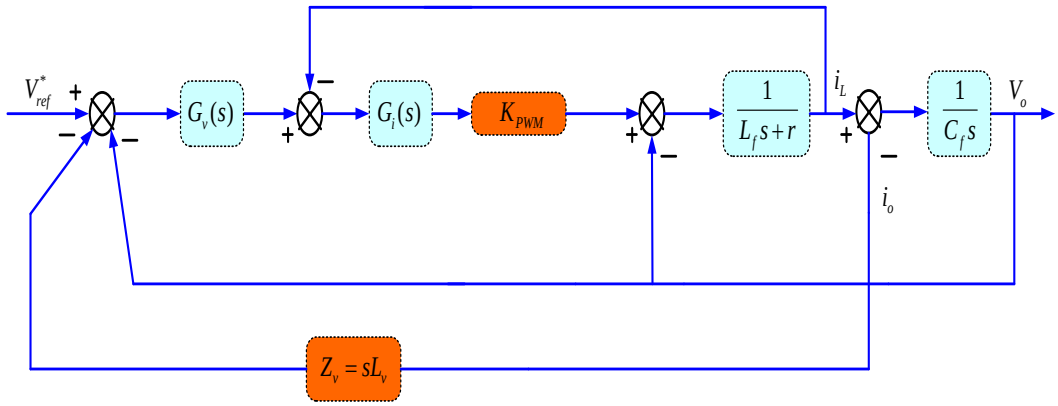

Figure 3.8: Virtual inductance control diagram

In the conventional droop control method, the mismatch of the output impedance of the inverter and the line impedance affects the distribution of the load power. In order to improve the effect of power sharing, the concept of virtual impedance was proposed [Xiongfei et al., (2015), Guerrero et al., (2005), Qinghai et al., (2014)]. The virtual impedance method control block diagram is shown in Figure 3.8.

The droop control strategy based on virtual impedance includes three nested loops.

The inner loop is a dual loop consisting of current and voltage loop. The intermediate link introduces a virtual impedance, forcing the equivalent output impedance of the DG inverter to achieve better power sharing. The outer loop is a power loop, where active and reactive powers are calculated[Chunxue and Zhengxi (2012), Guerrero et al., (2005)].This method can achieve accurate power sharing, has better dynamic modification performance and is suitable for inductive line impedance conditions.

Virtual impedance control has become a necessary condition for multi voltage source DG inverter operated in parallel for normal operation in the microgrid system. Equivalent output impedance of the DG inverters is affected by multiple factors, filter parameters, voltage and current control loop parameters, the differences of these factors led to inconsistencies of power sharing between the parallel DG inverters[Ruiqi et al., (2014), Guerrero et al., (2005), Guerrero et al., (2007)]. The given voltage reference changes after the virtual inductance has been added and the output voltage equation is given by:

$$V_{ref} = V_{ref}^{*} - Z_{vir} i_o \tag{3.6.1}$$

$$V_o = G_i(s)G_v(s)V_{ref}^{*} - [G_i(s)G_v(s)\,Z_{vir}(s) + Z_o(s)]i_o \tag{3.6.2}$$

Virtual inductor is expressed as:

$$Z_{vir} = sL_v, Z_o(s) = \frac{B_1 s^2 + B_2 s}{B_3 s^3 + B_4 s^2 + B_5 s + B_6} \tag{3.6.3}$$

$$\begin{aligned} B_1 &= L + L_v K_{pi} K_{pwm} K_{pv} \\ B_2 &= r + K_{pi} K_{pwm} + L_v K_{pi} K_{pwm} K_{vi} \\ B_3 &= LC, B_4 = K_{pi} K_{pwm} C + rc \\ B_5 &= K_{pi} K_{pwm} K_{vi} \\ B_6 &= K_{pi} K_{pwm} K_{vi} \end{aligned} \tag{3.6.4}$$

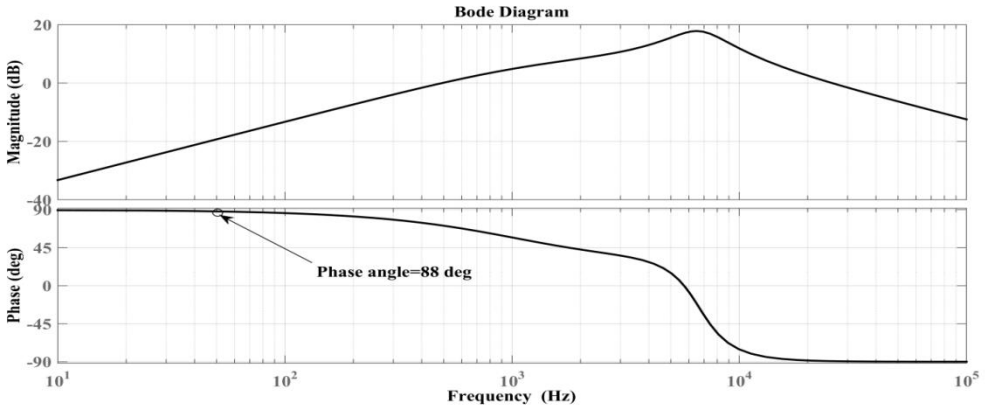

Figure 3.9: Bode diagram of inverter output impedance with virtual inductor.

If the line impedance is inductive, virtual inductors are added the control loop of the *P-f/Q-V* droop control to improve the power decoupling effect. Impedance angle at 50 Hz is 88° as shown in the Figure 3.9. The parallel inverter output impedance tends to more inductive, which has a major role in improving the power sharing.

3.7 SIMULATION RESULTS

In order to verify the feasibility of the direct and reverse droop control. Simulation model of DG inverter is built in MATLAB/SIMULINK and parameters are shown in Appendix.

Case 1: Power sharing analysis of direct (P-f/Q-V), reverse (P-V/Q-f) droop control under inductive line impedance with constant power load.

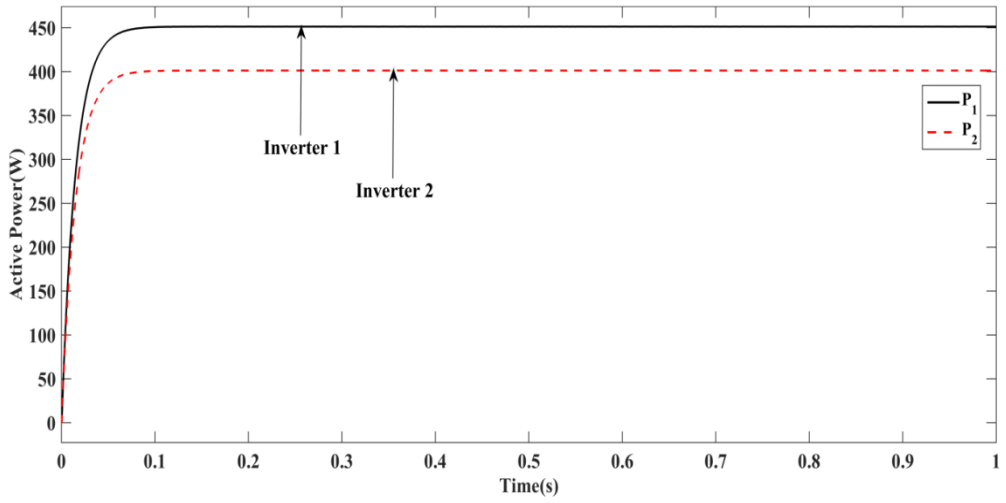

Figure 3.10: Active power sharing using reverse droop control under inductive line impedance.

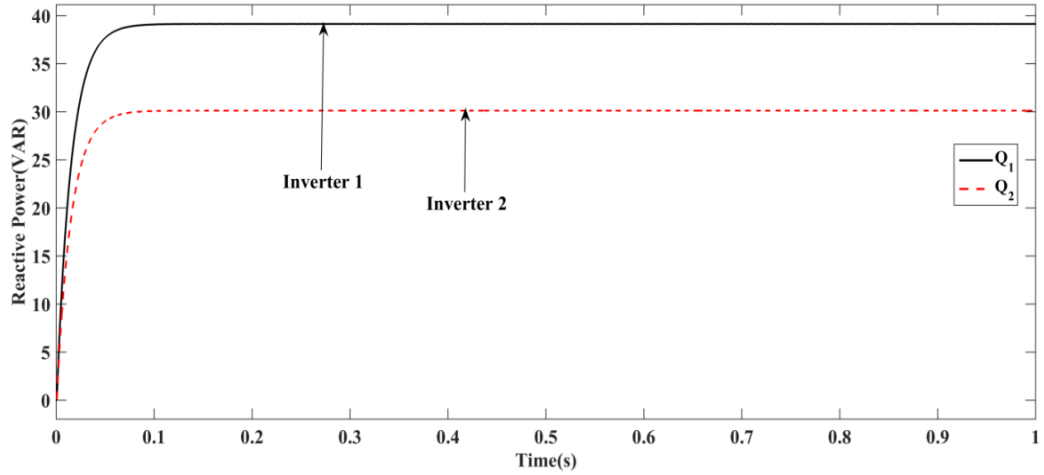

Figure 3.11: Reactive power sharing using reverse droop control under inductive line impedance.

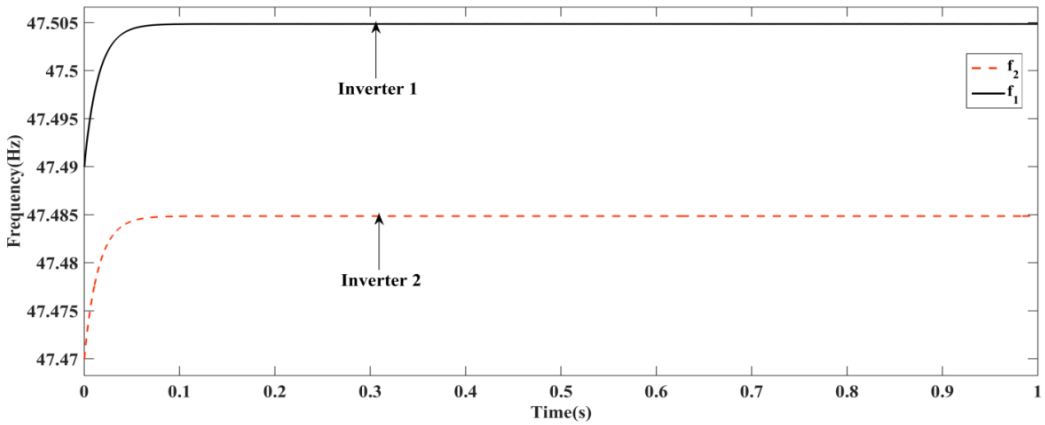

Figure 3.12: Parallel DG inverters output frequency using reverse droop conrol under inductive line impedance.

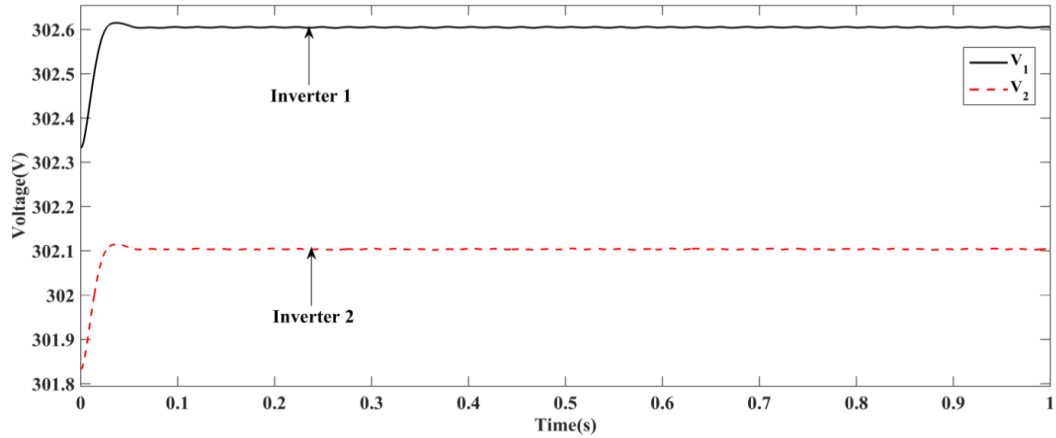

Figure 3.13: Parallel DG inverters output voltage amplitude using reverse droop control under inductive line impedance.

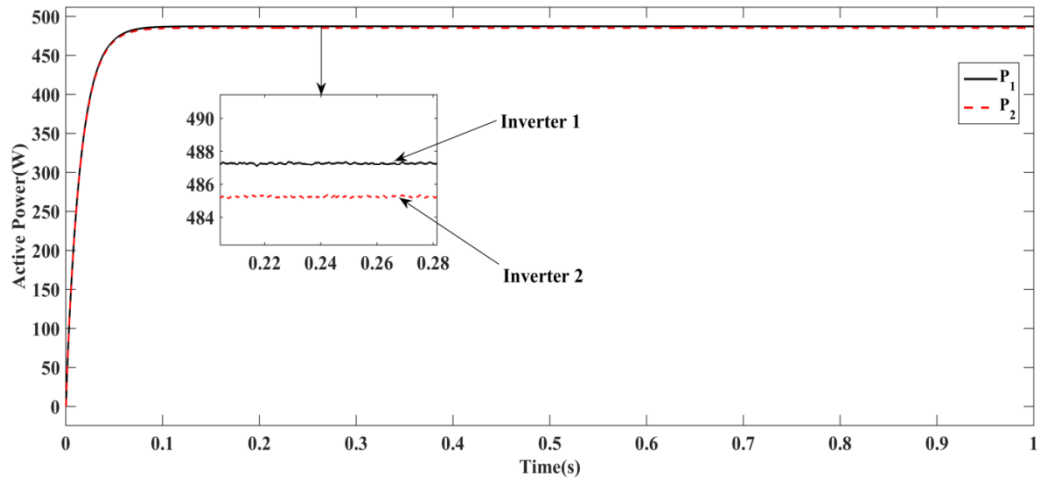

Figure 3.14 : Active power sharing using direct droop control under inductive line impedance.

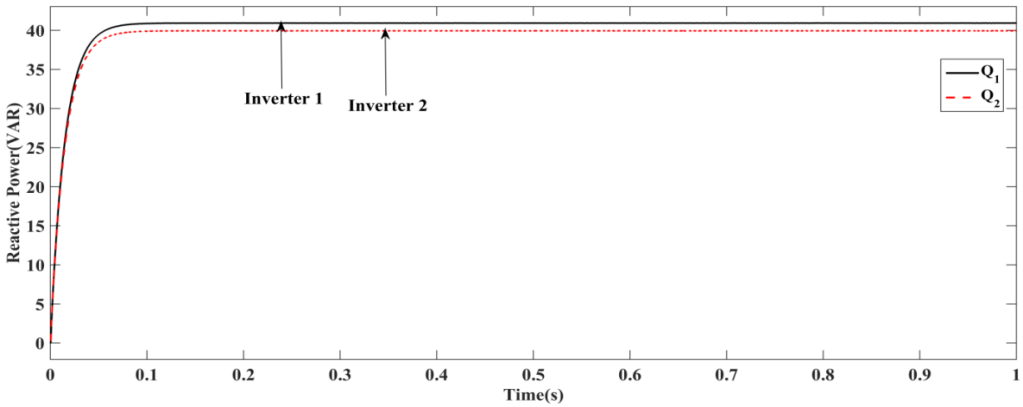

Figure 3.15: Reactive power sharing using direct droop control under inductive line impedance.

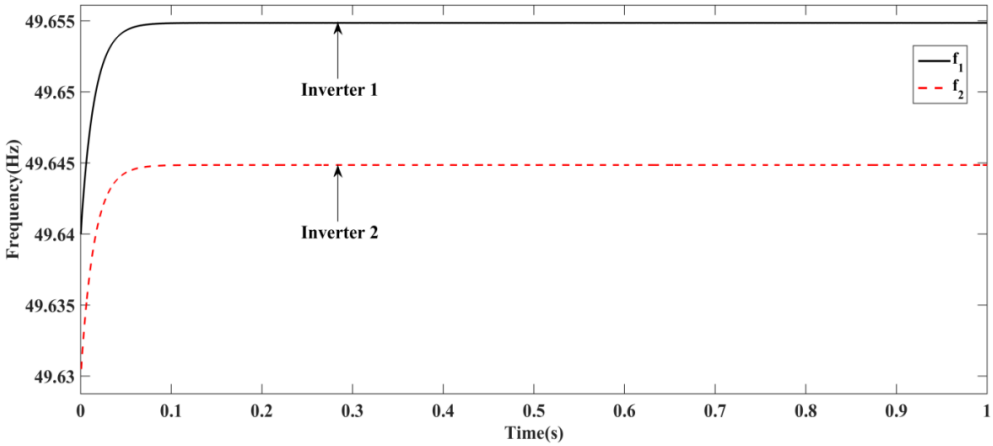

Figure 3.16: Parallel DG inverters output frequency using direct droop control under inductive line impedance.

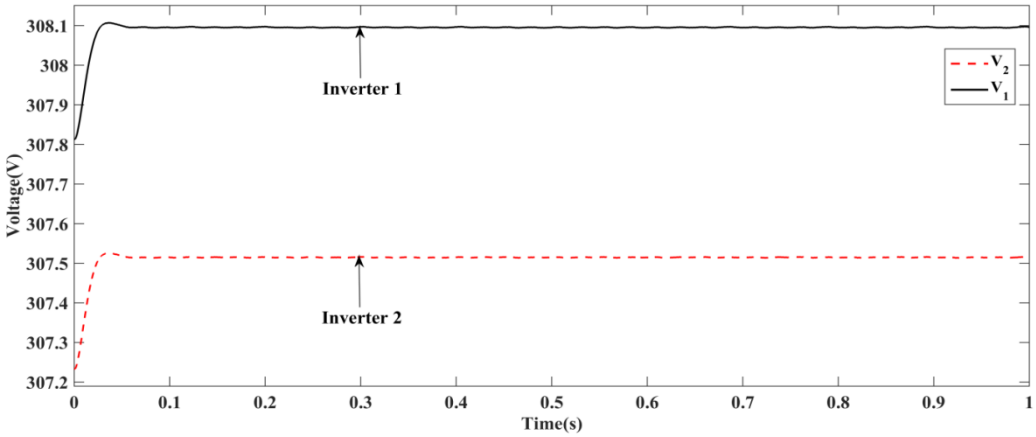

Figure 3.17: Parallel DG inverters output voltage amplitude using direct droop control under inductive line impedance.

Power sharing of parallel DG inverters is investigated with common load of P_{load}=1000W,Q_{load}=100VAR and line impedance of $R_{1Line} + jX_{1Line}$=0.002+j0.3Ω, $R_{2Line} + jX_{2Line}$=0.003+j0.4Ω. Intially reverse droop control is applied to the parallel DG inverters and output power of parallel inverters does not reach to a given proportional load sharing, because of the poor decoupling of power as shown in the Figure 3.10, 3.11. When the line impedance is inductive reverse droop control cannot realize the equalization of active and reactive power.

The parallel inverter voltage amplitude drop is significantly more compared to the given rated voltage amplitude of 311V and frequency variation of parallel inverters is more than ±0.6Hz compared with rate value of frequency 50Hz. so, when the line impedance is inductive with reverse droop control, frequency accuracy is reduced, the voltage amplitude drop rate exceeds the specified range as shown in the Figure 3.12,3.13. Now with the same parameters direct droop control is applied to the each DG inverters is able to share the load of active power P_1=486 W,P_2=484 W as shown in the figure 3.14.and reactive power of Q_1=39 VAR,Q_2=37 VAR as shown in the Figure 3.15.Frequency and voltage amplitude varaiations of DG inverters has a small deviation,frequency fluctations is not greater than 1% as shown in the Figure 3.16 and voltage amplitude has a slight decline V_1=308.1 V,V_2=307.5 V which is not greater than 5% as shown in the Figure 3.17.

Case 2: Power sharing analysis of direct droop control under inductive line impedance with step change in load.

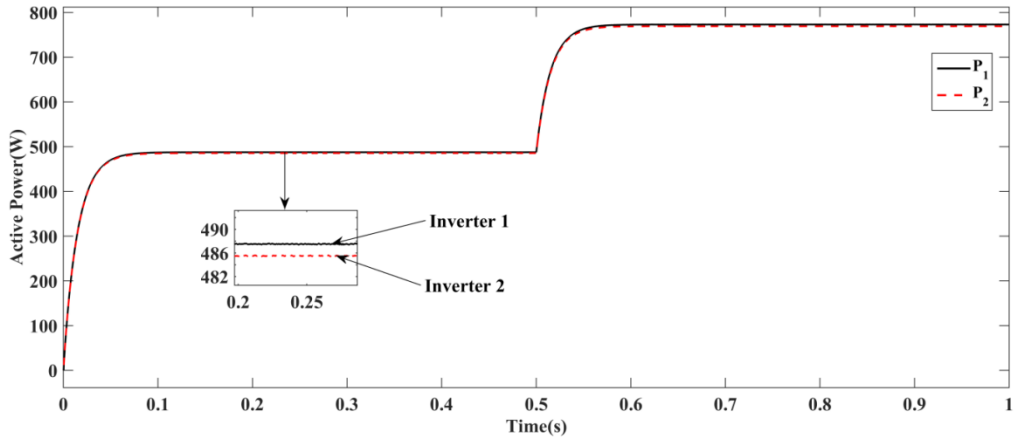

Figure 3.18: Active power sharing using direct droop control under inductive line impedance with step change in load.

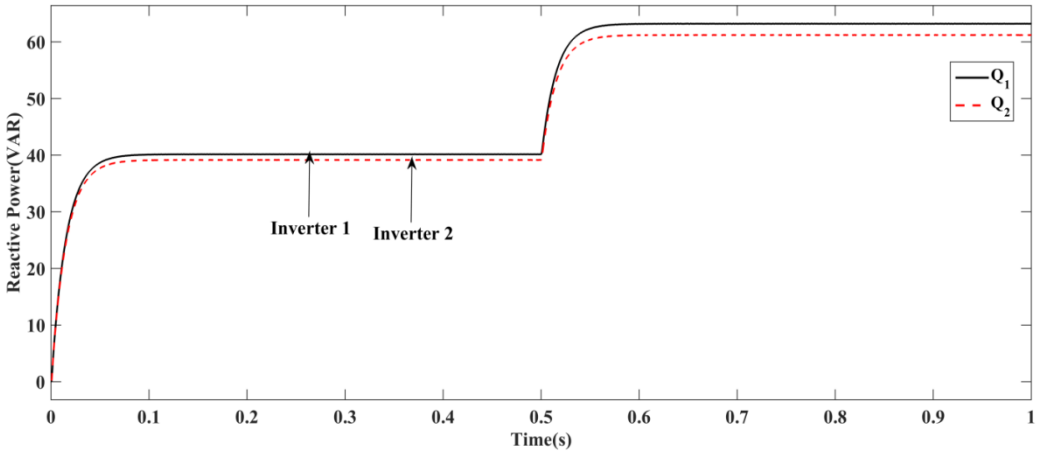

Figure 3.19: Reactive power sharing using direct droop control under inductive line impedance with step change in load.

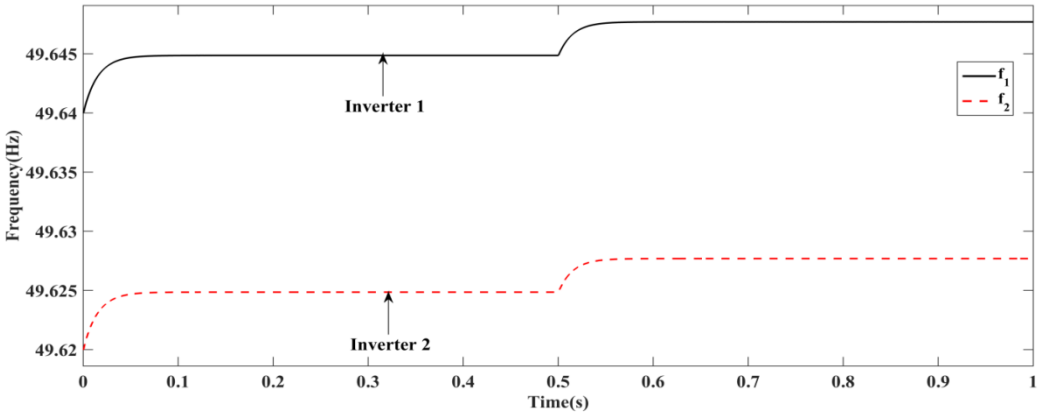

Figure 3.20: Parallel DG inverters output frequency using direct droop control under inductive line impedance with step change in load.

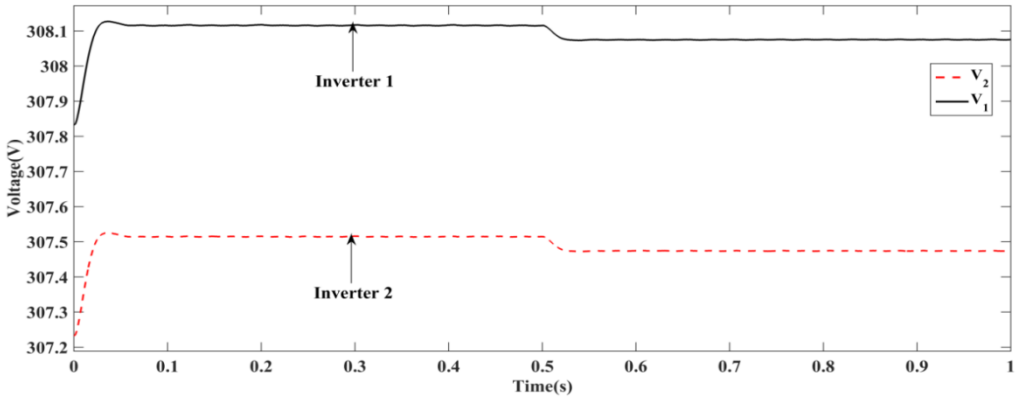

Figure 3.21: Parallel DG inverters output voltage amplitude using direct droop control under inductive line impedance with step change in load.

Power sharing of parallel DG inverters is investigated with common load of P_{load}=1000W, Q_{load}=100VAR and at 0.5 s sudden local load value of P_{load} = 600 W, Q_{load} = 50 VAR is added to verify the dynamic response and line impedance of $R_{1Line} + jX_{1Line}$ =0.002+j0.3Ω, $R_{2Line} + jX_{2Line}$ =0.003+j0.4Ω. Direct droop control is applied to the each DG inverters is able to share the load of active power P_1=486 W,P_2=484 W as shown in the Figure 3.18 and reactive power of Q_1=39 VAR,Q_2=37 VAR as shown in the Figure 3.19 and at load change at 0.5s P_1=772 W,P_2=768 W, Q_1=62 VAR,Q_2=59 VAR. Frequency and voltage amplitude variations of DG inverters has a small deviation, frequency fluctuations is not greater than 1% as shown in the Figure 3.20 and voltage amplitude has a slight decline V_1=308.1 V,V_2=307.5 V which is not greater than 5% as shown in the Figure 3.21.

Case 3: Power sharing analysis of direct droop control under inductive line impedance with frequent changes in load.

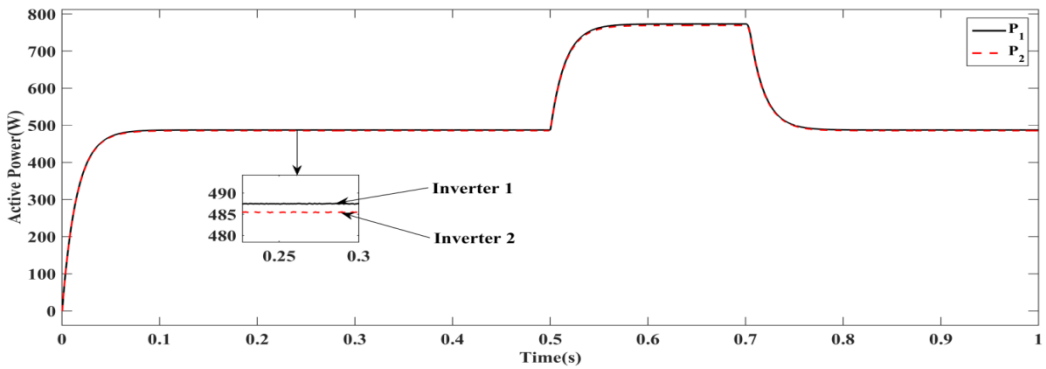

Figure 3.22: Active power sharing using direct droop control under inductive line impedance with frequent changes in load.

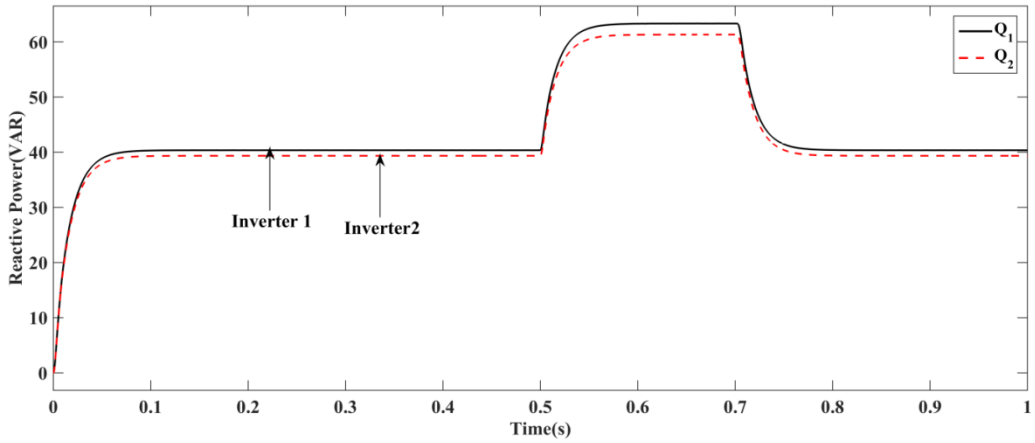

Figure 3.23: Reactive power sharing using direct droop control under inductive line impedance with frequent changes in load.

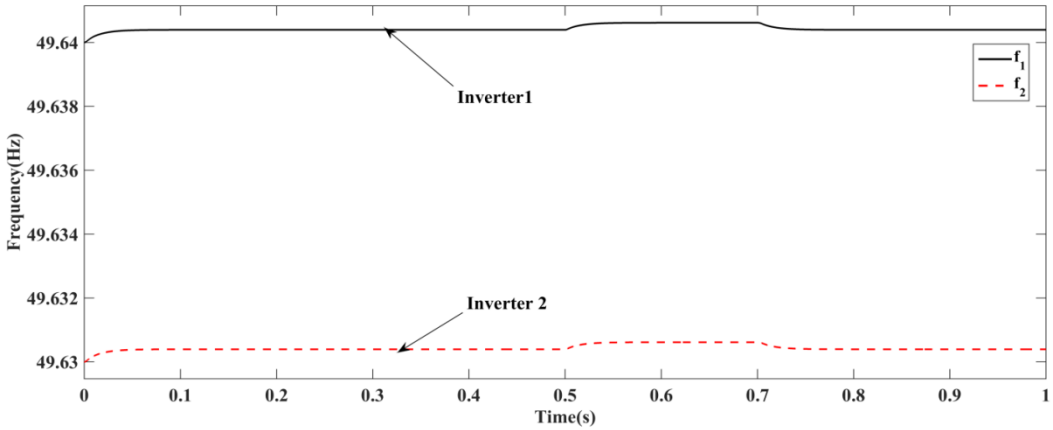

Figure 3.24: Parallel DG inverters output frequency using direct droop control under inductive line impedance with frequent changes in load.

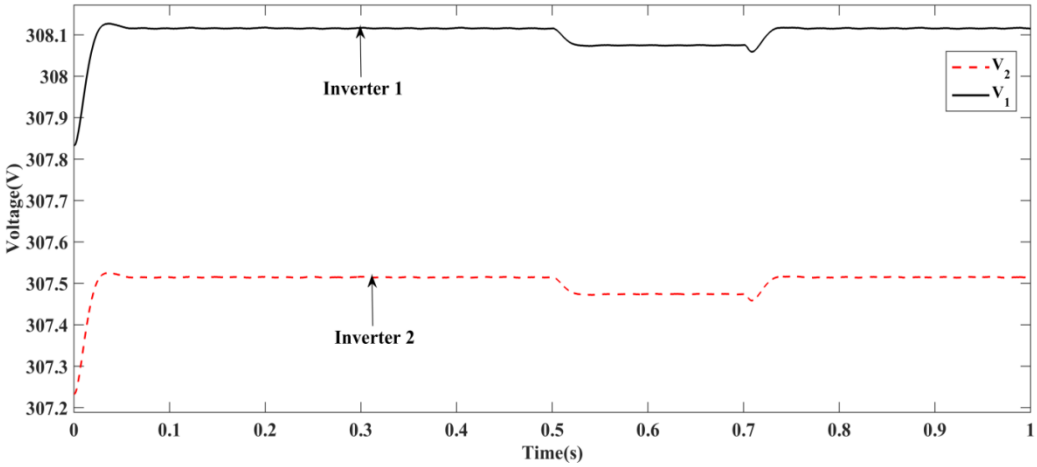

Figure 3.25: Parallel DG inverters output voltage amplitude using direct droop control under inductive line impedance with frequent changes in load.

Power sharing of parallel DG inverters is investigated with common load of P_{load}=1000W, Q_{load}=100VAR and at 0.5 s sudden local load value of P_{load} = 600 W, Q_{load} = 50 VAR is added and removed at 0.7s to verify the dynamic response and line impedance of $R_{1Line} + jX_{1Line}$ =0.002+j0.3Ω, $R_{2Line} + jX_{2Line}$ =0.003+j0.4Ω.

Direct droop control is applied to the each DG inverters is able to share the load of active power P_1=486 W,P_2=484 W as shown in the Figure 3.22 and reactive power of Q_1=39 VAR,Q_2=37 VAR as shown in the Figure 3.23 and at load change at 0.5s P_1=772 W,P_2=768 W, Q_1=62 VAR,Q_2=59 VAR.

Frequency and voltage amplitude variations of DG inverters has a small deviation, frequency fluctuations is not greater than 1% as shown in the Figure 3.24 and voltage amplitude has a slight decline V_1=308.1 V,V_2=307.5 V which is not greater than 5% as shown in the Figure 3.25.

Case 4: Power sharing analysis of direct droop control with virtual inductors under inductive line impedance.

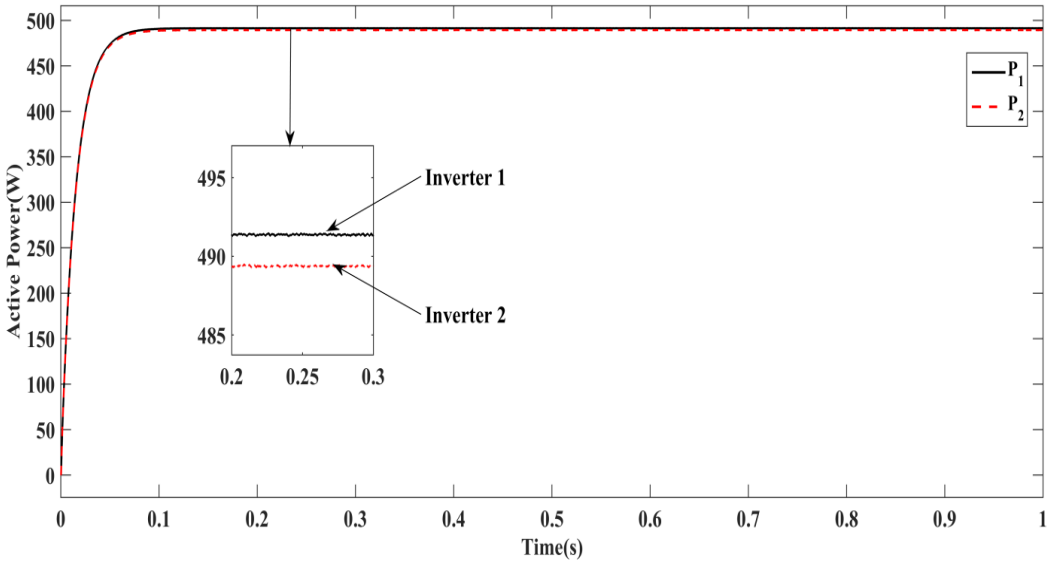

Figure 3.26: Active power sharing using direct droop control with virtual inductors under inductive line impedance.

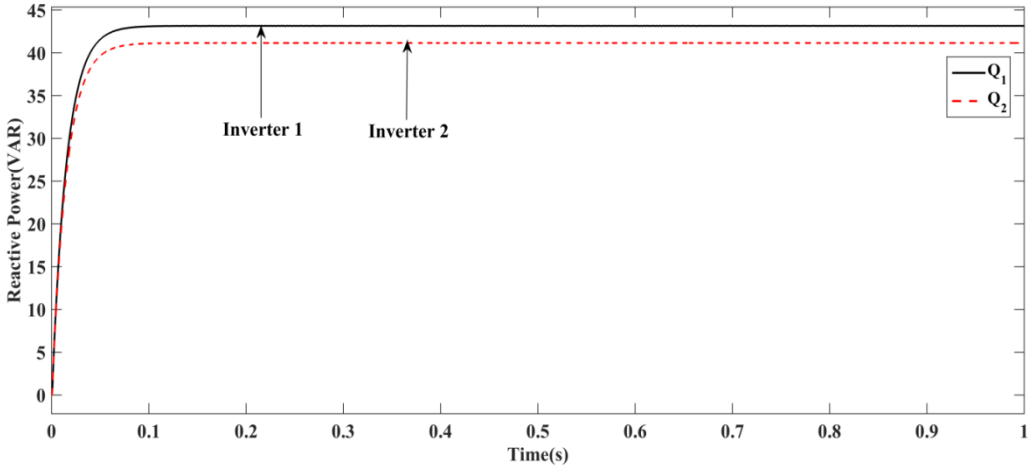

Figure 3.27: Reactive power sharing using direct droop control with virtual inductors under inductive line impedance.

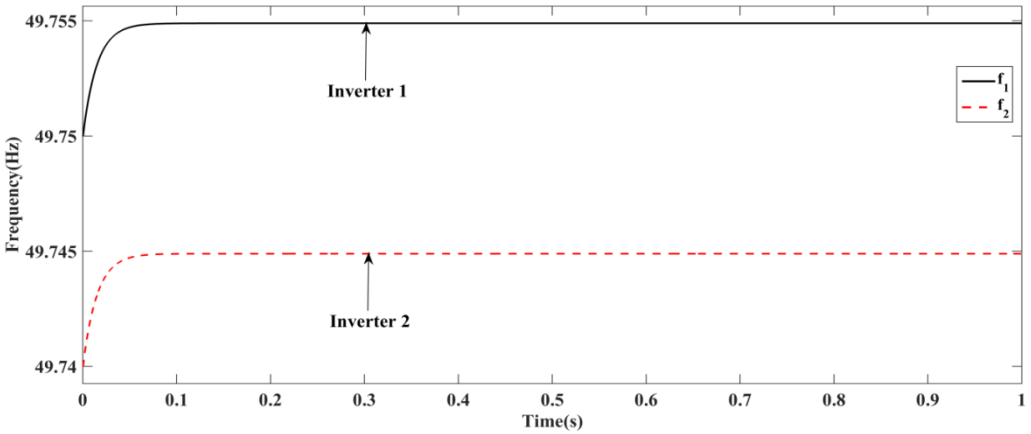

Figure 3.28: Parallel DG inverters output frequency using direct droop control with virtual inductors under inductive line impedance.

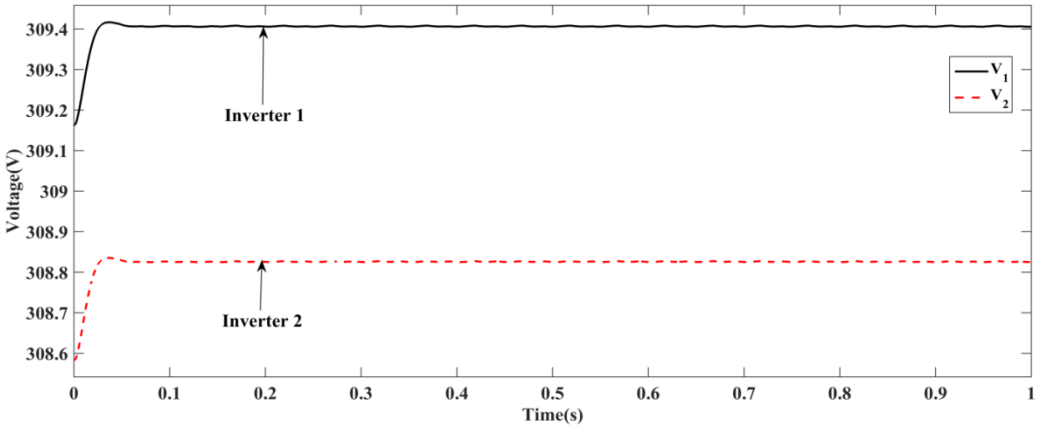

Figure 3.29: Parallel DG inverters output voltage amplitude using direct droop control with virtual inductors under inductive line impedance.

Power sharing of parallel DG inverters is investigated with common load of P_{load}=1000W,Q_{load}=100VAR and line impedance of $R_{1Line} + jX_{1Line}$ =0.002+j0.3Ω, $R_{2Line} + jX_{2Line}$ =0.003+j0.4Ω. Direct droop control based on virtual inductors can reduce the influence of the line impedance difference on the parallel inverters by setting the total output impedance of the DG inverters to be inductive, which improves decoupling of power and improves the proportional load sharing P_1=490 W, P_2=488 W, Q_1=43 VAR, Q_2=41 VAR as shown in the Figure 3.26, 3.27 and frequency variation of DG inverters is within the range of 49.74 Hz to 49.75 Hz, the maximum fluctuation of 0.004 Hz as shown in the Figure 3.28. Voltage variation of DG inverters is V_1=309.4 V, V_2=308.8 V as shown in the Figure 3.29. Thus, the direct droop control with virtual inductors improves power sharing compared to direct droop control.

Case 5: Power sharing analysis of direct droop control with virtual inductors under inductive line impedance with step change in load.

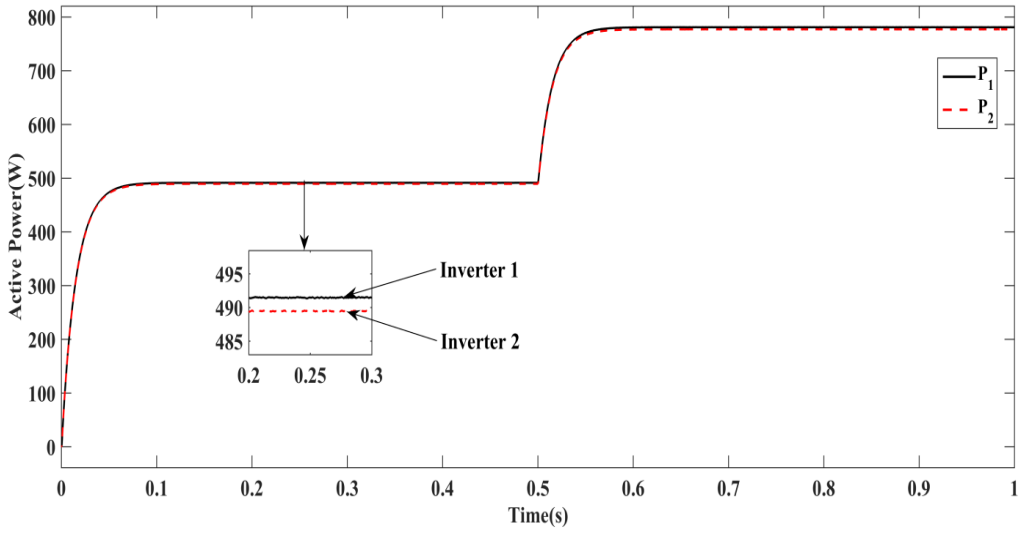

Figure 3.30: Active power sharing using direct droop control with virtual inductors under inductive line impedance with step change in load.

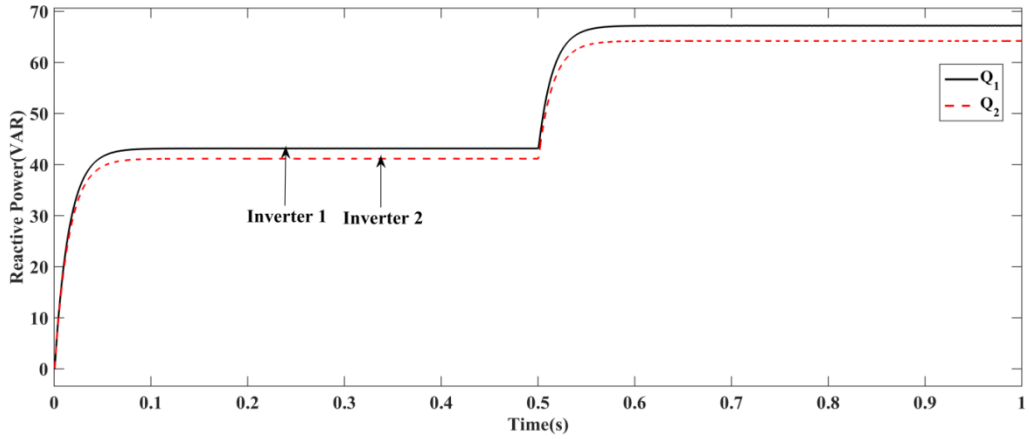

Figure 3.31: Reactive power sharing using direct droop control with virtual inductors under inductive line impedance with step change in load.

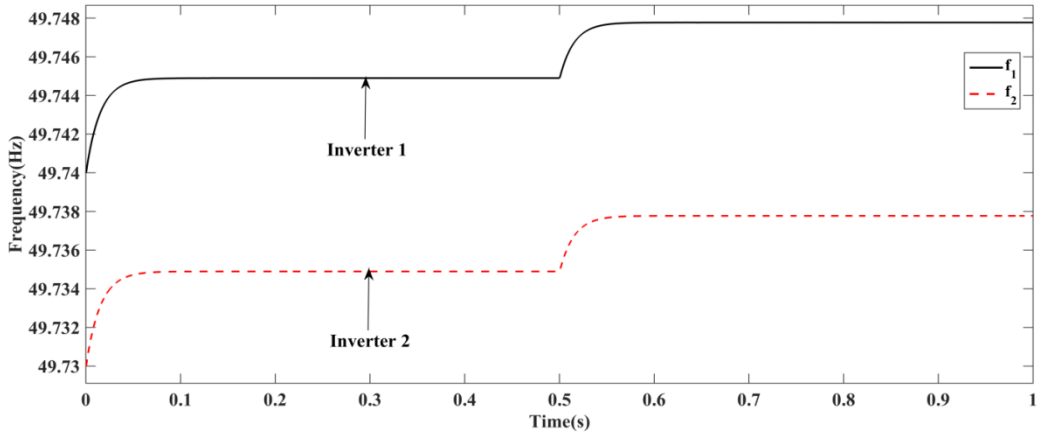

Figure 3.32: Parallel DG inverters output frequency using direct droop control with virtual inductors under inductive line impedance with step change in load.

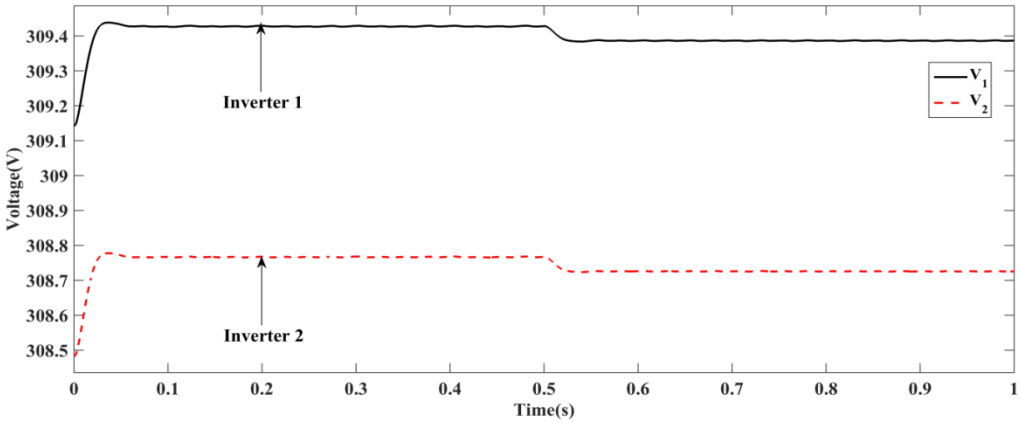

Figure 3.33: Parallel DG inverters output voltage amplitude using direct droop control with virtual inductors under inductive line impedance with step change in load.

Power sharing of parallel DG inverters is investigated with common load of P_{load}=1000W, Q_{load}=100VAR and at 0.5 s sudden local load value of P_{load} = 600 W, Q_{load} = 50 VAR is added to verify the dynamic response and line impedance of $R_{1Line} + jX_{1Line}$ =0.002+j0.3Ω, $R_{2Line} + jX_{2Line}$ =0.003+j0.4Ω. Direct droop control based on virtual inductors can reduce the influence of the line impedance difference on the parallel inverters by setting the total output impedance of the DG inverters to be inductive, which improves decoupling of power and improves the proportional load sharing P_1=490 W, P_2=488 W, Q_1=43 VAR, Q_2=41 VAR and at load change at 0.5 s, P_1=780 W, P_2=776 W, Q_1=67 VAR, Q_2=64 VAR as shown in the Figure 3.30,3.31 and frequency variation of DG inverters is within the range of 49.73 Hz to 49.74 Hz, the maximum fluctuation of 0.004 Hz as shown in the Figure 3.32. Voltage variation of DG inverters is V_1=309.4 V, V_2=308.9 V as shown in the Figure 3.33. Thus, the direct droop control with virtual inductors improves power sharing compared to direct droop control.

Case 6: Power sharing analysis of direct droop control with virtual inductors under inductive line impedance with frequent changes in load.

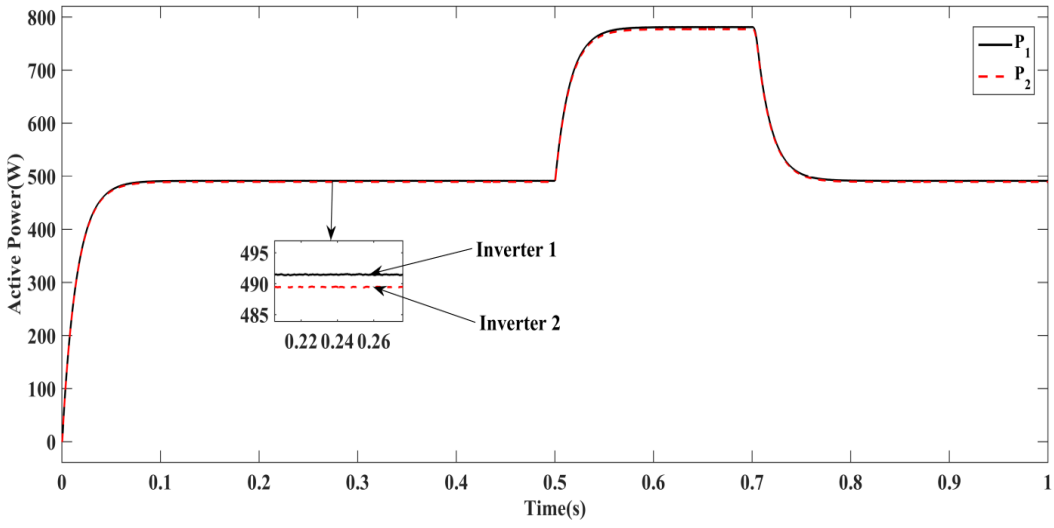

Figure 3.34: Active power sharing using direct droop control with virtual inductors under inductive line impedance with frequent changes in load.

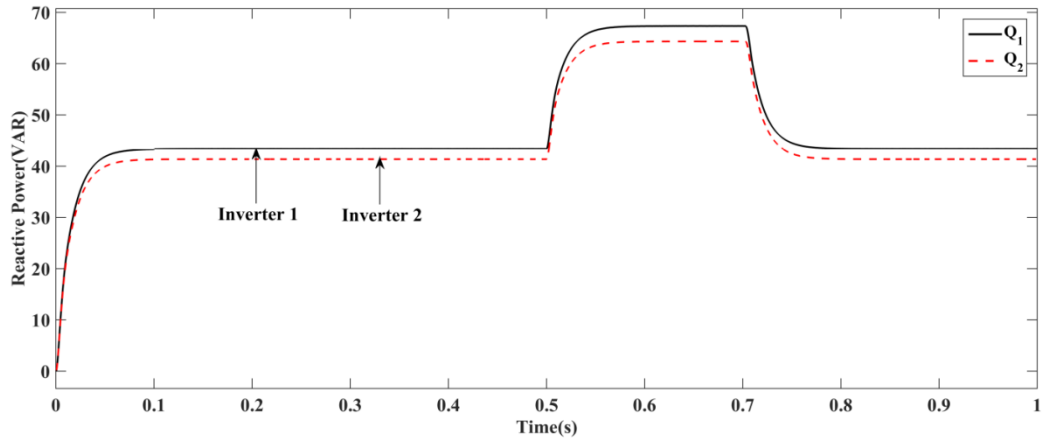

Figure 3.35: Reactive power sharing using direct droop control with virtual inductors under inductive line impedance with frequent changes in load.

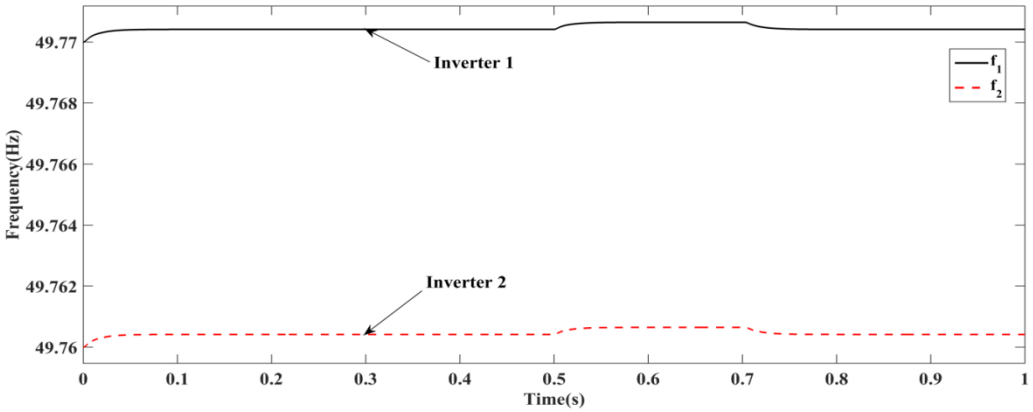

Figure 3.36: Parallel DG inverters output frequency using direct droop control with virtual inductors under inductive line impedance with frequent changes in load.

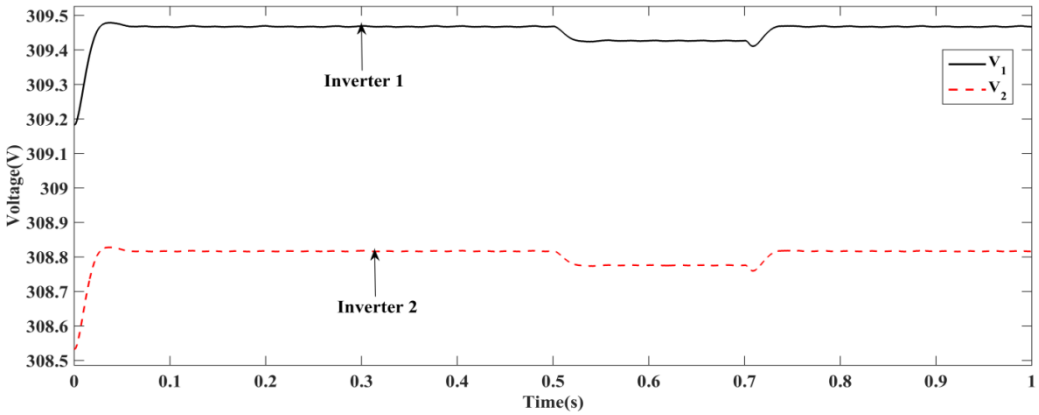

Figure 3.37: Parallel DG inverters output voltage amplitude using direct droop control with virtual inductors under inductive line impedance with frequent changes in load.

Power sharing of parallel DG inverters is investigated with common load of P_{load}=1000W, Q_{load}=100VAR and at 0.5 s sudden local load value of P_{load} = 600 W, Q_{load} = 50 VAR is added and removed at 0.7s to verify the dynamic response and line impedance of $R_{1Line} + jX_{1Line}$ =0.002+j0.3Ω, $R_{2Line} + jX_{2Line}$ =0.003+j0.4Ω. Direct droop control based on virtual inductors can reduce the influence of the line impedance difference on the parallel inverters by setting the total output impedance of the DG inverters to be inductive, which improves decoupling of power and improves the proportional load sharing P_1=490 W, P_2=488 W, Q_1=43 VAR, Q_2=41 VAR and at load change at 0.5 s, P_1=780 W, P_2=776 W, Q_1=67 VAR, Q_2=64 VAR as shown in the Figure 3.34,3.35 and frequency variation of DG inverters is within the range of 49.76 Hz to 49.77 Hz, the maximum fluctuation of 0.004 Hz as shown in the Figure 3.36. Voltage variation of DG inverters is V_1=309.4 V, V_2=308.9 V as shown in the Figure 3.37. Thus, the direct droop control with virtual inductors improves power sharing compared to direct droop control.

3.8 CONCLUSION

Analyzing the power transmission characteristics of distributed generation units in microgrid, the direct droop control is deduced and the limitation of direct droop controller is analyzed. Secondly, on the basis of this, the structure of the general droop controller and the conditions and characteristics of proportionally sharing the load capacity in the inverter parallel system using the controller are explained in detail. In order to match the total output impedance of the DG inverter in parallel operation, the direct droop control strategy based on virtual inductance is used to improve the total output impedance characteristic of DG inverter and the influence of virtual inductance on the total output impedance of inverter is analyzed in detail and the power distribution between inverters is improved. The simulation results verify the effectiveness of the adopted control strategy.

Chapter 4

4 REVERSE DROOP CONTROL (P-V/Q-F) OF PARALLEL DISTRIBUTED GENERATION INVERTERS IN MICROGRID

4.1 INTRODUCTION

Microgrids are small power distribution systems which comprise various micro sources, energy storage systems, energy conversion devices, loads, control and protection systems. The microgrid itself is a self-contained system capable of self-control, self-protection and self-management [Xinfa et al.,(2014)]. It can also be connected to the utility grid as a whole through the point of common coupling, operating in islanding or grid-connected mode according to the need of grid system and user loads [Ming et al., (2009)].

As the name implies, peer-to-peer control means that every DG in the microgrid system shares the same control position. Each DG can exert control based on local measurements instead of communications equipment [Pogaku et al., (2007)]. Droop control method is usually adopted in each DG, which can share the random fluctuation of load and energy automatically. It can realize microgrids plug and play at the same time. When the microgrid's operation mode is switched under droop control, there is no need to change the control method [Long (2014)]. The conventional droop control method uses the P-f and Q-V characteristic curves to emulate the external characteristic of the synchronous motor in the utility grid [Haoran et al., (2015)]. So that DGs adjust the amplitude and frequency of output voltage according to their own droop control curves in order to achieve rational allocation of power.

The virtual inductance is introduced to the direct droop control for better power decoupling control [Su et al., (2013), Linchuan et al., (2017)]. However, the effect of virtual impedance on the output voltage drop is not considered and the reactive power distribution issues with the unbalanced line impedance have not been solved in these papers. As for the shortcoming of conditional virtual impedance method, a virtual negative impedance method was proposed to make the total output impedance purely inductive, offsetting the resistive component of impedance and restraining the system

current circulation, but without enhancements of voltage quality and power distribution accuracy [Jin et al., (2016)]. In another approach [Junli et al., (2015)], dynamic virtual impedance is adapted to makes it change with the load current and voltage drop, thus enhancing the power quality. But the unbalanced line impedance has been neglected. In order to reduce reactive power sharing errors in direct droop control, a virtual impedance optimization method based on the minimization of system global reactive power sharing error was proposed in [Yixin et al., (2016)]. Nevertheless, the optimization calculation of the power sharing error function is complicated and the effect of virtual impedance on the output voltage is not considered in this paper. In [Yuqin et al., (2015)], the output voltage is regulated and fine adjustment to accommodate changes of load power, resulting good sharing of the load power and better power quality. However, the article does not consider the situation that the rated capacities of inverters are different.

The line impedance is predominantly resistive for low-voltage microgrid [Dawei et al., (2010)], where P-V/Q-f droop control strategy is more suitable. P-V/Q-f droop control strategy, which is very similar to the direct droop control, utilizing the droop characteristics of active power-voltage (P-V) and reactive power-frequency (Q-f) when the line impedance is resistive and is easy to implement with low loss and small frequency variation [Susu (2013)]. Similarly, this control method also has an active power sharing problem when the line impedance is unbalanced [Hou et al., (2016)]. In [Yan et al., (2016)], virtual impedance is added on the basis of droop control so that the total output impedance is matched with the rated capacity of the inverter to improve the power distribution. However, the effect of the virtual impedance on the output voltage needs to be reduced by modifying the droop characteristic curve.

The low-voltage microgrid system with multiple distributed generation sources, an improved Reverse(P-V/Q-f) droop control strategy based on the introduction of virtual resistance is adopted, which can achieve a reasonable sharing of power according to DGs capacities and guarantee a certain output power quality in the condition of resistive line impedances.

4.2 BLOCK DIAGRAM OF REVERSE DROOP CONTROL (P-V/Q-f)

Microgrid as a whole is composed of a voltage source inverters using reverse droop control as shown in the Figure 4.1, then assuming that the DG inverter dc bus voltage V_{dc} essentially unchanged.L_{f1},L_{f2} is a three phase filter inductor, r_1,r_2 filter inductor equivalent resistance, C_{f1},C_{f2} is a three phase filter capacitor.

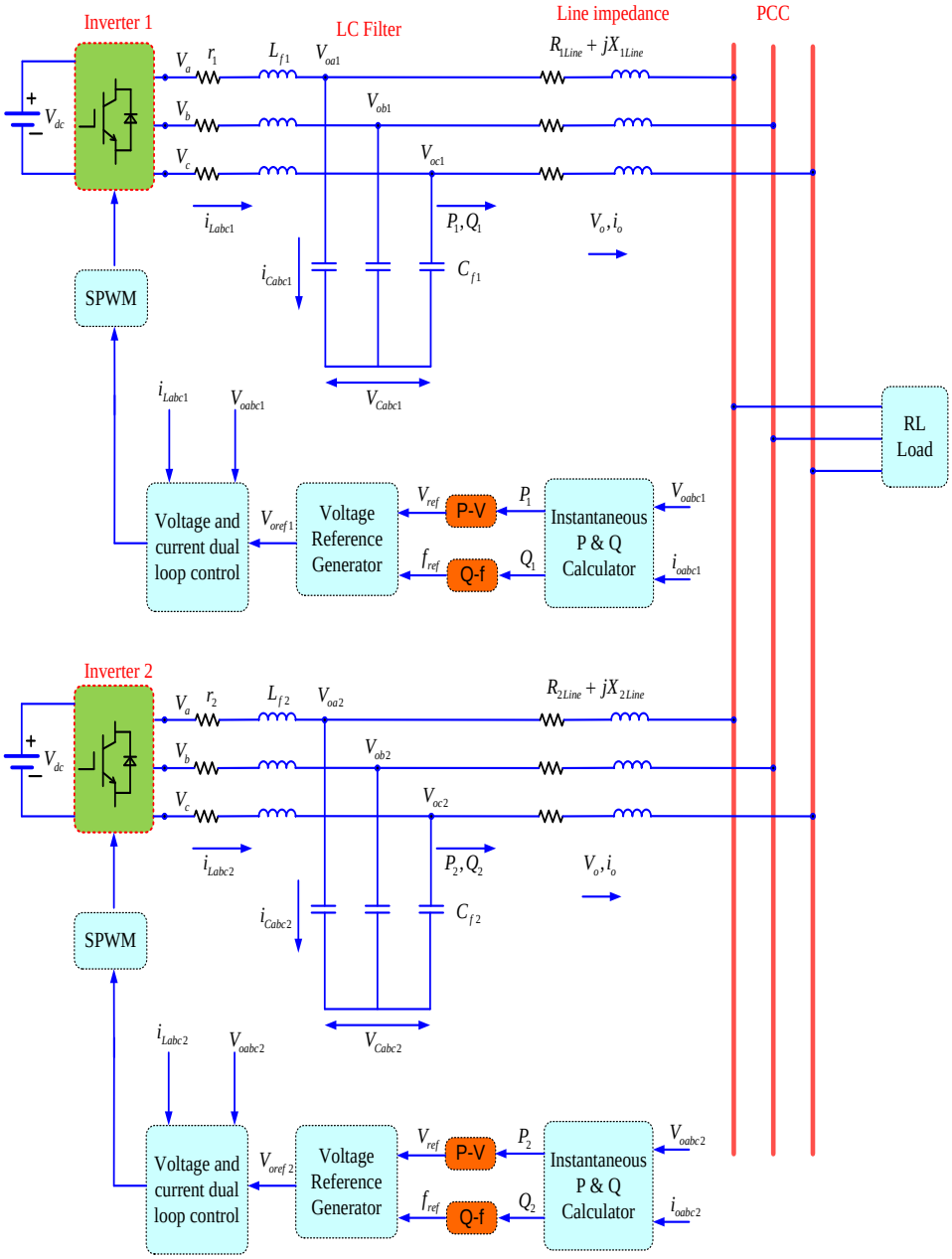

Figure 4.1: Block diagram of three phase parallel DG inverter in microgrid using reverse droop control.

Comprehensive equivalent line impedance of the transmission line of two DG inverters is expressed as $Z_1=R_1+jX_1$ $Z_2=R_2+jX_2$.PCC represents a common connection point for DG inverters.It is necessary to provide voltage and frequency support for microgrid operation and distribute load reasonably[Chen (2014), Wang (2014), Zhongming (2015)].

Under the condition of no communication, the power distribution is achieved by reverse droop control to regulate the parallel system of multiple DG inverters. The principle is: Each inverting DG source detects its own output power and compares it with the load power and then obtains the reference value of the output voltage amplitude and frequency according to the droop characteristics, so that the voltage amplitude and frequency are continuously adjusted in a loop and finally each DG inverter is realized. The DG source output power is consistent with the load power[Xumiao (2015), Zhang (2015)].

4.3 CONTROL DIAGRAM OF REVERSE DROOP CONTROL (P-V/Q-F)

In a microgrid, a reverse droop control is used to adjust the voltage and frequency of the DG inverters output, so that the micro-grid can operate under different load requirements. As can be seen from Figure 4.2, where L_f is the filter inductor, C_f is the filter capacitor, r is the filter inductor equivalent resistance and Z_{Load} is the load impedance, the reverse droop control model of microgrid can be divided into two parts: voltage and current loop control model and power droop control model. First, the output voltage and current of the microgrid power supply are obtained by sampling the DG inverter module. The output power of the microgrid power supply is obtained by the power calculation unit and the low-pass filter and then calculated according to the active power droop controller and the reactive power droop controller respectively. The reference voltage values V_{dref} and V_{qref} is finally adjusted by the voltage PI control and i_{dref} and i_{qref} are adjusted by the current P control to obtain controllable sinusoidal modulation signal m to the DG inverter[Shang (2013), Yajuan (2012)] .

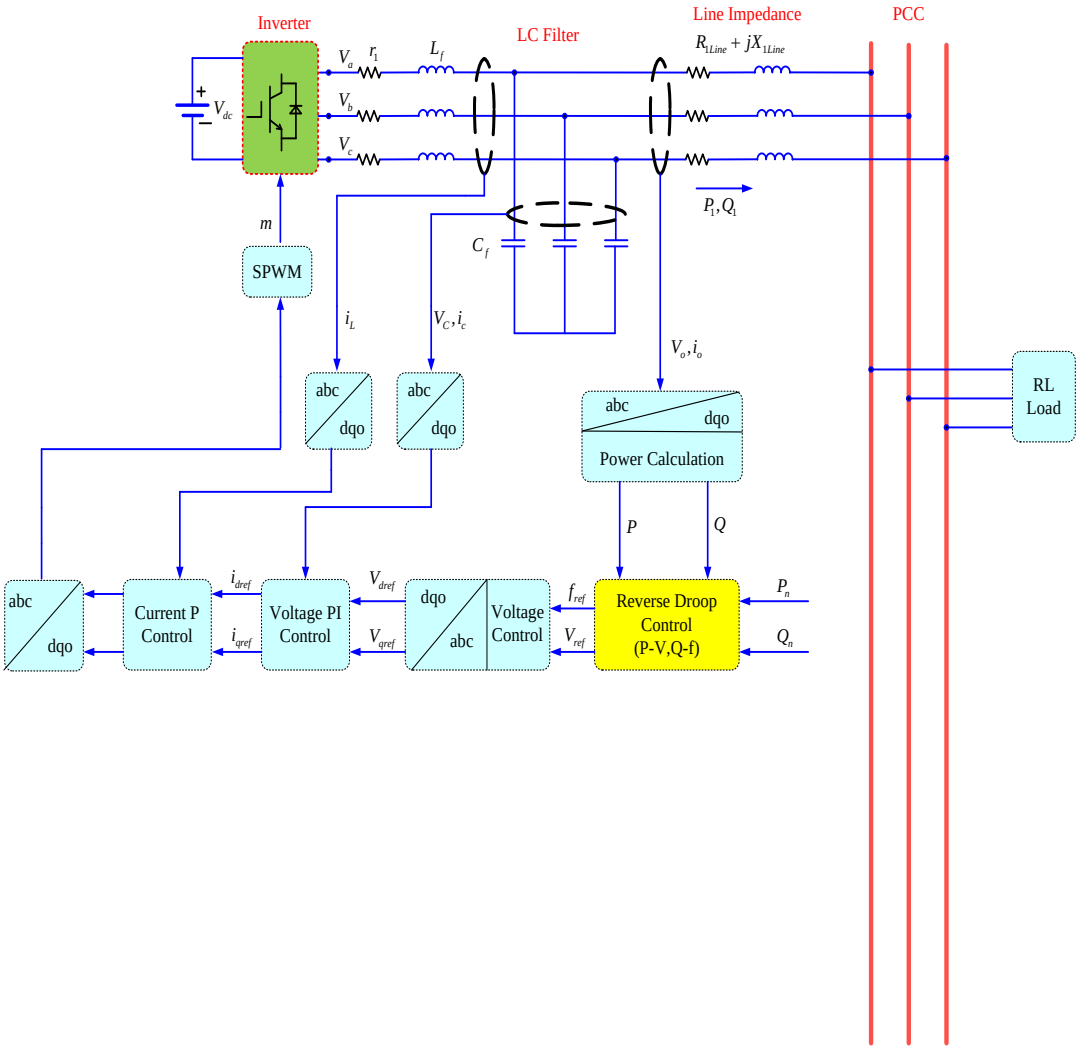

Figure 4.2 Control diagram of reverse droop control

4.4 PROPORTIONAL LAOD SHARING OF PARALLEL DISTRIBUTED GENERATION INVERTERS USING REVERSE DROOP CONTROL

If the load is distributed according to the capacity, the droop co efficient needs to be inversely proportional to the capacity, namely:

$$m_{PV1}P_1 = m_{PV2}P_2 = ... = m_{PVn}P_n \tag{4.5.1}$$

$$n_{Qf1}Q_1 = n_{Qf2}Q_2 = ... = n_{Qfn}Q_n \tag{4.5.2}$$

When the distributed inverter power supply with different capacity is running in parallel, it is necessary to realize the exact load sharing according to the rated capacity, and the condition that the droop coefficient of each inverter is inversely proportional to the rated capacity, namely the equation (4.5.1) and (4.5.2).

However, only by setting the Droop coefficient and the capacity is inversely proportional to the power cannot be accurately allocated; the following is a detailed analysis of the conditions for the accurate distribution of active and reactive power[Zhang (2015), Jinxiao (2013), Xumiao (2015).

(a) Equalization of reactive power

The parallel operation of two DG inverters is analyzed, after stable operation, the working frequency of the two parallel inverters is the same, $f_1=f_2$, therefore, according to the equation (3.2.15), if you want to achieve power according to the proportion of rated capacity accurately, only meet the following two conditions[Zhang (2015), Meiqin (2013), Jinxiao (2013)]:

$$f_1 = f_2 \tag{4.5.3}$$

$$n_{Qf1}Q_1 = n_{Qf2}Q_2 \tag{4.5.4}$$

If the reactive power of the inverter can be divided evenly, the following form can be found:

$$n_{Qf1}\frac{V_1V_o}{R_1}\delta_1 = n_{Qf2}\frac{V_2V_o}{R_2}\delta_2 \tag{4.5.5}$$

If $\delta_1 = \delta_2, V_1 = V_2$,then

$$\frac{n_{Qf1}}{R_1} = \frac{n_{Qf2}}{R_2} \tag{4.5.6}$$

(b) Active power equalization

Under the premise that the rated output voltages of the two inverters are equal and the droop coefficient is inversely proportional to the rated active power, the equation is satisfied[Zhang (2015), Meiqin (2013), Jinxiao (2013)]:

$$V_1 = V_2 \tag{4.5.7}$$

$$m_{PV1}P_1 = m_{PV2}P_2 \tag{4.5.8}$$

According to the formula (4.5.8), if the active power is to be accurately shared according to the rated capacity ratio, it is necessary to satisfy $V_1=V_2$, that is, $\Delta V=0$.

If $\Delta V=0$ is ensured, the active power of the inverter output is accurately divided according to the rated capacity ratio, which must satisfy:

$$\frac{R_1}{m_{PV1}} = \frac{R_2}{m_{PV2}} \tag{4.5.9}$$

$$\delta_1 = \delta_2 \tag{4.5.10}$$

According to the above analysis, under the reverse droop control strategy, the conditions for accurately distributing the active and reactive power according to the rated capacity ratio are satisfied by the equations (4.5.11) , (4.5.12) and (4.5.13), namely:

$$\begin{aligned} &V_1 = V_2 \\ &f_1 = f_2 \\ &m_{PV1}P_1 = m_{PV2}P_2 \\ &n_{Qf1}Q_1 = n_{Qf2}Q_2 \end{aligned} \tag{4.5.11}$$

$$\begin{aligned} &V_1 = V_2 \\ &\frac{R_1}{m_{PV1}} = \frac{R_2}{m_{PV2}} \end{aligned} \tag{4.5.12}$$

$$\begin{aligned} &\delta_1 = \delta_2 \\ &\frac{R_1}{n_{Qf1}} = \frac{R_2}{n_{Qf2}} \end{aligned} \tag{4.5.13}$$

Equations (4.5.11), (4.5.12) and (4.5.13) show that the parallel operation of inverters with different capacities can accurately share the load according to the rated capacity ratio and the following conditions must be met at the same time[Shang (2013), Yajuan (2012), Wang (2014)]:

1. The reference voltage and the set value of the reference voltage under the rated power of each inverter in the droop controller are the same;

2. The Droop coefficient of each inverter is inversely proportional to its rated capacity;

3. The transmission impedance of the inverter to the load is inversely proportional to the rated capacity of the inverter.

4. The amplitude and phase of the output voltage of each inverter in parallel operation should be consistent.

The line impedance of each DG inverter unit to the common bus is also uncertain. It is related to its geographical location and it is difficult to meet the condition that the line impedance is inversely proportional to the capacity.

Therefore, according to the reverse droop control method, it is very difficult to realize that the DG inverter can share the load accurately according to the rated

proportion and the application in the distributed generation system has certain limitation. So, reverse droop control method has to be improved.

4.5 SELECTION OF REVERSE DROOP (P-V/Q-F) CONTROL AND VIRTUAL RESISTANCE METHOD

From the 3rd chapter, Figure 3.1 shows that the impedance between the output end of the DG inverter and the public load is composed of two parts:

The DG inverter itself has output impedance Z_{inv} and line impedance Z_{Line}. The output impedance Z_{inv} of the DG inverter itself is determined by the control parameters [Jiarong et al., (2009), Mingrui et al., (2014)].

The output impedance of the DG inverter itself is mainly inductive and the line impedance is determined by the line conditions in the microgrid. The line impedance parameters in the microgrid are shown in Table 3-1.

It can be seen from Table 4.1 that the impedance of the line in the low-voltage microgrid is mainly resistive and the magnitude of the impedance is determined by the length of the line[Engler (2005), Chun et al., (2010)].

Table 4.1: Line impedance typical parameters

Type of line	R(Ω/Km)	X(Ω/Km)	R/X
Low voltage line	0.642	0.083	7.70
Medium voltage line	0.161	0.190	0.85
High voltage line	0.06	0.191	0.31

From the above analysis, it can be seen that the output impedance of the inverter is complex and its nature is uncertain. In general, the output impedance of the inverter itself is small and the output impedance characteristic is determined by the line impedance. However, the impedance of the line at the output end of the inverter in the microgrid is flexible and it is not possible to use the reverse droop control directly[Shang (2013), Chen (2014)].

There are two main solutions to this problem: decouple the output power or construct the output impedance of the inverter. Decoupling the output power requires knowing exactly the information of the output impedance and requires real-time on-line impedance measurement. This technology is still under research and is not mature

enough. Therefore, the output impedance of the DG inverter is altered using virtual resistance method as shown in the figure 4.3[Shang (2013), Guerrero et al., (2007), Ziqiang et al., (2013)]:

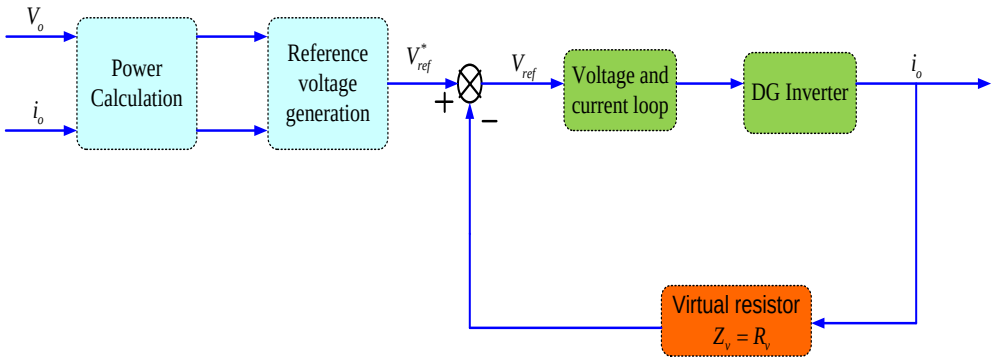

Figure 4.3: Virtual resistance block diagram.

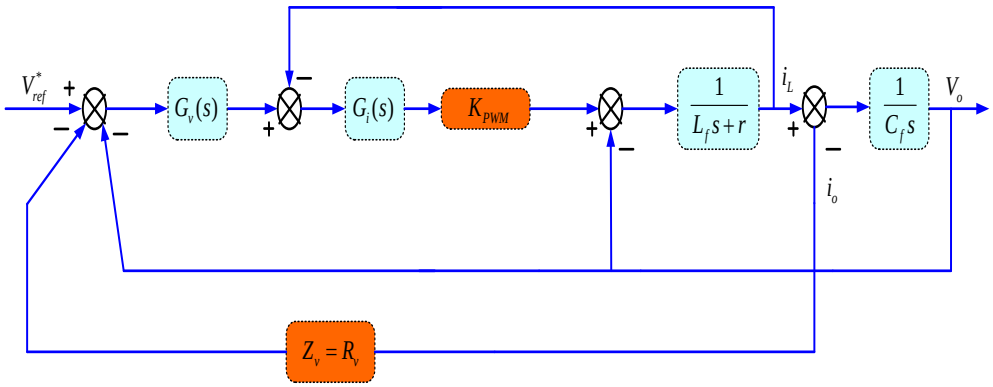

Figure 4.4: Virtual resistance control diagram.

As can be seen from Figure 4.4, the given voltage reference changes after the virtual resistance has been added and the output voltage equation is given by[Chen (2014), Yajuan et al., (2016)]:

$$V_{ref} = V^*_{ref} - Z_{vir} i_o \tag{4.5.1}$$

$$V_O = G_i(s) G_V(s) V^*_{ref} - [G_i(s) G_V(s) Z_{vir}(s) + Z_O(s)] i_O \tag{4.5.2}$$

Virtual impedance has two forms of virtual resistor and virtual inductor, respectively. The output impedance of the DG inverter is constructed into resistive or inductive. The addition of inductive impedance will be affected by high-frequency harmonic currents, large high-frequency current components will cause large voltage drop and

reduce the steady state characteristic of the system. In addition, the impedance of the line in the microgrid is generally resistive. If the output impedance of the inverter is forced to be inductive, a large amount of virtual inductance is required to make the output impedance of the inverter much more inductive than its resistance. The output impedance is resistively matched to the inverter line impedance, which is easier to control and more suitable for microgrids. Therefore, this chapter uses the form of virtual resistors to construct the DG inverter's output impedance as resistive[Shang (2013),Wang(2014),Jiaxing et al., (2014)].

In the conventional reverse droop control method, the mismatch of the output impedance of the inverter and the line impedance affects the distribution of the load power. In order to improve the effect of power sharing, the concept of virtual resistance was proposed [Guerrero et al., (2007), Guerrero et al., (2005), Zhang (2015)]. The virtual resistance method control block diagram is shown in Figure 4.4.

The reverse droop control strategy based on virtual resistance includes three nested loops:

The inner loop is a dual loop consisting of current and voltage loop. The intermediate link introduces a virtual resistance, forcing the equivalent output impedance of the DG inverter to achieve better power sharing. The outer loop is a power loop, where active and reactive powers are calculated. When the load is suddenly changed, the voltage amplitude and frequency are adjusted to obtain a good power sharing effect.This method can achieve accurate power sharing, has better dynamic modification performance and is suitable for resistive line impedance conditions[Guerrero et al., (2007), Chen (2014) , Lin (2017), Ziqiang (2013)].

Virtual resistor is expressed as:

$$Z_{vir}(s) = R_v, Z_o(s) = \frac{C_1 s^2 + C_2 s + C_3}{C_4 s^3 + C_5 s^2 + C_6 s + C_7} \tag{4.5.3}$$

$$\begin{aligned} &C_1 = L, C_2 = r + K_{pi}K_{pwm}K_{pv}R_v, C_3 = R_v K_{pi}K_{pwm}K_{vi}, C_4 = LC \\ &C_5 = rC + K_{pi}K_{pwm}C, C_6 = 1 + K_{pi}K_{pwm}K_{vi}, C_7 = K_{pi}K_{pwm}K_{vi} \end{aligned} \tag{4.5.4}$$

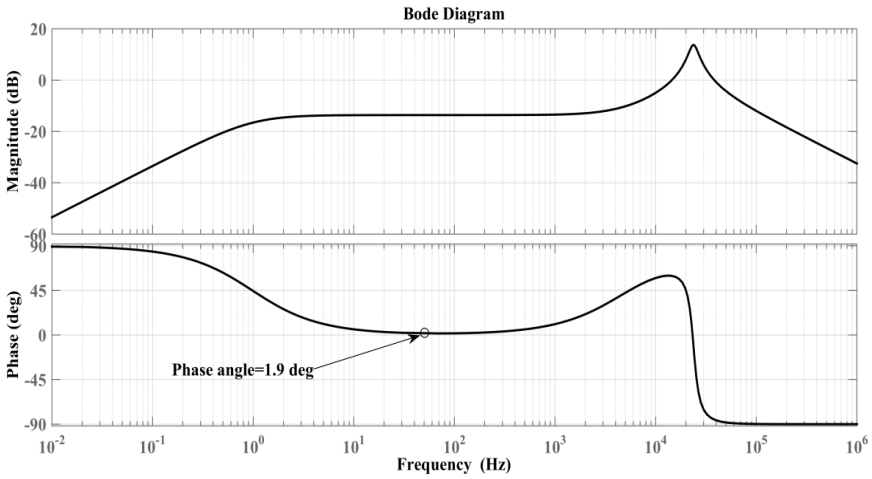

Figure 4.5: Bode diagram of inverter output impedance with virtual resistor.

If the line impedance is resistive, virtual resistor is added the control loop of reverse(*P-V/Q-f)*droop control to improve the power decoupling effect. Impedance angle at 50 Hz is 1.9° as shown in the Figure 4.5. The parallel inverter output impedance tend to be more resistive, which has a major role in improving the power sharing.

4.6 SIMULATION RESULTS

In order to verify the feasibility of the Direct and Reverse droop control. Simulation model of DG inverter is built in MATLAB/SIMULINK and parameters are shown in Appendix.

Case 1: Power sharing analysis of direct (P-f/Q-V), reverse (P-V/Q-f) droop control under resistive line impedance with constant power load.

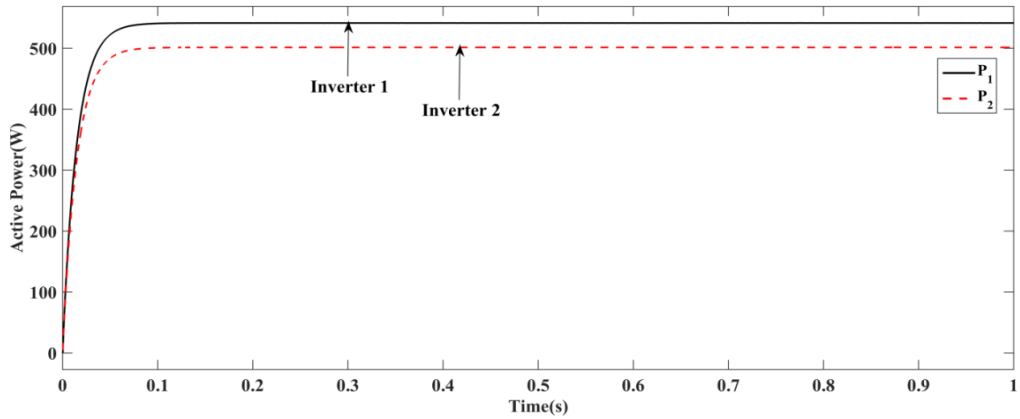

Figure 4.6 : Active power sharing using direct droop control under resistive line impedance.

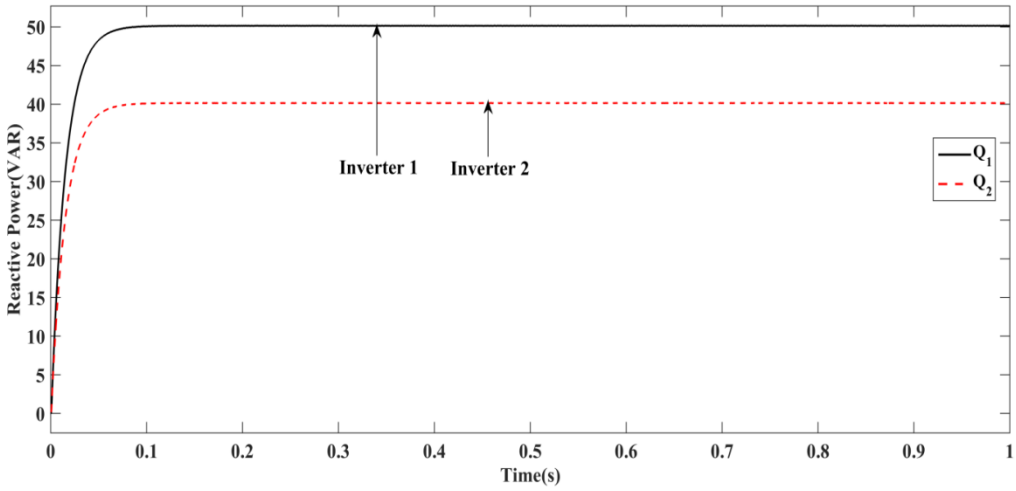

Figure 4.7 : Reactive power sharing using reverse droop control under resistive line impedance.

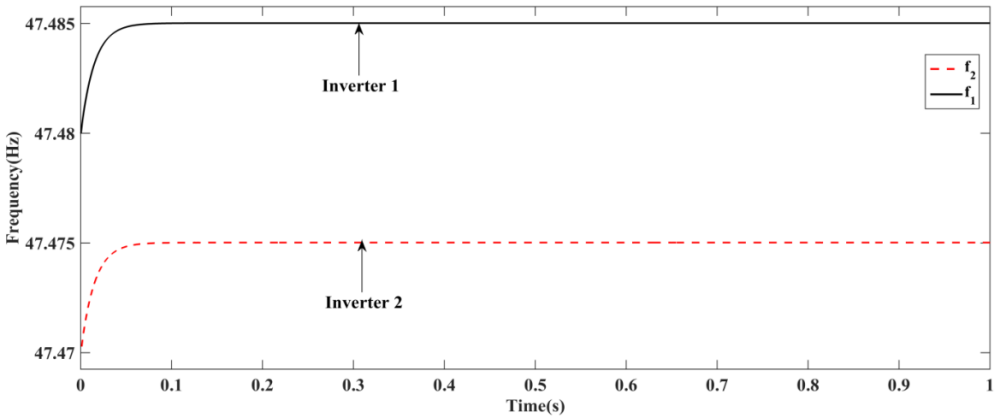

Figure 4.8: Parallel DG inverters output frequency using reverse droop control under resistive line impedance.

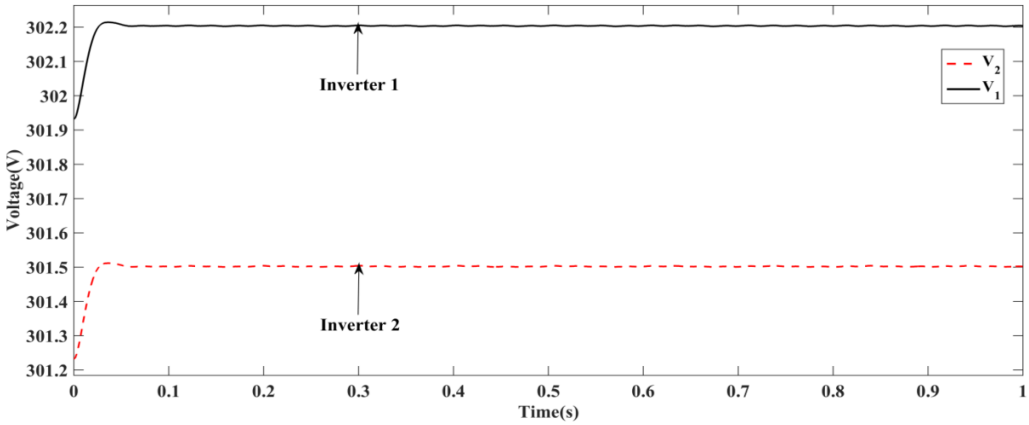

Figure 4.9: Parallel DG inverters output voltage amplitude using reverse droop control under resistive line impedance.

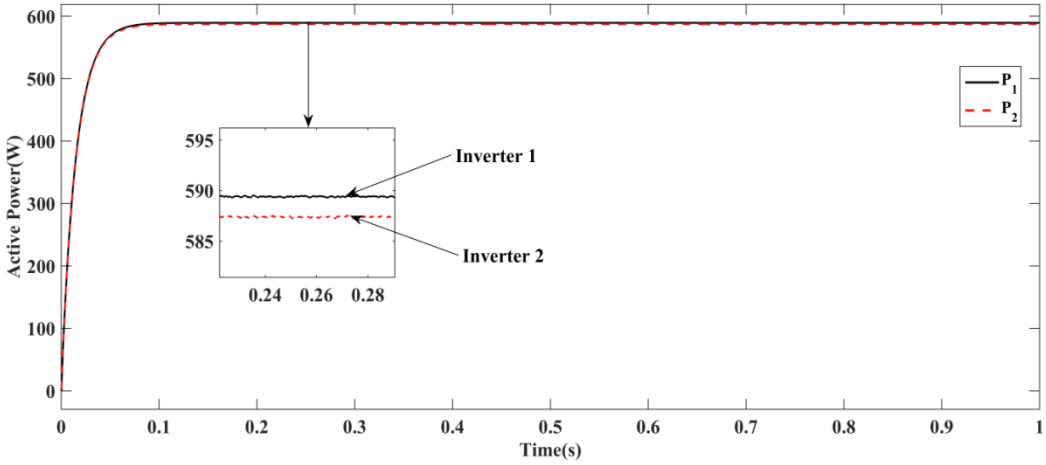

Figure 4.10 :Active power sharing using reverse droop control under resistive line impedance.

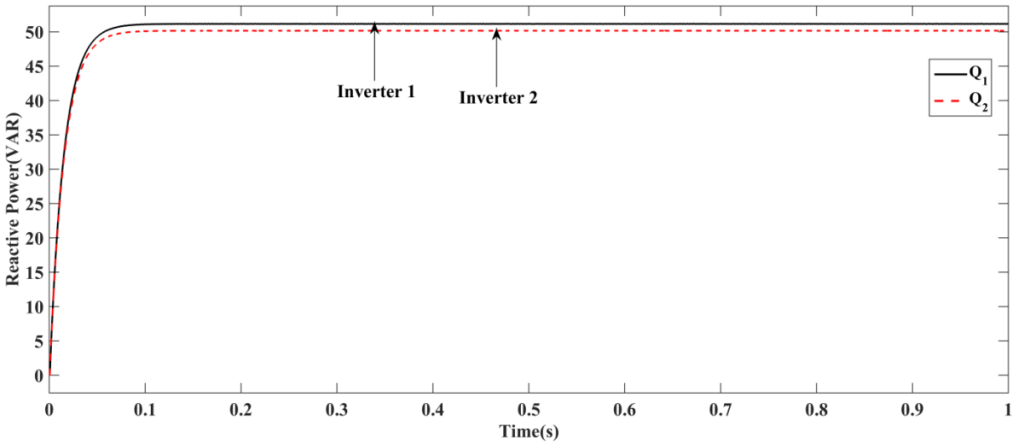

Figure 4.11: Reactive power sharing using reverse droop control under resistive line impedance.

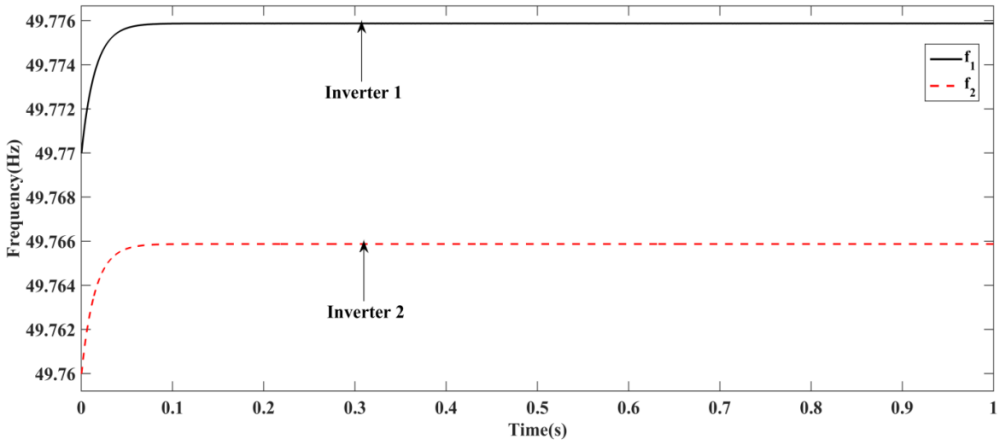

Figure 4.12: Parallel DG inverters output frequency using reverse droop control under resistive line impedance.

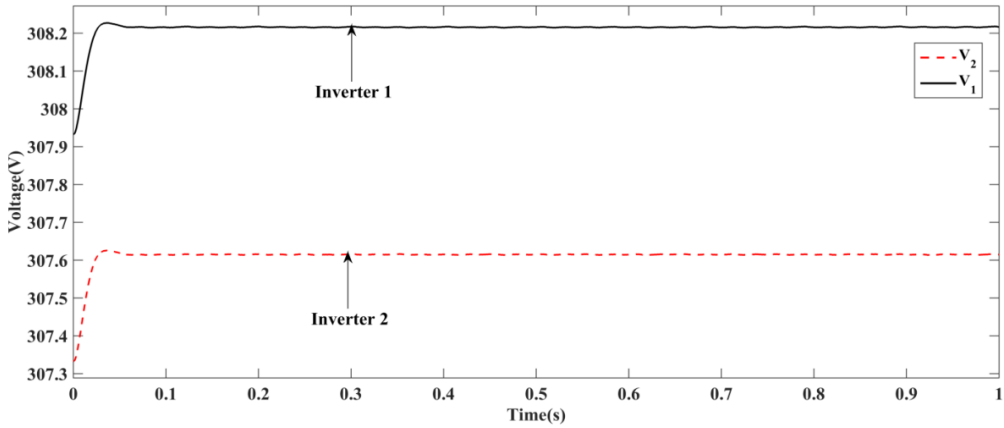

Figure 4.13: Parallel DG inverters output voltage amplitude using reverse droop control under resistive line impedance.

Power sharing of parallel DG inverters is investigated with common load of P_{load}=1200W,Q_{load}=120VAR and line impedance of $R_{1Line} + jX_{1Line}$=0.6+j0.002Ω, $R_{2Line} + jX_{2Line}$=0.7+j0.003Ω. Intially direct droop control is applied to the parallel DG inverters and output power of parallel inverters does not reach to a given proportional load sharing, because of the poor decoupling of power as shown in the Figure 4.6,4.7. When the line impedance is resistive direct droop control cannot realize the equalization of active and reactive power.

The parallel inverter voltage amplitude drop is significantly more compared to the given rated voltage amplitude of 311V and frequency variation of parallel inverters is more than ±0.6Hz compared with rate value of frequency 50Hz. so, when the line impedance is resistive with direct droop control, frequency accuracy is reduced, the voltage amplitude drop rate exceeds the specified range as shown in the Figure 4.8,4.9. Now with the same parameters reverse droop control is applied to the each DG inverters is able to share the load of active power P_1=588 W,P_2=586 W as shown in the Figure 4.10 and reactive power of Q_1=50 VAR,Q_2=48 VAR as shown in the Figure 4.11.Frequency and voltage amplitude variations of DG inverters has a small deviation,frequency fluctations is not greater than 1% as shown in the Figure 4.12 and voltage amplitude has a slight decline V_1=308.2 V,V_2=307.6 V which is not greater than 5% as shown in the Figure 4.13.

Case 2: Power sharing analysis of reverse droop control under resistive line impedance with step change in load.

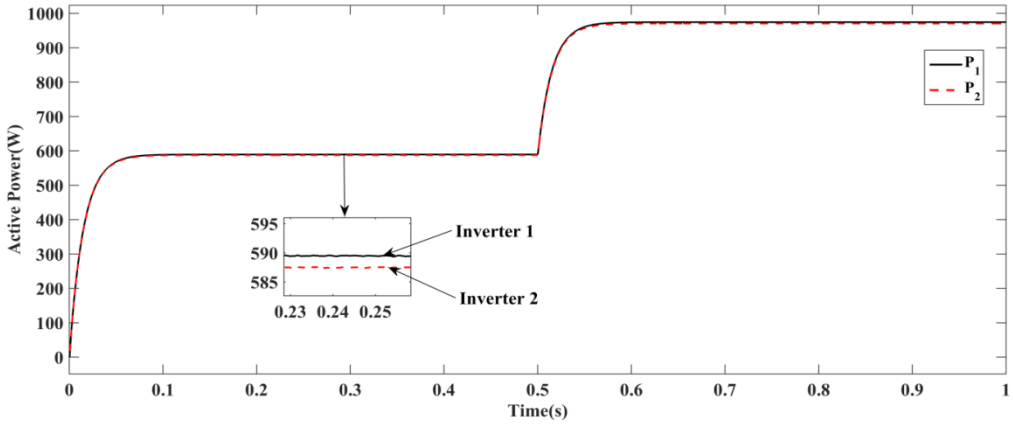

Figure 4.14 : Active power sharing using reverse droop control under resistive line impedance with step change in load.

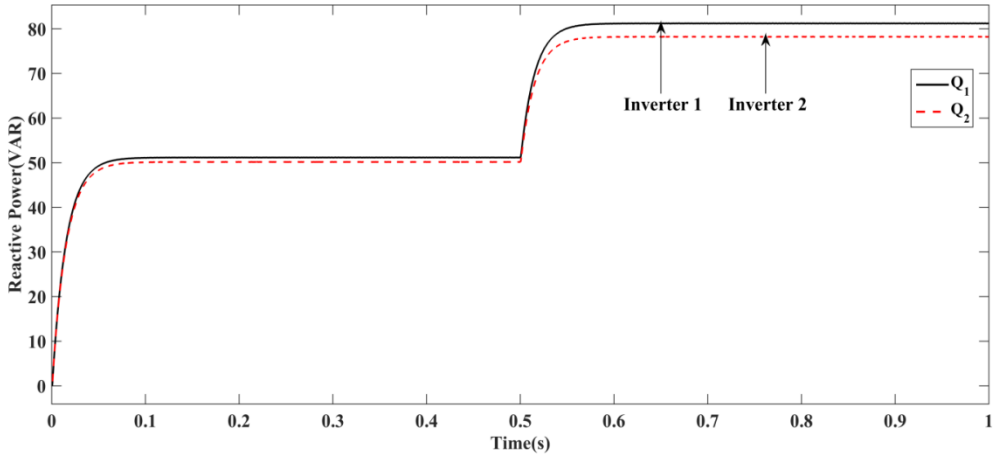

Figure 4.15: Reactive power sharing using reverse droop control under resistive line impedance with step change in load.

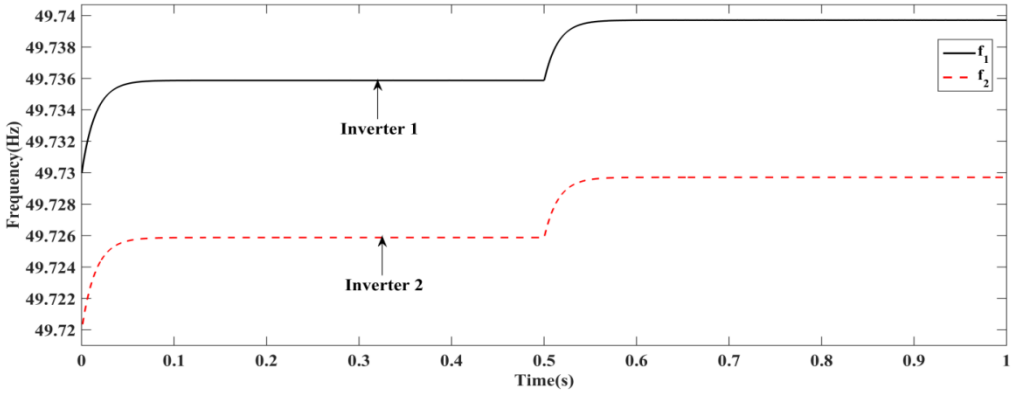

Figure 4.16: Parallel DG inverters output frequency using reverse droop control under resistive line impedance with step change in load.

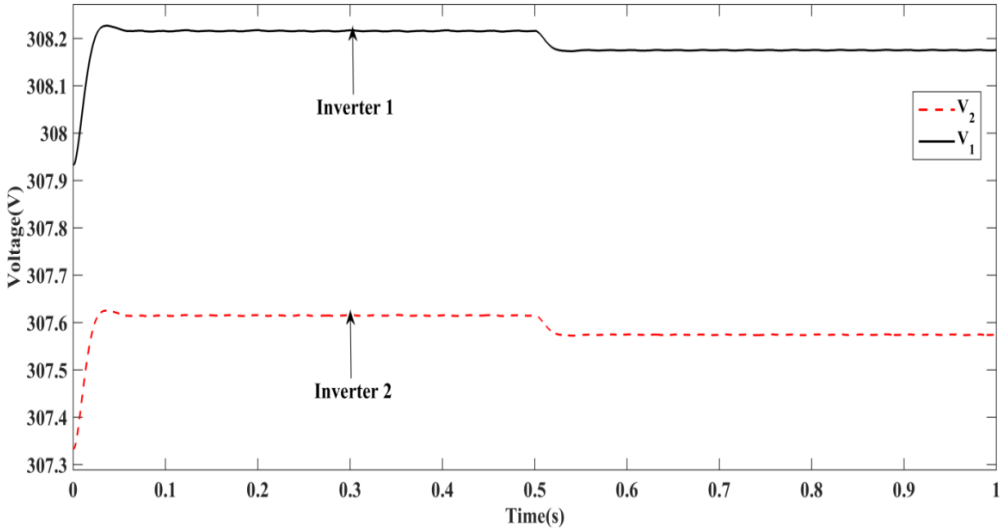

Figure 4.17: Parallel DG inverters output voltage amplitude using reverse droop control under resistive line impedance with step change in load.

Power sharing of parallel inverters is investigated with common load of P_{load} = 1200 W, Q_{load} = 120 VAR and at 0.5 s sudden local load value of P_{load} = 800 W, Q_{load} = 80 VAR is added to verify the dynamic response and line impedance of $R_{1Line} + jX_{1Line}$ =0.6+j0.002Ω, $R_{2Line} + jX_{2Line}$ =0.7+j0.003Ω.

Reverse droop control is applied to the each DG inverters is able to share the load of active power P_1=588 W,P_2=586 W as shown in the Figure 4.14 and reactive power of Q_1=50 VAR,Q_2=48 VAR as shown in the Figure 4.15 and at load change at 0.5s P_1=974 W,P_2=970 W, Q_1=80 VAR,Q_2=76 VAR.

Frequency and voltage amplitude variations of DG inverters has a small deviation, frequency fluctuations is not greater than 1% as shown in the Figure 4.16 and voltage amplitude has a slight decline V_1=308.2 V,V_2=307.6 V which is not greater than 5% as shown in the Figure 4.17.

Case 3: Power sharing analysis of reverse droop control under resistive line impedance with frequent changes in load.

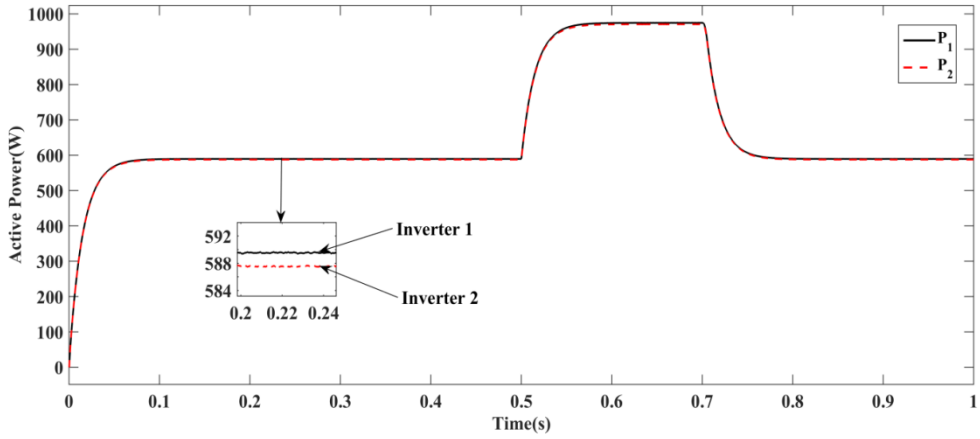

Figure 4.18: Active power sharing using reverse droop control under resistive line impedance with frequent changes in load.

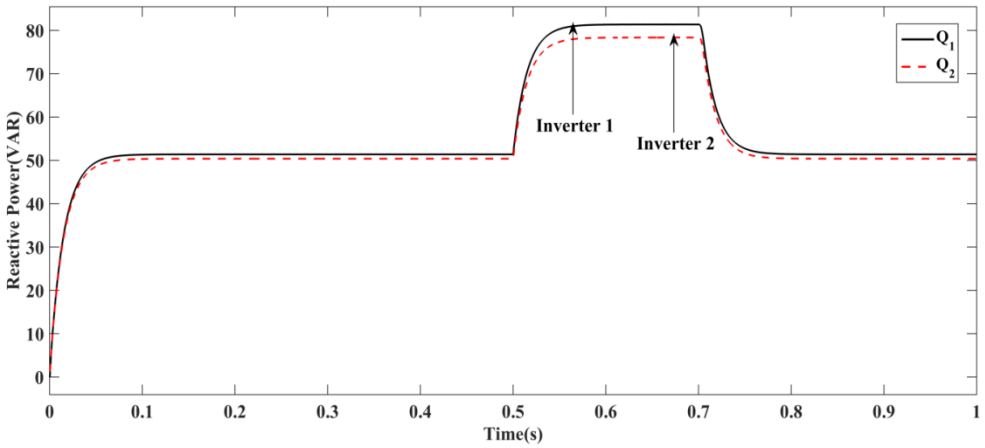

Figure 4.19: Reactive power sharing using reverse droop control under resistive line impedance with frequent changes in load.

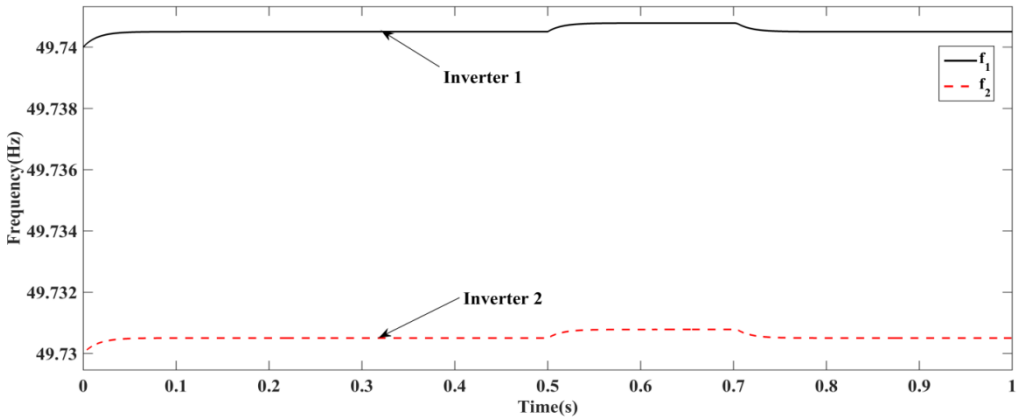

Figure 4.20: Parallel DG inverters output frequency using reverse droop control under inductive line impedance with frequent changes in load.

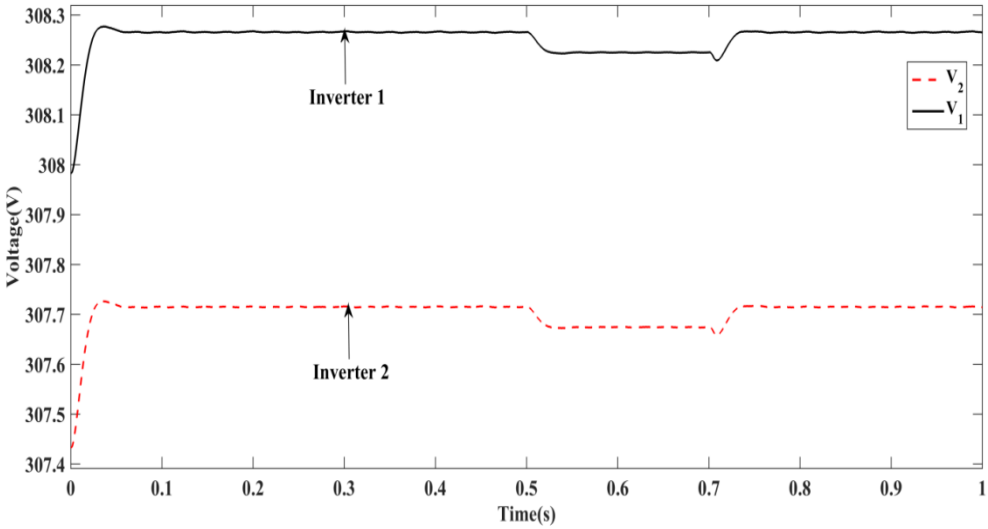

Figure 4.21: Parallel DG inverters output voltage amplitude using reverse droop control under resistive line impedance with frequent changes in load.

Power sharing of parallel inverters is investigated with common load of P_{load} = 1200 W, Q_{load} = 120 VAR and at 0.5 s sudden local load value of P_{load} = 800 W, Q_{load} = 80 VAR is added and removed at 0.7s verify the dynamic response and line impedance of $R_{1Line} + jX_{1Line}$ =0.6+j0.002Ω, $R_{2Line} + jX_{2Line}$ =0.7+j0.003Ω.

Reverse droop control is applied to the each DG inverters is able to share the load of active power P_1=588 W,P_2=586 W as shown in the Figure 4.18 and reactive power of Q_1=50 VAR,Q_2=48 VAR as shown in the Figure 4.19 and at load change at 0.5s P_1=974 W,P_2=970 W, Q_1=80 VAR,Q_2=76 VAR.

Frequency and voltage amplitude variations of DG inverters has a small deviation, frequency fluctuations is not greater than 1% as shown in the Figure 4.20 and voltage amplitude has a slight decline V_1=308.2 V,V_2=307.6 V which is not greater than 5% as shown in the Figure 4.21.

Case 4: Power sharing analysis of reverse droop control with virtual resistors under resistive line impedance.

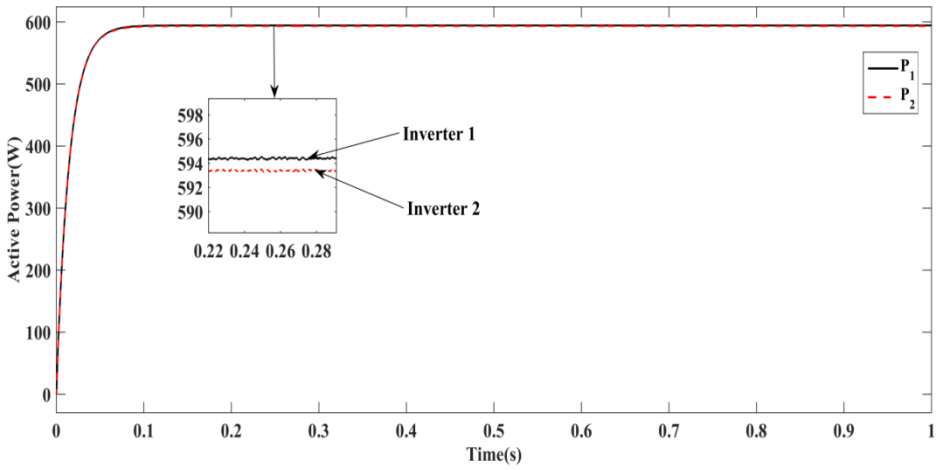

Figure 4.22: Active power sharing using reverse droop control with virtual resistors under resistive line impedance.

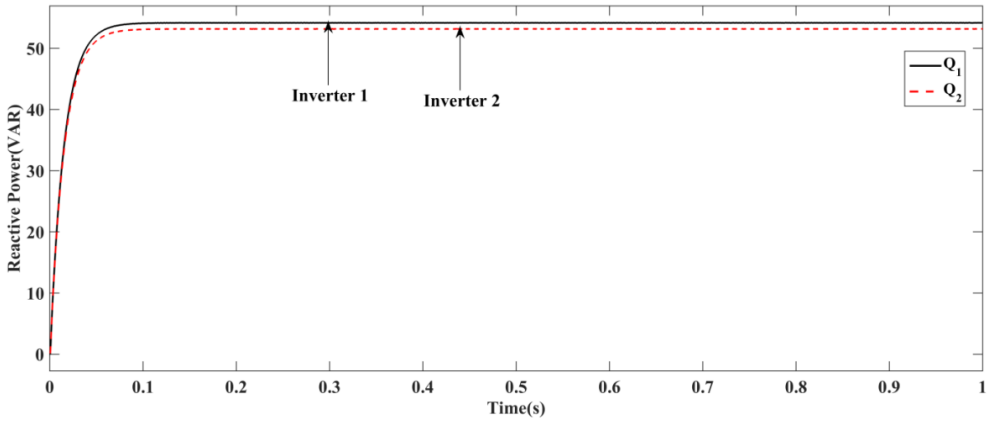

Figure 4.23: Reactive power sharing using reverse droop control with virtual resistors under resistive line impedance.

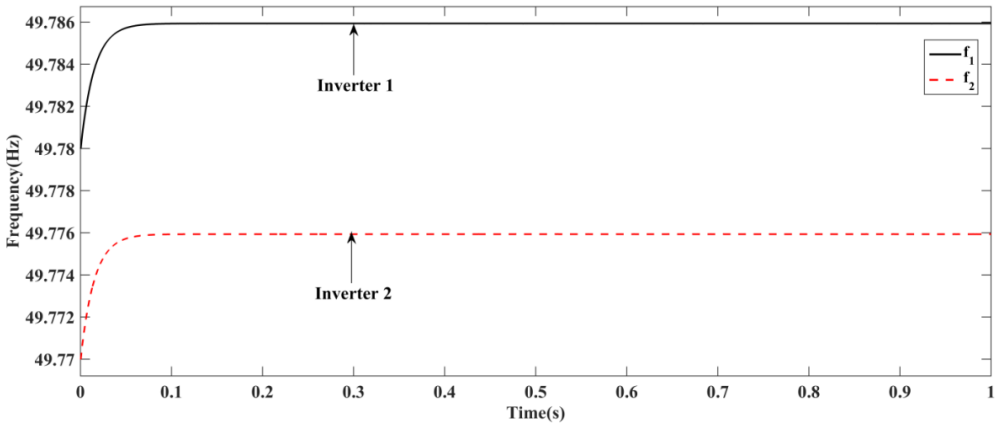

Figure 4.24: Parallel DG inverters output frequency using reverse droop control with virtual resistors under resistive line impedance.

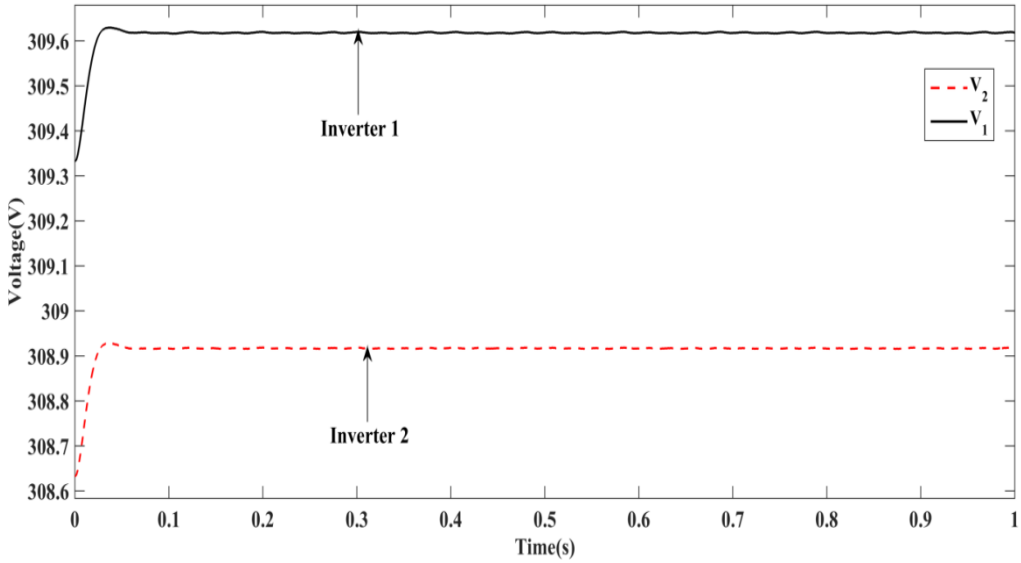

Figure 4.25: Parallel DG inverters output voltage amplitude using reverse droop control with virtual resistors under resistive line impedance.

Power sharing of parallel inverters is investigated with common load of P_{load} = 1200 W, Q_{load} = 120 VAR and line impedance of $R_{1Line} + jX_{1Line}$ =0.6+j0.002Ω, $R_{2Line} + jX_{2Line}$ =0.7+j0.003Ω. Reverse droop control based on virtual resistors can reduce the influence of the line impedance difference on the parallel inverters by setting the total output impedance of the DG inverters to be resistive, which improves decoupling of power and improves the proportional load sharing P_1=593 W, P_2=592 W, Q_1=54 VAR, Q_2=53 VAR as shown in the Figure 4.22,4.23.

Frequency variation of DG inverters is within the range of 49.77 Hz to 49.78 Hz, the maximum fluctuation of 0.004 Hz as shown in the Figure 4.24.

Voltage variation of DG inverters is V_1=309.6 V, V_2=308.9 V as shown in the Figure 4.25. Thus, the reverse droop control with virtual resistors improves power sharing compared to reverse droop control.

Case 5: Power sharing analysis of reverse droop control with virtual resistors under resistive line impedance with step change in load.

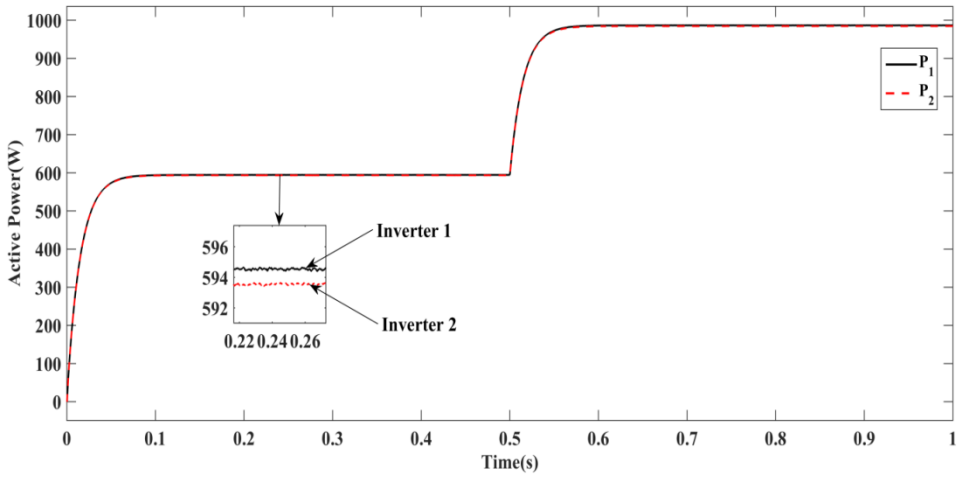

Figure 4.26: Active power sharing using reverse droop control with virtual resistors under resistive line impedance with step change in load.

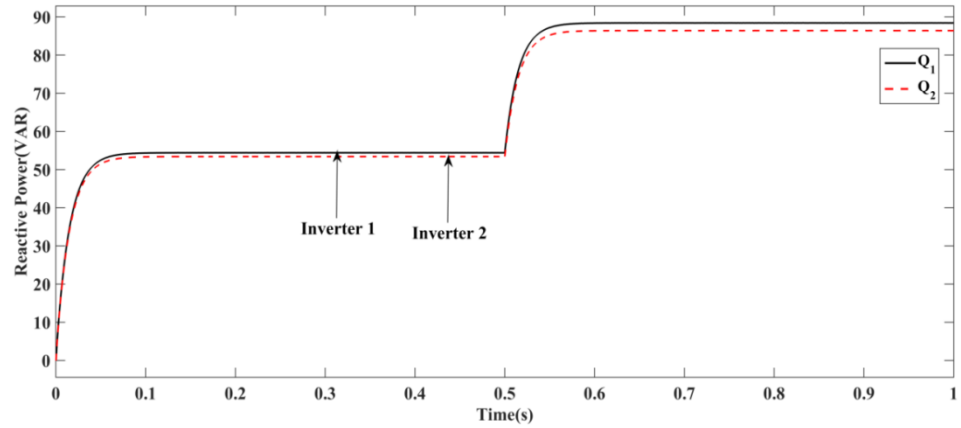

Figure 4.27: Reactive power sharing using reverse droop control with virtual resistors under resistive line impedance with step change in load.

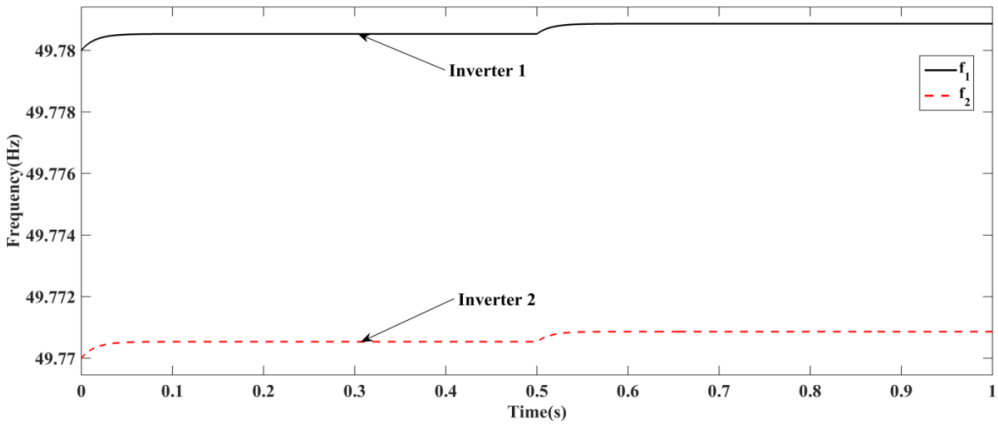

Figure 4.28: Parallel DG inverters output frequency using reverse droop control with virtual resistors under resistive line impedance with step change in load.

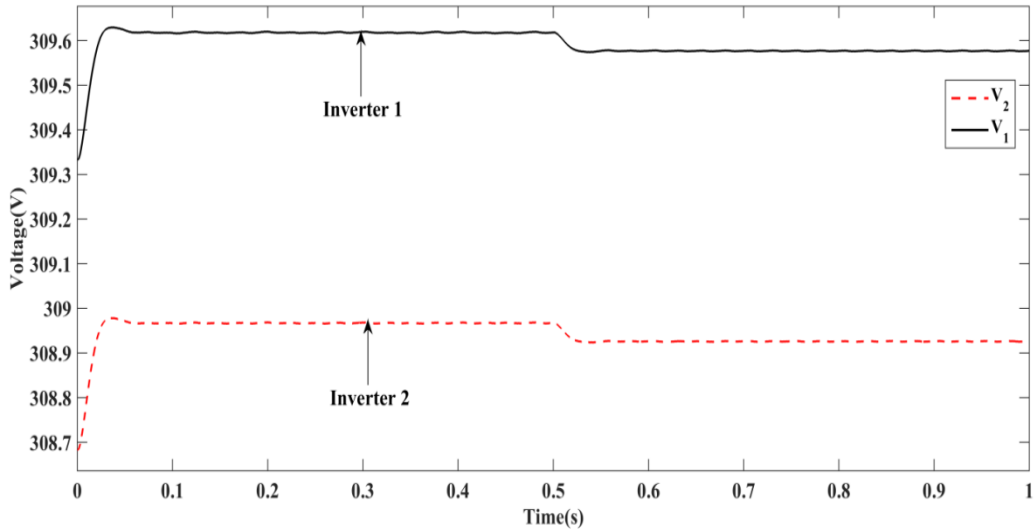

Figure 4.29: Parallel DG inverters output voltage amplitude using reverse droop control with virtual resistors under resistive line impedance with step change in load.

Power sharing of parallel inverters is investigated with common load of P_{load} = 1200 W, Q_{load} = 120 VAR and at 0.5 s sudden local load value of P_{load} = 800 W, Q_{load} = 80 VAR is added to verify the dynamic response and line impedance of $R_{1Line} + jX_{1Line}$ =0.6+j0.002Ω, $R_{2Line} + jX_{2Line}$ =0.7+j0.003Ω.

Reverse droop control based on virtual resistors can reduce the influence of the line impedance difference on the parallel inverters by setting the total output impedance of the DG inverters to be resistive, which improves decoupling of power and improves the proportional load sharing P_1=593 W, P_2=592 W, Q_1=54 VAR, Q_2=53 VAR and at load change at 0.5 s, P_1=934 W, P_2=931 W, Q_1=88 VAR, Q_2=85 VAR as shown in the figure 4.26,4.27 and frequency variation of DG inverters is within the range of 49.77 Hz to 49.78 Hz, the maximum fluctuation of 0.004 Hz as shown in the Figure 4.28. Voltage variation of DG inverters is V_1=309.6 V, V_2=308.9 V as shown in the Figure 4.29. Thus, the reverse droop control with virtual resistors improves power sharing compared to reverse droop control.

Case 6: Power sharing analysis of reverse droop control with virtual resistors under resisive line impedance with frequent changes in load.

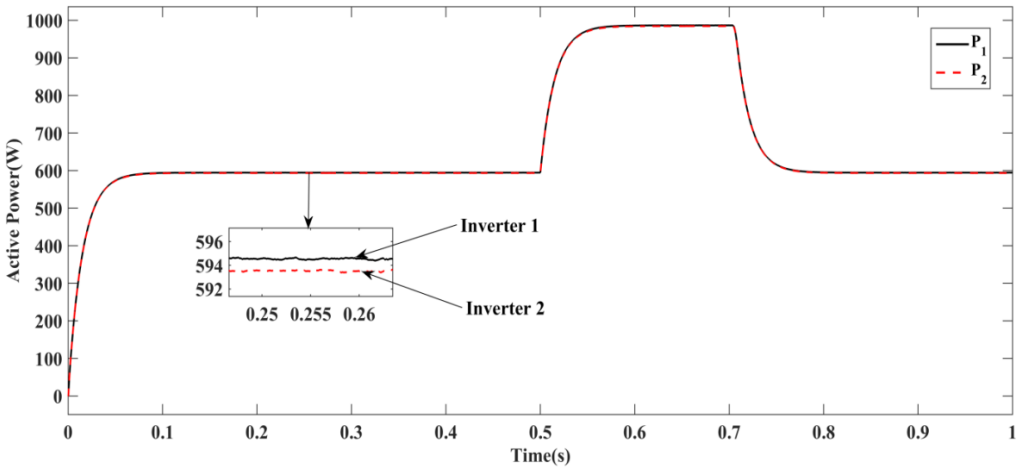

Figure 4.30: Active power sharing using reverse droop control with virtual resistors under resistive line impedance with frequent changes in load.

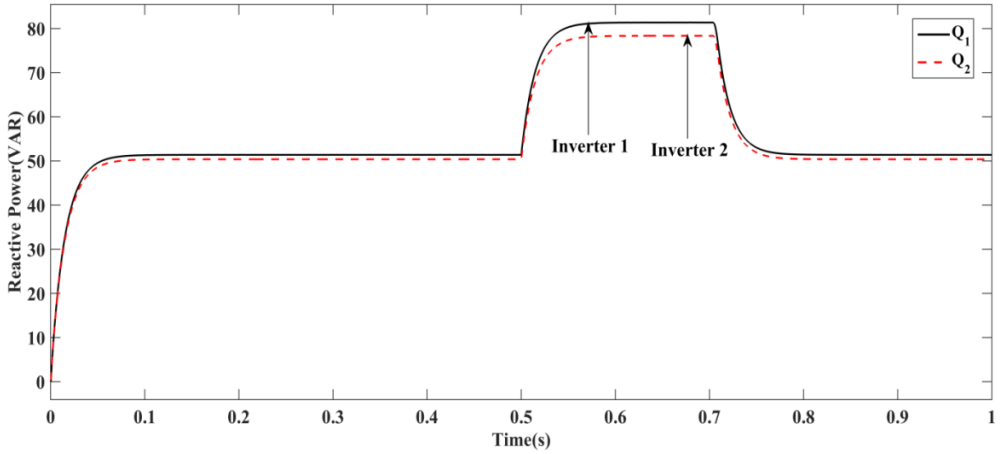

Figure 4.31: Reactive power sharing using reverse droop control with virtual resistors under resistive line impedance with frequent changes in load.

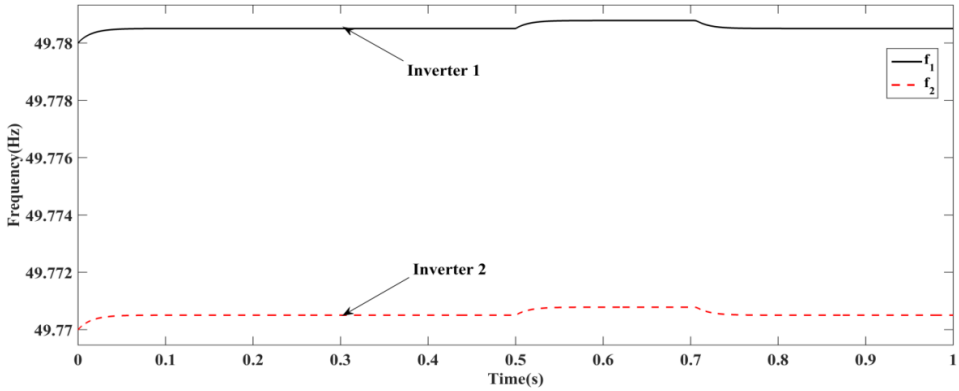

Figure 4.32: Parallel DG inverters output frequency using reverse droop control with virtual resistors under resistive line impedance with frequent changes in load.

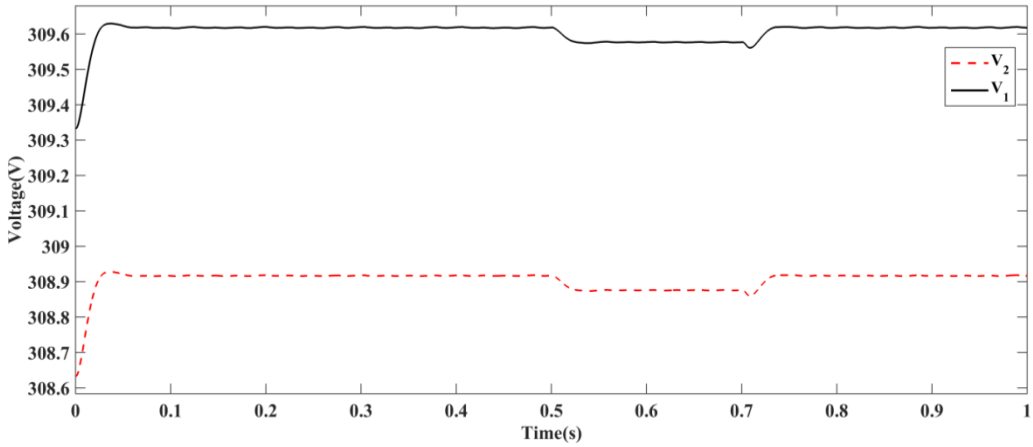

Figure 4.33: Parallel DG inverters output voltage amplitude using reverse droop control with virtual resistors under resistive line impedance with frequent changes in load.

Power sharing of parallel inverters is investigated with common load of P_{load} = 1200 W, Q_{load} = 120 VAR and at 0.5 s sudden local load value of P_{load} = 800 W, Q_{load} = 80 VAR is added and removed at 0.7s verify the dynamic response and line impedance of $R_{1Line} + jX_{1Line}$ =0.6+j0.002Ω, $R_{2Line} + jX_{2Line}$ =0.7+j0.003Ω. Reverse droop control based on virtual resistors can reduce the influence of the line impedance difference on the parallel inverters by setting the total output impedance of the DG inverters to be resistive, which improves decoupling of power and improves the proportional load sharing P_1=593 W, P_2=592 W, Q_1=54 VAR, Q_2=53 VAR and at load change at 0.5 s, P_1=934 W, P_2=931 W, Q_1=88 VAR, Q_2=85 VAR as shown in the Figure 4.30,4.31 and frequency variation of DG inverters is within the range of 49.77 Hz to 49.78 Hz, the maximum fluctuation of 0.004 Hz as shown in the Figure 4.32. Voltage variation of DG inverters is V_1=309.6 V, V_2=308.9 V as shown in the Figure 4.29. Thus, the reverse droop control with virtual resistors improves power sharing compared to reverse droop control.

4.7 CONCLUSION

In the low voltage distributed generation system, the impedance of the lines is resistive, so reverse droop control is adopted to realize power distribution among parallel DG inverters. This chapter analyzes the conditions that the DG inverter power supply needs to be satisfied by proportional power sharing and points out the limitations of the traditional reverse droop control in the distributed generation system with uncertain line impedance. An improved power allocation strategy based on virtual resistance is adopted and its theoretical analysis is carried out, which eliminates the influence of line impedance on power distribution accuracy of distributed generation system .The simulation model based on Matlab/simulink is built and the simulation of the same capacity of parallel DG inverters is carried out under the condition of restive and inductive line impedance, which verifies the correctness and validity of the power allocation strategy based on the virtual resistance.

Chapter 5

5 SECONDARY CONTROL OF DISTRIBUTED GENERATION INVERTERS IN MICROGRID

5.1 INTRODUCTION

Distributed Generation (DG) in microgrids is connected to the common bus via power electronic interfaces and corresponding feeders. The state of the microgrid and the large power grid is monitored by a secondary central controller [Bidram et al., 2013)]. According to the operation demand, the common point static switch is controlled so that the microgrid can operate in both islanding and grid-connected mode and ensure seamless switching between modes [He et al.,2015)]. In grid-connected operation of microgrid, the voltage and frequency reference of DG unit is set by central controller. The power distribution between microgrid and grid can be easily realized by inverter PQ control to maintain the bus voltage of PCC at rated voltage 10% of the range of fluctuations. Therefore, to meet the load on the voltage quality needs[Dengke et al.,2012].

When the microgrid is switched from grid-connected to island operation, DG uses voltage amplitude and frequency droop control to ensure the stability of voltage and frequency of the microgrid system. However, at this time, there are problems of frequency and voltage adjustment, coordination between energy supply and demand, power quality and also due to the microgrid impedance characteristics, topology and other factors[Ahn et al., (2010)]. When using droop control for power regulation, stability is difficult to be guaranteed due to the multiple DGs participating in the voltage amplitude and frequency regulation of the system. When the load changes over a wide range, a large droop coefficient needs to be selected to achieve a fast power balance, resulting in a large voltage amplitude and frequency offset[Xiaofeng et al., (2013)]. The traditional droop control method is difficult to achieve the coordinated operation of multiple distributed power in the microgrid to ensure that the distributed power supply accurately distributes the load power according to its capacity while maintaining the stability of the microgrid frequency and voltage.Therefore, the operation control based on hierarchical control is of great

practical significance for the research on the stability of voltage and frequency of microgrid[Ham et al., (2017), Barik et al., (2015)]. In [Guo and Wen (2014)] adopts the second regulation, collects microgrid voltage and frequency information from the centralized controller and compares with microgrid reference voltage and frequency. The command value of the error obtained after the voltage and frequency recovery controllers are sent to the local controller to adjust to make the voltage and frequency offset equal to zero. However, due to the existence of a central node, system reliability and scalability are poor and the failure of the communication link has an impact on the control effect and stability of the system and the plug-and-play feature is lacking.

While these improved methods can restore voltage amplitude and frequency to some extent, they also have some drawbacks. A droop control method based on virtual power flow is proposed in [Hu et al., 2014], but this method cannot effectively eliminate the deviation in voltage amplitude. In [Wu et al., 2015], a secondary control method based on load estimation is proposed. This method can effectively restore the voltage amplitude and frequency while achieving power sharing between parallel inverters. However, this method makes the secondary adjustment relatively slow. The secondary control method proposed in [Xuan et al.,(2011)] achieves frequency recovery by dynamically changing the droop characteristic of the main power supply.

However, this method has high requirements on the capacity of the main power supply and thus is not applicable in many practical engineering situations. The central controller is used for hierarchical control in [Guerrero et al., (2011)], but the dependence of this method on the central controller reduces its reliability.In [Shafiee et al., (2014)], the reliability of the system is improved by using the distributed secondary controller, but the small difference of parameters will result in power sharing errors between the parallel DG inverters and the dependence of the method on the communication line is reduced.

Based on the existing research, this chapter proposes a distributed secondary control to achieve voltage and frequency recovery. At the same time, the system frequency and voltage amplitude are regulated by a proportional integral (PI) controller. This method not only can accurately restore the voltage amplitude and

frequency, but also can quickly achieve power sharing between parallel DG inverters. Simulation results verify the effectiveness of the proposed method.

5.2 VOLTAGE AND FREQUENCY STABILITY ANALYSIS OF DISTRIBUTED GENERATION INVERTERS

The problem of voltage stability can be considered to be that when the system is distributed, the voltage fluctuation should not exceed the rated value ±5%. Voltage instability will have serious consequences, such as: damage to equipment, the quality of industrial products and production, ,even caused large areas of power outages, voltage collapse and other major accidents[Pengyu (2017)].

In power system, voltage is an important energy index, so it is necessary to standardize the voltage amplitude so that the voltage deviation and fluctuation must be within a reasonable range. China's "power system and reactive power technology guide" stipulates the voltage tolerance range, as shown in table 5.1[Yong (2015)]:

Table 5.1: Allowable voltage deviations

User voltage level	Allowable voltage offset	User voltage level	Allowable voltage deviation
≥35KV	±10%	380V	±7%
10KV	±7%	220V	-10% to -5%

Frequency is also an important power quality index, the frequency instability on the power system will also have a great impact, so in order to avoid the frequency fluctuations in the network, "Power Industry Technical Code" stipulates that frequency rate fluctuation should be ensured within the ±0.5Hz, that is, the inverter output frequency is guaranteed within the 50±0.5Hz [Yonggang (2012)].

5.3 DISTRIBUTED GENERATION INVERTER SECONDARY CONTROL OVERVIEW

5.3.1 Centralized Secondary Control

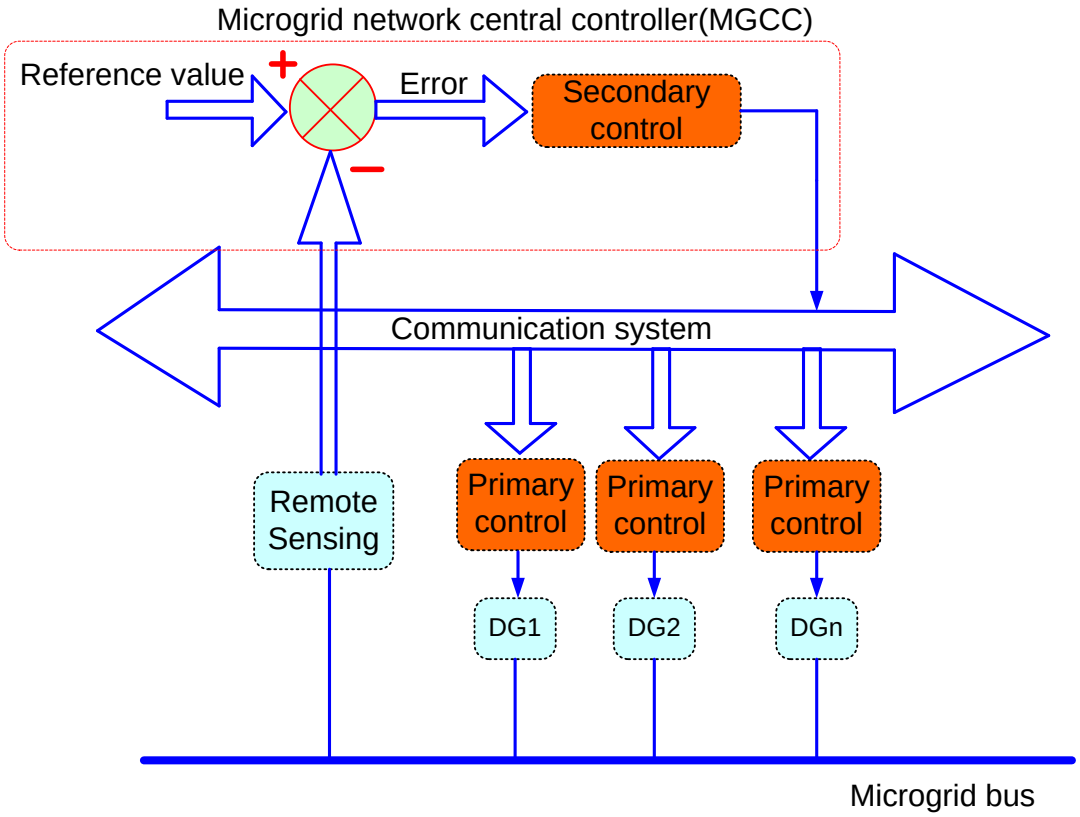

Figure 5.1: Centralized secondary control

Under normal circumstances, the micro-grid control is decentralized control, level three control is centralized control and level two control can be both centralized control and decentralized control [Guerrero et al., (2011)].

The traditional secondary control method uses a centralized control structure of a microgrid (Micro-grid Central Controller, MGCC), which requires a complex bi-directional communication network, due to a failure of the MGCC controller enough to stop the action of level secondary control. Therefore, the reliability of this system is not high [Huo et al., (2012), Pengyu (2017)].

The traditional centralized secondary control realizes the regulation function through the microgrid central controller (MGCC). Figure 5.1 shows the overall system architecture of centralized secondary control, consisting of a series of locally controlled DG units and a two level secondary controller that passes data back to the

MGCC controller through a low bandwidth communication system after acquiring a range of parameters through a remote sensor module [Guerrero et al., (2013)]. Then, the secondary controller compares the variables to the reference value and sends the output signal to the first-level control of each DG unit through the communication channel.

The advantage of centralized level two control is that the communication system is not busy because only one way information transmission (from sensor to MGCC and then from MGCC to each DG unit) is available. The disadvantage is that MGCC is not very reliable, because a MGCC controller's error action is enough to stop entire microgrid system [Ahumada et al., (2016)].

(a) Frequency Control

Frequency as a control variable that can provide power consumption and generate relevant information has an important advantage and the frequency of large power grid depends mainly on the output active power of synchronous generator, so the secondary controller of traditional large power grid is designed to restore frequency. This secondary controller, known in Europe as a load-frequency controller, is called an automatic generation controller in the United States and consists of an n controller with a dead zone [Yonggang (2012), Cuiyun (2013)].

These two-level controllers recover frequencies when the deviations are above a certain value. In order to recover the frequency, a secondary controller similar to a large power grid is implemented in MGCC[Xumiao (2015)]. The principle of frequency recovery compensator in centralized level two control is as follows:

$$\delta f = K_{pf}(f_{MG}^{*} - f_{MG}) + K_{if}\int (f_{MG}^{*} - f_{MG})dt \tag{5.3.1}$$

K_{pf} and K_{if} are the relevant parameters of the frequency PI compensator in the centralized secondary controller. After obtaining the micro-grid frequency f_{MG}, the remote sensor module is compared with the reference value f_{MG}^{*}, then the processing difference is δf to the first level controller of all DG units.

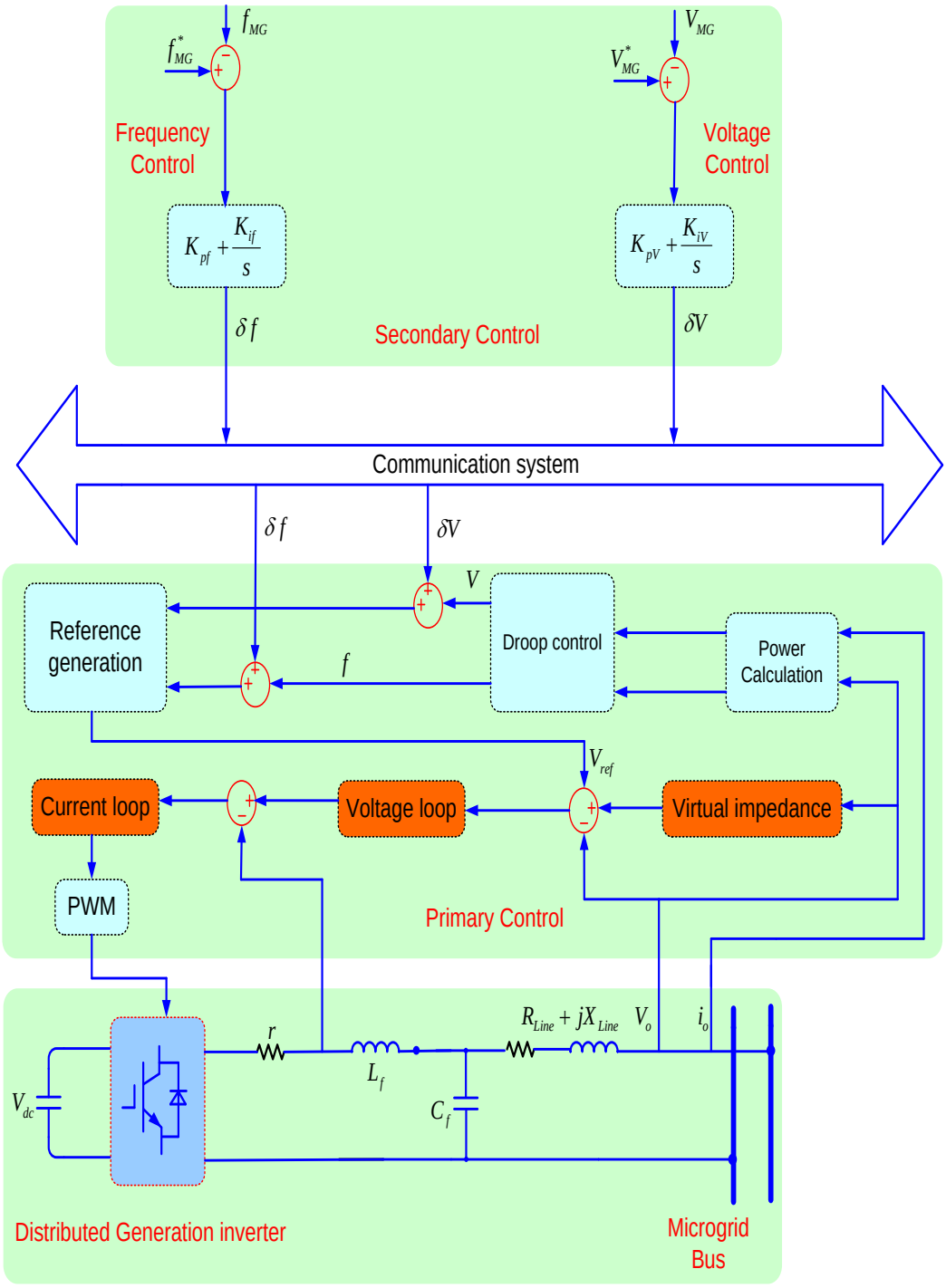

Figure 5.2: Specific details of centralized secondary control for a DG unit

(b) Voltage Control

Similar to frequency control, voltage control also takes a similar process. When the voltage effective value of the microgrid exceeds the rated range, a PI controller

compensates for the voltage amplitude of the micro-grid and sends the voltage amplitude deviation through the low bandwidth communication system to each DG unit[Savaghebi et al., (2012), Zhongming (2015), Yong (2015)]. In this way, there are both frequency recovery control and voltage amplitude recovery control in the central controller of microgrid system. The voltage amplitude recovery control loop is as follows:

$$\delta V = K_{pv}(V_{MG}^{*} - V_{MG}) + K_{iv}\int (V_{MG}^{*} - V_{MG})dt \tag{5.3.2}$$

K_{pv} and K_{iv} are the relevant parameters of the voltage PI compensator in the centralized two-level controller. The voltage amplitude deviation value of the micro-grid is δV to the first level controller of all DG units.

Figure 5.2 shows the specific centralized secondary control details for each DG in the microgrid and it can be seen that in order to restore the micro-grid voltage and frequency, the micro-grid frequency and bus voltage amplitude are measured and sent to MGCC via the communication system, which is compared with the reference value in MGCC[Guerrero et al.,(2013)] .

The processed difference is then sent through the communication system to the first level controller of all DG units. The processed difference is then sent through the communication system to the first level controller of all DG units[Pengyu (2017)].

5.3.2 Distributed Secondary Control

Unlike the centralized secondary control, the distributed secondary control uses the primary and secondary controllers together as the local controller, so that the microgrid can adjust the frequency, voltage and power in each local DG unit, thus avoiding the use of MGCC and natural attributes of wireless networks are utilized[Shafiee et al.,(2014),Bidram et al.,(2013)].

In this way, even if a single DG unit fails, it will not cause the entire system to collapse. Figure 5.3 shows the overall system architecture of distributed secondary control.

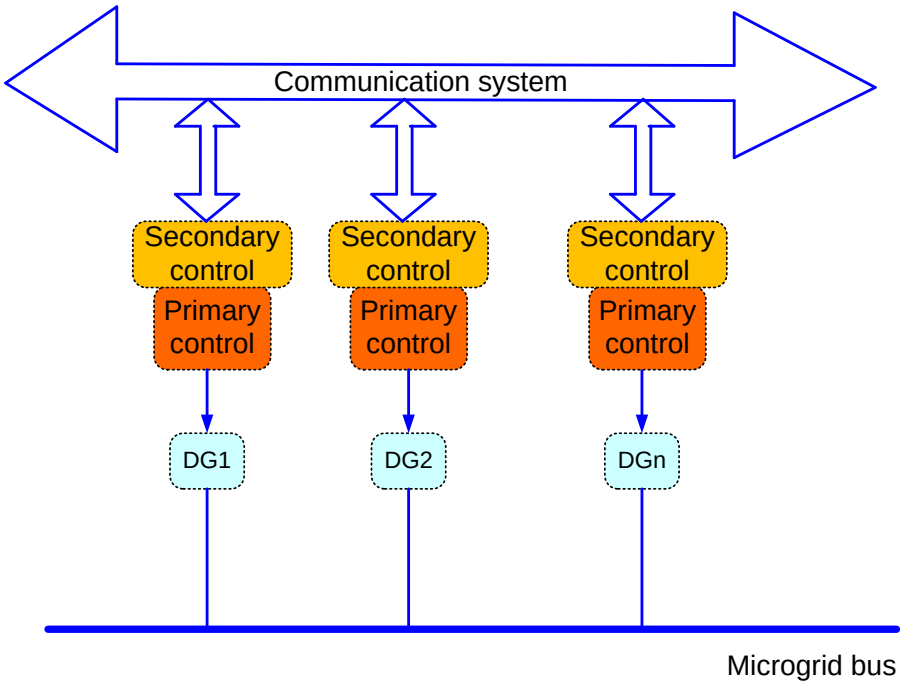

Figure 5.3: Distributed secondary control

(a) Frequency control

In order to compensate for the frequency deviation caused by the droop controller, the use of secondary frequency control was proposed. However, in order to avoid the instability of the micro-grid system which may be caused by different DG inverters, the method requires communication [Yuen et al., (2011), Pengyu (2017)].

In the distributed secondary control strategy, each DG measures the frequency value in each sample time and sends it to other DGs. The frequency of other DG measurements is averaged and then the frequency of internal DG restore is as follows:

$$\delta f_{DG_k} = K_{pf}(f^*_{MG} - \bar{f}_{DG_k}) + K_{if}\int (f^*_{MG} - \bar{f}_{DG_k})dt \tag{5.3.3}$$

Where, $\bar{f}_{DG_k} = \dfrac{\sum_{i=1}^{N} f_{DG_i}}{N}$

K_{pf} and K_{if} are the parameters of the PI controller, f^*_{MG} is the microgrid frequency parameter. $\bar{f}_{DG_k}$ is the average frequency of all DG units. δf_{DG_k} is the control signal generated by the DG_k secondary control at each sampling time. Here, i=1,2,……,N,k=1,2,….,n. N is the number of measurement frequency values, n is the number of DG units.

(b) Voltage control

Similar to frequency control, voltage control requires each inverter to measure the voltage value and then compensate for the voltage amplitude deviation caused by the droop control. The advantage of this method compared to centralized secondary control is that it does not require the use of sensors, only the terminal voltage of each DG [Savaghebi et al., (2012), Yong (2015)].At this point, the voltage is restored as follows:

$$\delta V_{DG_k} = K_{pv}(V_{MG}^{*} - \bar{V}_{DG_k}) + \mathrm{K}_{iv}\int (V_{MG}^{*} - \bar{V}_{DG_k})\,\mathrm{dt} \tag{5.3.4}$$

Where, $\bar{V}_{DG_k} = \dfrac{\sum_{i=1}^{N} V_{DG_i}}{N}$

Here δV_{DGk} is the recovery voltage value of DG_k, which is within each sample time.

Here, δV_{DG_k} is the recovery voltage value of DG_k, which is obtained by PI control of the difference between the microgrid voltage parameter V_{MG}^{*} and the DG voltage average value $\bar{V}_{DG_k}$ in each sample time. According to the above method, the secondary control can eliminate the voltage amplitude deviation caused by the primary control within each DG unit.

Figure 5.4 shows the specific distributed secondary control details for each DG of the microgrid. The distributed secondary control is placed between the communication system and the primary control. At this time, with the centralized secondary control only measuring the frequency and voltage amplitude of the microgrid.

The secondary control of each DG in the distributed secondary control is the measurement values (frequency, voltage amplitude and reactive power) of all other DG units need to be collected by the communication system, then averaged and the appropriate signals sent to the primary control to eliminate the steady-state error [Guerrero et al.,(2013), Shafiee et al., (2014), Bidram et al., (2013)].

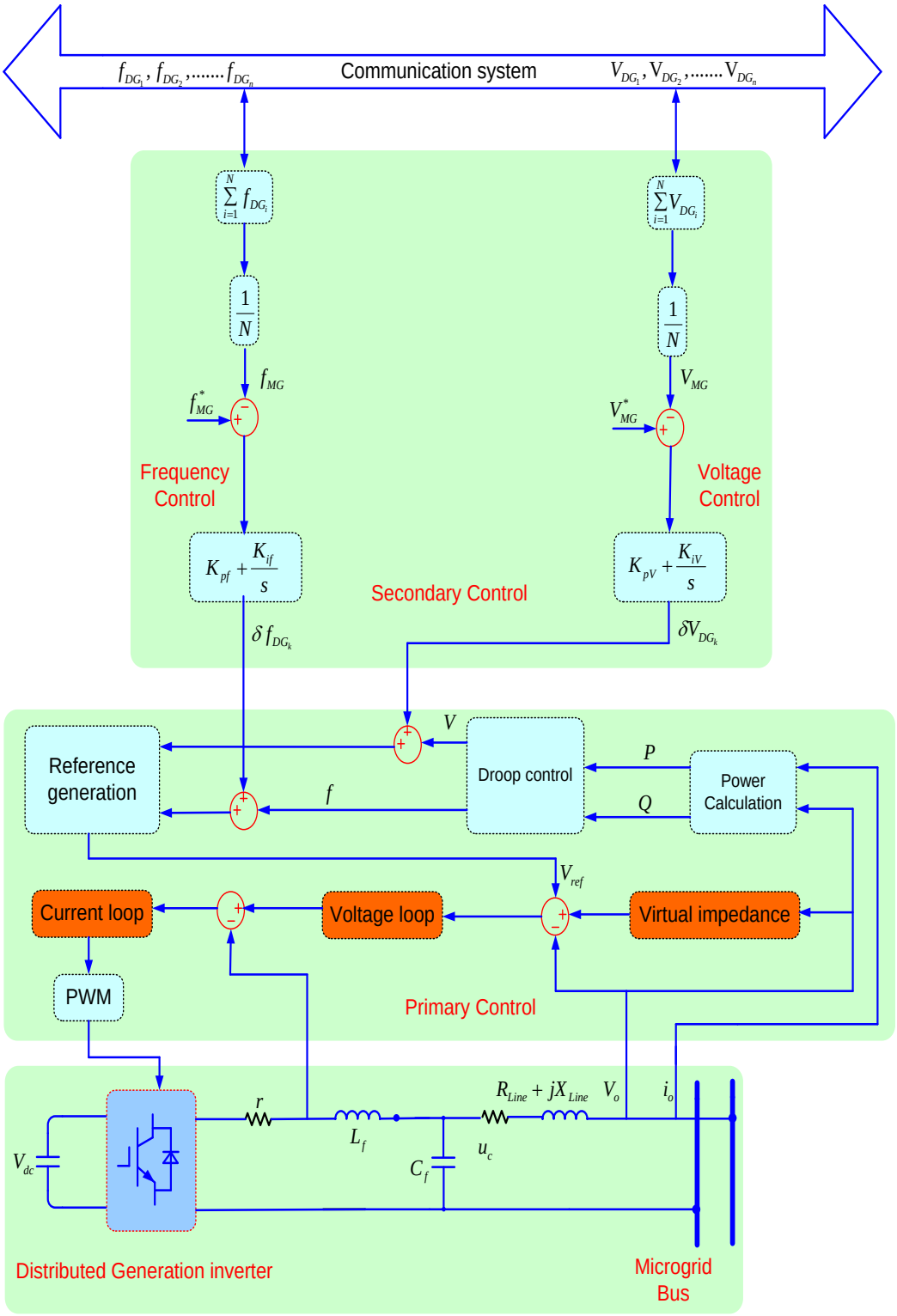

Figure 5.4: Details of distributed secondary control for a DG unit

5.4 IMPROVED DISTRIBUTED SECONDARY CONTROL

If the microgrid can be operated stably and efficiently, the choice of control method is very important. If the control method is selected to be suitable, the frequency and voltage of the microgrid can be effectively adjusted and the load power between the DGs can be accurately distributed. Decentralized control method requires only local information of the DG and therefore its stability is high. The centralized control method needs all the information of all DGs, its reliability is low.

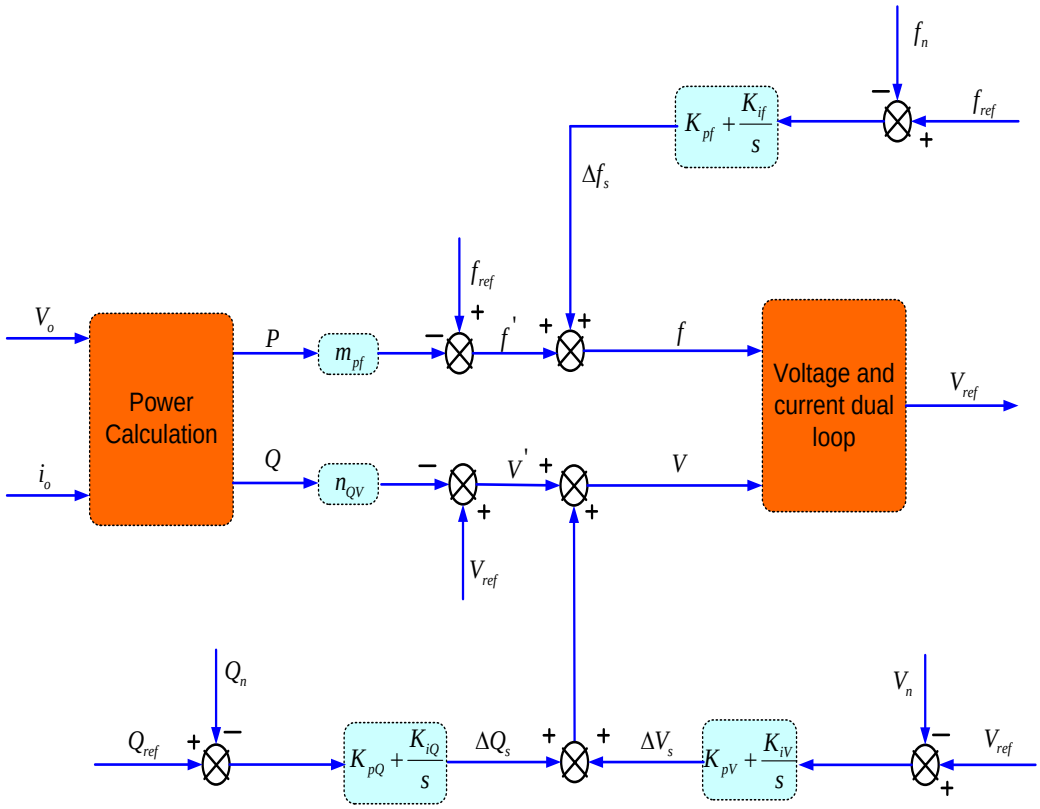

Figure 5.5 Control block diagram of secondary control with Direct(*P-f/Q-V)* droop control

In the distributed control method, each DG control unit only needs its local and neighboring DG information. Because the distributed DG controller does not need the central controller to collect the entire control information, the entire DG system will not cause large deviations due to the failure of a single DG control unit and the distributed control system has higher reliability. The distributed control method of the microgrid can maintain the stability of frequency and voltage while ensuring the

accurate distribution of load power by integrating the advantages of traditional decentralized control and centralized control methods.

In the islanding type microgrid with traditional direct and reverse droop control, when the load power fluctuates frequently, the output voltage and frequency of the DG inverter will have a large deviation from the rated value and adding the virtual impedance(resistors and inductors) will also cause the inverter output voltage to decrease. When the impedance value of the connection line is inconsistent, the voltage drop from the DG unit to the PCC point will be different, causing the active and reactive power to be unreasonably distributed.

In order to ensure the quality of the voltage and distribute the active and reactive power with high accuracy, voltage, frequency, active and reactive power are introduced into the secondary regulation so that the voltage and frequency maintain the rated output and the power is distributed rationally. Each DG unit includes conventional direct and reverse droop control and secondary regulation, eliminating the need for a central controller and enhancing system stability. When the reactive power increase, causes the voltage amplitude to decrease, the voltage is adjusted to the nominal value by the voltage droop control curve by the voltage secondary regulation control. When the increase in the load power causes the frequency to decrease, the frequency shifts to the nominal value by shifting the frequency upwards frequency droop control curve by the frequency secondary adjustment.

The secondary reactive power regulation directly controls the distribution of reactive power, so that the reactive power distribution is not affected by the voltage of the DG terminal, thereby eliminating the problem that the reactive power cannot be evenly distributed due to the inconsistence of line impedance and realizing highly accurate distribution of reactive power.

After introducing the secondary regulation control, the inverter output voltage and frequency reference values are f_{ref} and V_{ref} respectively, as shown in equations below:

$$f_n = f_{ref} - m_{Pf} P_n + \Delta f_s \tag{5.4.1}$$

$$V_n = V_{ref} - n_{QV} Q_n + \Delta V_s + \Delta Q_s \tag{5.4.2}$$

where,

$$\Delta f_s = (K_{pf} + \frac{K_{if}}{s})(f_{ref} - f_n)$$
$$\Delta V_s = (K_{pV} + \frac{K_{iv}}{s})(V_{ref} - V_n) \quad (5.4.3)$$
$$\Delta Q_s = (K_{pQ} + \frac{K_{iQ}}{s})(Q_{ref} - Q_n)$$

In the formula, K_{pf} and K_{if} are the proportional and integral coefficient of the frequency adjustment. K_{pV}, K_{iV} voltage ratio adjustment of the proportional and integral coefficient; K_{pQ}, K_{iQ} are the proportional and integral coefficient of the reactive power adjustement.

Δf_s, ΔV_s and ΔQ_s are the frequency, voltage and reactive power secondary regulation output values, respectively. The control block diagram of the DG inverter that adds the secondary voltage, frequency and reactive power adjustment for Direct (*P-f/Q-V*)droop control is shown in Figure 5.5.

It can be seen from the figure that the voltage secondary adjustment compares the output voltage of the inverter with a reference value and then adjusts the difference through a proportional-integral controller and then superimposes the voltage value V' of the conventional droop control output and the voltage V input after compensation is obtained. Voltage and current double loop control, eventually restore the voltage to the rated value.

According to the Figure 5.5, the voltage two regulation by comparing the output voltage of the inverter with the reference value, then the difference is adjusted by the proportional integral regulator controller, then superimposed to the traditional droop control output voltage value V', the compensated voltage V input to the voltage and current double loop control, finally the voltage is restored to the rated value.

In the same way, secondary adjustments can be made to the frequency and reactive power to keep the frequency at a rated value and the reactive power can be distributed with high accuracy.

The control block diagram of the DG inverter that adds the secondary voltage, frequency and reactive power adjustment for Reverse(*P-V/Q-f*) droop control is shown in Figure 5.6.

In the formula, K_{pf} and K_{if} are the proportional and integral coefficient of the frequency adjustment. K_{pV}, K_{iV} voltage ratio adjustment of the proportional and

integral coefficient; K_{pP}, K_{iP} are the proportional and integral coefficient of the active power adjustement. Δf_s, ΔV_s and ΔQ_s are the frequency, voltage and active power secondary regulation output values, respectively.

$$V_n = V_{ref} - m_{PV} P_n + \Delta V_s + \Delta P_s \tag{5.4.4}$$

$$f_n = f_{ref} + n_{Qf} Q_n + \Delta f_s \tag{5.4.5}$$

where,

$$\begin{aligned} \Delta f_s &= (K_{pf} + \frac{K_{if}}{s})(f_{ref} - f_n) \\ \Delta V_s &= (K_{pV} + \frac{K_{iV}}{s})(V_{ref} - V_n) \\ \Delta P_s &= (K_{pP} + \frac{K_{iP}}{s})(P_{ref} - P_n) \end{aligned} \tag{5.4.6}$$

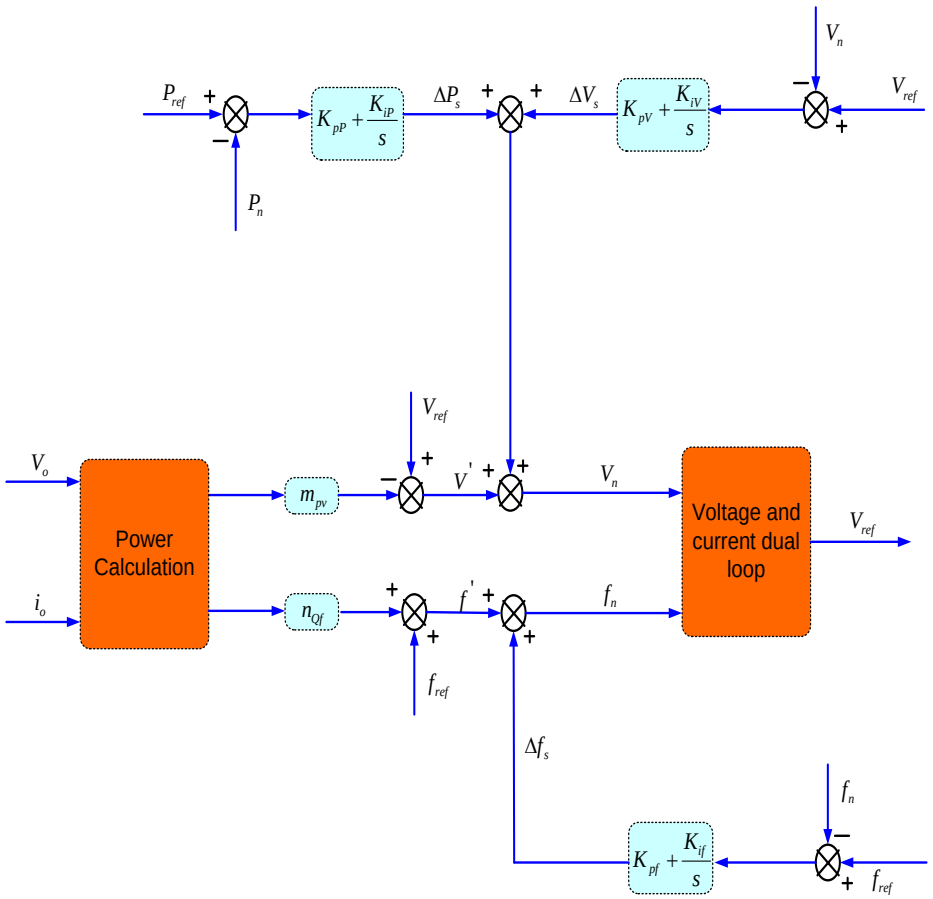

Figure 5.6 Control block diagram of secondary control with Reverse (*P-V/Q-f*)droop control

It can be seen from the figure that the voltage secondary adjustment compares the output voltage of the inverter with a reference value, and then adjusts the difference through a proportional-integral controller and then superimposes the voltage value V' of the reverse droop control output and the voltage V input after compensation is obtained. Voltage and current double loop control, eventually restore the voltage to the rated value.According to the Figure 5.6, the voltage two regulation by comparing the output voltage of the inverter with the reference value, then the difference is adjusted by the proportional integral regulator controller, then superimposed to the reverse droop control output voltage value V', the compensated voltage V input to the voltage and current double loop control, finally the voltage is restored to the rated value.In the same way, secondary adjustments can be made to the frequency and active power to keep the frequency at a rated value and the active power can be distributed with high accuracy.

Frequency control:In the frequency recovery control in Figure 5.7(a),5.8(a), it is assumed that the initial operating point of the inverter is A and the output power P_{ref} and frequency f_{ref} at this time. When the load decreases, the operating point moves to B, the output power increases to P' and the output frequency rises to f'. If the slope of the droop curve does not shift down at the same time and the operating point changes to C, the frequency can be restored to f_{ref}, i.e, when the load changes, by continuously correcting P_{ref} until it reaches P′, i.e, the inverter works in the droop curve 2, the secondary adjustment of the output frequency of the inverter can be realized. Therefore, for different power DGs, the secondary control mainly responds to changes in the nominal frequency.

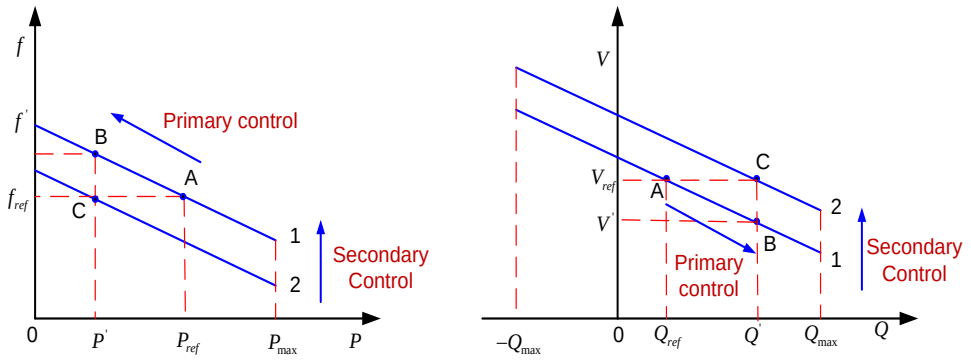

(a)Frequency recovery (b) Voltage amplitude

Figure 5.7: Secondary control response using direct droop control

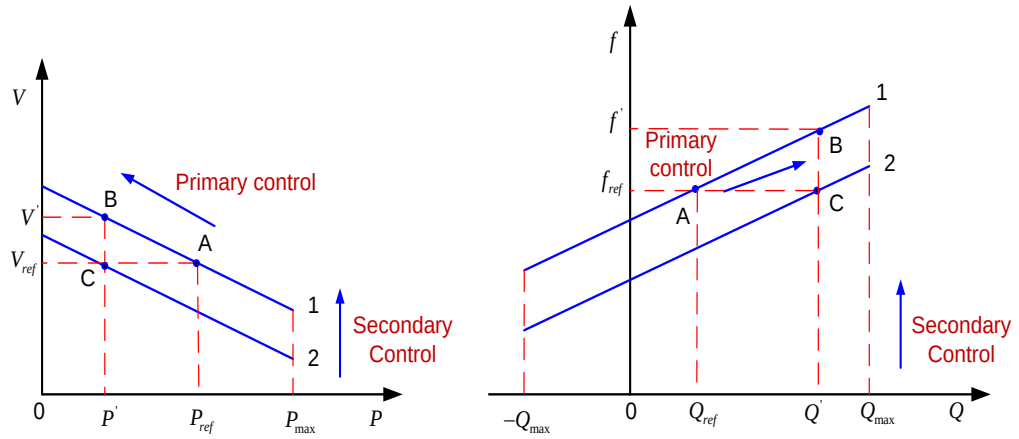

(a)Frequency recovery (b) Voltage amplitude

Figure 5.8: Secondary control response using reverse droop control

Voltage Control:A similar method can be used for distributed voltage control. As shown in Figure 5.7(b),5.8(b), it is assumed that the initial operating point of the inverter is A, the output power Q_{ref} and the voltage V_{ref}. When the load increases, the operating point moves to B, the output reactive power increases to Q' and the output voltage drops to V'. If the slope of the droop curve does not shift upwards and the operating point changes to C, the voltage can be restored to V_{ref}, i.e, when the load changes, Q_{ref} can be continuously corrected until it reaches Q', i.e, the DG inverter works in the droop curve 2 and the secondary adjustment of the inverter output voltage can be realized. Therefore, the voltage deviation caused by the direct and reverse droop control is reduced by calculating the voltage deviation of each inverter.

5.5 SIMULATION RESULTS

In this section, two simulation models of distributed generation inverters connected in parallel are built to verify the Direct (*P-f/Q-V)* and Reverse (*P-V/Q-f*) improved droop control strategy with resistive and inductive line impedance to ensure the rational allocation of power between parallel inverters. The simulation parameters are shown in the Appendix A.

Case 1: Power sharing analysis of secondary control with *P-V/Q-f* reverse droop control under resistive line impedance.

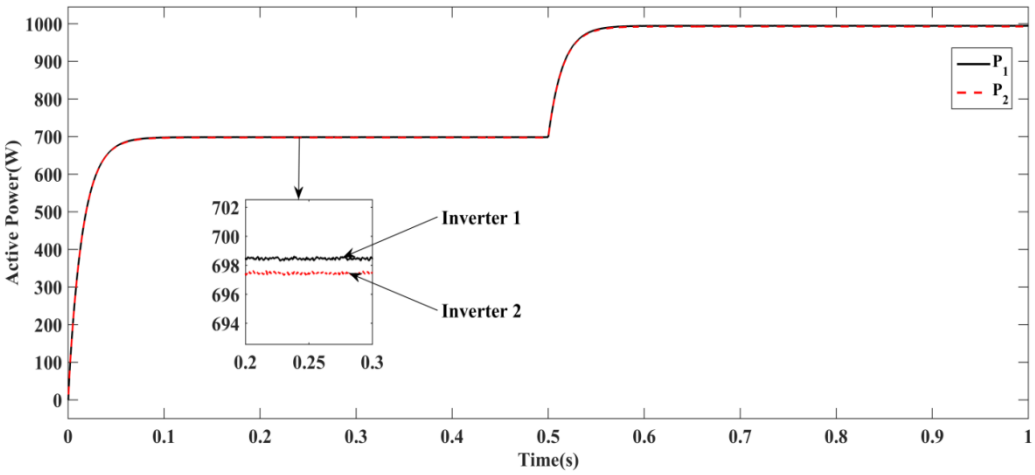

Figure 5.9: Active power sharing of parallel DG inverters using secondary control with virtual resistors under inductive line impedance.

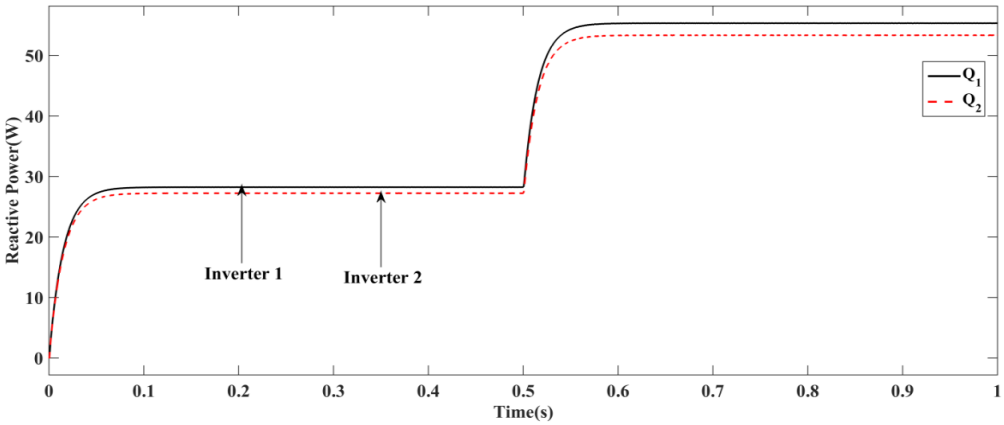

Figure 5.10: Reactive power sharing of parallel DG inverters using secondary control with virtual resistors under inductive line impedance.

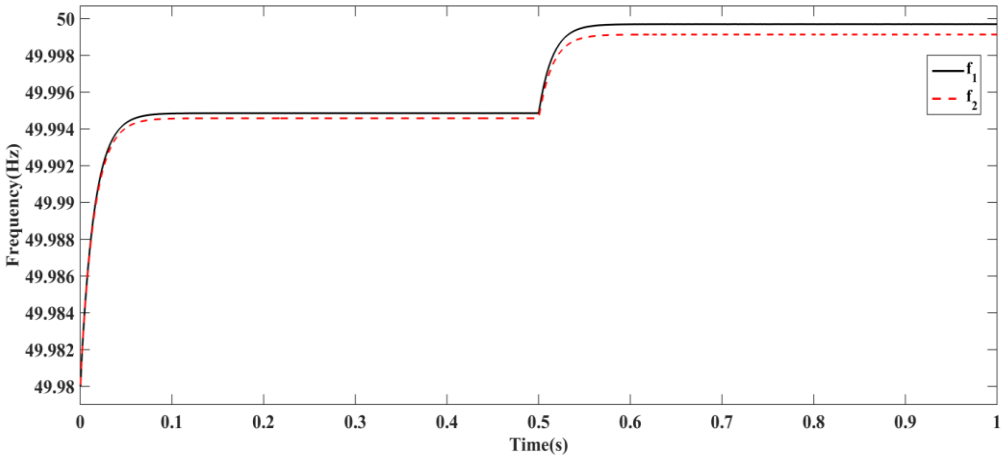

Figure 5.11 Parallel DG inverter output frequency using secondary control with virtual resistors under resistive line impedance.

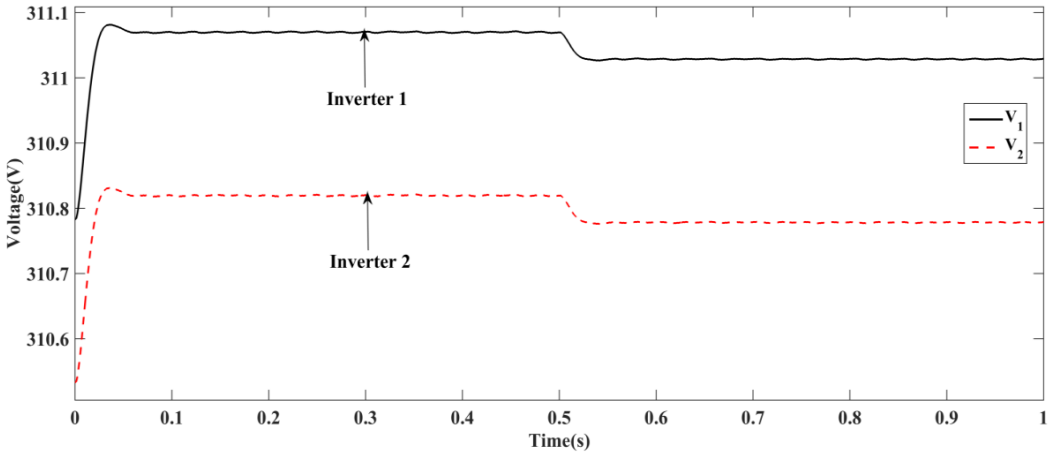

Figure 5.12 Parallel DG inverter output frequency using secondary control with virtual resistors under resistive line impedance.

Power sharing of parallel DG inverters is investigated with common load of P_{load} = 1400 W, Q_{load} = 60 VAR and at 0.5 s sudden local load value of P_{load} = 600 W, Q_{load} = 60 VAR is added to verify the dynamic response and line impedance of $R_{1Line} + jX_{1Line}$ = 0.6+j0.002 Ω, $R_{2Line} + jX_{2Line}$ = 0.7+j0.003 Ω. *P-V/Q-f* droop control based on virtual resistors with secondary control can reduce the influence of the line impedance difference on the parallel inverters by setting the total output impedance of the DG inverters to be resistive, which improves decoupling of power and improves the proportional load sharing P_1=697 W, P_2=696 W, Q_1=28 VAR, Q_2=27 VAR and at load change at 0.5 s, P_1=990 W, P_2=988 W, Q_1=54 VAR, Q_2=52 VAR as shown in the Figure 5.9-5.10 and frequency variation of DG inverters is within the range of 49.99 Hz to 50.001 Hz, the maximum fluctuation of 0.004 Hz as shown in the Figure 5.11. Voltage variation of DG inverters is V_1=311 V, V_2=310.8 V as shown in the Figure 5.12. Thus, the improved secondary control for reverse(*P-V/Q-f)* droop control, ensures voltage amplitude and frequency are restored to the rated value of 50 Hz and 311 V.

Case 2: Power sharing analysis of secondary control with *P-f/Q-V* direct droop control under inductive line impedance.

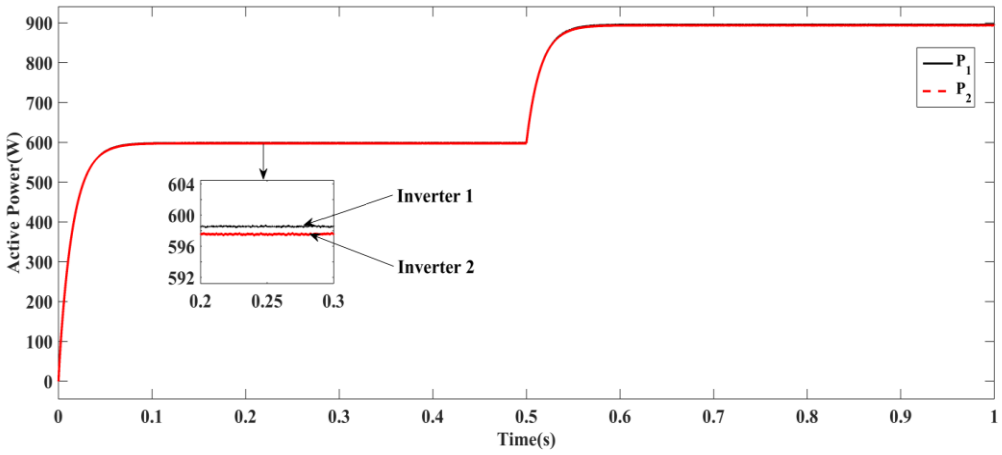

Figure 5.13 Active power sharing of parallel DG inverters using secondary control with virtual inductors under inductive line impedance.

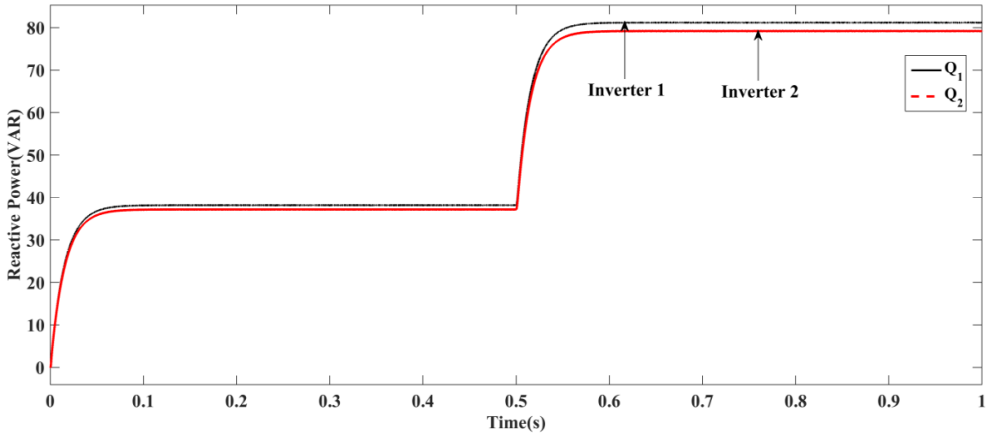

Figure 5.14 Reactive power sharing of parallel DG inverter using secondary control with virtual inductors under resistive line impedance.

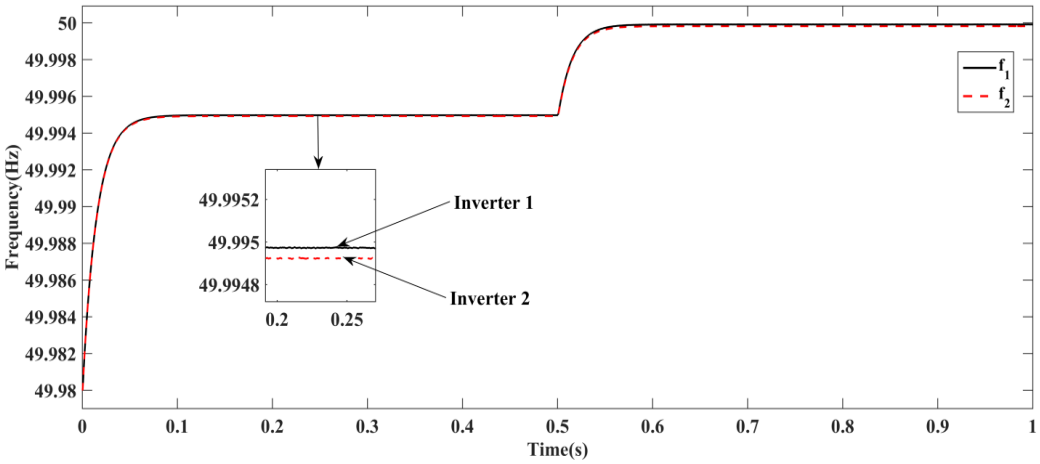

Figure 5.15 Parallel DG inverter output frequency using secondary control with virtual inductors under resistive line impedance.

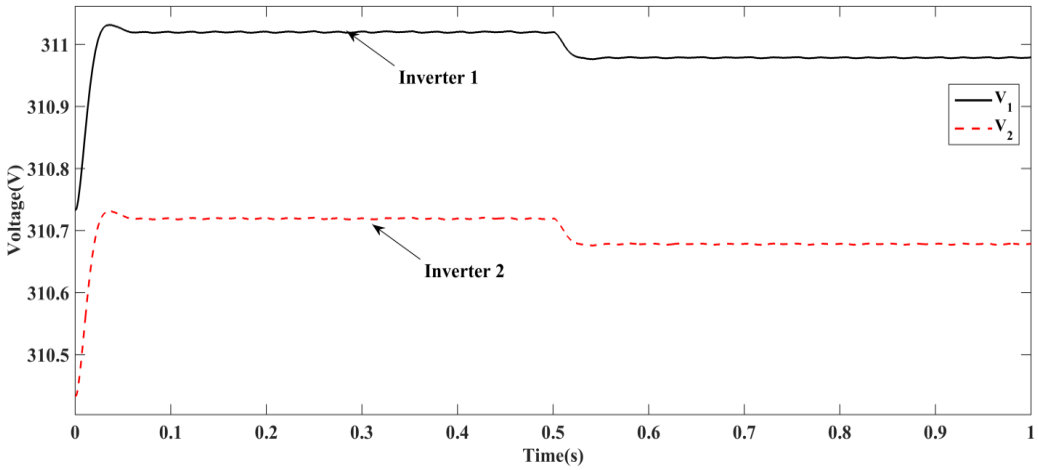

Figure 5.16 Parallel DG inverter output voltage using secondary control with virtual inductors under resistive line impedance.

Power sharing of parallel DG inverters is investigated with common load of P_{load} = 1200 W, Q_{load} = 80 VAR and at 0.5 s sudden local load value of P_{load} = 600 W, Q_{load} = 90 VAR is added to verify the dynamic response and line impedance of $R_{1Line} + jX_{1Line}$ = 0.002+j0.3 Ω, $R_{2Line} + jX_{2Line}$ = 0.003+j0.4 Ω. *P-f/Q-V* droop control based on virtual inductors with secondary control can reduce the influence of line impedance difference on the parallel DG inverters by setting the total output impedance of the DG inverters to be inductive, which improves decoupling of power and improves the proportional load sharing P_1=597 W, P_2=596 W, Q_1=38 VAR, Q_2=37 VAR and at load change at 0.5 s, P_1=892 W, P_2=890 W, Q_1=79 VAR, Q_2=77 VAR as shown in the Figure 5.13-5.14 and frequency variation of DG inverters is within the range of 49.99 Hz to 50.01 Hz, the maximum fluctuation of 0.004 Hz as shown in the Figure 5.15. Voltage variation of DG inverters is V_1=311.1 V, V_2=310.7 V as shown in the Figure 5.16. Thus, the improved secondary control for direct(*P-f/Q-V)* droop control, ensures voltage amplitude and frequency are restored to the rated value of 50 Hz and 311 V.

Case 3: Power sharing analysis of secondary control with *P-V/Q-f* reverse droop control under resistive line impedance (Frequent load changes).

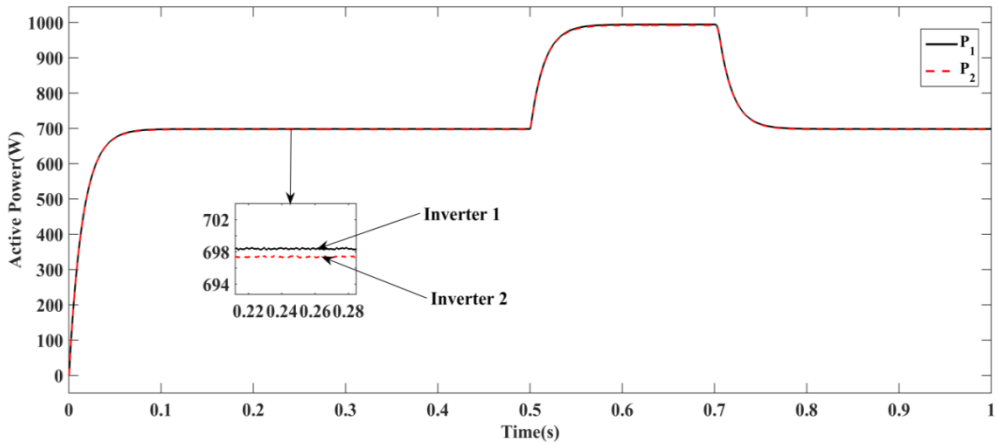

Figure 5.17 Active power sharing of parallel DG inverters using secondary control with virtual resistors under inductive line impedance (frequent load changes).

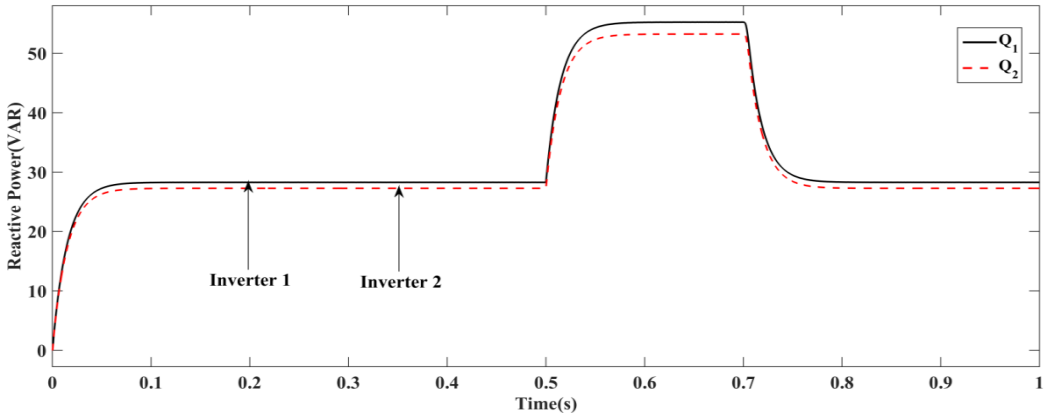

Figure 5.18 Reactive power sharing of parallel DG inverters using secondary control with virtual resistors under inductive line impedance(frequent load changes).

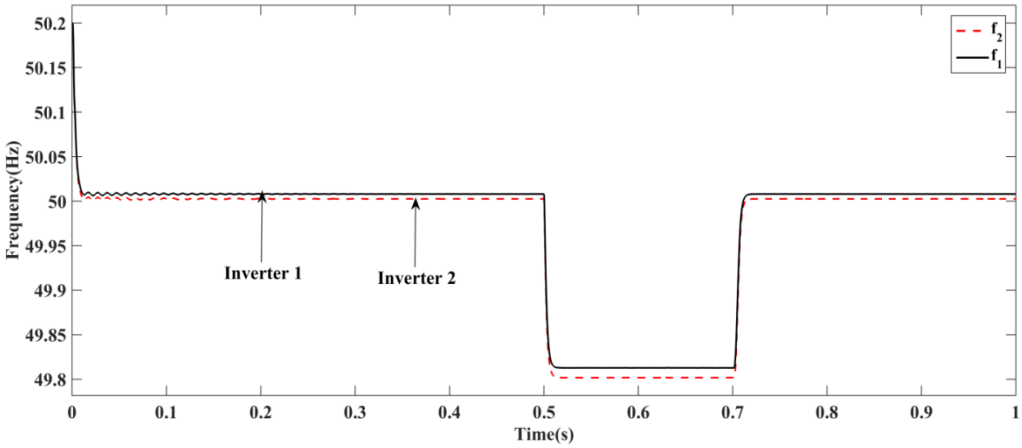

Figure 5.19 Parallel DG inverter output frequency using secondary control with virtual resistors under resistive line impedance(frequent load changes).

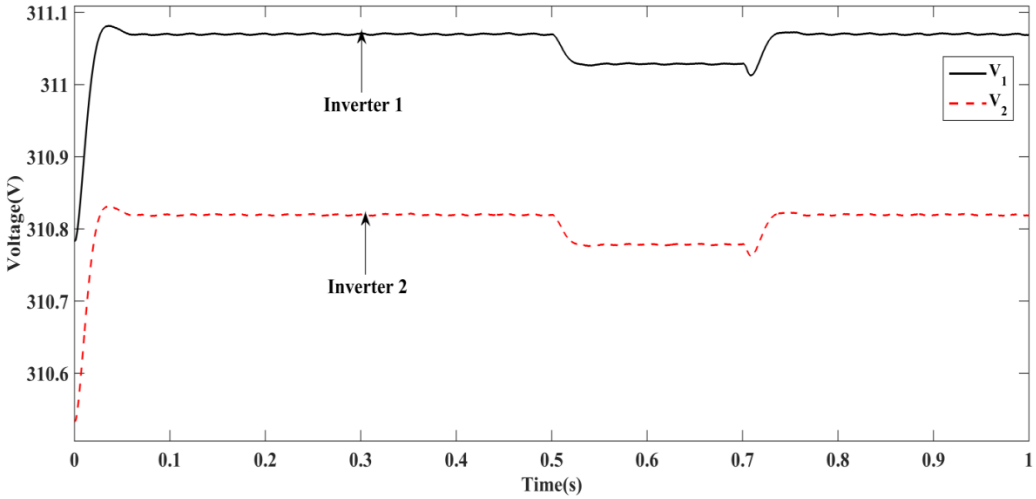

Figure 5.20 Parallel DG inverter output frequency using secondary control with virtual resistors under resistive line impedance(frequent load changes).

Power sharing of parallel DG inverters is investigated with common load of P_{load} = 1400 W, Q_{load} = 60 VAR and at 0.5 s sudden local load value of P_{load} = 600 W, Q_{load} = 60 VAR is added and removed at 0.7s to verify the dynamic response and line impedance of $R_{1Line} + jX_{1Line}$ = 0.6+j0.002 Ω, $R_{2Line} + jX_{2Line}$ = 0.7+j0.003 Ω. *P-V/Q-f* droop control based on virtual resistors with secondary control can reduce the influence of the line impedance difference on the parallel inverters by setting the total output impedance of the DG inverters to be resistive, which improves decoupling of power and improves the proportional load sharing P_1=697 W, P_2=696 W, Q_1=28 VAR, Q_2=27 VAR and load change at 0.5 s, P_1=990 W, P_2=988 W, Q_1=54 VAR, Q_2=52 VAR as shown in the Figure 5.17-5.18 and frequency variation of DG inverters is within the range of 49.98 Hz to 50.001 Hz, as shown in the Figure 5.19. Voltage variation of DG inverters is V_1=311.1 V, V_2=310.8 V as shown in the Figure 5.20. Thus, the improved secondary control for reverse (*P-V/Q-f)* droop control, ensures voltage amplitude and frequency are restored to the rated value of 50 Hz and 311 V.

Case 4: Power sharing analysis of secondary control with *P-f/Q-V* direct droop control under inductive line impedance(Frequent load changes).

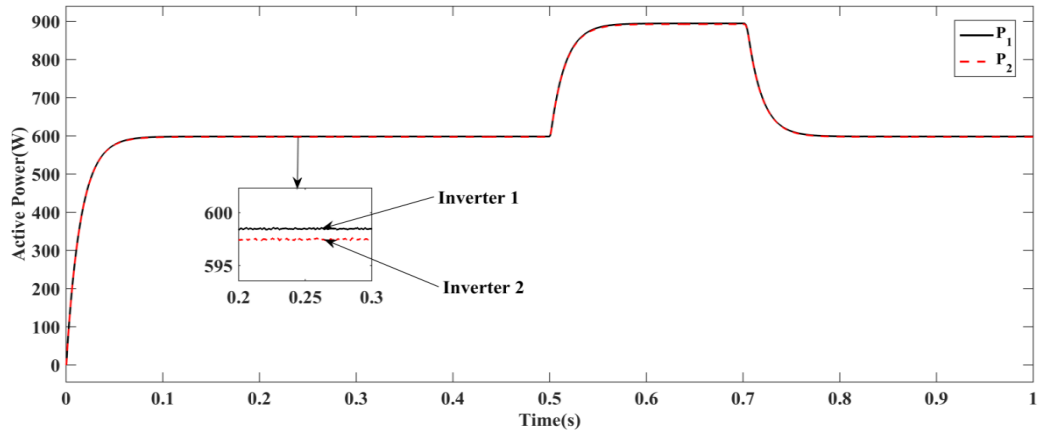

Figure 5.21 Active power sharing of parallel DG inverters using secondary control with virtual inductors under inductive line impedance(frequent load changes).

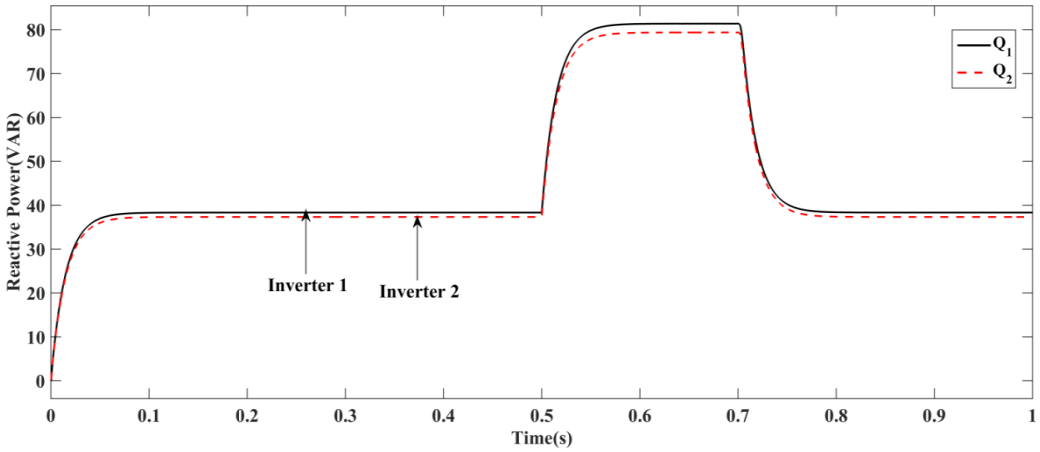

Figure 5.22 Reactive power sharing of parallel DG inverter using secondary control with virtual inductors under resistive line impedance(frequent load changes).

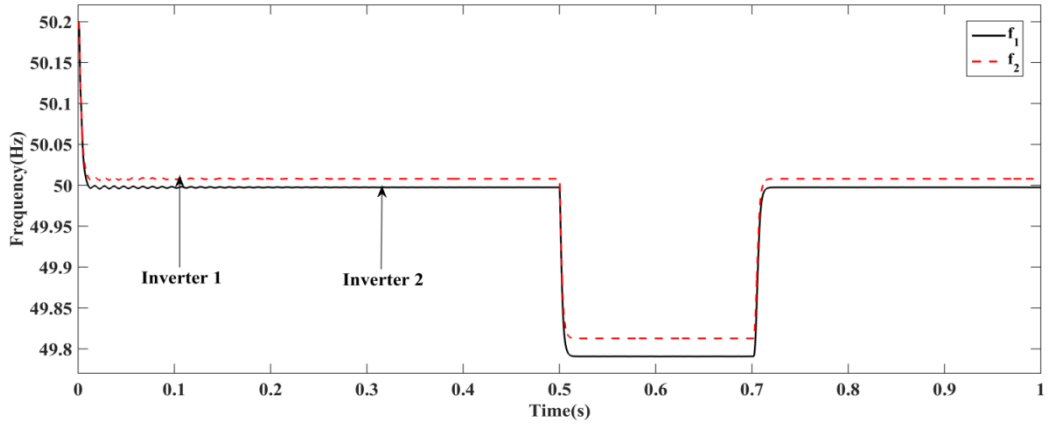

Figure 5.23 Parallel DG inverter output frequency using secondary control with virtual inductors under resistive line impedance(frequent load changes).

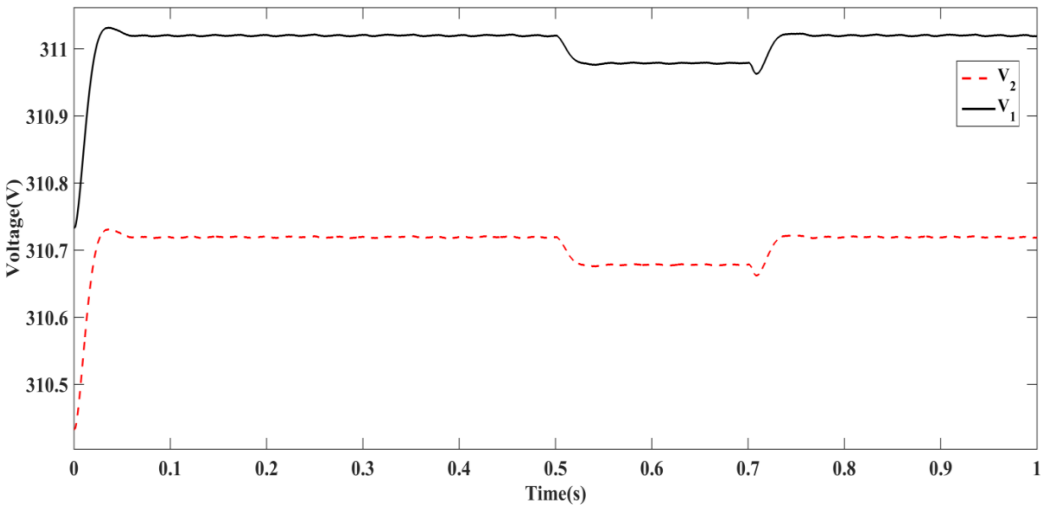

Figure 5.24 Parallel DG inverter output voltage using secondary control with virtual inductors under resistive line impedance(frequent load changes).

Power sharing of DG parallel inverters is investigated with common load of P_{load} = 1200 W, Q_{load} = 80 VAR and at 0.5 s sudden local load value of P_{load} = 600 W, Q_{load} = 90 VAR is added and removed at 0.7s to verify the dynamic response and line impedance of $R_{1Line} + jX_{1Line}$ = 0.002+j0.3 Ω, $R_{2Line} + jX_{2Line}$ = 0.003+j0.4 Ω. *P-f/Q-V* droop control based on virtual inductors with secondary control can reduce the influence of line impedance difference on the parallel DG inverters by setting the total output impedance of the DG inverters to be inductive, which improves decoupling of power and improves the proportional load sharing P_1=597 W, P_2=596 W, Q_1=38 VAR, Q_2=37 VAR and at load change at 0.5 s, P_1=892 W, P_2=890 W, Q_1=79 VAR, Q_2=77 VAR as shown in the Figure 5.21-5.22 and frequency variation of DG inverters is within the range of 49.98 Hz to 50.01 Hz, as shown in the Figure 5.23. Voltage variation of DG inverters is V_1=311 V, V_2=310.7 V as shown in the Figure 5.24. Thus, the improved secondary control for direct (*P-f/Q-V)* droop control, ensures voltage amplitude and frequency are restored to the rated value of 50 Hz and 311 V.

5.6 CONCLUSION

Aiming at the problem that the voltage and frequency deviate from the rated value of the active and reactive power under the traditional direct and reverse droop control method, such as the high accuracy distribution between the parallel inverter and the large load, the control strategy of two times regulating the voltage, frequency and reactive powers of DG Unit is proposed. The voltage and frequency can be maintained at rated values through secondary regulation and the active and reactive power also achieves higher precision of the distribution.

Chapter 6

6 CONCLUSIONS AND FUTURE SCOPE

6.1 CONCLUSIONS

At present, the new energy revolution centered on the development of renewable energy and new energy has been opened on a global scale. As an important technical support of uninterruptible power supply system, distributed generation, new energy, microgrid, inverter parallel technology is also one of the key technologies in power system application, and it has very definite practical significance. In this thesis, the droop control applied parallel power sharing technology and power flexible distribution technology and related problems of the DG inverter system are discussed and studied. The main research results are summarized as follows:

(1) The background and significance of the research topic are introduced. The research status of the micro-grid all over the world is analyzed and the main research directions are explained. The basic structure and common control strategy of the microgrid are introduced. The main control methods of the DG inverter type interface in the microgrid are described. The basic control principle and main control module are analyzed and the focus is on the droop control technology.

(2) The advantages and disadvantages of different main circuits of the distributed generation source inverter and the topology structure of the filter are analyzed. Based on the mathematical model of distributed generation inverter, the closed-loop control of voltage instantaneous value in three-phase static coordinate system and the output voltage control strategy of inverter based on voltage and current cancellation in dq rotating coordinate system are analyzed. The output voltage control strategy based on the proportional integral controller is adopted in the dq coordinate system, which reduces the number of variables. The influence of controller parameters on the voltage closed-loop transfer function and the equivalent output impedance of the DG inverter is analyzed.

(3) Analyzes the basic structure and principle of droop control. Secondly, on the basis of this, the structure of the droop controller and the conditions and characteristics of proportionally sharing the load capacity in the DG inverter parallel system using the controller are explained in detail. In order to solve the problem of

power sharing and power coupling at the same time, this chapter adopts an improved virtual inductance method. In the virtual inductance control method, the effect of virtual inductance is analyzed from the perspective of equivalent impedance, and the Bode plot of the output impedance under typical control parameters is analyzed. Finally, the simulation of the control mode is carried out. In parallel with the DG inverters, the improved direct droop control and the direct droop control power allocation results are compared and analyzed. The simulation results verify the effectiveness of the improved direct droop control method.

(4) In the low-voltage micro-grid, the impedance of transmission line is resistive, which makes the traditional direct droop control not to be used normally and the power coupling between active and reactive is unable to realize the proportional load sharing. The difference of the droop control between the microgrid and traditional grid was analyzed based on the power transmission characteristics, the the reverse droop control that suits for the low voltage microgrid was adopted as the basis of the study in this chapter. The virtual resistance method is used to realize active and reactive power decoupling control for the coupling between active and reactive power in low voltage microgrid. The virtual resistance strategy is adopted to eliminate the influence of differences between line impedance on power distribution. The influences of different line impedances on DG inverter power distribution are simulated and the effectiveness of the scheme is verified.

(5) Analysis of improved direct and reverse droop control with secondary control for DG parallel inverters in microgrid is proposed considering line and output impedance. Due to the voltage and frequency deviation in direct and reverse droop control, especially when the microgrid is operating in islanded mode, the stability of the system will be affected if the offset is too large. The voltage and frequency control was used to guarantee the stability of the whole system in this chapter. The proposed distributed secondary for direct and reverse droop control , a compensates the virtual resistors and inductors voltage drop and line impedance differences, to improve output voltage amplitude and frequency accuracy to the reference value. Simulation results show the rationality and effectiveness of the proposed improved control method.

6.2 FUTURE SCOPE

In this thesis, some discussions and research on DG inverter parallel control and related problems based on droop control and virtual impedance technology have been made and some achievements have been made, but the following aspects still need to be further developed:

The improved control strategy studied in this thesis improves the power accuracy of the inverter parallel system and the dynamic and steady-state performance of the power distribution, but it is mainly explained by linear load in the simulation, that is, only the fundamental power component is considered.

When the inverter parallel system has a non-linear load, the harmonic current has not been analyzed in depth based on the proposed scheme for the allocation between the parallel inverter units.

The focus of this thesis is on the power sharing controller and the power distribution controller. The output voltage quality of a parallel system is determined by the joint action of all parallel units, so the research design of the voltage controller is also critical. The synchronization precision of each inverter is low because of the parallel technology based on droop control, so the stable operation of the parallel system with impedance support is needed. The stand-alone DG inverter control aims to design the inverter close to the ideal voltage source.

Single inverter voltage control technology such as proportional resonance control, repetitive control, no beat control, optimal control and so on, if applied to the shunt inverter voltage controller, the influence of the power distribution of the parallel system and the design of the impedance level are necessary to ensure the stability of the parallel system, which remains to be discussed.

In addition, different PWM (Pulse width modulation) modulation techniques, such as bipolar, unipolar and unipolar frequency multiplier SPWM modulation and SVPWM modulation. The influence of modulation on the parallel circulation (including the power-frequency circulation and the switching sub-circulation) is still to be studied.

LIST OF PUBLICATIONS

International Journals

1. Chethan Raj D, D.N.Gaonkar, Josep M Guerrero. (2018). "Improved Pf/QV and PV/Qf droop controllers for parallel distributed generation inverters in AC microgrid". *International journal of sustainable Cities and Society*, Volume 41, no.1, pp-421-442.

2. Chethan Raj D, D.N.Gaonkar.(2017). "Multiple Inverters operated in parallel for proportional load sharing in microgrid". *International journal of power electronics and drive systems*, Volume 8, no.2, pp:654-666, 2017.

3. Chethan Raj D, D.N.Gaonkar, Josep M Guerrero "Power sharing control strategy of parallel inverters in AC microgrid using improved reverse droop control". *International journal of power electronics*, Volume 11, no.1, pp:116-137, 2020.

International Conferences

1. Chethan Raj D, D N Gaonkar. (2016). "Frequency and voltage droop control of parallel inverters in microgrid". *2nd (IEEE) International conference on control, instrumentation,energy and communication*, pp:407-411.

2. Chethan Raj D, D N Gaonkar.(2014). "Coordination control of microgrid". *9th (IEEE) International conference on Industrial and Information systems*, pp:1-6.

APPENDIX

Parameters of Parallel DG inverters

Symbol	Value	Description
f_s	10 kHz	Inverter switching frequency.
L_f	3 mH	Filter inductor.
C_f	15 µF	Filter capacitor.
r	0.2 Ω	Filter inductor equivalent resistance.
V_{dc}	700 V	DC link voltage.
f	50 Hz	Fundamental frequency.
R_v	2 Ω	Virtual resistors.
L_v	6 mH	Virtual inductors.
m_{pf1},m_{pf2} n_{QV1},n_{QV2}	0.000025 rad/s/W, 0.0014 V/VAR	Direct*(P-f/Q-V)*droop control coefficients.
m_{PV1}, m_{PV2} n_{Qf1},n_{Qf2}	0.0014 V/W, 0.000025 rad/s/VAR	Reverse*(P-V/Q-f)* droop control coefficients.
V_o	311 V	Output voltage of inverter(microgrid system voltage).
K_{pf}, K_{if}	0.25, 6.1	Frequency secondary adjustment parameters for direct droop control
K_{pV}, K_{iV}	0.4, 2.1	Voltage secondary regulation parameters for direct droop control
K_{pQ}, K_{iQ}	0.06, 0.7	Reactive secondary adjustment parameters for direct droop control
K_{pf}, K_{if}	0.3, 5	Frequency secondary adjustment parameters for Reverse droop control
K_{pV}, K_{iV}	0.6, 2.6	Voltage secondary regulation parameters for Reverse droop control
K_{pP}, K_{iP}	0.04, 0.9	Reactive secondary adjustment parameters for Reverse droop control
Inverter 1,2.	3 KVA	Inverter rating

REFERENCES

Ackermann,T., Anderson,G. and Soder,L. (2001). "Distributed generation: a definition*." J.Electric power system research*, 57(3), pp.195-204.

Ackermann,T. and Knyazkin,V. (2002). "Interaction between distributed generation and the distribution network:Operation aspects." *Proc., IEEE/PES Transmission and distribution conf. Asia pacific*, pp.1357-1362.

Ahmed,M.A. and Istvn,E. (2005). "Impact of distributed generation on the stability of electrical power systems." *IEEE power engineering society general meeting*, pp.1056-1063.

Ahn,S.J., Park,J.W., Chung,Y., Moon,S., Kang,S.H. and Nam,S.R. (2010). "Power sharing method of multiple distributed generators considering control moded and configurations of a microgrid." *IEEE Trans. on Power delivery*, 25(3), pp.2007-2016.

Ahumada,C., Cardenas,R., Saez,D. And Guerrero,J.M. (2016). "Secondary control strategies for frequency restoration in islanded microgrids with consideration of communication delays." *IEEE trans. on smart grid*, 7(3), pp.1430-1441.

Augustine,S., Lakshminarasamma,N. and Mishra,M.K. (2016). "Control of photovoltaic based low voltage dc microgrid system for power sharing with modified droop algorithm." IET power electronics, 9(6), pp.1132-1143.

Augustine,S., Mishra,M.K. and Lakshminarasamma.,N. (2015). "Adaptive droop control strategy for load sharing and circulating current minimization in low voltage standalone dc microgrid." *IEEE trans. on sustainable energy*, 6(1), pp.132-141.

Balijepalli,V.V.S.K.M., Khaparde,S.A., Dobariya,c.V., (2010). "Deployment of microgrids in india." *Proc. IEEE PES Generating meeting*, pp.1-6.

Bansal,R. and Manditereza,P.T. (2016). "Renewable distributed generation: the hidden challenges-a review from the protection perspective." J.*Renewable and Sustinable Energy reviews*, 58(1),pp.1457-1465.

Barik,M.A., Pota,H.R. and Ravishankar,J. (2015). "Hierarchical control approach for microgrid load sharing with renewable energy sources." IEEE Power & Energy Society General Meeting, pp.1-5.

Bidram,A., Davoudi,A., Lewis,F.K. and Guerrero,J.M. (2013). “Distributed co-operative secondary control of microgrids using feedback linearization.” *IEEE Trans. on Power system*. 28(3), pp.3462-3470.

Bidram,A., Davoudi,F., Lewis,F.K. and Qu,Z. (2013). “Secondary control of microgrids based on distributed cooperative control of multi agent systems.” *IET Generation transmission and distribution*, 7(8), pp.822-831.

Blaabjerg,F., Chen,Z. and Kjaer,S.B. (2004). “Power electronics as efficient interface in dispersed power generation systems.” *IEEE trans. on Power electronics*, 19(5), pp.1184-1194.

Brabandere, K D., Bolsens, B. and Van J.(2007). “A voltage and frequency droop control method for parallel inverters.” *IEEE trans. on Power electronics*, 22(4), pp.1107-1115.

Braun,M., Degner,T. and Vandenbergh,M.(2006). “Laboratory DG grid.” European Commission.

Broeck,H.V.D. and Boeke,U. (1998). “A simple method for parallel operation of inverters.” *Proc., IEEE/International Telecommunications Energy Conference*, pp.143-150.

Chandorkar, M. C., Divan, D. M. and Adapa, R. (1993). “Control of parallel connected inverters in standalone ac supply systems.” *IEEE Trans. on Industry Applications*, 29(1), pp.136-143.

Changyoung,W., Yinhai,Z. and Zhongchao,Z. (2000). “Characteristics and design of LC filter in current source active power filter.” *J.Telecom power technologies*, 12(4), pp.12-14.

Chen,Y., Guerrero,J.M., Shuai,Z., Chen,Z., Zhou,L. and Luo,A. (2016). “Fast reactive power sharing, circulating current and resonance suppression for parallel inverters using resistive-capacitive output impedance.” *IEEE transactions on Power electronics*, 31(8), pp.5524-5537.

Chen.D.(2014). “Research on control strategy of parallel operated inverters based on virtual resistance in low voltage microgrid.” *Master thesis*, Yanshan university,China.

Cheng,Y.J. and Sng,E.K.K. (2006). “A novel communication strategy for decentralized control of paralleled multi inverter systems.” *IEEE Trans. On Power Electronics*, 21(1), pp. 148-156.

Chengshan, W., Zhaoxia, X. and Shouxiang, W. (2009). “Multiple feedback loop control scheme for inverters of the microsource in microgrids.” *Transactions of China Electro Technical society*, 24(2), pp.100-107.

Chengshan,W., Zhaoxia,X. and Shouxiang,W. (2008). “Synthrtical control and analysis of microgrid.” *J.Automation of electric power systems*, 32(7), pp.98-103.

Chiang,S.J., Lin,C.H., Yen.C.Y. (2004). “Current limitation control technique for parallel operation of UPS inverters.” *Proc. IEEE Power Electronics Specialists Conference*, pp.1922-1926.

Chun,M.X., Qiang,B.D. and Wen,R.X. (2010). “Study on control strategies of a low voltage microgrid.” *J.Automation of electric power systems*, 34(19), pp.91-96.

Chunxue,W. and Zhengxi,L. (2012). “A simplified control method of parallel inverters based on virtual impedance control loop.” *Trans. on china electrotechnical society*, 27(6), pp.63-68.

Cuiyun,Li.(2013). “Research on voltage and frequency recovery control in microgrid based on droop characteristic, *Master thesis*, Yanshan University, China.

Dahraie,m.V., Moghaddam,A.A. and Guerrero,J.M. (2018). “Evaluation of reliability in risk constrained scheduling of autonomous microgrids with demand response and renewable resources.” *IET Renewable power generating*, 12(6), pp.657-667.

Das,P.P. and Chattopadhyay,S. (2015). “A d-q voltage droop control method for inverter paralleling without any communication between individual inverters.” *Proc., IEEE energy conversion congress and exposition conference*, pp.3794-3801.

Dawei,C. and Guiping,Z. (2010). “Power transmission characteristics of low voltage microgrids.” *J. trans. on china electrotechnical society*, 25(7), pp.117-123.

Debnath,D. and Chatterjee,K. (2016). “Solar photovoltaic-based stand-alone scheme incorporating a new boost inverter.” *IET Power electronics*, 9(4), pp.621-630.

Deng,H., Oruganti,R. and Srinivasan,D. (2005). “PWM methods to handle time delay in digital control of a UPS inverter.” IEEE power electronics letters, 3(1), pp. 1-6.

Dengke,G., Jianguo,J. and Yuhua,Z. (2012). “Design of microgrid control strategy using voltage amplitude and phase angle droop control.” *J.Automation of electric power systems*, 36(5), pp.29-34.

Dong,J., Feng,T.T., Sun,H.X., Cai,H.X., Li,R. and Yang,Y. (2016). “Clean distributed generation in china:Policy options and international experience.” *J.Renewable and Sustainable energy reviews*, 57(1), pp.753-764.

Dragicevic,T., Lu,X., Vasquez,J.C. and Guerrero,J.M. (2016). “DC microgrids-Part I:A review of control strategies and stabilization techniques.” *IEEE trans. on power electronics*, 31(7), pp.4876-4891.

Driesen,J. and Katiraei,F. (2008). “Design for distributed energy resources.” *IEEE power and energy magazine*, 6(3), pp.30-40.

Dugan,R.C. and Mcdermott,T.E. (2002). “Distributed generation.” *IEEE Industry application magazine*, 8(2), pp.19-25.

Eid,B.M., Rahim.N.A., Selvaraj,J. and Kateb,A.H.E .(2016). “Control method and objectives for electronically coupled distributed energy resources in microgrids: A Review.” IEEE systems journal, 10(2), pp.446-458.

Engler,A. (2005). “Applicability of droops in low voltage grids.” J.Distributed energy resources, 1(1), pp.1-6.

European Comission. “Strategic research agenda for europe’s electricity networks of the future.”[EB/OL].http://www.smartgrids.eu.

Gao,F. and Iravani,M.R. (2008). “A control strategy for a distributed generation unit in grid connected and autonomous modes of operation.” *IEEE trans. on power delivery*, 23(2), pp.850-859.

Golsorkhi,M.S. and Lu, D. D. C. (2015). “ A Control Method for Inverter-Based Islanded Microgrids Based on V-I Droop Characteristics.” *IEEE trans. on power delivery*, 30(3), pp. 1196-1204.

Guerrero, J. M., Berbel, N.,Devicuna, L.G., Matas, J., Miret, J. and Castilla M. (2006). “Droop control method for the parallel operation of online uninterruptible

power systems using resistive output impedance." *IEEE Twenty first Annual Applied Power Electronics Conference and Exposition*, pp.1716-1722.

Guerrero, J. M., Garciade,V.L., Matas,J., Castilla,M. and Miret,J. (2005). "Output impedance design of parallel connected ups inverters with wireless load sharing control." *IEEE trans. on industrial electronics*, 52(4), pp. 1126-1135.

Guerrero, J. M., Vicuna, L, G, de., Matas J, Castilla, M. and Miret, J. (2004). "A wireless controller to enhance dynamic performance of parallel inverters in distributed generation systems." *IEEE trans. on Power electronics*, 19(5), pp.1205-1213.

Guerrero, J.M., Hang, L. and Uceda, J. (2008). "Control of distributed uninterruptible power supply systems." *IEEE Trans. on Industrial Electronics*, 55(8), pp. 273-281.

Guerrero, J.M., Matas J., Vicuna L., Castilla M. and Miret, J. (2007). "Decentralized control for parallel operation of distributed generation inverters using resistive output impedance." *IEEE Trans. on industrial electronics*, 54(2), pp.994-1004.

Guerrero,J.M., Blaabjerg,F., Zhelev,T., Hemmes,K., Monmasson,E., Jemei,S., Comech,M.P., Granadino,R. and Frau,J.I. (2010). "Dsitributed Generation:Toward a new energy paradigm." *IEEE trans. on industrial electronics*, 60(4), pp.195-204.

Guerrero,J.M., Chandorkar,M., Lee,T. and Loh,P.C. (2013). "Advanced control architectures for intelligent microgrids-part-I: Decentralized and hierarchical control." *IEEE trans. on Industrial electronics*, 6094), pp.1254-1262.

Guerrero,J.M., Vasquez,J.C., Matas,J. and Vicuna,L.G.De. (2011). "Hierarchical control of droop controlled ac and dc microgrids-A general approach towards standardization." *IEEE Trans. on Industrial electronics*, 58(1), pp.158-172.

Guo,F. and Wen,C. (2014). "Distributed control subjected to constraints on control inputs: A case study on secondary control of droop controlled inverter based microgrids." *Proc., 9th IEEE Conf.Ind.Electron.Appl., Hangzhou, China*, pp.1119-1124.

Guo,Q.(2016). "Research on parallel technology of distributed inverter system for flexible power sharing control." *Phd thesis*, Zhejiang University, China.

Guo,Q., Wu,H., Lin,L. and Bai,Z. (2016). "Secondary voltage control for reactive power sharing in an islanded microgrid." *Journal of Power Electronics*, 16(1), pp.329-339.

Gupta,A., Dolla,S. and Chatterjee,K. (2018). "Hybrid AC-DC microgrid: Systematic evaluation of control strategies." IEEE trans. on smart grid, 9(4), pp.3830-3843.

Han,H., Liu,Y., Sun,Y., Su, M. and Guerrero,J.M. (2015). "An improved droop control strategy for reactive power sharing in islanded microgrid." *IEEE trans. on power electronics*, 30(6), pp. 3133-3141.

Han,Y., Li,H., Shen,P., Coelho,E.A.A. and Guerrero,J.M. (2017). "Review of active and reactive power sharing strategies in hierarchical controlled microgrids." *IEEE Trans. on Power electronics*, 32(3), pp.2427-2451.

Haoran,L., Xuhong,Y. and Chengchen,F. (2015). "Control strategy research of output impedance analysis and improved droop control based on multiple inverters parallel." *J.power system protection and control*, 43(20), pp.29-35.

Hasanzadeh,A., Onar,O.C., Mokhtari,H. and Khaligh,A. (2010). "A Proportional resonant controller based wireless control strategy with a reduced number of sensors for parallel operated UPSs." *IEEE trans. on power delivery*, 25(1), pp.468-478.

Hatziargyriou,N. (2007). "Overview of microgrid R&D in Europe." *Symposium on microgrids*,Nagoya.

Hatziargyriou,N., Asano,H., Iravani,R. and Marnay.C. (2007)."Microgrids:An overview of ongoing research,development and demonstration projects.' *IEEE power and energy magazine*, 5(4), pp.78-94.

He,J., Li,Y. and Blaabjerg,F. (2015). "An enhanced islanding microgrid reactive power imbalance power and harmonic power sharing scheme." *IEEE Trans. on Power electronics*, 30(6), pp.3389-3401.

He,J. and Li,Y.W. (2012). "An Enhanced Microgrid Load Demand Sharing Strategy." *IEEE trans. on power electronics*." 27(9), pp.3984-3995.

He,Z., Wang,X., Xing,Y. and Ma,Y. (2008). "Presynchronization control for parallel inverters based on power line communication." *Proc., IEEE Power Electronics Specialists Conference*, pp.3243-3247.

He,Z. and Xing,Y. (2008). "Distributed control for UPS modules in parallel operation with RMS voltage regulation." *IEEE trans. on industrial electronics*, 55(8), pp. 2860-2869.

Hou,X., Sun,Y., Yuan,W., Han,H., Zhong,C. and Guerrero,J.M. (2016). "Conventional P-ω/Q-V droop control in highly resistive line of low voltage converter based AC microgrid. *J.Energies*, 9(11), 943-963.

Hsieh,H.M., Wu,T.F., Wu,Y.E., Nien,H.S. and Wu,Y.E. (2005). "A compensation strategy for parallel inverters to achieve precise weighting current distribution." *Proc., IEEE Industry Applications Conference*, pp.954-960.

Hu,J., Zhu,J., Dorrell,D.G. and Guerrero, J.M. (2014). "Virtual flux droop method-A new control strategy of inverters in microgrids." *IEEE Trans. on power electronics*, 29(9), 4704-4711.

Hua, H., Xou X., Yang J, Wu. J., Su,M. and Guerrero, J.M. (2016). "Review of power sharing control strategies for islanding operation of ac microgrids." *IEEE trans. on smart grid*, 7(1), pp.1200-1214.

Huo,M., Hu,H., Xing,H. and Guerrero,J.M. (2012). "Multilayer control for inverters in parallel operation without intercommunications." *IEEE Trans. on Power electronics*, 27(8), pp.3651-3663.

IEEE std. 1547(2003). IEEE standard for interconnecting distributed resources with electric power system.

Jiarong,K., Yunya,W. and Shaojun,X. (2009). "Design of control parameters for parallel connected inverters." *trans. on china electro technical society*, 24(9), pp.120-127.

Jiaxin,L., Yingchao,Z., Xisen,Q., Song,C. and Zhengming,Z. (2014). "Analysis of virtual output impedance for parallel connected inverters with wireless load sharing control." *J.Power supply*, 51(1), pp.55-60.

Jin,L., He,Z., Zhang,Y., Nie,J. and Zhang,M. (2016). "A new virtual impedance method for parallel inverters with droop control." *IEEE vehicle power and propulsion conference*, Hangzhou, China, pp.1-4.

Jinxiao,L. (2013). “Research on the three phase inverters in parallel without interconnection based on virtual impedance control.” *Master thesis,* Yanshan university, China.

Jordehi.,A.R. (2016). “Allocation of distributed generation units in electric power systems: A review.’ *J.Renewable and Sustainable energy reviews*,56(1), pp.893-905.

Jun,Y., Hongbiao,D., Te,Z. and Yi,T. (2015). “Improved droop control strategy for inverters parallel operation in microgrid.” J.power system technology, 39(4), pp.932-937.

Junhu,Y., Xiaoqing,H., Zengjic,C. and Kai,G. (2012). “Analysis on the dynamic performance of microgrid based on droop control of inverters.” *J.Southern power system technology*, 6(4), pp.1674-1678.

Junli,Y., Chunhua,P. and Chen,C. (2015). “Droop control strategy based on dynamic virtual impedance in low voltage microgrid.” *J.Power system protection and control,* 43(21), pp.1-6.

Junzhao,C., Wenxi,W. and Jiangbo,C. (2016). “Control strategy of sharing power in proportion for autonomous microgrid by virtual inductance.” *J.High voltage engineering*, 42(7), pp.2142-2148.

Kakigano,H., Miura,Y. and Ise,T. (2009). “Configurationand control of a DC microgrid for residential houses.” *Transmission and Distribution Conference & Exposition:Asia and pacific, Seoul,* pp.1-4.

Katiraei,F. and Iravani,M.R. (2006). “Power management strategies for a microgrid with multiple distributed generation units.” *IEEE Trans. on power systems*, 21(4), pp.1821-1831.

Kayalvizhi,S. and Kumar,V.D.M. (2017). “Frequency control of microgrid with wind perturbations using levy walks with spider monkey optimization algorithm.” *International Journal of Renewable Energy Research*, 7(1), pp.146-156.

Khaledian,A. and Golkar,M.A. (2017). “Analysis of droop control method in an autonomous microgrid.” *J.Applied research and technology*, 15(4), pp.371-377.

Khaparde,S.A., (2007).”Infrastructure for sustainable development using renewable energy technologies in india.” *Proc. IEEE PES general Meeting*, pp.1-16.

Khattam,W.E.I. and Salama,M.M.A. (2004). “Distributed generation technologies definitions and benefits.” *J.Electric power systems research*,71(2), pp.119-128.

Kim,H. and Sul, S.K. (2009). “Analysis on output LC filters for pwm inverters.” *IEEE International power electronics and motion control conference*, Wuhan, China, pp.384-389.

Kroutikova,N., Aramburo,C.A.H. and Green,T.C. (2007). “State-space model of grid-connected inverters under current control mode.” *IET electric power applications*, 1(3), pp.329-338.

Lasseter,R.H., Eto,J.H., Schenkman.,B., Stevens,J., Volkommer,H., Klapp,D., Linton,E., Hurtado,H. and Roy,J. (2011). “CERTS microgrid laboratory test.” *IEEE trans. on Power delivery*, 26(1), pp.325-332.

Lassetter,R.H., Akhil,A. and Marnay,C. (2002). “Integration of distributed energy resources:the CERTS microgrid concept.” Consortium for electric reliability technology solutions white paper.

Lee,C.T., Chu,C.C. and Cheng,P.T. (2013). “A new droop control method for the autonomous operation of distributed energy resource interface converters. *IEEE trans. on Power electronics*, 28(4), pp.1980-1993.

Lee,P.K., Lai,L.L. and Chan,S.W. (2011). “A practical approach of energy efficiency management reporting systems in microgrid.” *IEEE power and energy society general meeting*, pp.1-5.

Lee,W.C., Lee,T.K., Lee,S.H., Kim,K.H., Hyun,D.S. and Suh,I.Y. (2004). “A master and slave control strategy for parallel operation of three phase UPS systems with different ratings.” *Proc., IEEE Applied Power Electronics and Exposition Conference*,Anaheim, USA, pp.456-462.

Li,Y. and Li,W. (2009). “Decoupled power control for an inverter based low voltage microgrid in autonomous operation.” *Proc., IEEE Power electronics and motion control conference*, China, pp.2490-2496.

Li,Y.W. and Kao,C.N. (2009). “An accurate power control strategy for power electronics interfaced distributed generation units operating in a low voltage multibus microgrid.” *IEEE trans. on power electronics*, 24(12), pp.2977-2988.

Liaoyuan,L., Zhao,L., Wei,L. and Hao,M. (2016). “Wireless current sharing scheme for parallel operation of inverters using resistive output impedance.” *J.trans. on china electrotechnical society*, 31(8), pp.43-50.

Lin,L. (2017). “Research on some key issues of current sharing and flexible power distribution for paralleled multi inverter system.” *PhD thesis*, Zhejiang university, China.

Linchuan,W., Jian,W. and Zhilong,S. (2017). “Research on droop control strategy of microgrid based on virtual impedance.” *J.Electric switchgear*, 1(1), pp.41-44.

Long,L. (2014). “Research on power sharing strategy and smooth switch method in a microgrid.” *Master thesis*, Southwest jiaotong university, China.

Lopes,J.A.P., Moreira,C.L. and Madureira,A.G. (2006). “Defining control strategies for microgrid island operation.” *IEEE trans. on power systems*, 21(2), pp.916-924.

LYNCH,J. (2006). “Northern power system update on madriver microgrid and related activites[EB/OL].http://der.lbl.gov.

Mahmood,H., Michaelson,D. and Jiang,J. (2015). “Reactive power sharing in islanded microgrids using adaptive voltage droop control.” *IEEE trans. on smart grid*, 6(6), pp.3052-3060.

Majumder,R. (2014). “A hybrid microgrid with DC connection at back to back converters.” *IEEE trans. on smart grid*, 5(1), pp.251-259.

Maria,H.(2014). “World Energy outlook[C].Paris: International Energy Agency.

Mazumder,S.K., Acharaya,K. and Tahir,M. (2005). “Wireless control of spatially distributed power electronics.” Proc., *IEEE Applied Power Electronics and Exposition Conference*, Austin, USA, pp.75-81.

Meiqin,M.(2013). “Research on droop control based uniform controller for dual mode invertersd in a microgrid.” *Master thesis*, Hefei university of technology, China.

Meiqin,M., Yatao,S., Zheng,D., Kai,S. and Liuchen,C. (2015). “Accurate power control and unified control of coverters for microgrid based on local measurement.” *J.Automation of electric power systems*, 39(21), pp.37-45.

Meng,L., Sanseverino,E,R., Luna,A., Dragicevic,T., Vasquez,J.C. and Guerrero, J.M. (2016). “Microgrid supervisory controllers and energy management systems:A literature review.” *J. Renewable and sustainable energy reviews*,60(1), pp.1263-1273.

Micallef,A., Apap,M., Staines,C.S. and Guerrero,J.M. (2015). “Single phase microgrid with seamless transition capabilities between modes of operation.” *IEEE trans. on smart grid*, 6(6), pp.2736-2745.

Michael,H. and Natalie,P. (2011). “Smart grids initiatives in Europe.” Austrian Federal Ministry for transport, innovation and technology.

Ming,D., Yuan,Z.Y. and Meiqin,M. (2009). “Key technologies for microgrids being researched.” *J.Power system technology*, 33(1), pp.1-11.

Mingrui, Z., Zhichao, D. and Shaobo, W. (2014). “Research on droop control strategy and parameters selection of microgrids.” *Trans. of china electro technical society*, 29(2), pp.136-144.

Mohamed,A.R.I. and El-Saadany, E. F. (2008). “Adaptive decentralized droop controller to preserve power sharing stability of paralleled inverters in distributed generation microgrids.” *IEEE trans. on Power electronics*, 23(6), pp. 2806-2816.

Mohan,V., Singh,J.G. and Ongsakul,W. (2017). “Sortino ratio based portfolio optimization considering EVs and Renewable energy in microgrid power market.” *IEEE trans. on Sustainable energy*, 8(1), pp.219-229.

Morozumi,S. and Nara,K. (2007). “Recent trend of new type power delivery system and its demonstrative project in japan.” *IEEE trans. on Power and energy*, 12797), pp.770-775.

Morozumi,S. (2006). “Overview of microgrid research and development activities in japan.” *International symposium of Microgrids*, Montreal.

Morozumi,S. (2007). “Microgrid demonstration projects in japan.” *Proc., Power conversion conference, Nagoya*, pp.635-642.

Mortezapour,V. and Lesani,H. (2017). “Hybrid AC/DC microgrids:A generalized approach for autonomous droop based primary control in islanded operations.” *J.Electrical power and energy systems*, 93(1), pp.109-118.

Ministry of New and Renewable Energy, Annual Report (2015). Online, Available:www.mnre.gov.in.

Nunna, H. S. V. S. K. and Srinivasan,D. (2017). “Multiagent based transactive energy framework for distribution systems with smart microgrids.” *IEEE trans. on industrial informatics*, 13(5), pp.2241-2250.

Nunna, H. S. V. S. K., and Doolla, S. (2012). “Demand response in smart distribution system with multiple microgrids.” *IEEE trans. on Smart Grid*, 3(4), pp.1641–1649.

Pecaslopes,J.A., Moreira,C.L. and Resende,F.O.(2005). “Control strategies for microgrids black start and islanded operation.” *J.Distributed energy rersources*, 1(3), pp.241-261.

Pei,Y., Jiang,G., Yang,X. and Wang,Z. (2004). “Auto master slave control technique of parallel inverters in distributed AC power systems and UPS.” *Proc., IEEE Power electronics specialists conference,*Aachen, Germany, pp.2050-2053.

Peng,L., Ling,Z. and Yinbro,S. (2009). “An effective way for large scale renewable energy power generation connected to the microgrid.” *J.North china electric power university*, 36(1), pp.10-14.

Peng,Li. and Chengshan,W. (2010). “Development and challenges of distributed generation the microgrid and smart distribution system.” *J.Automation of electric power systems*, 34(2), pp.10-16.

Pengyu,C. (2017). “Voltage frequency recovery and reactive power allocation basede on consensus algorithm.” *Master thesis*, Shenyang Agricultural University, China.

Pesaram,M.H.A., Huy,P.D. and Ramachandaramurthy,V.K.,(2017). “A review of the optimal allocation of distributed generation:objectives,constraints,methods and algorithms.” *J.Renewable and Sustainable energy reviews*, 75(1), pp.293-312.

Piboonwattanakit,K. and Khanngern.W. (2007). “Design of the two parallel inverter modules by circular chain control technique.” *Proc. IEEE Power Electronics and Drive Systems Conference*, Bangkok, Thailand, pp.1518-1522.

Pogaku,N., Prodanovic,M. and Green,T.C. (2007). “Modeling analysis and testing of autonomous operation of an inverter based microgrid.” *IEEE trans. on power electronics*, 22(2), pp.613-625.

Poh,C.L., Ding,L. and Blaabjerg,F. (2011). “Autonomous control of interlinking converters in hybrid AC-DC microgrids with energy storages.” *IEEE energy conversion congress and exposition(ECCE), Phoenix*,USA, pp.652-658.

Qian,G., Liaoyuan,L., Hongyan,W., Zhihong,B. and Hao,M. (2015). “An improved droop control strategy for accurate reactive power sharing among distributed generators.” *J.Automation of electric power systems*, 39(15), pp.30-34.

Qingchang,Z. (2013). “Robust Droop Controller for Accurate Proportional Load Sharing Among Inverters Operated in Parallel.” *IEEE trans. on industrial electronics*, 60(4), pp. 1281-1290.

Qinghai,Z., An,L., Yandong,C., Chuwu,P. and Ziqing,P. (2014). “Analysis of output impedance for parallel inverters and voltage control strategy.” *trans. on china electrotechnical society*, 29(6), pp.98-105.

Qinglin,Z., Zhongying,C. and Weiyang,W. (2006). “Improved control for parallel inverter with current sharing control scheme.” *Proc., IEEE Power electronics and motion control conference*, Shanghai, China, pp.1-5.

Rajesh,K.S., Dash,S.S., Rajagopal,R. and Sridhar,R.(2017). “A review on control of ac microgrid.” *J.Renewable and sustainable energy reviews*.” 71(1), pp.814-819.

Ricchiuto,D., Mastromauro,R.A., Liserre,M., Trintis,I. and Nielsen,S.N. (2013). “Overview of multi DC bus solutions for DC microgrids.” *Proc., IEEE International Symposium on power electronics for distributed generation systems*, Rogers, USA, pp.1-8.

Rokrok,E. and M. E.H. Golshan. (2010). “Adaptive voltage droop scheme for voltage source converters in an islanded multibus microgrid.” *IET Generation Transmission & Distribution*, 2010, 4(5), pp.562-578.

Rocabert.J., Luna,A., Blaabjerg,F. and Rodriguez,P. (2012). “Control of power converters in ac microgrid.” *IEEE trans. on power electronics*, 27(11), pp.4734-4749.

Roslan,A.M., Ahmed,K.H., Finney,S.J. and William.B.W. (2011). “Improved instantaneous average current-sharing control scheme for parallel-connected inverter considering line impedance impact in microgrid networks.” *IEEE trans. on Power Electronics*, 26(3), pp.702-716.

Rowe,C.N., Summers,T.J., Betz,R.E., Cornforth,D.J. and Moore,T.G. (2013). “Arctan power–frequency droop for improved microgrid stability.” *IEEE trans. on Power electronics*, 28(8), pp. 3747-3759.

Ruiqi,W., Yan,C., Shumin,S., Zhanxin,J., Baoxian,L. and Chaoying,L. (2014). “Control and performance analysis of microgrid based on co-ordinate rotational virtual impedance.” *J.power system protection and control*, 42(12), pp.78-86.

Sao,C.K. and Lehn,P.W. (2005). “Autonomous load sharing of voltage source converters.” *IEEE transactions on power delivery*, 20(2), pp. 1009-1016.

Savaghebi,M., Jalilian,A., Vasquez,C.J. and Guerrero,J.M.(2012). “Secondary control scheme for voltage unbalance compensation in an islanded droop controlled microgrid.” *IEEE trans. on smart grid*, 3(2), pp.797-807.

Sen,S. and Kumar,V.(2018). “Microgrid modeling:A comprehensive survey.” *J.Annual reviews in control*, Accepted (In press).

Shafiee,Q., Guerrero, J.M. and Vasquez, J.C. (2014). “Distributed secondary control for islanded microgrid-A novel approach.” *IEEE trans. on Power electronics*, 29(2), pp.1018-1031.

Shah,S. and Sensarma,P.S. (2010). “Three degree of freedom robust voltage controller for instantaneous current sharing among voltage source inverters in parallel.” *IEEE trans. on Power electronics*, 25(12), pp.3003-3014.

Shang,S. (2013). “Research on P-V/Q-F droop control technology of microgrid inverter.” *Master thesis*, Yanshan university, China.

Shanxu,D., Bangyin,L., Yong,K. and Jian,C. (2004). “Parallel operation technique of inverters in UPS based on distributed logic control.” *J.Power electronics*, 38(2), pp.56-58.

Shanxu,D., Jian,C. and Feng,F. (2003). “Wireless parallel operation scheme of inverters based on power line communication.” *J.Automatic of electric power systems*, 27(24), pp.28-31.

Shaohua,X., Jianlin,L. and Dong,H. (2015). “Stability analysis and control strategy of parallel storage inverter system working under the microgrids’s island condition.” *J.High voltage engineering*, 41(10), pp.3266-3273.

Shinji,T., Yokoyama,A. and Hayashi,Y. (2009). “Distributed generation in japan.” *IEEE power and energy society general meeting*, Calgary, pp.1-5.

Shuai,Z., Sun,Y., Shen,Z.J., Tian,W., Tu,C., Li,Y. and Yin,X. (2016). “Microgrid stability:classification and a review.” *J.Renewable and sustainable energy reviews*, 58(1), pp.167-179.

Siri,K., Lee,C.Q. and Wu, T.(1992). “Current distribution control for parallel connected converters.” *IEEE trans. On Aerospace and Electronic Systems*, 28(3), pp.829-840.

Stevens,J., Vollkommer,H. and Klapp,D. (2007). “CERTS microgrid system tests.” *Power engineering society general meeting*,Tampa,USA, pp.1-4.

Stevens,J. (2004). “Development of sources and a test bed for CERTS microgrid testing.” *IEEE power engineering society general meeting*, Denver,USA, pp.1-2.

Su,J., Zheng,J., Cui,D., Li,X., Hu,Z. and Zhang,C. (2013). “An integrated control strategy adopting droop with virtual inductance in microgrid.” *J.Engineering*, 5(1), pp.44-49.

Sun,X., Lee,Y. and Xu,D. (2003). “Modeling, analysis, and implementation of parallel multi-inverter systems with instantaneous average-current-sharing scheme.” *IEEE trans. on power electronics*, 18(3), pp. 844-856.

Sun,X., Wong,L., Lee,Y. and Xu,D. (2006). “Design and analysis of an optimal controller for parallel multi-inverter systems.” *IEEE trans. on Circuits and systems II: Express Briefs*, 53(1), pp. 56-61.

Susu,S.(2013). “The study of droop control in low voltage microgrid.” *Ph.d thesis*, Yanshan university, China.

Tan,J., Lin,H., Zhang,J., Ying,J. (2003). “A novel load sharing control technique for paralleled inverters.” *Proc., IEEE Power Electronics Specialist Conference*, Acapulco, Mexico, pp.1432-1437.

Tao,Y., Liu,Q., Deng,Y., Liu,X. and He,X. (2015). “Analysis and mitigation of inverter output impedance impacts for distributed energy resource interface.” *IEEE trans. on power electronics*, 30(7), pp. 3563-3576.

Tianzhi,F., Xinbo,R., Lan,X. and Aizhong,L. (2008).“An improved distributed control strategy of parallel inverters.” *Proceedings of the CSEE*, 28(33), pp.30-36.

Tuladhar,A., Jin,H., Unger,T. and Mauch,K. (2000). “Control of parallel inverters in distributed ac power systems with consideration of line impedance effect.” *IEEE trans. on industry application*, 36(1), pp.131-137.

Unamuno,E. and Barrena,J.A. (2015). “Hybrid AC/DC microgrids-Part I:Review and classification of topologies.” *J.Renewable and sustainable energy reviews*, 52(1), pp.1251-1259.

Vasquez,J.C., Guerrero,J.M., Luna,A., Rodriguez,P. and Teodorescu,R. (2009). “Adaptive droop control applied to voltage source iverters operating in grid connected and islanded modes.” *IEEE trans. on industrial electronics*, 56(10), pp.4088-4096.

Vluski,R., Kumar,J., Venkata,S.S., Vishwakarma,D., Scheider,K., Sani,A.M., Terry,R. and Agate,W. (2017). “Microgrid controller design, implementation and deployment:A journey from conception to implementation at the philadelphia navy yard*.” IEEE power and energy magazine*, 15(4), pp.50-62.

Wang,J.(2014). “Control strategy research for parallel connected distributed generation in a low voltage microgrid.” *Master thesis*, Yanshan University,China.

Wang,J. and Dan,Z. (2016). “Research on construction and development trend of microgrid in china.” *J.power system technology*, 40(2), pp.451-458.

Wang,X., Lei,Y.W., Blaabjerg,F. and Loh.P.C. (2015). “Virtual impedance based control for voltage source and current source converters.” *IEEE trans. on Power electronics*, 30(12), pp.7019-7037.

Wei, X., Zhu, G.,Lu, J. and Xu,X. (2016). “Instantaneous current-sharing control scheme of multi-inverter modules in parallel based on virtual circulating impedance.” *IET Power Electronics*, 9(5), pp. 960-968.

Wei,H., Hui,S.C., Ping,W.Z. and Hua,Z.J. (2009). “A review on microgrid technology containing distributed generation system.” *J.Power system technology*, 33(9), pp.14-18.

Wei,Y., Min,C., Shanke,M., Mingzhi,G. and Zhaoming,Q. (2009). “Paralleing control technique of microgrid inverters based on improved droop method.” *J.Automation of electric power systems*, 33(6), pp.77-80.

Wei,Y.C., Minmatas, J., Guerrero, J. M. and Qian, Z. M. (2011). “Design and analysis of the droop control method for parallel inverters considering the impact of the complex impedance on the power sharing.” *IEEE trans. on industrial electronics*, 58(2), pp.576-587.

Wu, T., Liu, Z., Liu, S.W. and You,Z. (2016). “A unified virtual power decoupling method for droop controlled parallel inverters in microgrids.” *IEEE trans. on power electronics*, 31(8), pp.5587-5603.

Wu,T., Liu,J., Liu,Z., Wang,S. and Liu,B. (2015). “Load power estimation based secondary control for microgrids.” *Proc., International Conference on Power Electronics and ECCE Asia , Seoul, Korea*, pp.722-727.

Wu,T.F., Chen,Y.K. and Huang,Y.H. (2000). “3C strategy for inverters in parallel operation achieving an equal current distribution.” *IEEE trans. on industrial electronics*, 47(2), pp. 273-281.

Wu,X., Panda,S.K. and J. Xu. (2007). “Effect of Pulse-Width Modulation Schemes on the Performance of Three-Phase Voltage Source Converter.” *Proc., IEEE industrial electronics society conference*,Taipei, Taiwan, pp.168-173.

Xiaodong,C. (2016). “Research on control strategy of shipboard microsource inverter based on the droop control, *Master thesis*, Dalian maritime university, China.

Xiaofei,L., Xin,A. and Yonggang,W. (2011). “Study of single phase HFAC microgrid based on MATLAB/SIMULINK.” *4th International conference on electric utility deregulation and restricting and power technologies(DRPT)*, pp.1104-1108.

Xiaofeng,S., Juan,W., Yanjun,T. and Li,X. (2013). “Control of DG connected inverters based on self adaptable adjustment of droop coefficient.” *Proceedings of the CSEE*, 33(36), pp.71-78.

Xiaofeng,S., Yalin,Y., Wei,Z., Hong,S. and Guangjun,T. (2014). “An adaptive droop control method for inverters in microgrid.” *J.Power system technology*, 38(9), pp.2386-2391.

Xie,B.H., Zheng,S. and Ni,M. (2017). “Microgrid development in china: A method for renewable energy and energy storage capacity configuration in a megawatt-level isolated microgrid.” *IEEE electrification Magazine*, 5(2), pp.28-35.

Xin, C., Changhua, Z. and Qi, H. (2017). “Small signal stability analysis of microgrid using droop control with differential term.” *J. Automation of electric power system*, 41(3), pp.46-53.

Xinfa,Y., Jian,S., Zhipeng,L.U., Haitao,L. and Rui,L. (2014). “Overview on microgrid technology.” *Proceedings of the CSEE*, 34(1), pp.57-70.

Xing,Y., Huang,L., Sun,S. and Yan,Y.(2002). “Novel control for redundant parallel UPSs with instantaneous current sharing.” *Proc., IEEE Power Conversion Conference*, Osaka, Japan, pp. 959-963.

Xuan,Z. and Jinjun,L. (2011). “A novel power distribution strategy for parallel inverters in islanded mode microgrid.” *J. Power supply*, 9(1), pp.38-42.

Xumiao,Z. (2015). “Based on the droop control microgrid inverters control system research.” *Master thesis*, Yanshan university, China.

Yajuan, G., Guerrero, J. M., Zhao, X., Vasquez, J. C. and Guo, X. (2016). “ A new way of controlling parallel connected inverters by using synchronous reference frame virtual impedance loop part-I:control principle.” *IEEE trans. on power electronics*, 31(6), pp. 4576-4593.

Yajuan, G., Weiyang, W. and Xiaoqiang, G. (2011). “Control strategy for three phase inverters dominated microgrid in autonomous operation.” *Proceedings of the CSEE*, 31(33), pp. 52-60.

Yajuan,G.(2012). “Study on control of three phase voltage source inverters in microgrid.” *Master thesis*, Yanshan university,China.

Yajuan,G. and Weiyang,W.(2010). “An improved droop controller for gridconnected voltage source inverter in microgrid.” *Proc., IEEE international symposium on power electronics for distributed generation systems*, Hefei, China, pp. 823-828.

Yan,L., Zhencai, C., Danyue,W. and Jianhua,L. (2016). “A control strategy of load distribution based on virtual impedance in an islanded mode microgrid.” *J.Electrical measurement and instrumentation*, 53(9), 67-73.

Yandong,C.(2014). “Research on the key techniques of multi inverter control system in microgrid.” *PhD thesis*, Hunan university, China.

Ye,Z., Li,G. and Hongjie,J. (2015). “Improved droop control method for microgrid based additional damping.” *J.Automation of electric power systems*, 39(18), pp.25-30.

Yixin, Z., Fang, Z., Feng, W. and Baoquan,B. (2016). “Virtual impedance optimization method for microgrid reactive power sharing control.” *Proceedings of the CSEE*, 36(17), pp.4552-4563.

Yong,S. (2015). “Control Strategies of microgrid inverters and microgrid system.” *Phd Thesis*, Hefei university of technology, China.

Yonggang,W.(2012). “Analysis of frequency stability of microgrid based on droop control.” *Master thesis*, North china electric power university, China.

Yuen,C., Oudalov,A. and Timbus,A. (2011). “The Provision of frequency control reserves from multiple microgrids.” *IEEE trans. on industrial electronics*, 58(1), pp.173-183.

Yuqin,X. and Huanjun,M. (2015). “Parallel operation technology of inverters based on improved droop control.” *J.Power system protection and control*, 43(7), pp.103-107.

Zhang,C., Xu,Y., Dong,Z.Y. and Ravishankar,J.(2017). “Three-Stage Robust Inverter-Based Voltage/Var Control for Distribution Networks with High-Level PV.” *IEEE trans. on smart grid*, pp.1-12.

Zhang,S.(2015). “Power control of paralleled inverters with different power ratings based on the current droop control.” *Master thesis*, Yanshan university, China.

Zhang,X.(2015). “Research on the control strategy for paralleled inverters with different capacities in distributed generation systems.” *Master thesis*, Yanshan university, China.

Zhang,Z.(2013). “Research on droop control strategy for microgrid inverter.” *Master thesis*, Nanjing university of aeronautics and astronautics, China.

Zhao,B., Yang,Y., Zhang,X., Xue,M., Li,P., Xu,C. and Zhou,D. (2016). "Implementation of a dual microgrid system with flexible congigurations and hierarchical control in china." *J.Renewable and sustainable energy reviews*, 65(1), pp.113-123.

Zhen,L. and Wei,B. (2014). "Research on control strategy of synchronous voltage source converter based on complex virtual impedance in microgrid." *J.Modern electric power*, 31(2), pp.60-65.

Zheng,Z., Weihua,S., Chunwei,S., Hui,L. and Li,R. (2016). "Circuit based analysis of typical control schemes of voltage source inverter." *Proceedings of the CSEE*, 36(18), pp.4980-4989.

Zhongming, Z. (2015). "Research on the low voltage microgrid decoupling droop control strategy." *Master thesis,* Southwest jiaotong University, China.

Zhongyi, H. (2008). "Research on the control and parallel operation control for pwm inverters."*Phd thesis*, Nanjing university of aeronautics and astronautics, China.

Zhongyi,H., Yan,X., Biaojie,Q. and Xiaona,W. (2010). "Control for inverters in parallel operation with presynchronized voltage references." *trans. on china electrotechnical society*, 25(4), pp.115-121.

Zhu,Y.X., Zhuo,F., Wang,F., Liu,B.Q. and Zhao,Y.J. (2015). "A wireless load sharing strategy for islanded microgrid based on feeder current sensing." *IEEE trans. on power electronics*, 30(12), pp.6706-6719.

Ziqiang,P., An,C., Yandong,C., Zhiyong,C., Jigen,L. and Chunming,T. (2013). "A frequency divided virtual resistance based control strategy for multi parallel inverters." *J.Power system technology*, 37(11), pp.3276-3280.

Zixin,Li., Ping,W., Hua,L.Y., Haibin,Z., Xiasong,S. and Fanqiang,G. (2009). "400Hz high power voltage source inverter with digital control." *Proceedings of the CSEE*, 29(6), pp.36-42.

Brief Bio-Data

Mr. Chethan Raj D is a research scholar in the Department of Electrical & Electronics Engineering, National Institute of Technology Karnataka (NITK), Surathkal, Mangalore, INDIA.

Address:

Mr. Chethan Raj D,
Bagalgunte Village,
Bengaluru,Karnataka – 560073, INDIA.
Phone: +91 9738128573
Email:chethanraj9@gmail.com.